GENERATION EXPANSION PLANNING UNDER EXTENDED CONDITIONS USING SIMHEURISTICS APPROACH

KONGRITH KOMASATID

A THESIS SUBMITTED IN PARTIAL FULFILLMENT
OF THE REQUIREMENT FOR THE DEGREE OF
DOCTOR OF ENGINEERING IN ELECTRICAL ENGINEERING
FACULTY OF ENGINEERING
KING MONGKUT'S INSTITUTE OF TECHNOLOGY LADKRABANG
2020

KMITL-2020-EN-D-018-104

GENERATION EXPANSION PLANNING UNDER EXTENDED CONDITIONS USING SIMHEURISTICS APPROACH

KONGRITH KOMASATID

A THESIS SUBMITTED IN PARTIAL FULFILLMENT
OF THE REQUIREMENT FOR THE DEGREE OF
DOCTOR OF ENGINEERING IN ELECTRICAL ENGINEERING
FACULTY OF ENGINEERING
KING MONGKUT'S INSTITUTE OF TECHNOLOGY LADKRABANG
2020

KMITL-2020-EN-D-018-104

Thesis Title	Generation Expansion Planning under Extended Conditions using Simheuristics Approach
Student	Mr.Kongrith Komasatid
Student ID.	57601004
Degree	Doctor of Engineering
Program	Electrical Engineering
Year	2020
Thesis Advisor	Assoc. Prof. Dr. Somchat Jiriwibhakorn

ABSTRACT

This thesis presents a new stochastic optimization, so-called "Simheuristics" for solving a generation expansion planning problem considering the extended conditions other than those considered in the official power development plan (PDP). Firstly, the load leveling application of Lithium-based energy storage system is considered in the Thailand power system. The load leveling strategy involves storing the cheap energy and release it during the expensive marginal cost of generation. Secondly, the generation planning framework is enhanced with the flexible generation planning to cope with the increasing variable renewables. Thirdly, the import of liquefied natural gas is assumed 100% in 2028. The risk-hedging against the uncertainty of spot prices is considered in generation planning. Lastly, the reduction target of carbon dioxide emission is considered 25% for the electricity sector to achieve the 1.5°C global climate change. For this reason, the carbon tax and emission trading schemes are evaluated for mitigation options. The proposed method has been demonstrated with the Thailand generation system (PDP2018) considering the extended conditions. The simulation result shows that the proposed method is suitable for practical generation planning.

หัวข้อวิทยานิพนธ์	การวางแผนขยายกำลังการผลิตไฟฟ้าภายใต้การพิจารณาเงื่อนไขด้วยวิธีจำลองสถานการณ์ฮิวริสติกส์
นักศึกษา	นายคงฤทธิ์ โกมาสถิตย์
รหัสประจำตัว	57601004
ปริญญา	วิศวกรรมศาสตรดุษฎีบัณฑิต
สาขาวิชา	วิศวกรรมไฟฟ้า
พ.ศ.	2563
อาจารย์ที่ปรึกษาวิทยานิพนธ์	รศ.ดร. สมชาติ จิริวิภากร

บทคัดย่อ

วิทยานิพนธ์นี้ นำเสนอวิธีการหาคำตอบที่เหมาะสมภายใต้ความไม่แน่นนอนที่ชื่อ “วิธีจำลองสถานการณ์ฮิวริสติกส์” สำหรับวางแผนขยายกำลังผลิตไฟฟ้า ซึ่งพิจารณาเงื่อนไขเพิ่มเติมที่นอกเหนือจากที่ได้พิจารณาในแผนพัฒนากำลังผลิตไฟฟ้าของประเทศไทย ฉบับ พ.ศ. 2561 - 2580 โดยเงื่อนไขแรกได้พิจารณาการใช้ประโยชน์จากระบบกักเก็บพลังงานโดยใช้แบตเตอรีลิเธี่ยมในโหมดการจัดการระดับของโหลด ซึ่งจะสะสมพลังงานในช่วงที่เชื้อเพลิงมีราคาถูก จากนั้นจะปล่อยพลังงานเพื่อลดปริมาณการผลิตไฟฟ้าของโรงไฟฟ้าในช่วงที่ราคาเชื้อเพลิงมีราคาแพง เงื่อนไขที่สองได้พิจารณากรอบการวางแผนเพิ่มเติมสำหรับเสริมกำลังผลิตไฟฟ้าที่มีความยืดหยุ่น เพื่อรองรับพลังงานผันแปรที่มีแนวโน้มเพิ่มสูงขึ้น เงื่อนไขที่สามได้พิจารณาการป้องกันความเสี่ยงจากความไม่แน่นอนของราคาเชื้อเพลิงสำหรับผลิตไฟฟ้า ซึ่งเกิดขึ้นจากสัดส่วนของเชื้อเพลิงที่ได้จัดหามาจากตลาดจรที่มีแนวโน้มเพิ่มมากขึ้น และเงื่อนไขที่สี่ได้พิจารณาเครื่องมือทางนโยบายสำหรับการแก้ปัญหาโลกร้อนและการเปลี่ยนแปลงสภาพภูมิอากาศ ซึ่งประกอบด้วยแนวทางจัดเก็บภาษีคาร์บอน และตลาดซื้อขายคาร์บอน โดยวิธีที่นำเสนอได้นำมาสาธิตวางแผนขยายกำลังการผลิตไฟฟ้าของประเทศไทย ช่วงปี 2561-2580 จากผลการทดสอบแสดงให้เห็นว่า วิธีที่นำเสนอสามารถนำไปประยุกต์ในทางปฏิบัติได้อย่างมีประสิทธิภาพ

Acknowledgment

This thesis was written during my pursuing the D. Eng (electrical engineering) at the faculty of engineering, King Mongkut's Institute of Technology Ladkrabang. I would like to thank my supervisor, Assoc. Prof. Dr. Somchat Jiriwibhakorn for your endless patience, discussions, and supervision throughout the academic study for my research.

I would like to thank the five academic examiners: Asst. Prof. Dr. Parnjit Damrongkulkamjorn, Asst. Prof. Dr. Nirudh Jirasuwankul, Asst. Prof. Dr. Chai Chompoo-Inwai, Asst. Prof. Dr. Chow Chompoo-Inwai, and Assoc. Prof. Dr. Somchat Jiriwibhakorn to fulfill this doctoral thesis.

Besides, I would like to thank all of my colleagues in the generation and transmission planning division at EGAT who support me in the data to fulfill my research.

Last, thank you to my family, especially Mrs.Lertluck and Mr. Komol Komasatid for their love, eternity, and financial support. Finally, I also would like to thank my beloved Miss. Apiwattanaree Saengkum for her encouragement and support.

Kongrith Komasatid

Table of Contents

Notation

To the greatest extent, the individual notation used in this doctoral thesis attempts to describe the unique meaning. In the case of extra meaning in a specific context, the notation is explained clearly. In general, the indices are represented by italics lowercase while member sets are uppercase with the special font style. Equation format is designed by chapter and number within the section, e.g. (2.1) stand for Section 2, Equation 1. The scientific units and references are represented in "[]", e.g. [MWh] stand for megawatt-hour unit, [10] stand for the tenth reference in section References. The scalar and constant parameters are written in normal style while the matrices are written in italic boldface. Generally, a row vector is an $1 \times j$ matrix, e.g. A={a_1, .. , a_j }, and a column vector $i \times 1$ matrix represents by $A^\intercal$ ($\intercal$ means 'transpose operator' as is customary). The subscript refers to the indices of variables and constant parameters. The superscript reserves for special descriptions, e.g. min/max value, group of power plants, and so on. The function is denoted by bold character and indicate by (■). Finally, we reserve the special superscript with bracket, e.g. $(.)^{(iter)}$ means for additional meanings.

Indices

d	Index of decision spaces,
e	Index of the energy function,
f	Index of fuel types,
g	Index of power plant units,
h	Index of operating hours or duration hours,
i	Index of function or row index of a matrix,
j	Index of function or row index of a matrix,
l	Index of system net load,
ω	Index of scenario path, and
t	Index of the planning stage.

Sets

$\mathcal{G}$	Set of all generating units in generation fleets,
$\mathcal{G}^N$	Set of new candidate generating units, $\mathcal{G}^N \subset \mathcal{G}$
$\mathcal{G}^E$	Set of existing generating units, $\mathcal{G}^E \subset \mathcal{G}$
$\mathcal{G}^C$	Set of committed generating units, $\mathcal{G}^C \subset \mathcal{G}$
$\mathcal{G}^R$	Set of retired generating units, $\mathcal{G}^R \subset \mathcal{G}^E$
$\mathcal{G}^{\mathrm{th}}$	Set of thermal units,
$\mathcal{G}^{\mathrm{H}}$	Set of hydroelectricity with storage units,
$\mathcal{G}^{\mathrm{ESS}}$	Set of EES units,
$\mathcal{D}$	Set of decision spaces,
$\mathcal{T}$	Set of study periods,
$\mathcal{H}$	Set of operating hours,
$\mathcal{L}$	Set of system net load,
$\mathcal{F}$	Set of feasible candidate solutions,
F	Set of fuel types of power plants,
$\mathcal{G}^{\mathrm{VSPP}}$	Set of VSPP units,
$\mathcal{G}^{\mathrm{SPP}}$	Set of SPP units,
$\mathcal{E}$	Set of the energy function,
$\mathcal{C}$	Set of the cuckoo nest,
Ω	Set of all possible scenario,
$\mathbb{I}$	Set of a row of function,
$\mathbb{J}$	Set of a column of function,

Variables

X	Vector in $\mathbb{Z}^{ng}_{\geq 0}$ representing the existing generating power plants;
U	Vector in $\mathbb{Z}^{nn}_{\geq 0}$ representing the new-built power plants,
C	Vector in $\mathbb{Z}^{nc}_{\geq 0}$ representing the committed power plants,
R	Vector in $\mathbb{Z}^{nr}_{\geq 0}$ representing the retired power plants,
E^{PPS}_g	Vector in $\mathbb{R}^{ng}_{\geq 0}$ representing expected produced energy [MWh],
E^{ESS}_g	Vector in $\mathbb{R}^{ng}_{\geq 0}$ representing expected produced energy [MWh],

Constants parameters

cap_g	Vector in $\mathbb{R}_{\geq 0}^{nn}$ representing the contract capacity of power plants [MW],
C_g^{Inv}	Vector in $\mathbb{R}_{\geq 0}^{nn}$ representing the unit capital cost [$/MW],
C_g^{FOM}	Vector in $\mathbb{R}_{\geq 0}^{ng}$ representing the fixed O&M cost [$/MW],
C_g^{VOM}	Vector in $\mathbb{R}_{\geq 0}^{ng}$ representing the variable O&M cost [$/MWh],
AHR_g	Vector in $\mathbb{R}_{\geq 0}^{ng}$ representing the average heat rate [MMBTU/MWh],
FC_g	Vector in $\mathbb{R}_{\geq 0}^{ng}$ representing the fuel cost [$/MMBTU],
$C_g^{\text{SO}_2}$	Vector in $\mathbb{R}_{\geq 0}^{ng}$ representing the coefficient of sulfur dioxide [$/kg],
C_g^{PM}	Vector in $\mathbb{R}_{\geq 0}^{ng}$ representing the coefficient of particulate matter [$/kg],
SCC	Vector in $\mathbb{R}_{\geq 0}^{ng}$ representing the carbon tax [$/kg$_{CO_2}$],
$\delta_g^{\text{SO}_2}$	Vector in $\mathbb{R}_{\geq 0}^{ng}$ representing the SO_2 emission factor [kg/MWh],
δ_g^{PM}	Vector in $\mathbb{R}_{\geq 0}^{ng}$ representing the particulate matter factor [kg/MWh],
$\delta_g^{\text{CO}_2}$	Vector in $\mathbb{R}_{\geq 0}^{ng}$ representing the CO_2 emission factor [ton-kg/MWh],
$\mathcal{D}_g$	Vector in $\mathbb{Z}_{\geq 0}^{ng}$ representing the investment limitation [$],
γ_g	Vector in $\mathbb{R}_{\geq 0}^{nr}$ representing the decommissioning factor [$/MW],
ET	Vector in $\mathbb{R}_{\geq 0}^{\text{T}}$ representing yearly carbon dioxide emission target [kg-CO_2],
M_f^{min}, M_f^{max}	Vector in $\mathbb{R}_{\geq 0}^{ng}$ representing minimum and maximum fuel mix ratio [%],
γ_g	Vector in $\mathbb{R}_{\geq 0}^{nr}$ representing the decommissioning factor [$/MW],
p_g	Vector in $\mathbb{R}_{\geq 0}^{ng}$ representing the availability of generating units [fraction],
q_g	Vector in $\mathbb{R}_{\geq 0}^{ng}$ representing the unavailability of generating units [fraction],
$\text{H}_g^{\text{operate}}$	Vector in $\mathbb{R}_{\geq 0}^{ng}$ representing the operating hours of hydro units [hour],
$\text{H}_g^{\text{discharge}}$	Vector in $\mathbb{R}_{\geq 0}^{ng}$ representing the discharging hours of hydro units [hour],
MC_g^{charing}	The short-run marginal cost of charging energy [MWh],
$MC_g^{\text{discharing}}$	The short-run marginal benefit of discharging energy [MWh],
EL_g	The energy limit corresponding to energy marginal analysis [MWh],
η_g^{cycling}	The cycling/round-trip efficiency of ESS generating unit [MWh],
K_g	The movable energy block of generating unit [dimensionless],
SoC_g	The state of charging energy [MWh],
DoD_g	The depth of discharging energy [MWh],
E^{load}	The total load energy [MWh],
L	The typical electricity load [MW],

d	The duration that system net load greater or equal to load [hour],
δ^d	The discounted rate [% per year],
ε	The generating system reliability criteria [% per year],
$IEAR$	Interrupted energy assessment rate [million $/MWh],
LOLP	Loss-of-Load probability index [%],
$\mathrm{Prob}^{\mathrm{discover}}$	The discovering probability of maximum iterations [%],
T	Number of planning periods,
ng	Number of all generating units,
nn	Number of new candidate options,
nc	Number of committed power plants,
nr	Number of retired power plants,
nd	Number of deterministic constraints,
np	Number of probabilistic constraints,
nh	Number of maximum operating hour,
nt	Number of nest of tricked bird,
e^{total}	Number of cumulative energy blocks,
iter	Number of iterations,
$\mathrm{iter}^{\max}$	Number of maximum iterations,

Symbols

$(.)^{(t)}$	Variables of time stage t,
$(.)^{(iter)}$	Variables of iteration $iter$,
$(.)^{(s)}$	Variables of scenario s,
$(.)^{(h)}$	Variables of operating hour h,
$(.)^{(*)}$	Optimized value of the objective function,
$(.)^{(\mathrm{iter})}$	Iteration of variable,

Functions

$\phi(\blacksquare)$	Function of equality constraint,
$\psi(\blacksquare)$	Function of inequality constraint,
$\theta(\blacksquare)$	Function of salvage value from generating units, in $\mathbb{R}_{\geq 0}^{ng}$ [%],

$\mathrm{LOLP}(\blacksquare)$ Function of LOLP evaluation using probabilistic production simulation from generating units, in $\mathbb{R}_{\geq 0}^{ng}$ [%],

$NPV^{(t)}(\blacksquare)$ Function of net present value from planning horizon, in $\mathbb{R}^{\mathrm{T}}$ [$],

$\mathrm{ELDC}^{(i)}(\blacksquare)$ Function of ELDC, in $\mathbb{R}_{\geq 0}^{ng}$ [fraction],

$\mathrm{Levy}(\blacksquare)$ Function of number generator, in $\mathbb{R}_{+}^{nt}$ [dimensionless],

$\mathrm{EF}(e)^{(i)}$ The energy function of LDC, returning value in $\mathbb{R}_{\geq 0}^{ng}$ [MWh],

$EF'(e)^{(i)}$ The intermediate variable of the energy function, in $\mathbb{R}_{\geq 0}^{ng}$ [MWh],

Planning Models

GEP-I Deterministic multi-year GEP considering generating reliability without decommissioning cost consideration,

GEP-II Deterministic multi-year GEP considering generating reliability without external cost consideration

GEP-III The GEP-I planning model with enhanced flexibility planning,

S-GEP-I The stochastic GEP considering official PDP2018's assumptions, and

S-GEP-II The S-GEP-I planning model considering all extended conditions.

List of Tables

List of Figures

Chapter 1
Introduction

1.1 Preface

Thailand electricity planning is a process to optimize the long-term generation expansion plan, so-called PDP (power development plan) in the electric supply industry (ESI) to serve national electricity demand. Based on PDP 2018 [1], the Ministry of Energy together with a state-owned enterprise, well-known as Electricity Generating Authority of Thailand (EGAT), prepares PDP to provide the energy supply to Thailand electricity demand at optimum plan while satisfying security, economy, and environment. An independent organization or Thailand's Load Forecast Sub-committee (TLFS) plays a role for electricity forecasting, considering three key assumptions into the load model: (1) Energy Efficiency Development Plan: EEDP, (2) Alternative Energy Development Plan: AEDP, and (3) Electric Vehicle Plan. The approval processes are considered by Energy Regulatory Commission (ERC) then endorsed by the National Energy Policy Council (NEPC) and finally acknowledged by the Cabinet, respectively (as shown in Figure 1.1).

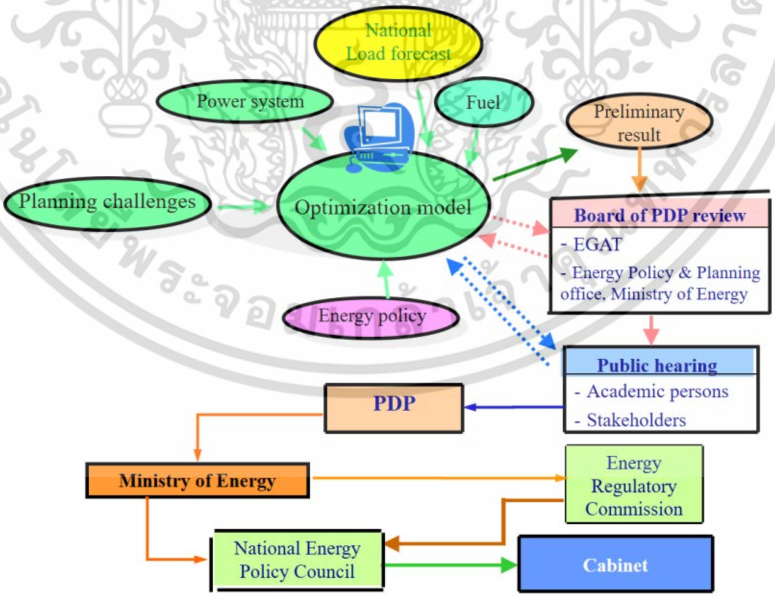

Figure 1.1 PDP approval processes based on PDP 2018 [2]

The Thailand market structure (number 2 as shown in Figure 1.2) is an enhanced single buyer which EGAT is a single buyer taking care of generation, purchasing, and selling bulk electricity. EGAT purchases electricity from private power producers and neighboring countries, i.e., foreign independent power producers (FIPP) then sell electricity to the domestic distribution companies, i.e. provincial electricity authority (PEA), metropolitan electricity authority (MEA) and cross-border electricity trading, i.e. Lao PDR and Malaysia. The private power producers are categorized by contract capacity: 1) independent power producers (IPPs) which contracted capacity > 90 MW, 2) small power producers (SPPs) which contracted capacity of 10-90 MW and 3) very small power producers (VSPP) which contracted capacity less than 10 MW. The electricity price is defined by customer types and implemented as a uniform tariff throughout the whole country.

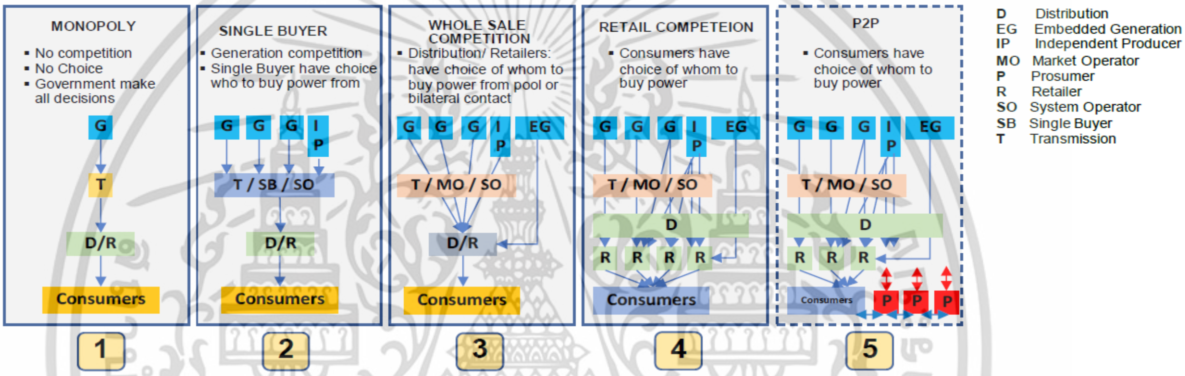

Figure 1.2 General market structures, adopt from [3]

As the market structure described above, Thailand's electric supply industry is governed by governmental agencies (e.g. energy policy and planning office, Ministry of Energy) and regulated by regulatory bodies (e.g. the energy regulatory commission) as shown in Figure 1.3.

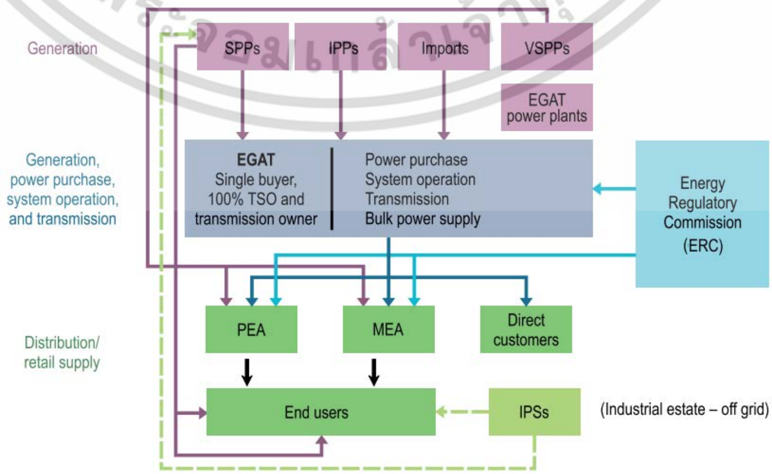

Note: TSO = transmission system operator; IPSs = independent power supply.

Figure 1.3 Thailand electric supply industry [4]

1.2 New planning challenges

The objective of traditional PDP is to optimize the investment cost and operating cost resulting in selected technologies, resources, contracted capacities, commercial operate date, and connecting zones of new-build power plants to serve national electricity demand subject to the energy policies under certainty parameters. The new planning challenges are listed as following:

1.2.1 Climate Change Policy

The last ice age or "glacial period" ended in the past 18 million years and the interglacial period started in about 11 million years ago. The glacial-interglacial epoch can be explained by Milankovitch's theory which describes the collective effects (eccentricity, axial tilt, and precession of the Earth's orbit) of change to the Earth's movement. Focusing on the global climate system, the interglacials period can be observed at high sea level, high average surface temperature, and high atmospheric carbon dioxide. For instance, the intensity [part per million: ppm] of the glacial period stays below 190 ppm then increases abruptly to 270 ppm of the interglacial period in the Pre-Industrial Revolution as illustrated in Figure 1.4.

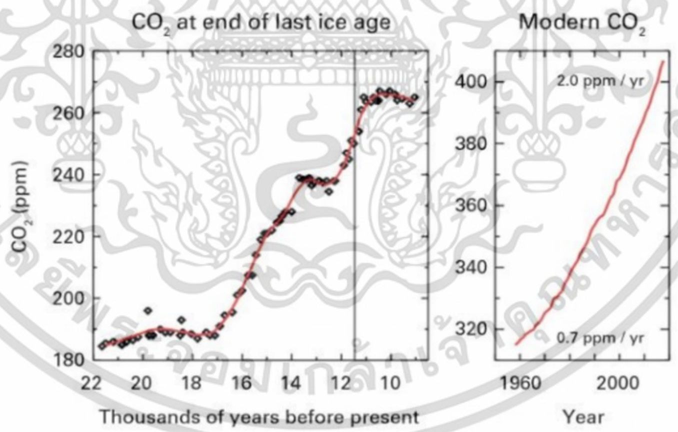

Figure 1.4 Atmospheric carbon dioxide of Thousand years before present (Holocene) [5]

Since the Industrial Revolution, hydroelectricity, nuclear power plant, and fossil-fired power plants (oil, coal, gas, diesel, bunker oil, and so on) have been the majority technologies producing electricity worldwide. In the late 19th, The Intergovernmental Panel on Climate Change (IPCC) [7] reports that the average surface temperature rises

0.6±0.2°C and atmospheric concentration significantly increases 40% from 280 ppm in 1750 to 400 ppm in 2019 (as shown in Figure 1.5).

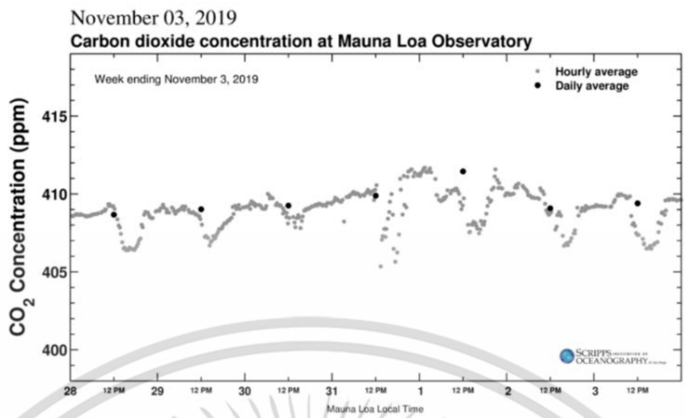

Figure 1.5 Atmospheric carbon dioxide concentration [6]

In the context of sustainable development goal 13 of the United Nations (UN), the government of Thailand decided to include the Nationally Appropriate Mitigation Actions (NAMAs) target [8] into the electricity policy to reduce the emission by 7-20 % of the power sector in 2020. The NAMAs corporates the 2°C climate change policy into PDP formulation. In the Conference of Parties 21 (COP21), Thailand intends to reduce emission by 20-25 percent from projected business-as-usual (BAU) level by 2030 as Nationally Determined Contribution (NDC) target. As low-carbon development may pay high cost to mitigate the climate change problem, it is important to study the positive effect on the environmental advantage of policy instruments (e.g., carbon tax scheme [9], emission trading scheme [10], and so on).

1.2.2 System impacts from renewable integration

Based on AEDP 2015 [11], the Ministry of Energy (Thailand) sets a target of 27.99% of renewable energy by 2036. As of 2014 result, the shares of renewable reached one-fifth of policy comprising wind, solar photovoltaics (PV), biomass, biogas, hydro, municipal solid waste, and new alternative energy as shown in Table 1.1.

The need for climate change mitigation makes the markets of renewable energy grow rapidly worldwide due to emission-free characteristics and zero variable cost. On the other hand, the high penetration of renewable energy creates new challenges to planning philosophy are as follows:

Table 1.1

Renewable energy resources target of AEDP 2015

Renewable energy resources	2014 (MW)	2036 target (MW)	%Capacity of 2036
Municipal solid waste	66.72	500	0.71%
Industrial waste	0	50	0.07%
Biomass	2451.82	5,570	7.92%
Biogas (waste/solid/water)	311.5	600	0.85%
Mini hydro	142.01	376	0.53%
Biogas (energy crop)	0	680	0.97%
Wind energy	224.47	3,002	4.27%
Solar energy	1,298.51	6,000	8.53%
Hydropower	0	2,906.4	4.13%
Total capacity (MW)	**4,449.03**	**19,684.4**	**27.99%**

A. Need for system flexibility

Some types of renewable energy perform as the variable renewable energy (VRE) [12], i.e. onshore/offshore wind, solar PV, and small hydroelectricity, due to the uncertainty and variability characteristics. The variability refers to the generation profile of VRE that fluctuates according to the natural resources (e.g., wind speed and direction, solar radiation, hydro stream, and so on). The uncertainty refers to the plant availability that intermittent depends on the meteorological situations (e.g., weather conditions, and so on).

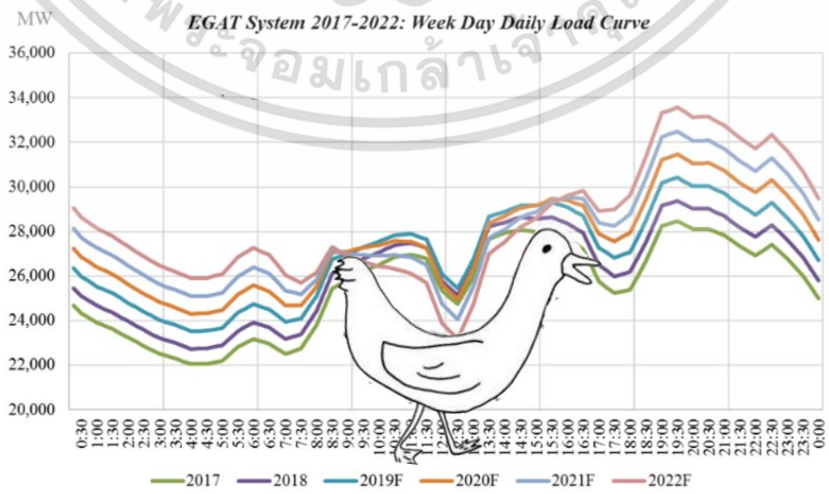

Figure 1.6 Thailand's duck curve effect of netload profile [13]

As of 2018 Thailand generation system, the electricity demand curve in EGAT's system is reshaping significantly, so-called *duck curve effect* [13] as shown in Figure 1.6. The dispatchable-power plants (nuclear, fossil-fired power plants and hydroelectricity) are stressed to ramp down the electricity power to match the high supply of PV generation during noon, and then ramp up to serve the electric power during sunset. In long-term planning, flexibile generation technologies (e.g., fossil dispatchable-power plants, energy storage, demand response, and so on) [14] are required to be invested for the upcoming PDP considering reliable power system operation.

B. Need for frequency security

From past to present, the synchronous machines of conventional generation technologies (e.g., thermal, steam, and combined cycle technologies) have the advantage for generation-load balance, so-called 'system inertia' which resist the rate of change of frequency (RoCoF) [15]. The importances of system inertia are that: (1) increasing load (decreasing system frequency), the stored kinetic energy in rotating machines are released to compensate instantaneously the shortfall generation, and (2) increasing generation (increasing system frequency), the kinetic energy is harvested in the rotating machines to reduce the surplus generation. In contrast, the inverter-based generations (IBGs) [16], i.e. onshore/offshore wind and solar photovoltaics have no contribution to system inertia. Recently, IBGs are committed to increase the installed capacity for reducing carbon dioxide emission and environmental impact. With this reason, the *frequency security* is recognized as the new dimension of generation expansion planning (GEP) since frequency dynamics may be deteriorated as a result of the decreasing trend of system inertia [17].

1.2.3 Grid Energy Storage Utilization

The grid energy storage system (ESS) [18] are essential and critical parts of the micro grid and smart grid. As of today, we can transform the electrical energy to other forms that are: (1) gravitational potential energy (e.g. hydroelectricity with large reservoir), (2) electrochemical energy (e.g. hydrogen, flow batteries, lithium-ion batteries), (3) kinetic energy (e.g. flywheels), (4) magnetic fields (e.g. superconducting magnetic energy storage), (5) electric field (e.g. supercapacitor energy storage), and (6) thermal storage, (e.g. molten salt energy storage). Figure 1.7 organizes the ESS technology in power system.

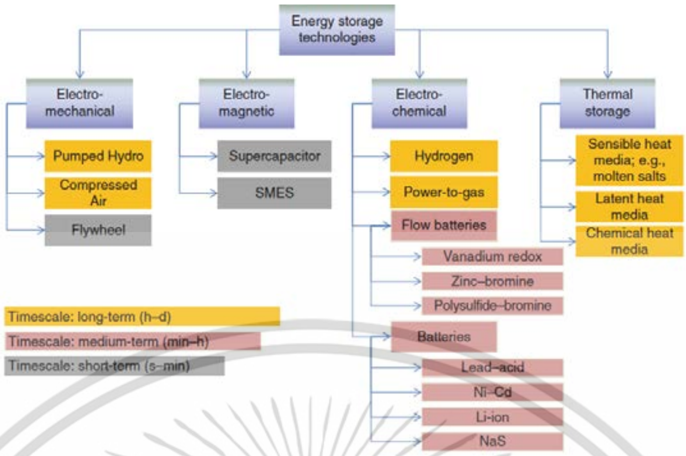

Figure 1.7 Overview of energy storage technologies in power system applications [19]

ESS gradually expands the operation applications as shown in Figure 1.8. In Thailand power system operation, hydroelectricity is applied in many applications that are: (1) hydroelectricity (with large-storage) releases the stored water to displace the on-peak period, so-called *"peak-shaving application"* [20], and (2) *load leveling application* which pumped-storage hydroelectricity stores the water of lower reservoir during cheap cost to the upper reservoir, then release the stored energy to displace the expensive energy at on-peak period [21].

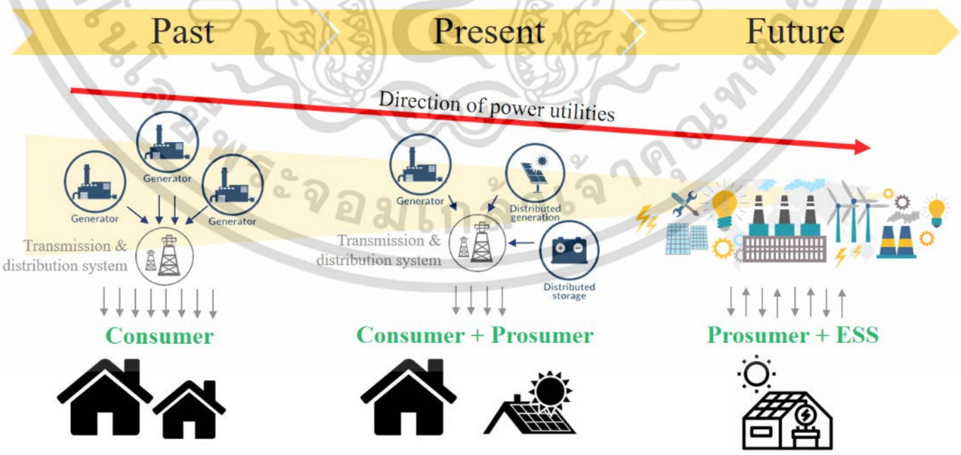

Figure 1.8 The direction of power utilities in the future [22]

Although hydroelectricity (with reservoir) and pumped-storage hydroelectricity are mature technology as shown in Figure 1.9. The technological advancements of the Lithium-based battery energy storage system (Lithium-BESS) are observed the decreasing investment cost and improving round-trip efficiency. Thus, Lithium-BESS have potential benefits [23] in the energy management system that are: (1) to smooth the variable power of wind and solar generation, so-called "hybrid firm", (2) to provide primary reserve when real-time power unbalance, (3) to arbitrage the cheap energy then sell in the expensive period, and so on. The techno-economic feasibility is required to confirm the cost and benefit of Lithium-BESS for load leveling application in the Thailand power system.

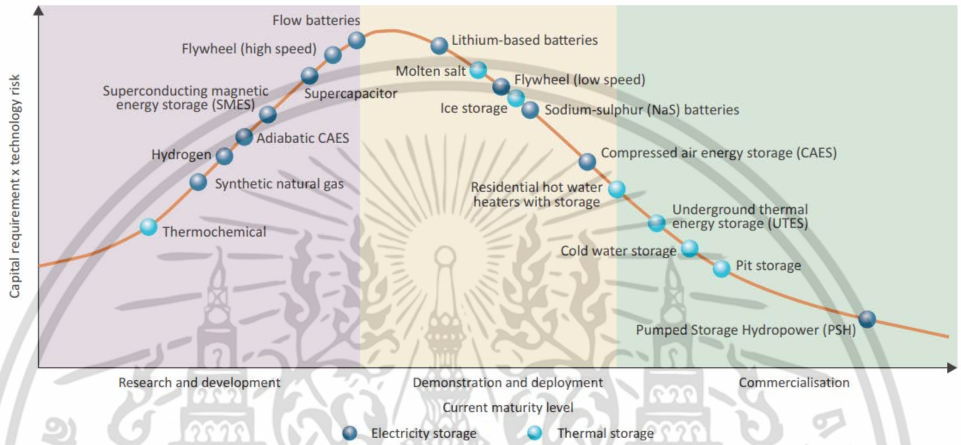

Figure 1.9 Technological advancement of ESSs [24]

1.2.4 Fossil fuel price uncertainty:

PDP2015 focuses on system adequacy, which is modeled as a single nodal generation model, subjecting to the energy policy under certainty parameters [25]. Refer to Thailand's 2019 fuel report [26], the primary fossil fuels are 60.89% natural gas, 39.07% coal-fired, and 0.07% diesel-fired. So, fossil fuel prices influence the generation cost/price of power plants (as seen in Figure 1.10).

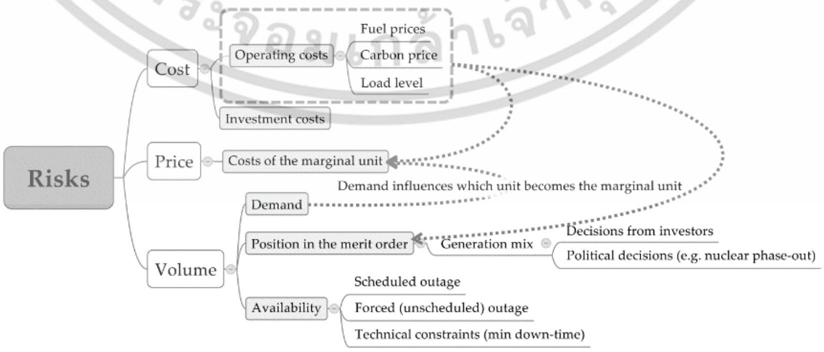

Figure 1.10 Risks classification related power plant investments, adopted from [27]

The traditional long-term contract prices [28] have the advantage of risk-hedging. For instance, long-term take-or-pay contracts have linked the natural gas seller (well-known as Public Company Limited: PTT), and buyer (EGAT) for 15 to 20 years with obligations as a bilateral contract. In the take-or-pay concept, the buyer is required to use a pre-specified minimum quantity whether or not to use it, the seller is required to deliver the annual contract quantity (ACQ). Generally, the price contract is depending on the Dubai crude oil price and restricts the maximum and minimum values. Risks are shared along the gas value chain as the price of the seller and volume of buyers.

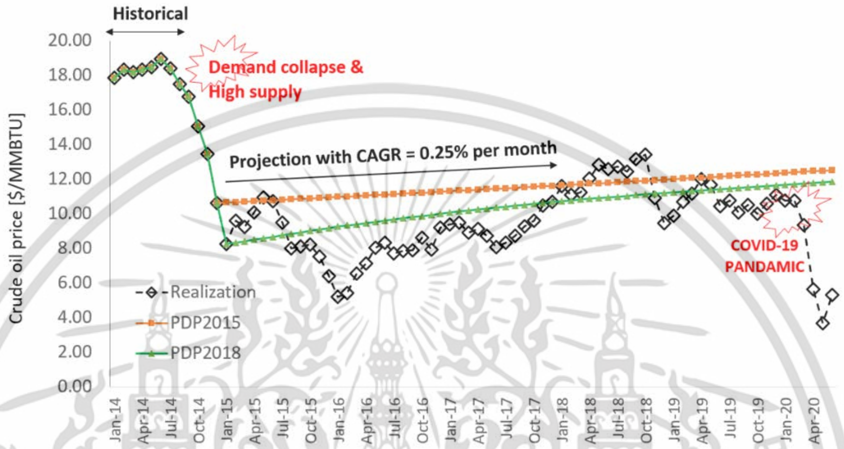

Figure 1.11 Crude oil price of Singapore hub [29]

Unfortunately, an increasing proportion of spot and short-term prices are occurring in the Thailand power system, because the long-term contract prices became increasingly uncompetitive [1.30]. With this reason, spot prices and volatility are becoming the market-driven forward contract. Figure 1.11 reveals the monthly commercial fuel prices of the Singapore spot market. The prices of these fuels perform strong volatility in the short-term (day period) and mean-reverting behavior in medium-term (month- and year-periods). It is important to account for the uncertainty of fuel prices into the optimization model for robust generation investment planning.

1.3 Objectives

Research questions are stated as follows:

a) What are instrumental policies that can mitigate the climate change problem in an efficient cost-benefit way?

b) How to develop the conventional framework to incorporate system flexibility and frequency security for higher variable renewables?

c) How to develop the load-leveling application of Lithium BESS for techno-economics assessment in the optimization model?

d) How to develop the new stochastic optimization considering the fuel risk-hedging for generation expansion planning?

Refer to research questions, this doctoral thesis is intended to fulfill the research gaps are as follows:

Assesses the emission trading/carbon tax scheme

The first issue relates to the instrumental policies for climate change mitigation which comprise: (1) command-and-control, (2) moral suasion, (3) incentives, and so on. The scope of this doctoral thesis focuses on the incentive approaches which value the price of carbon dioxide emission. This can be implemented either through a price-based incentive (e.g. carbon tax scheme) or a quantity-based incentive (e.g. emission trading scheme).

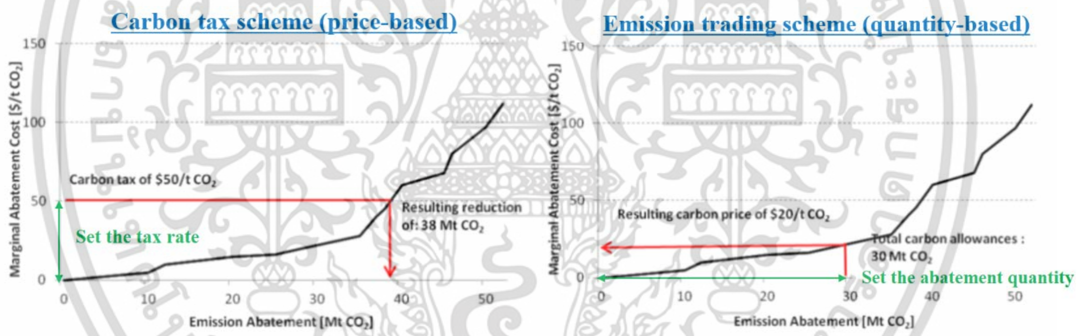

Figure 1.12 MCC curve comparison for a price-based (left) and quatity-based incentives (right), adopted from [1.31]

Theoretically, the price-based incentive and quantity-based incentive have the same outcome which aims to reduce the environmental impacts, i.e. greenhouse gases, harmful gases, and particular matter. The concept is described by using the marginal abatement cost (MAC) curve [31] as shown in Figure 1.12. The policy instruments for climate change mitigation are introduced as follows:

First, the carbon tax scheme is a price-based incentive for climate change policy by setting up the tax rate. In the case of the carbon tax scheme, the carbon cost impacts to high carbon-intensive technology. Therefore, the fuel switching effect could occur in a generation investment portfolio. As a result of the carbon tax scheme, the high-efficiency low emission technologies are invested in the power system.

Last, the emission trading scheme is a quantity-based incentive for climate change policy by the cap-and-trade principle. The CO_2 reduction target is capped (the initial emission allowance). Each firm can emit the CO_2 emission within the CO_2 credit. If the excess emission occurs, each firm can either invest cleaner options or purchase the unused allowance from the carbon market.

This doctoral thesis demonstrates the carbon tax and emission trading schemes for the efficient policy instruments of Thailand's context.

Develops two-stage GEP incorporating flexibility and frequency security

The second issue relates to the generation expansion planning (GEP) framework. The traditional way copes with the adequacy assessment which optimizes the generation portfolio using the net-present value approach. The traditional framework is depicted as shown in Figure 1.13.

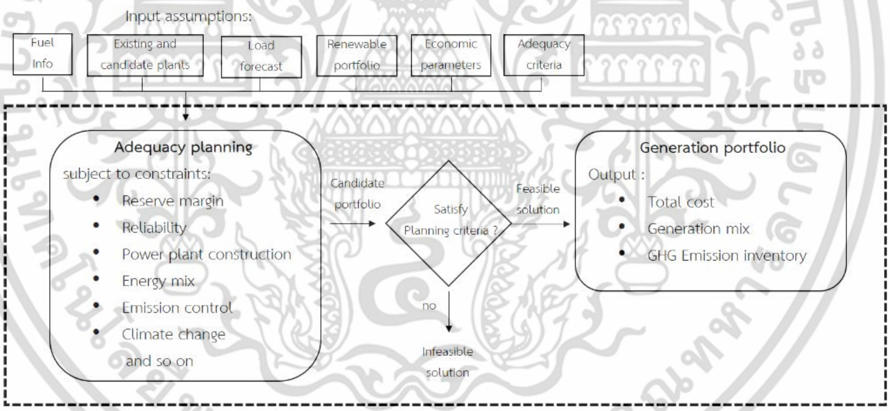

Figure 1.13 Overview of traditional generation expansion planning

Increasing variability and uncertainty caused by VRE call for *frequency security* and *system flexibility*. This doctoral thesis proposes the two-stage GEP framework to enhance flexibility planning in the second stage with the embedded dispatch simulation (with special spinning reserve constraint for inertial frequency response and governor action). **Figure 1.13** visualizes the conceptual idea of the proposed framework. The principles are briefly described are as follows;

- The first stage follows the conventional framework considering generation adequacy. The outcomes of the first stage are considered as candidate plans and are sent to the second stage.
- The second stage evaluates system flexibility with embedded dispatch simulation. The candidate plans that can not satisfy the operational flexibility need to be added the dummy gas turbine and be sent back to first stage planning. Otherwise, the candidate plan is feasible for frequency security and system flexibility

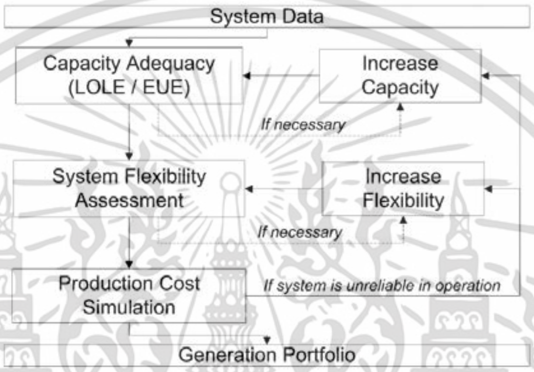

Figure 1.14 Proposed two-stage generation expansion planning framework, adopted from [17]

Enhances probabilistic production simulation incorporating ESS

The third issue relates to the probabilistic production simulation (PPS) enhancement to incorporate the load leveling application of Lithium-BESS. Figure 1.15 describes the relations between GEP and PPS which evaluates the production cost of the generating units of each candidate plan. The original PPS evaluates the expected produced energy based on the equivalent load approach covering only the thermal power plant. The original PPS algorithm is required to improve the operation of ESS due to ESS is playing an increasingly important role in the Thailand power system.

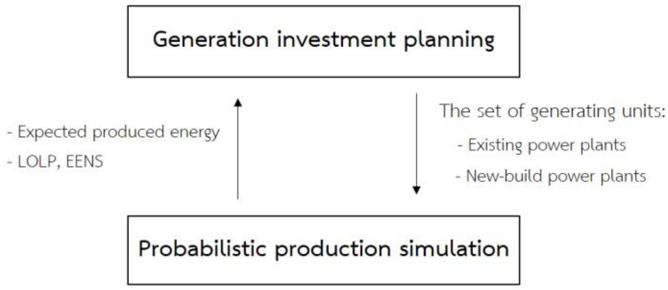

Figure 1.15 Interaction between GEP and PPS

In this doctoral thesis, the PPS has enhanced the load leveling model into the original PPS. Firstly, the valley-filling and the peak-shaving operations are modeled into original PPS to accommodate the charging-load and the discharged-energy of ESS operations, respectively. Lastly, valley-filling mode and peak-shaving mode are combined to form the load leveling operation for ESS operation. The economic operation of ESS is evaluated by using the piecewise cost-benefit curve (PCBC).

Develops an efficient stochastic optimization

The fourth issue relates to the stochastic method to optimize the GEP under uncertainty parameter, e.g. fuel price. Many experts apply many approaches to solve the stochastic optimizations such as sample-average approximation [32], two-stage recourse optimization [33], chance-constrained programming [34], mean-risk value [35], value-at-risk [36] and so on. This thesis improves a new stochastic optimization (as shown in Figure 1.9), so-called "Simheuristics" [37] which are the hybrid approaches based on "Simulation-Based" and "Metaheuristics". The main advantages of the Simheuristics are extending the metaheuristic approach for compromising solution quality and monte-carlo simulation for decision-making under risk and uncertainty.

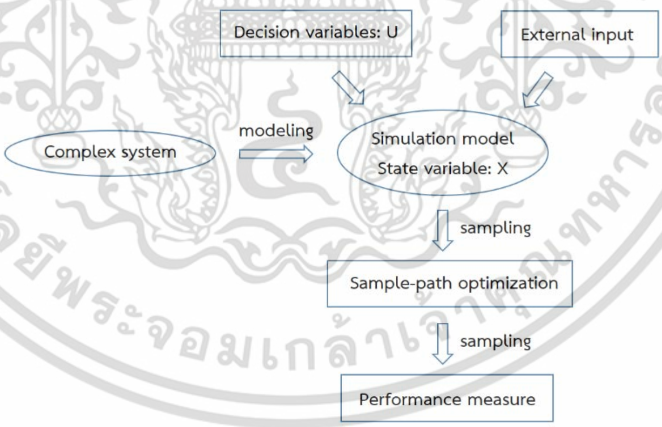

Figure 1.16 Overview of Simheuristic approach, adopted from [37]

However, the simulation time of monte-carlo simulation is computationally expensive optimization based on the *central limit theorem* [38]. For this reason, the quasi monte-carlo simulation using Sobol sequence [39] is applied to expedite the convergence characteristics. Moreover, the efficient metaheuristic method is developed for the Simheuristic approach, so-called "hybrid cuckoo search optimization, and dynamic programming”. Finally, the proposed Simheuristic is used to solve the Thailand generation expansiopn planning considering extended conditions.

1.4 Thesis outline

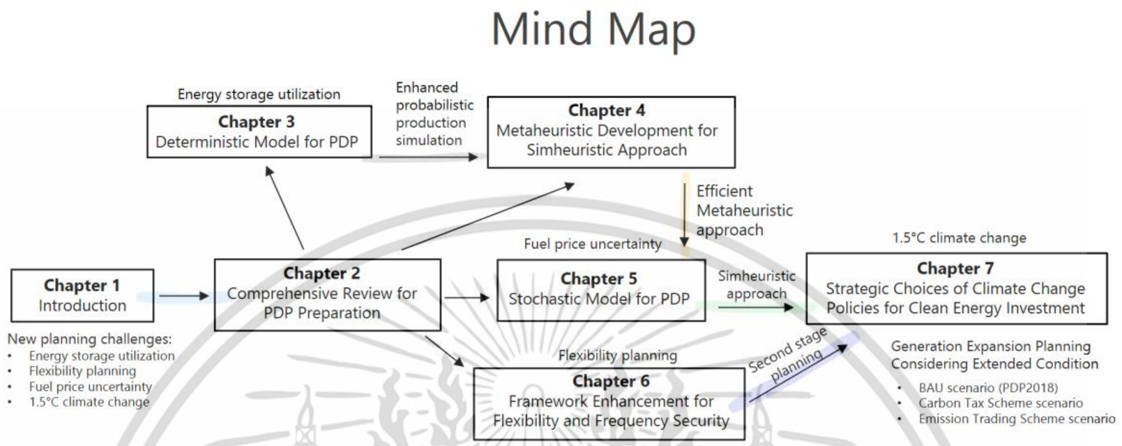

Figure 1.17 Mind map of thesis

The relationship of the content is shown in Figure 1.17, and the details are organized as follows:

Chapter 1 introduces the emerging problem statements of the electricity planning model. Then, the literature is reviewed from the famous journals and conferences. Consequently, the research objective and thesis outline are provided.

Chapter 2 presents the comprehensive reviews for PDP preparation. The important data are emphasized to proceed the preliminary-PDP. This chapter provides in-depth information which the readers can understand as well as specialist, smoothly.

Chapter 3 presents the deterministic model for PDP, categorized as generation expansion planning (GEP) problem in combinatorial optimization. The GEP is observed as the large-scale nonlinear characteristics and is recognized as the NP-hard problem. The objective function (i.e. investment cost, O&M cost, environment cost, external cost, outage cost, and salvage costs) and general constraints (i.e. adequacy, reliability, investment limitation, fuel diversification, pollution control, and carbon dioxide emission) are formulated into the optimization model. Furthermore, the probabilistic production simulation is developed based on the latest journals. Finally, the viability feasibility of Lithium-ion BESS with load-leveling application is conducted for Thailand power system planning.

Chapter 4 presents the metaheuristic method development for the Simheuristic approach. The proposed method is a hybrid approach between the cuckoo search and the dynamic programming, so-called “hybrid CSDP”. The efficient techniques, i.e. feasible search concept, hybrid structure, and memory exploration search are applied because of solution quality and convergence characteristic. The hybrid CSDP is evaluated with classical and metaheuristics methods using the small-scale 1996 Korea’s generation system with a 20-year planning horizon. The simulation results reveal that the hybrid CSDP outperforms the other methods with high solution quality (high probability to find the global optimal solution), good robustness (low standard deviation), and fast convergence characteristics (low iteration to reach optimal solution).

Chapter 5 presents the stochastic model development, namely “Simheuristics” to solve the generation expansion planning considering the uncertainty of fuel price. The main improvements are the aggregated scenario, efficient metaheuristic approach (hybrid CS-DP), and the robust decision making. The proposed method is tested on the Thailand generation system (PDP2015).

Chapter 6 presents the interesting descriptions relating the system flexibility and frequency security. The two-stage planning is proposed to invest the flexible generation into the generation portfolio. The optimization model of operation simulation is provided. The proposed framework is demonstrated in the IEEE RTS system considering 30% solar PV penetration.

Chapter 7 studies generation expansion planning considering the emission trading and carbon tax schemes in Thailand generation system. The related concept and optimization model are discussed. The Simheuristics approach is demonstrated base on the extended conditions of Thailand generation system (official PDP2018).

Chapter 8 gives the conclusion. Furthermore, the research gaps are recommended to continue the research in the future.

Chapter 2

Comprehensive Review for PDP Preparation

Preface

In Chapter 1, we discussed the overview of the Thailand electricity generation system. The important data for the preliminary PDP preparation is shown in Figure 2.1. This chapter is aimed to briefly review the important data that are: (1) energy policies, (2) electricity demand, (3) generation system (4) fuel information (5) economic aspects, and, (6) planning criteria.

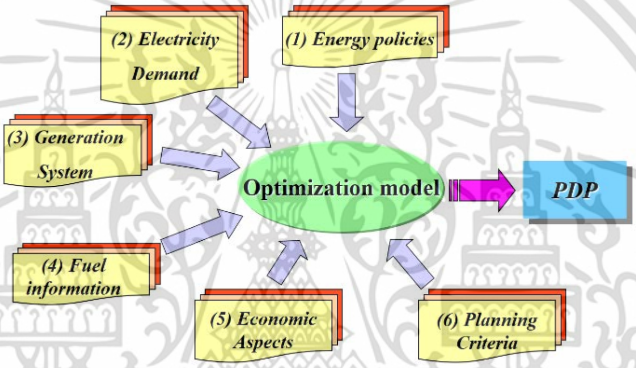

Figure 2.1 Important data of optimization model for preliminary PDP

2.1 Energy policies

A. National policies

In 2015, the ministry of energy had prepared Thailand integrated energy blueprint (TIEB) comprising (1) power development plan, (2) energy efficiency plan [38], (3) alternative energy development plan, (4) gas plan [39] and (5) oil plan [40]. The key assumptions that impact the Thailand generation planning are summarized in Table 2.1.

Table 2.1

Interrelation among PDP and other plans in TIEB

Energy plan	Impact to PDP
Energy efficiency development plan (EEDP)	This plan includes energy efficiency that impacts the future demand (the higher efficiency is, the lower energy require)
Alternative energy development plan (AEDP)	The renewable portfolio aims to share 25% in energy balance (by installed capacity); In this study, renewable generation is considered as ‘negative load’.

Energy plan	Impact to PDP
Gas plan	This plan relates the imported liquefied natural gas (LNG) that require in case of insufficient indigenous gas.
Oil plan	This plan relates to the growth of oil usage in generation capacity

B. Global climate change policy

Pre-2012 period:

In 1979, the first world climate conference recognized climate change as a serious problem. Later, the IPCC was established in 1988. In 1995, the first session of the Conference of the Parties (COP) became the Kyoto protocol [41] which the developed countries (Annex I parties) are committed mitigating the global warming and climate change problem, while the developing countries act as a voluntary basis. Thailand, a country in non-annex I parties (developing country) voluntarily participates in the United Nation framework convention on climate change (UNFCC) to mitigate the global warming problem within below $2C^{\circ}$ temperature rising (comparing to the pre-industrial era).

Target at pre-2020 period:

The first commitment aims to reduce 5% atmospheric emission covering six GHGs in the period 2008-2012. The second commitment tighten the reduction target to 18% in the period 2013-2020. In December 2014, the COP20 was held in Lima, Peru which Thailand government declared the Nationally Appropriate Mitigation Actions (NAMAs) [42] by the statement:

"... Thailand will endeavor, on a voluntary basis, to reduce its GHG emissions in the range of 7 – 20 percent below the business as usual (BAU) in energy and transportation sectors in 2020, subject to the level of international support provided in the form of technology development and transfer, finance, and capacity building from NAMA preparation and implementation. ..."

In 2017, Thailand's GHG emission inventory reports 225.613 million tonnes of kilogram carbon oxide equivalent per year ($MTCO_2e$) or 0.75% of global emission. As the power sector emitted around 28.19% of national emission, the PDP aims to reduce emission intensity [$kgCO_2/kWh$] through the increased renewable portfolio.

Target at post-2020 period:

In 2015, COP21 took place in Paris, France which Thailand government has announced Intended Nationally Determined Contribution (NDC) [43] as a statement:

"... Thailand intends to reduce its greenhouse gas emissions by 20 percent from the projected business-as-usual (BAU) level by 2030. The level of the contribution could increase up to 25 percent, subject to adequate and enhanced through a balanced and ambitious global agreement ..."

To achieve a 2°C climate change policy, all countries cooperate to combat global warming and climate change problems. Ministry of Natural Resources and Environment prepared Thailand's Nationally Determined Contribution Roadmap on Mitigation 2021-2030 [44] to comply with the INDC target.

As described above, Figure 2.2 depicts the baseline emission (emission from BAU) and target emission (reduction from BAU) considering the NAMA and INDC targets.

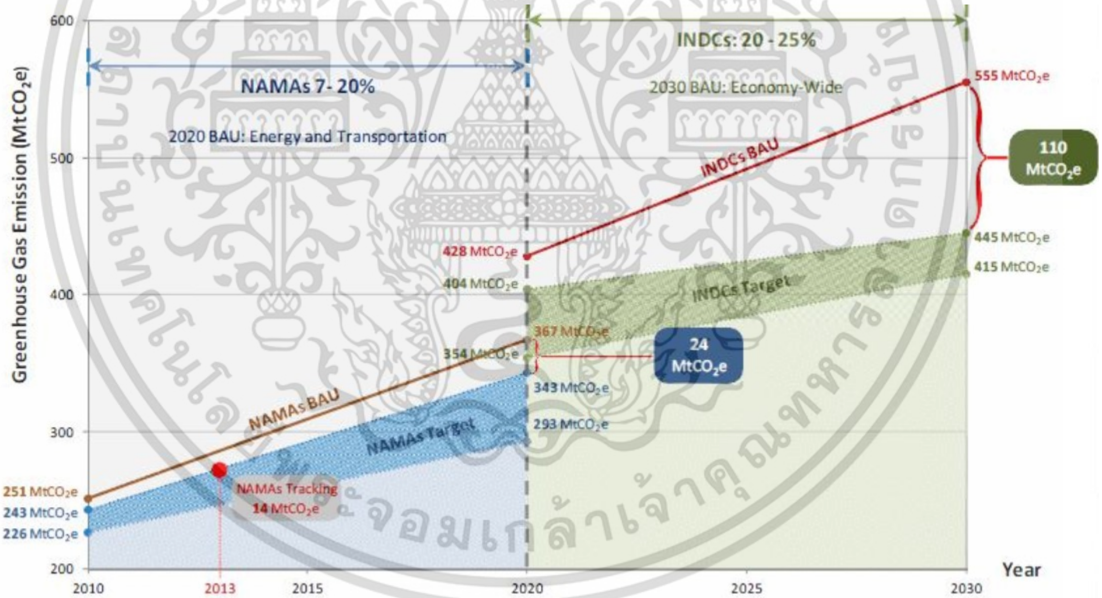

Figure 2.2 NAMA and INDC target as Thailand climate change policy [45]

2.2 Electricity demand

A. Bottom-up structure

Figure 2.3 depicts the bottom-up structure of Thailand national electricity demand based on PDP2015. The net electricity demand is required to supply reliably via transmission system comprising: (1) domestic demand (e.g. MEA's, PEA's and EGAT's customers), and (2) foreign customer (e.g. Lao PDR). Base on Figure 2.3, VSPP generation is behind-the-meter of EGAT's meter; So it is considered as inherent load characteristics. Furthermore, it should be noted that the independent power supply (IPS) is not included in load forecasting.

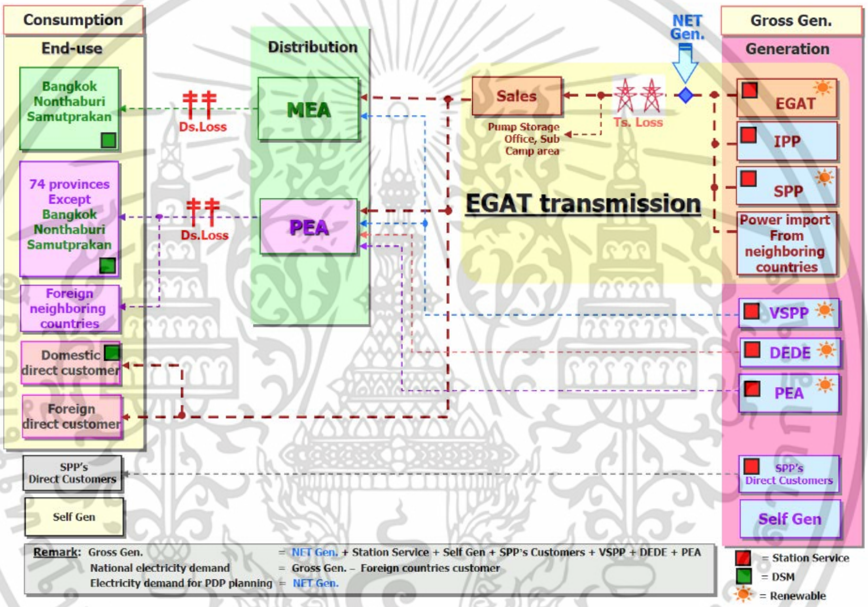

Figure 2.3 Overall Thailand national electricity demand

B. Net load duration curve definition

The power balance of electricity demand (hereafter collectively referred to as an "original load") is shifting towards high variability and uncertainty as increasing variable renewables (i.e. wind, photovoltaics, and small hydroelectricity). The net electricity demand (hereafter collectively referred to as a "net load") is defined as the original load subtracted by the variable generation (coincident time as illustrated in Figure 2.4). The load duration curve (LDC) can be derived by sorting the chronological net load in descending order with losing temporal information [46]. The interesting issue should be pointed out that the risk of overproduction is observed when increasing the penetration of renewables and the operation time of base-load power plants is reduced.

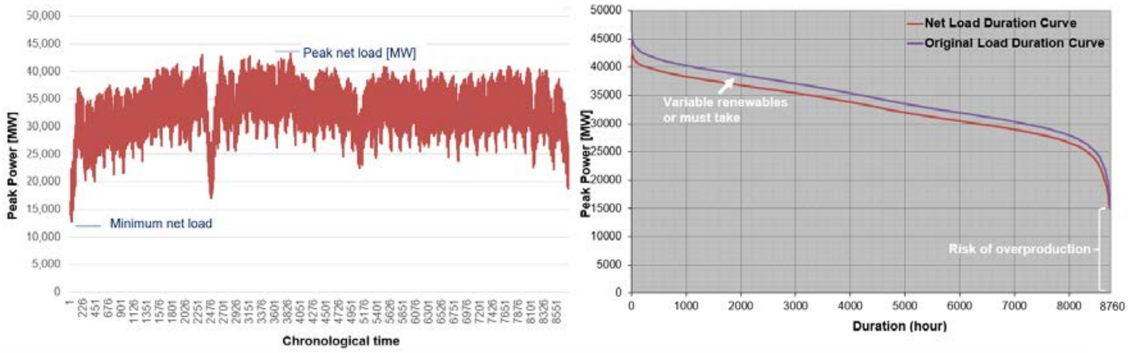

Figure 2.4 Net load duration curve definition

We consider a chronological load with maximum periods mh (normally 8760 hours for hourly load consideration), a set of operating hour $\mathcal{H}$, and system net load $\mathcal{L}$; Mathematical speaking, the net load duration curve function defines any point (h, l) representing a number of hour duration $\mathrm{D} \in \mathbb{R}_+$ (duration that greater or equal to system net load $\mathrm{NL} \in \mathbb{R}$); Let $\mathrm{NL}^{\mathrm{min}}$ and $\mathrm{NL}^{\mathrm{max}}$ be a minimum and maximum system netload, respectively; The total load energy E^{load} [MWh] can be calculated using below equation:

$$E^{\mathrm{load}} = \int_0^{nh} LDC(\mathrm{D})d\mathrm{D} = \text{Area under graph} \qquad (2.1)$$

The LDC can be converted to the probability function $(\mathrm{L}, \mathrm{Prob})$ by divide with nh; Prob means the cumulative probability [fraction].

C. Electricity demand forecast.

According to the time scale, electricity demand can be categorized as (1) long-term load change by load growth, (2) mid-term load change due to seasonality and weather, and (3) short-term load change that varies by the generation of variable renewables [47]. The generation expansion planning considers only the long-term demand forecasting.

From a previous study, the long-term demand forecasting is observed with a strong correlation with the gross domestic product (GDP) under the year-planning horizon [48]. With the above discussion, the GDP growth estimation conducted by the Office of the National Economic and Social Development Board (NESDB) is demonstrated in Table 2.2-2.3. In this thesis, the long-term original demand is adopted from PDP and subtract with the variable renewables (by using actual 2015 SPP and VSPP generation that scaling-up with contracted capacity).

Table 2.2

2015-2024 GDP growth estimation vs net load

Year	2015	2016	2017	2018	2019	2020	2021	2022	2023	2024
GDP	4.0%	4.4%	4.7%	4.3%	4.1%	4.2%	4.2%	4.1%	4.0%	4.1%
%Growth		4.10%	3.31%	3.31%	3.31%	3.31%	3.31%	2.50%	2.50%	2.50%
Net Load	27,307	28,389	29,285	30,213	31,175	32,171	33,204	33,990	34,799	35,630
Original Load	28,465	29,632	30,613	31,627	32,673	33,755	34,872	35,744	36,638	37,553

Table 2.3

2025-2034 GDP growth estimation vs net load

Year	2025	2026	2027	2028	2029	2030	2031	2032	2033	2034
GDP	4.0%	4.0%	4.0%	3.9%	3.8%	3.8%	3.9%	3.8%	3.8%	3.8%
%Growth	2.50%	2.50%	2.10%	2.10%	2.10%	2.10%	2.10%	1.67%	1.67%	1.67%
Net Load	36,484	37,362	38,106	38,867	39,646	40,444	41,259	41,906	42,565	41,931
Original Load	38,492	39,455	40,283	41,129	41,993	42,875	43,775	44,506	45,249	46,005

2.3 Generation systems

The generation system can be categorized by primary resources (i.e., fossil power plant, nuclear power plant, and renewable energy) as shown in Figure 2.5.

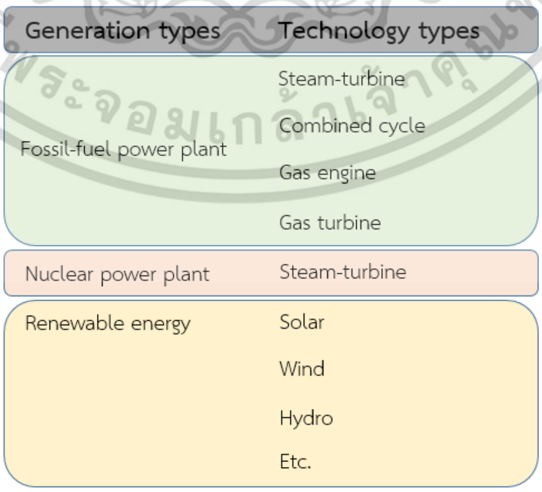

Figure 2.5 Overview generation system categorizes by primary sources

2.3.1 Fossil fuel power plant

A. Steam turbine

Steam turbine (alternatively, called a thermal power plant) follows the principle of the Rankine cycle. The fuel feeding systems for steam turbine are (1) fossil-fired power plant which thermal energy come from fossil fuels (e.g. pulverized coal, natural gas-fired, bunker and so on), and (2) nuclear power plant which thermal energy come from the nuclear reactor; Refer to PDP2015, the five nuclear power plants are chosen to mitigate the carbon dioxide emission. Unfortunately, after the Fukushima disaster [49] occurred, nuclear power plants are postponed. The merit and demerit are summarized as follows;

Merit: Well-known technology and low operating cost compared to other energy resources.

Demerit: The fossil fuels generate the byproduct GHG, e.g. carbon dioxide, harmful substance, e.g. sulfur dioxide which impacts to environment and ecology. Thermal efficiency is around 35% depending on the life usage of the power plant.

B. Combined cycle power plant

A combined-cycle power plant is a hybrid between steam and gas turbine power plants. The configurations are (1) *single shaft* which one gas turbine and one steam turbine are coupled on single shaft synchronous generator; In 2008, the first multi-shaft project was Chana power plant, and (2) *multi-shaft* which have one or more gas turbine and heat recovery steam generator (HRSG) supplying one steam turbine; The multi-shaft technology can be seen in overall Thailand power system. The merit and demerit are summarized as follows;

Merit: conversion efficiency of 50% or more with less capital cost compared to coal-fired steam power plant. Moreover, the combined-cycle power plant is fast cycling than the steam power plant

Demerit: A simple cycle combustion turbine has a lower thermal efficiency than a combined cycle technology.

C. Gas engine

Gas engine or diesel engine follow the principle of the Diesel cycle. The existing diesel engine locates in Mae-hong-son province. The merit and demerit are summarized as follows;

Merit: quick start/stop plant and maturity technology.

Demerit: high operation and maintenance cost.

D. Gas turbine power plant

Gas turbine power plant follows the principle of the Brayton cycle. The natural gas can be for gas turbines. The former gas turbine power plants are located at Sainoi and Nongchok. Nowadays, gas turbines are removed from the Thailand power system because of high operating and maintenance costs. The merit and demerit are summarized as follows;

Merit: The initial conversion efficiency reaches 33% without a warm-up period requirement.

Demerit: A simple cycle combustion turbine has a lower thermal efficiency than a combined cycle technology.

2.3.2 Renewable energy

Refer to AEDP 2015, the bulk renewable energy can be categorized as SPP and distributed renewables can be categorized as VSPP. The overall SPP (with firm-contract) connects to EGAT's transmission system, contradictorily the most VSPP (e.g., bagasse, gas, hydroelectricity, wind, solar, and so on) connect to distribution system which considers as behind-the-meter for national control center. Figure 2.6 shows the aggregated wind and solar PV generation (1 Jan 2015 - 7 Jan 2015).

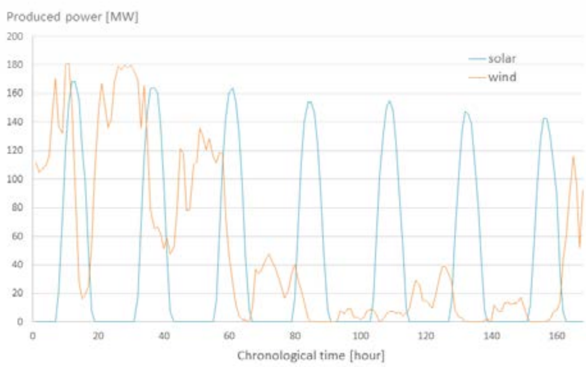

Figure 2.6 Weekly aggregated wind and solar PV generation at 8% penetration

A. Account for VSPP

In this doctoral thesis, the *negative load approach* [50] is applied to cope with the variability and uncertainty of VSPPs. Firstly, the original load is derived from the practical generation profiles (e.g., bagasse, gas, hydroelectricity, wind, solar and so on). Secondly, the renewable profiles are generated by the scaling-up approach (generate by using cumulative capacity and normalized generation profiles). Lastly, the chronological original load is subtracted by renewable profile to form the system net load as equation (2.2):

$$\mathrm{NL}_{\mathrm{net}}^{(h)} = \mathrm{NL}_{\mathrm{org}}^{(h)} - \sum_{g \in \mathcal{G}^{\mathrm{VSPP}}} P_{\mathrm{VSPP}}^{(h)} \qquad \forall h \quad (2.2)$$

where $\mathrm{NL}_{\mathrm{net}}^{(h)}$ represents the system netload [MW] over operating hour h; $\mathrm{NL}_{\mathrm{org}}^{(h)}$ represents original load [MW]; $P_{\mathrm{VSPP}}^{(h)}$ represents the projected VSPPs profiles [MW] associated with a set of VSPPs's units $\mathcal{G}^{\mathrm{VSPP}} \subset \mathcal{G}$.

B. Account for SPP

This doctoral thesis applies a two-state generation model of probabilistic production cost [51] for SPP. The technical terms: dependable capacity, forced outage rate (FOR), and capacity factor are briefly reviewed as follows;

Generally speaking, the dependable capacity is used instead of capacity credit [52] for Thailand generation planning. The dependable capacity [53] is defined as the generating capability [%] that can carry the system load at the specified period (normally system netload). The concept of dependable evaluation can be depicted in Figure 2.7.

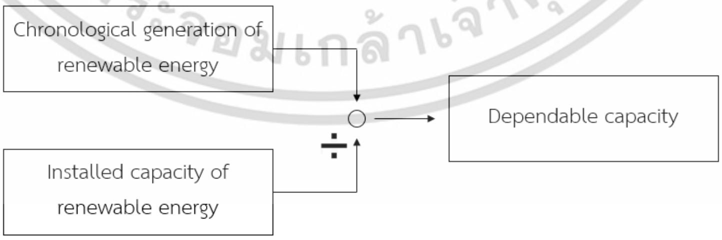

Figure 2.7 Dependable capacity concept

To account uncertainty of renewable energy, the two-state generation model [54-55] is applied. The capacity factor is calculated by using equation (2.3); The forced outage rate (FOR) which is steady-state unavailability is approximated by using the equation (2.4):

$$\%CF = \frac{\text{Annual produced energy}}{\text{Installed capacity}} \times 100 \quad (2.3)$$

$$\text{FOR}=1 - \%\text{CF} \quad (2.4)$$

where $\text{CF} \in \mathbb{R}$ denotes the faction of actually produced energy [MWh]; $FOR \in \mathbb{R}$ and $q \in \mathbb{R}$ represent the forced outage rate [%] and unavailability of generating units, respectively; In this doctoral thesis, the dependable capacity, FOR, and capacity factors are estimated using Equation (2.3-2.4) as following:

Table 2.4

Parameter estimations of non-firm generation profile (year 2559)

Descriptions	Bagasses	Gas	Hydro	Waste	Solar	Wind
Cumulative capacity [MW]	218	280	12.2	12	175	180
Capacity factor	46.8%	46.4%	25.9%	36.7%	23.4%	20.0%
FOR	53.2%	53.6%	74.1%	63.3%	76.6%	80.0%
Dependable capacity	62.6%	40.2%	50.0%	52.2%	84.5%	1.3%

Table 2.5

Parameter estimations of firm generation profile (year 2559)

Descriptions	SPP Gas	SPP Coal	SPP Fuel	Palm	Cane	Husk	Rubber	Wood
Cumulative capacity [MW]	2,666	370	5	8.8	96.8	90.8	20.2	90.5
Capacity factor	74.3%	53.2%	59.0%	85.4%	83.4%	72.8%	92.4%	52.0%
FOR	25.7%	46.8%	41.0%	14.6%	16.6%	27.2%	7.6%	48.0%
Dependable capacity	86.4%	68.4%	92.0%	100%	100%	57.3%	100%	59.6%

2.3.3 Generating cost

A. Fixed O&M and Variable O&M

In general, behavior of generating cost can be categorized as follows (1) **fixed cost** which relates to land, grid connection, power plant construction and so on. This cost is regarded as ‘sunk cost’ which can not be recovered or manageable, (2) **variable cost** which relates to fuel cost, variable O&M and a carbon tax/credit, sometimes is called “avoidable cost” and (3) **quasi-fixed cost** that these costs are mixed between fixed and variable cost, for example, the salary of the employee. Figure 2.8 depicts the different ration of cost in difference technologies. Capital intensive investments are nuclear and coal-fired technologies. The emission-free technologies are wind and solar generations.

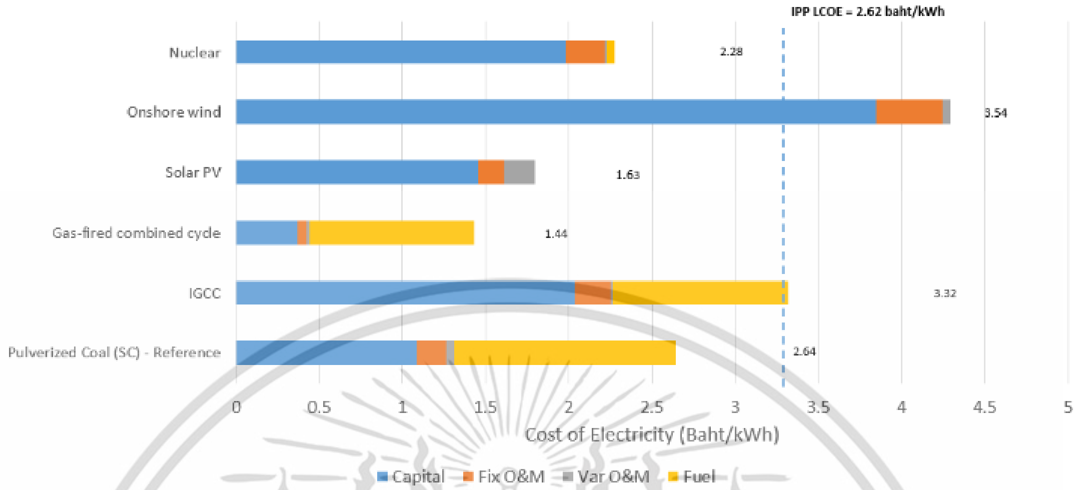

Figure 2.8 The mixture ratio of generating cost in different technologies

Additionally, VOM is defined as the variable operation & maintenance cost that changes depending on produced energy (exclude the fuel cost). FOM is defined as the fixed operation & maintenance cost that is constant and does not depend on the fuel cost. Table 2.6 shows the typical VOM, FOM, and FOR of each technology.

Table 2.6

Typical VOM, FOM, and FOR of each technology

Parameters	Thermal plant	Hydroelectricity	SolarPV & wind
Maintenance	6 / 4 / 2 week	N/A	N/A
FOR	6% /7% /10%	N/A	See section 2.3.2
VOM	25 [$/MWh]	1.452 [$/MWh]	N/A
FOM	1.05 [$/kW/yr]	10 [$/kW/yr]	N/A
Fuel cost	Depend on fuel type	Near zero	Near zero

B. Heat rate and thermal efficiency

To understand the heat rate or performance of power plant [56], the various terminologies are introduced as below;

Input-output curve characteristics measures the actual input heat of generating unit i generating P MW. For good accuracy, the input-ouput characteristics is modeled using a quadratic function.

Incremental heat rate is incremental input heat to change the operating point [MW] to another point. The incremental heat rate of power plants is not always increasing monotonically.

Average heat rate is the ratio of required input heat for a range of operating points.

Thermal efficiency measures the energy conversion of the power plant that uses the primary energy then transforms to the secondary energy (work or heat) in dimensionless.

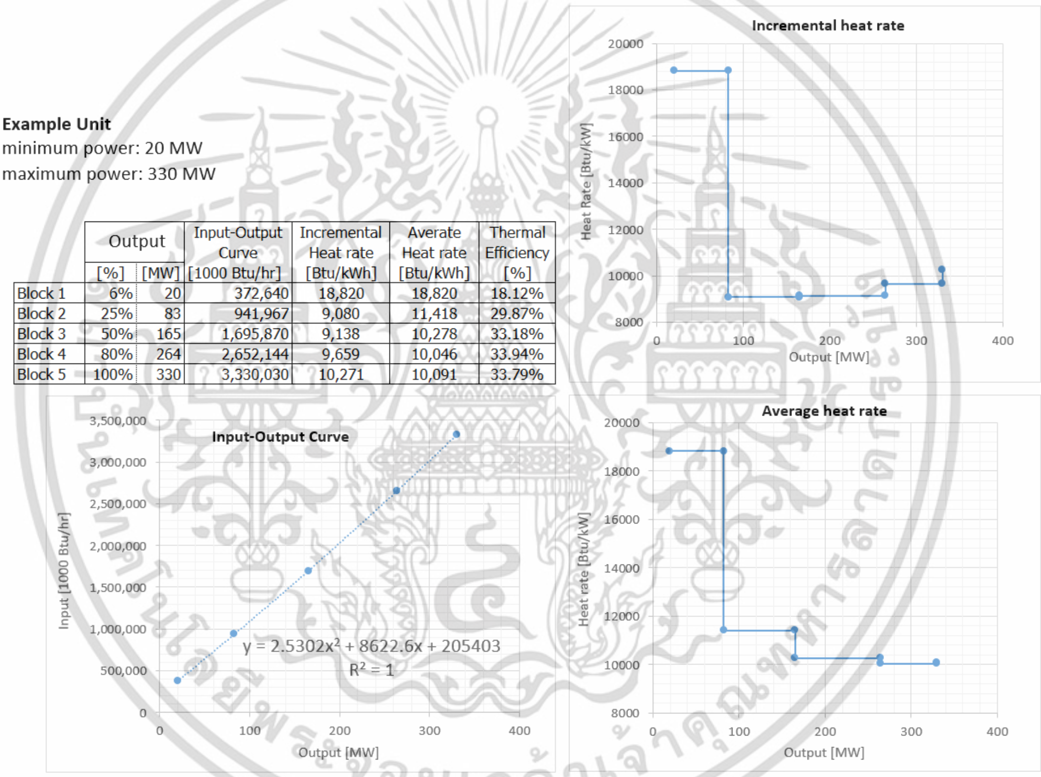

	Output [%]	Output [MW]	Input-Output Curve [1000 Btu/hr]	Incremental Heat rate [Btu/kWh]	Averate Heat rate [Btu/kWh]	Thermal Efficiency [%]
Block 1	6%	20	372,640	18,820	18,820	18.12%
Block 2	25%	83	941,967	9,080	11,418	29.87%
Block 3	50%	165	1,695,870	9,138	10,278	33.18%
Block 4	80%	264	2,652,144	9,659	10,046	33.94%
Block 5	100%	330	3,330,030	10,271	10,091	33.79%

Figure 2.9 Summary of heat rate data

Generally, these terminologies were written in mathematical equations as follows:

$$HR(P_i) = a_1 {P_i}^2 + a_2 P_i + a_3 \tag{2.5}$$

$$IHR(P_i) = \frac{\mathrm{d}}{\mathrm{d}P}\left(a_1 {P_i}^2 + a_2 P_i + a_3\right) = 2a_1 P_i + a_2 \tag{2.6}$$

$$AHR(P_i) = \frac{HR(P_i)}{P_i} \tag{2.7}$$

$$\eta^{th} \sim \frac{3.41}{AHR} \tag{2.8}$$

where equation (2.5) states the approximated input-output characteristics $HR(P_i)$ of generating unit i using quadratic function; equation (2.6) derives the incremental heat rate $IHR(P_i)$; The average heat rate $AHR(P_i)$ is calculated by equation (2.7); The thermal efficiency η^{th} is calculated using equation (2.8) and the relationships of all terms are depicted in Figure 2.9.

Table 2.7

Fuel requirements for electricity generation (As of Sept/2019)

Fuel Type	Electricity [MWh]	Amount	Unit	%Mix by Electricity
Natural gas				60.891%
East	1,751,501.94	12,906,313,379	MMscf.	19.2%
West	1,830,407.99	15,661,951,965	MMscf.	20.0%
Mixed Gas	1,231,539.80	9,984,552,343	MMscf.	13.5%
JDA	634,977.03	4,909,370,878	MMscf.	7.0%
NPO	113,122.60	975,618,949	MMscf.	1.2%
LKB	0	0	MMscf.	0%
Coal				39.073%
Lignite	2,153,802.17	2,064,416	Ton	23.6%
Bituminous	1,414,915.55	547,436	Ton	15.5%
Bunker oil				0%
0.5 % sulphur	0	0	liter	0%
2 % sulphur	0	0	liter	0%
Petroleum				~0.036%
Diesel	3,474.02	832,173	liter	~0.036%

C. Fuel cost

In power system planning, the average heat rates play a role in operating cost approximation. The fuel cost [$/MWh] can be written in mathematics as follows;

$$\text{Fuel Cost} = HR(\blacksquare) \times \text{Fuel Price} \tag{2.9}$$

where equation (2.9) denotes the fuel cost; $HR(\blacksquare)$ denotes the heat rate characteristics (model as a quadratic function) of power plant [MMBTU/MWh]; **Fuel Price** is contracted fuel price of power plant [$/MMBTU];

2.4 Fuel information

The technical information of commercial fuels for electricity generation is that: quantity, the security of supply, heat value, price, volatility and environmental impacts.

A. Quantity and indigenous source

For illustration, Table 2.7 shows the statistical fuel requirement for electricity generation in September 2019. The dependence of natural gas reaches a 60% requirement of total electricity generation. The domestic gas fields comprise of (i) offshore, (ii) onshore, and so on. Source of lignite occupies almost 100% from Mae Moh Mine (shares 62% of total coal consumption). For a planning point of view, the scarcity and abundance of commercial fuel are examined by using the reserve per production ration (R/P ratio) as follows;

$$\text{R/P ratio} = \frac{\text{reserve}}{\text{actual fuel rate per year}} \tag{2.10}$$

where equation (2.9) provides the domestic reserve [dimensionless] of fossil fuels; **reserve** denotes proved reserve [57] for natural gas or economic reserve [58] for lignite; Actual fuel rate and global reserves are derived from the annual report [59].

Table 2.8

Domestic fuel reserves at end of 2018

Descriptions	Domestic production	Domestic reserves	Domestic R/P ratio	Global reserves
Crude oil	47.26 [MMbbl/year]	136.88 [MMbbl]	2.9 [year]	50 [year]
Natural gas	1,105 Bcf/year	6,050 Bcf	5.5 [Year]	50.9 [year]
Coal	14,443 [thousand tonne]	825,000 [thousand tonne]	57 [Year]	132 [year]
Uranium	-	-	-	85 [year]

As the next 6 years, the depletion of proved natural reserves reveals the insecurity of supply. With this reason, the imported LNG via the floating storage and regasification unit (FSRU) or LNG receiving terminal is the solutions for the natural gas supply. The increasing of the imported LNG creates a higher electricity tariff and vulnerable problem [54].

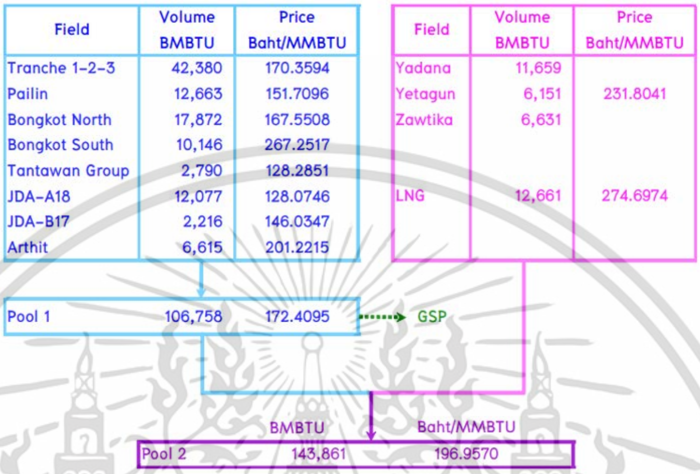

Figure 2.10 Example calculation of natural gas pooled price.

B. Pool prices for natural gas

Thailand's natural gas transmission is depicted in Figure 2.11. The PTT undertakes transportation and supply for electricity generation. The gas pricing concept is categorized as pool price#1 for the gas field produced from the gulf of Thailand and JDA, and pool price#2 for the gas field purchased natural gas from Myanmar and imported LNG. To calculate the pooled price, the weighted average cost approach is applied as below equation;

$$\mathrm{NG\#2} = \mathrm{NG\#1} \times \mathrm{Vol}^{\mathrm{gulf}} + \mathrm{NG}^{\mathrm{Myanmar}} \times \mathrm{Vol}^{\mathrm{Myanmar}} + \mathrm{NG}^{\mathrm{LNG}} \times \mathrm{Vol}^{\mathrm{LNG}} \quad (2.11)$$

where equation (2.11) describes the pooled natural gas price; $\mathrm{NG\#1}$, $\mathrm{NG}^{\mathrm{Myanmar}}$ and $\mathrm{NG}^{\mathrm{LNG}}$ are representing the wellhead prices of first pooled price, Myanmar and LNG, respectively; $\mathrm{Vol}^{\mathrm{gulf}}$, $\mathrm{Vol}^{\mathrm{Myanmar}}$ and $\mathrm{Vol}^{\mathrm{LNG}}$ are representing the natural gas volumes of the gulf of Thailand, Myanmar and LNG, respectively. Generally, the wellhead price is declared in the long-term contract driven by constant price [$/MMBTU], Dubai crude oil price [$/barrel], exchange rate [baht/$], consumer price index, and the USA producer price index for machinery and equipment: oil field and gas machinery.

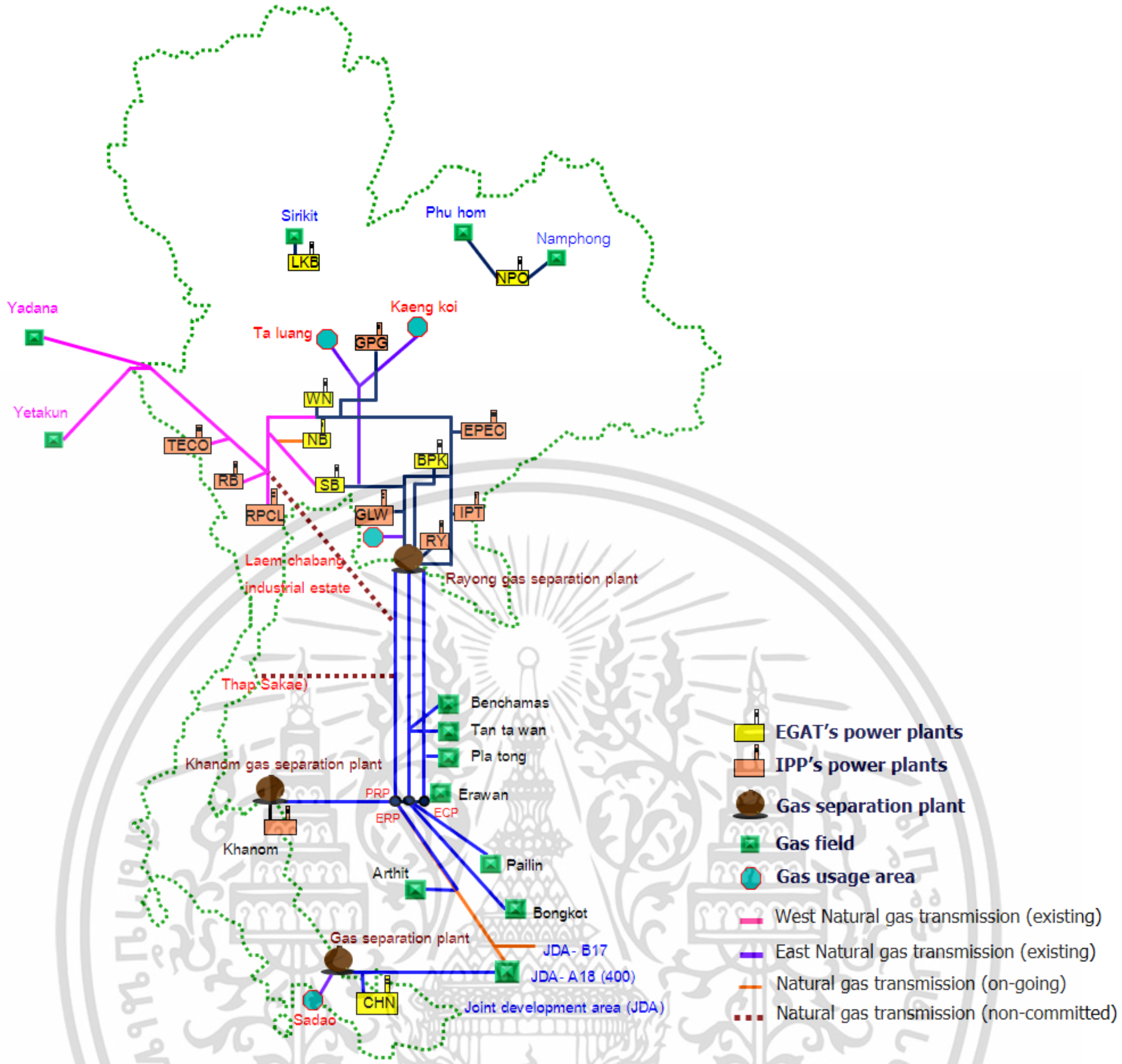

Figure 2.11 Existing natural gas transmission for electricity generation (as of 2010)

C. Heat value & Carbon dioxide emission

The greenhouse gases (GHGs) are any gases in the atmosphere which absorb and re-emits heat from The Sun. To calculate the emission rate [$\mathrm{kgCO_2/MWh}$] of the power plant, the calculation can be shown as below equation;

$$\text{Emission rate} = \frac{\text{Heat rate } \times \text{Emission factor}}{\text{Heat value}} \tag{2.12}$$

where equation (2.12) states the emission rate calculation; **Heat rate** represents the average heat rate [MMBTU/MWh] of power plant; **Emission factor** denotes emission factor [tonne $\mathrm{kgCO_2}$/TJ] which derives from IPCC guideline for national greenhouse inventory; **Heat value** denotes the net calorific value [MJ/unit] of each unit; η^{th} is the practical thermal efficiency of power plant [%].

Table 2.9

Emission rate of fossil fuels

Greenhouse gas	Chamical formula	100-year GWP	Source	Application
Carbondioxide	CO_2	1	Natural	Human respiration
Methane	CH_4	21	Natural	Baterial activity
Nitrous oxide	N_2O	310	Natural	Fertilizers wastes
Sulphur hexafluoride	SF_6	23,900	Man-made	Gaseous insulation for high voltage

Table 2.10

100-year global warming potential based on fifth assessment report

Fuel Type	Unit	2006 IPCC Guidelines			This thesis		
		Heat value [MJ/Unit]	Emission facor [tCO2/TJ]	Emission Per unit [kgCO_2/unit]	Heat rate [MMBTU /MWh]	Heat value [MMBTU /Unit]	Emission rate [kgCO_2 /MWh]
Natural gas (dry)	scf.	1.02	54.30	0.0554	745	967	426.92
Lignite	Ton	10,470	90.90	951.723	10.12	9,924	970.56
Bituminous	Ton	26,370	89.50	2,360.12	7.25	24,994	684.60
Bunker	liter	39.77	75.50	3.0026	9.46	3,7695	753.55
Diesel	liter	36.42	72.60	2.6441	9.42	3,4519	721.61

It's worth comparing the effect of different GHGs in the same unit, the global warming potential (GWP) was developed [60]. The GWP describes both absorbed radiative efficiency and how long GHGs stay in the atmosphere. Table 2.10 shows the 100-year time horizon global warming potential e.g., CO_2, CH_4 and N_2O and so on. This data is derived from the sixth assessment report of IPCC [61].

2.5 Economic aspects

2.5.1 Least-cost planning

Least-cost planning (cost-benefit analysis) is a standard planning method to evaluate the optimal generation portfolio (e.g. cost minimization) among feasible alternatives. The technical terms: net present value (NPV) and price escalation are introduced are as follows:

A. Net present value

The generation expansion planning using the net present value (NPV) is a concept to calculate all the costs (e.g. investment cost, O&M cost, outage cost, and so on) and return (salvage or residual value) taking into the account of the time value of money. The candidate plan that has the smallest NPV indicates the optimal plan for least-cost planning under the pre-defined objective function. The net present value function $NPV^{(t)}(\blacksquare)$ converting the future value to referenced value can be stated as follows;

$$NPV^{(t)}(\blacksquare) = \frac{1}{\left(1+\delta^{d}\right)^{t}}\text{cost/benefit} \tag{2.13}$$

where **cost/benefit** represent any costs (positive value) and return (negative value) in the monetary unit; δ^d denotes the discounted rate which relates to the weight average cost of capital (WACC); $\boldsymbol{t}$ is time period that discounts the cost to the reference year.

B. Price escalation

Normally, price escalation refers to the price adjustment due to some factors, e.g. inflation, customer price index, and so on. The price escalation can be stated as below.

$$\text{PV}^{(t+1)} = \text{PV}^{(t)} \times (1+\delta^{e})^{t} \tag{2.14}$$

where $\mathbf{PV}^{(t)}$ represent the present value [monetary unit] over time horizon t; δ^e denotes escalation rate [%];

2.5.2 Cost metrics

A. Levelized cost

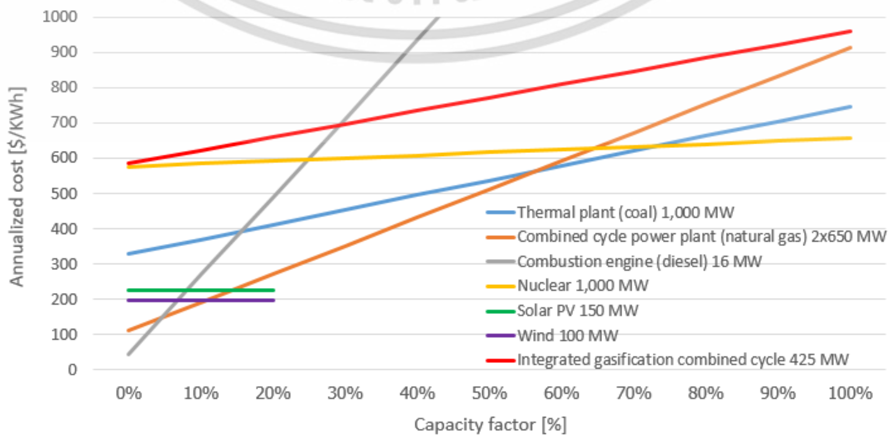

Figure 2.12 Annualized cost at the different capacity factor for PDP2015

The cost metric, so-called *'Levelized cost of electricity: LCOE'* or *'Levelized energy cost:* is introduced for generating cost comparison in different technologies. Figure 2.12 depicts the annualization of fixed and variable costs at pre-specific capacity factor $\%\mathrm{CF}$ per generating electricity [$/MWh]. This concept is calculated using the following formula:

$$\mathrm{LCOE@}\ \%\mathrm{CF} = \text{Fixed cost} + \text{Variable cost} \tag{2.15}$$

$$= \mathrm{CRF}^{\mathrm{Life}}(c^{Invest} + c^{FOM}) + \mathrm{CRF}^{\mathrm{Life}}(\, c^{VOM} + c^{Fuel}\,) \times 8760 \times \%\mathrm{CF} \tag{2.16}$$

In which,

$$\mathrm{CRF}^{\mathrm{Life}}(\blacksquare) = \text{Present cost}\ \frac{(1+\delta^{d})^{\mathrm{Life}}}{(1+\delta^{d})^{\mathrm{Life}} - 1} \tag{2.17}$$

where $\mathrm{CRF}^{\mathrm{Life}}(\blacksquare)$ denotes capital recovery function to annualized costs [$/MWh]; c^{Invest} denotes investment cost [$/kW]; c^{FOM} denotes fixed O&M costs [$/kW/year]; c^{VOM} represents O&M cost [$/kWh]; c^{Fuel} represents fuel cost [$/kWh]; $\mathbf{Life}$ denotes useful life of each power plant [year].

B. Screening curve

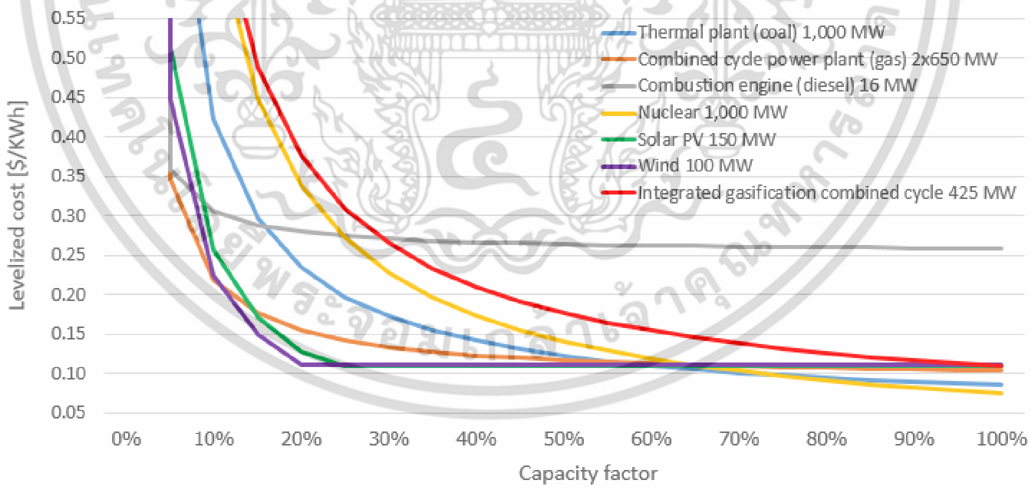

Figure 2.13 Screening curve of candidate options for PDP2015

Figure 2.13 illustrates the simplest approach to evaluate the candidate options in terms of investment and operating costs, the so-called 'Screening curve'. The screening curve is a function of the capacity factor $\%\mathrm{CF}$ and the annualized cost $\mathbf{LCOE}$ are as follow;

$$\text{Screening curve(\%CF, LCOE)} = \frac{\text{Annualized cost}}{\text{Produced energy}} \quad (2.18)$$

$$= \frac{\text{CRF}(c^{Invest} + c^{FOM})}{8760 \times \%\text{CF}} + \text{CRF}(\, c^{VOM} + c^{Fuel}\,) \quad (2.19)$$

where the annualized fixed costs are obtained from the investment cost c^{Invest} and fixed O&M costs c^{FOM} vai the capital recovery function; Parallelly, the annualized variable costs c^{VOM} are derived from the variable O&M cost and fuel cost c^{Fuel} via the capital recovery function.

C. Incremental abatement cost

The abatement cost is the true cost to reduce the negative impacts on the environment, e.g. acid rain from sulfur dioxide emission, global warming and climate change problems from GHGs, and so on. Therefore, the incremental abatement cost of each scenario is compared to the BAU plan. The simplest equation to calculate the incremental abatement cost [\$/ton-kgCO_2] is shown as follows;

$$\text{Incremental abatement cost} = \frac{\text{Cost difference}}{CO_2\text{reduction}} \quad (2.20)$$

$$= \frac{\text{Cost}^{\text{ BAU}} - \text{Cost}^{\text{ Scenario}}}{\text{CO}_2^{\text{BAU}} - \text{CO}_2^{\text{scenario}}} \quad (2.21)$$

where $\text{Cost}^{\text{ BAU}}$ denotes the cost of electricity generation of BAU scenario; $\text{Cost}^{\text{ Scenario}}$ denotes any scenario planning of electricity generation; CO_2^{BAU} is carbon dioxide emission [ton-kgCO_2] of BAU scenario; $\text{CO}_2^{\text{scenario}}$ is carbon dioxide emission [ton-kgCO_2] of any scenario.

2.6 Planning criteria

The planning criteria for generation planning are as follows:

○ *Reserve margin* is a deterministic approach for measuring the adequacy of generating units to supply the electricity demand taking into account the uncertainty of generation outage. Based on Thailand generation planning criteria, the maximum reserve margin R_{max} is required at least 15%. The reserve margin can be stated as the equation are as follows:

$$\text{Installed capacity } \geq (\text{Original Load} - \text{VRE}) + \text{Reserve} \quad (2.22)$$

$$\sum_{g=1}^{G}[Cap_g] \geq NL^{(t)} \times (1 + \mathrm{RM}^{\min}) \qquad \forall t, \quad (2.23)$$

where Cap_g denotes the installed capacity of generating unit g at the planning horizon t; $NL^{(t)}$ represents the system maximum net load ($NL^{(t)} = \mathrm{argmax}_{h\in 8760}\{NL_{net}^{(h)}\}$) at the planning horizon t; $\mathrm{RM}^{\min}$ denotes minimum planning reserve margin [%].

- *LOLP* is a probabilistic approach to measure the loss-of-load probability of customer service. Base on Thailand planning criteria, the LOLP criterion is set 0.00274 or 24 hours per year, approximately.
- *Energy mix* is deterministic criteria to measure both securities of supply and fuel dependence. Table 2.11 shows the fuel diversification trend based on PDP2015.

Table 2.11

Fuel diversification based on PDP2015 (by energy)

Year	Type of generating technologies					
	Foreign hydroelectricity	Lignite/Coal	Renewables	Natural gas	Nuclear	Diesel, Fuel oil
2015	6%	20%	9%	64%	-	0.8%
2021	8%	27%	18%	47%	-	0.1%
2026	8%	23%	18%	51%	-	0.1%
2031	13%	20%	19%	48%	-	0.1%
2036	15%	23%	20%	37%	5%	0.1%

- *NAMA & INDC* represent global warming and climate problems. As described in section 1.2.1, the NAMA target aims to reduce the 7-20% carbon dioxide emission in the energy and transportation segment from the BAU scenario (2010 emission is referenced as baseline). Moreover, the INDC aims to reduce the 20-25% carbon dioxide emission in economy-wide. Figure 2.14 summarises the target reduction of Thailand's NAMA/INDC.

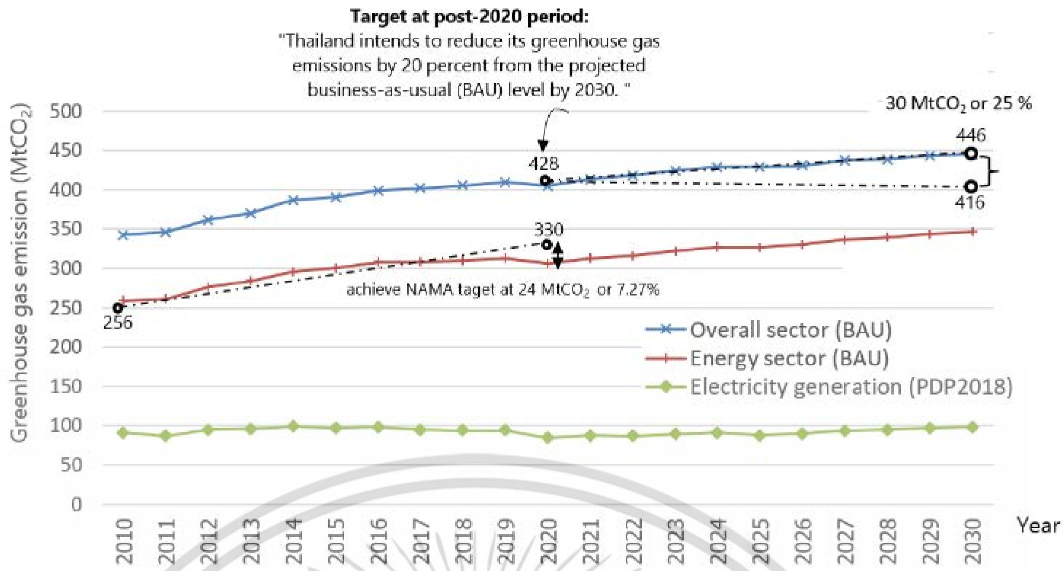

Figure 2.14 Required reduction of carbon dioxide emission considering NAMA/INDC policies

2.7 Example calculation 1: Overnight cost calculation

Descriptions

To demonstrates the overnight investment cost calculation. In this example calculation, the economic and power plant parameters are provided in Table 2.12.

Table 2.12

Coal-fired thermal power plant based on PDP2018

Economic parameters		Power plant performance	
Base year	Beginning 2018	Contract capacity [MW]	1,000
Discount rate	10%	Commissioning year	Ending 2023
Construction escalation rate	3%	Plant life [year]	30
Interest during construction rate	7%	Hear rate [MMBTU/MWh]	8,903
Percent of O&M to total capital cost	4%	Base cost (USD/kW)	2,101
Percent of FOM to total O&M	85%	Expenditure profile [%]	17%, 25%, 25%, 24%, 9%
Percent of VOM to total O&M	15%	Normal plant factor [%]	85%
FOM escalation rate	8%	Fuel Cost [USD/MMBTU]	4.26
VOM escalation rate	3%		
Fuel escalation rate	1%		

Step1: Calculates the Levelized cost of capital. First, calculate the annual base cost follow the given expenditure profile. The future cost is calculated using Eq. (2.14). The interest during construction (IDC) is calculated using Eq. (2.15).

$$\mathrm{IDC}_t = \left\{\frac{FV}{2} + \sum_{t=1}^{t-1} FV + \sum_{t=1}^{t-1} \mathrm{IDC}_t\right\} \times \%\mathrm{IDC} \quad (2.24)$$

where $\%\mathrm{IDC}$ stands for IDC rate; IDC_t is an interest during construction at year t. The spreadsheet of overnight investment cost for the 1,000-MW coal-fired power plant is shown in Table 2.13. The annualized capital cost is calculated using Eq. (2.16) are as follows;

$$\text{Annualized capital cost } = \sum_{t=1}^{Life} \frac{cost \times \delta^d}{1-(1+\delta^d)^{-t}} = 197.6\ million\ \$ \quad (2.25)$$

Table 2.13

The overnight investment cost for 1,000-MW coal-fired power plant

Year	Expenditure profile	Expenditure	Future cost	Accumulate	IDC	Accumulate IDC	Total
1	17%	250.0	250.0	0.0	8.8	0	258.8
2	25%	367.7	378.7	250.0	31.4	8.8	410.1
3	25%	367.7	390.1	628.7	60.5	40.1	450.5
4	24%	353.0	385.7	1,018.8	91.9	100.6	477.6
5	9%	132.4	149.0	1404.5	117.0	192.4	266.0
	100%	1,470.7	1,553.5				1862.9

Step2: Calculates the annualized costs of FOM, VOM, and fuel. Table 2.14 breakdowns the detailed calculation is as follows;

Table 2.14

Example calculation of annualized cost of VOM, FOM and fuel costs

Year	FOM [milliom \$]	VOM [milliom \$]	Fuel [\$/kw]
Base year	5.93	5.93	0.038
1st year	6.11	6.11	0.038
2nd year	6.29	6.29	0.039
3rd year	6.48	6.48	0.039

Year	FOM [milliom $]	VOM [milliom $]	Fuel [$/kw]
...	...	...	...
30th year	14.39	14.39	0.051

Use equation 2.13 to convert the future cost of FOM, VOM, and fuel cost to present value. The present value of FOM, VOM, and fuel cost are 200.26 million$, 75.1 million$ and 0.393 million$, respectively.

Again, use equation 2.16 to calculate the annualized cost of FOM, VOM, and fuel cost. The annualized costs of FOM, VOM, and fuel cost are 21.24 million$, 7.97 million$ and 0.042 million$, respectively.

The per unit of annualized cost are calculated are the following:

$$\text{annualized cost of FOM} = \frac{\text{annualized cost} \times 1000}{\text{contract capacity}} = \frac{21.24 \times 1000}{700} = 30.35 \text{ \$/kW}$$

$$\text{annualized cost of VOM} = \frac{\text{annualized cost} \times 1000}{\text{contract capacity} \times 8760 \times \%\text{CF}} = \frac{7.97 \times 1000}{700 \times 8760 \times 85\%} = 0.00153 \text{ \$/kWh}$$

$$\text{annualized cost of fuel} = 0.042 \text{ \$/kWh}$$

Figure 2.15 illustrate the production cost of example calculation.

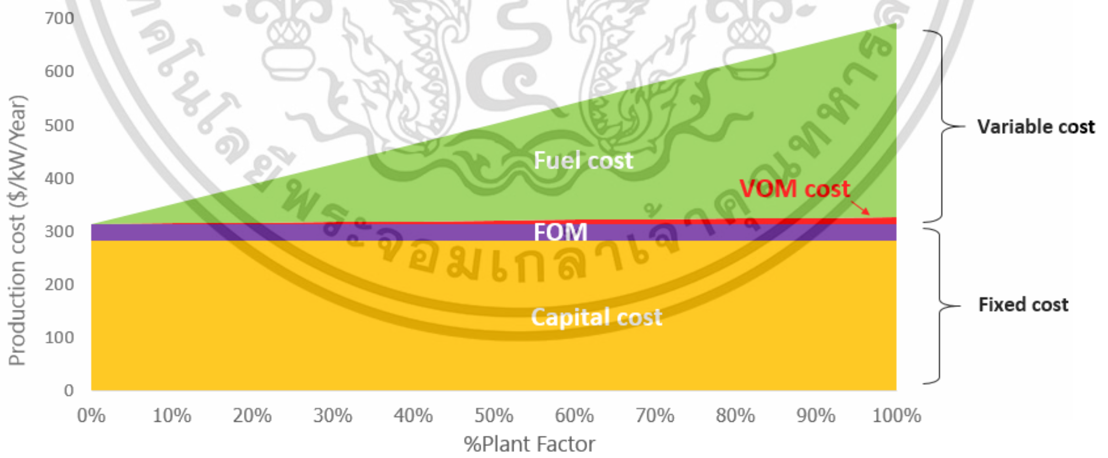

Figure 2.15 The production cost of a 1,000-MW coal-fired power plant

Chapter 3

Deterministic Model for PDP

The important assumptions and data are reviewed for preliminary PDP preparation in Chapter 2. In this chapter, the important processes, namely, generation expansion planning (GEP) and probabilistic production simulation (PPS) are discussed as insight-details. Figure 3.1 visualizes the relationship between the input assumptions and the optimization model. The GEP is a process to invest the new generating units for the generation fleets; the existing and new generating units are proceeded into the PPS to obtain the expected produced energy (for production cost calculation) and reliability indices (for system constraints of optimization model).

In the first section, the GEP is introduced to solve the deterministic model for PDP under certainty parameters. The mathematical equation states the cost models: (1) investment cost, (2) availability payment, (3) energy payment, (4) external cost, (5) outage cost, (6) decommissioning cost, and (7) salvage cost. The planning constraints comprise of that: (1) generation adequacy, (2) generating system reliability, (3) investment limitation, (4) fuel diversification, and (5) carbon emission target.

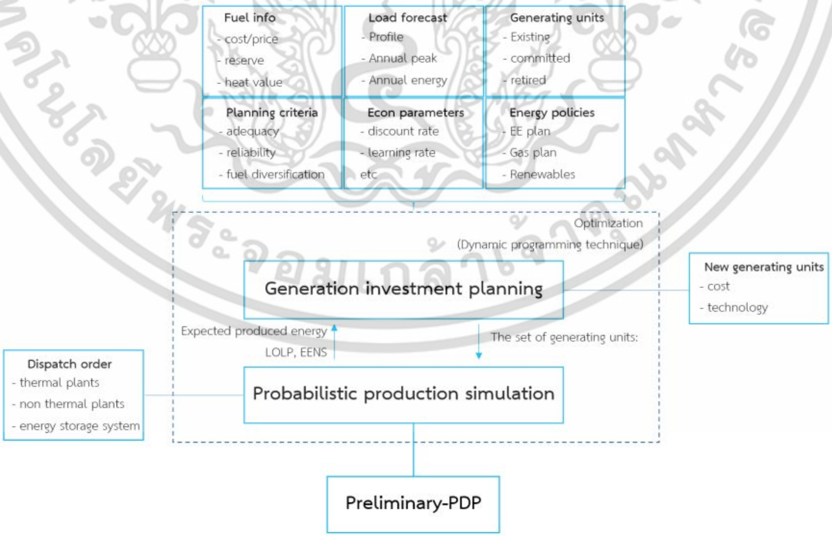

Figure 3.1 Overview of a deterministic model for preliminary-PDP preparation

In the second section, the PPS considering the generation outage is introduced to simulate the expected produced energy of existing and new generating units in each candidate plan. The reliability indices such as EENS and LOLP, are derived based on the energy equivalent function (EEF). The benefits of the EEF are accuracy and computational time. Unfortunately, the drawbacks of traditional PPS can not handle the operation of hydroelectricity and energy storage system (ESS) as well. The development of the PPS framework is necessary for system planning.

In the third section, the operation models: valley-filling and peak-shaving are enhanced into the traditional PPS. This enhancement yields the load-leveling operation for ESS which optimal operation is approximated using piece-wise benefit/cost curve analysis. Finally, the study case demonstrates the load leveling application of Lithium-based battery energy storage systems on the Thailand generation system.

3.1 General descriptions

3.1.1 Single-stage GEP problem

The single-stage GEP problem can be modeled as the combinatorial (discrete) optimization [62] as follows;

$$\text{minimization} \quad z(U) \tag{3.1}$$

$$\text{subject to} \quad U \in \Omega \tag{3.2}$$

The function $z : \mathbb{Z}_{\geq 0}^{nn} \rightarrow \mathbb{R}$ is an objective function or real-valued cost which aims to be optimized. The vector U represent a column-vector of independent decision variables: $U = [u_1, u_2, .., u_{nn}]^{\intercal}$ over each decision space $d \in \mathcal{D}$. In generation expansion planning, the decision variable denotes the non-negative integer variables $\mathbb{Z}_{\geq 0}$ of new-built power plants; decision space $\mathcal{D}$ means the maximum number to construct the new power plants of each candidate option over the planning horizon; $\mathcal{T}$ denotes the set of the planning horizon $\mathcal{T} = \{1,2, .. \mathrm{T}\}$ with the study period T. In addition, the search space $\mathbb{S}$ of combinatorial optimization is defined as:

$$\mathbb{S} = \{\mathcal{D}_1 \times \mathcal{D}_2 \times \ldots \times \mathcal{D}_{nn}\} \tag{3.3}$$

The *constraint set* $\mho = \{U : \phi(U) = 0, \psi(U) \leq 0\}$ where $\phi(\boldsymbol{U})$ represents equality constraint, e.g. state equation and so on, $\psi(U)$ represents inequality constraint, e.g. generating reliability, generation adequacy and so on. The global optimal solution U^* is defined as follows:

$$U^* \in \mathcal{F} \subseteq \mathbb{S} \tag{3.4}$$

where optimal objective function is $z(U^*) < z(U)$ for all $U \in \Omega \setminus \{U^*\}$ over feasible solutions $\mathcal{F}$ (satisfying all constraints).

The relations among all column vectors of an existing generating unit X, new-built power plants U, committed power plants C and retired power plants R can be defined as follows:

$$X = U + C - R \tag{3.5}$$

In which,

$$X_{g\in\mathcal{G}^E} = \begin{bmatrix} x_1 \\ x_2 \\ \dots \\ x_{ng} \end{bmatrix} \quad U_{g\in\mathcal{G}^N} = \begin{bmatrix} u_1 \\ u_2 \\ \dots \\ u_{nn} \end{bmatrix} \quad C_{g\in\mathcal{G}^C} = \begin{bmatrix} c_1 \\ c_2 \\ \dots \\ c_{nc} \end{bmatrix} \quad R_{g\in\mathcal{G}^R} = \begin{bmatrix} r_1 \\ r_2 \\ \dots \\ r_{nr} \end{bmatrix} \tag{3.6}$$

Let $\mathcal{G}^E$, $\mathcal{G}^N$, $\mathcal{G}^C$and $\mathcal{G}^R$ be the sets of a new candidate, existing, committed and retired generating units, respectively; The set of all generating units imply $\mathcal{G} = \mathcal{G}^E \cup \mathcal{G}^N \cup \mathcal{G}^C - \mathcal{G}^R$.

As mentioned before, the maximum members ng, nn, nc and nr represent a number of all generating, new candidate, committed and retired power plants, respectively.

3.1.2 Multi-stage GEP problem

Generally, multi-stage combinatorial optimization can be modeled by using forward dynamic programming that main problem is decomposed to subproblem $t \in \mathcal{T}$ (planning horizon), so-called "stage" in a recursive manner [63]. The candidate plans in each planning stage are called the "state" s of state-space set $S_t = \{s_1, s_2, \dots, s_{ns}\}$ over the planning horizon t. The candidate plans are solved stage-by-stage from the beginning until the final stage. The objective function and state equation over any time stage t are formulated using bellman's equation as follows;

$$\boldsymbol{Z}(s)^{(t-1)} = \text{minimization}\,\{\mathcal{V}^{(t)}(\boldsymbol{X}^{(t)}, \boldsymbol{U}^{(t)}) + \boldsymbol{Z}^{(t-1)}(\boldsymbol{X}^{(t-1)})\} \tag{3.7}$$

Subject to

$$\boldsymbol{X}^{(t)} = \boldsymbol{X}^{(t-1)} + \boldsymbol{U}^{(t)} + \boldsymbol{C}^{(t)} - \boldsymbol{R}^{(t-1)} \qquad \forall t \in [2, \mathrm{T}] \tag{3.8}$$

Any bold variables with superscript (t) refer to those variables in the planning year t; Let $\mathcal{V}^{(t)}{}_t(\boldsymbol{X}^{(t)}, \boldsymbol{U}^{(t)})$ represent the cost-to-go function of new-build power plants $\boldsymbol{U}^{(t)}$ associating the generating capacity $\boldsymbol{X}^{(t)}$ at planning year; $\boldsymbol{Z}^{(t-1)}(\boldsymbol{X}^{(t-1)})$ is the optimized cost at the planning year $t-1$. Equation (3.9)-(3.12) represent the set definition of existing generating units $\boldsymbol{X}^{(t)}$, new-build power plants $\boldsymbol{U}^{(t)}$, committed power plants $\boldsymbol{C}^{(t)}$ and retired power plants $\boldsymbol{R}^{(t)}$ as following:

$$\boldsymbol{X}^{(t)} = \left[X^{(1)}, X^{(2)}, \dots X^{(\mathrm{T})}\right] \quad ,\forall t \in \mathcal{T} \quad (3.9)$$

$$\boldsymbol{U}^{(t)} = \left[U^{(1)}, U^{(2)}, \dots U^{(\mathrm{T})}\right] \quad ,\forall t \in \mathcal{T} \quad (3.10)$$

$$\boldsymbol{C}^{(t)} = \left[C^{(1)}, C^{(2)}, \dots C^{(\mathrm{T})}\right] \quad ,\forall t \in \mathcal{T} \quad (3.11)$$

$$\boldsymbol{R}^{(t)} = \left[R^{(1)}, R^{(2)}, \dots R^{(\mathrm{T})}\right] \quad ,\forall t \in \mathcal{T} \quad (3.12)$$

Incorporating the NPV calculation considering the discount rate δ^d, the equation (3.7) is rewritten as follows;

$$NPV^{(t)}\left(\boldsymbol{Z}(s)^{(t)}\right) = \min\left(\frac{1}{\left(1+\delta^d\right)^t}\mathcal{V}^{(t)}\left(\boldsymbol{X}^{(t)}, \boldsymbol{U}^{(t)}\right) + \boldsymbol{Z}^{(t-1)}\left(\boldsymbol{X}^{(t-1)}\right)\right) \quad (3.13)$$

3.2 Mathematical formulation

3.2.1 Objective function

The objective of deterministic generation expansion planning is to minimize the discounted total costs (e.g. investment cost, fixed and variable O&M costs, outage cost, decommissioning cost, salvage cost and so on) within long-term planning horizons (15-20 years) under certainty parameters (e.g. fossil fuel cost, learning rate, future electricity demand and so on). The total cost can be modeled either single- or multi-objective functions. The single-objective function approach tradeoffs between the total costs in generation expansion planning, while the multi-objective function approach treats many solutions by Pareto-front [64] or Markowitz portfolio optimization [65]. In this doctoral thesis, the individual costs have complied into a single-objective function approach as follows;

$$\min z = \begin{bmatrix} CC\left(\boldsymbol{U}^{(t)}\right) + AP\left(\boldsymbol{X}^{(t)}\right) + EP\left(\boldsymbol{X}^{(t)}\right) + OC\left(\boldsymbol{X}^{(t)}\right) + \\ EC\left(\boldsymbol{X}^{(t)}\right) + DC\left(\boldsymbol{R}^{(t)}\right) - SC\left(\boldsymbol{X}^{(t)}\right) \end{bmatrix} \quad (3.14)$$

where $CC\left(\boldsymbol{U}^{(t)}\right)$, $AP\left(\boldsymbol{X}^{(t)}\right)$, $EP\left(\boldsymbol{X}^{(t)}\right)$, $EC\left(\boldsymbol{X}^{(t)}\right)$, $OC\left(\boldsymbol{X}^{(t)}\right)$, $DC\left(\boldsymbol{R}^{(t)}\right)$, and $SC\left(\boldsymbol{X}^{(t)}\right)$ represent investment, availability payment, energy payment, outage, external, decommissioning and salvage costs, respectively. The details of individual cost functions in equation (3.14) can be expressed as follows:

A. Investment cost

The investment cost function considers both direct and indirect terms (e.g., contingency and interest during construction) to build candidate generating units over the planning year is defined as follows:

$$CC(\,\boldsymbol{U}^{(t)}) = \sum_{t\in\mathcal{T}} \mathrm{NPV}^{(t)}\left(\sum_{g\in\mathcal{G}^N} C_g^{\mathrm{Inv}}\mathrm{cap}_g U_g^{(t)}\right) \tag{3.15}$$

Eq. (3.15) states that the investment cost of new candidate generating units $\mathcal{G}^N$ equals to the product of unit capital cost and new installed capacity [MW] over the planning horizon t. For unit $g \in \mathcal{G}^N$, let $C_g^{\mathrm{Inv}} \in \mathbb{R}_{\geq 0}^{nn}$ be a vector of unit capital cost [\$/MW]; similarly, we define unit g's contract capacity vector [MW] to be $\mathbf{cap}_g \in \mathbb{R}_{\geq 0}^{nn}$. The NPV calculation is assumed to occur in the beginning of the planning year t, and all generating units set imply $\mathcal{G} = \mathcal{G}^E \cup \mathcal{G}^N$.

B. Availability payment

The availability payment covers the fixed operation & maintenance cost that is required to keep the "availability status" of power plants for the operating year t.; This cost function can be expressed as follows;

$$AP(\,\boldsymbol{X}^{(t)}) = \sum_{t\in\mathcal{T}} \mathrm{NPV}^{(t)}\left(\sum_{g\in\mathcal{G}} C_g^{\mathrm{FOM}}\mathrm{cap}_g X_g^{(t)}\right) \tag{3.16}$$

Eq. (3.16) considers availability payment [million \$] per year t (equals the fixed O&M cost multiply with the installed capacity [MW]). We define the unit g's fixed O&M cost vector $C_g^{\mathrm{FOM}} \in \mathbb{R}_{\geq 0}^{ng}$ [\$/MW]; For simplicity, The NPV calculation is assumed to occur in the ending of the planning year t.

C. Energy payment

The energy payment covers the fuel and variable operation & maintenance costs of power plants to generate power for the operating year t; This cost function can be expressed as follows;

$$EP(\,\boldsymbol{X}^{(t)}) = \sum_{t\in\mathcal{T}} \mathrm{NPV}^{(t)}\left(\sum_{g\in\mathcal{G}} E_g^{\mathrm{PPS}}(AHR_g FC_g + C_g^{\mathrm{VOM}})\right) \tag{3.17}$$

Eq. (3.17) considers the sum of fuel cost and variable O&M cost; we define the expected produced energy $E_g^{\mathrm{PPS}} \in \mathbb{R}_{\geq 0}^{ng}$ of generating unit g (derive from probabilistic production simulation); As mentioned in Eq. (2.8), $AHR_g \in \mathbb{R}_{\geq 0}^{ng}$ represents the average heat rate [MMBTU/MWh] of generating units g, and fuel cost $FC_g \in \mathbb{R}_{\geq 0}^{ng}$ represents the fuel cost [$/MMBTU] relating to fuel type of generating units g; $C_g^{\mathrm{VOM}} \in \mathbb{R}_{\geq 0}^{ng}$ represents the variable O&M costs [$/MWh] of generating units g; For simplicity, The NPV calculation is assumed to occur in the ending of planning year t.

D. Outage cost

Generally, the unsupplied energy or EENS (expected energy not-served) is reduced when the power system strength is reinforced (the higher system expansion investment, the less unsupplied energy) [66]. Figure 3.2 depicts the optimal system investment concept considering reliability level and outage cost. The outage cost function can be expressed as follows;

$$OC(\boldsymbol{X}^{(t)}) = \sum_{t \in \mathcal{T}} \mathrm{NPV}^{(t)}(IEAR \cdot EENS^{(t)}) \tag{3.18}$$

where $IEAR \in \mathbb{R}_{\geq 0}$ stand for the interrupted energy assessment rate which reflects the outage cost of customers: industrial, commercial, residential segments in monetary term [million $/MWh]; $EENS \in \mathbb{R}_{\geq 0}$ stands for the expected energy not-served [MWh] representing the unsupplied energy [MWh]. For simplicity, The NPV calculation is assumed to occur in the ending of planning year t.

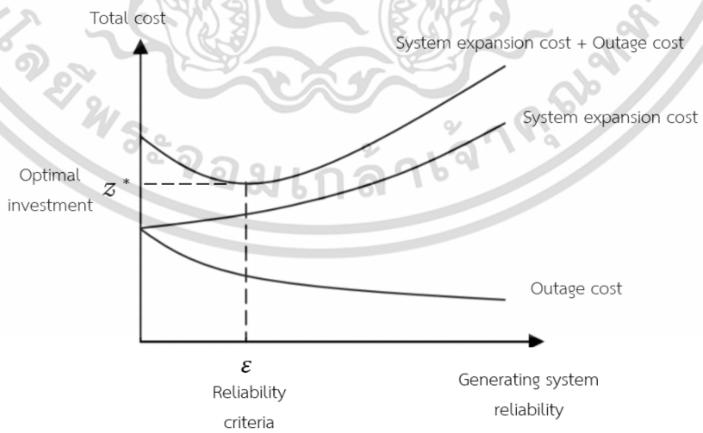

Figure 3.2 Reliability constrained generation expansion planning, adopted from [66]

D. External cost

The environmental problem from local pollutants (e.g. SO_2, PM and so on) and

GHG (e.g. CO_2) is still a major problem even though the new powet plants are equipped with the necessary emission control and cleaner technology deployment (e.g. electrostatic precipitator to control particulate matter, and flu-gas desulfurization to control sulfur dioxide [67]). The internalization of external cost (representing the true costs from negative impact to environment and society) into the generation expansion planning is an efficient policy instrument. The external cost function can be expressed as follows;

$$EC(\boldsymbol{X}^{(t)}) = \sum_{t\in\mathcal{T}} \mathrm{NPV}^{(t)} \left(\sum_{g\in\mathcal{G}} E_g^{\mathrm{PPS}} \left(C_g^{\mathrm{SO_2}} \delta_g^{\mathrm{SO_2}} + C_g^{\mathrm{PM}} \delta_g^{\mathrm{PM}} + SCC \cdot \delta_g^{\mathrm{CO_2}} \right) \right) \quad (3.19)$$

where $\delta_g^{\mathrm{SO_2}} \in \mathbb{R}_{\geq 0}^{ng}$ and $\delta_g^{\mathrm{PM}} \in \mathbb{R}_{\geq 0}^{ng}$ are representing the sulfur dioxide and particulate matter emission factor [kg/MWh], respectively; $\delta_g^{\mathrm{CO_2}} \in \mathbb{R}_{\geq 0}^{ng}$ represents carbon dioxide emission factor [ton-kg/MWh]; $C_g^{\mathrm{SO_2}} \in \mathbb{R}_{\geq 0}^{ng}$ and $C_g^{\mathrm{PM}} \in \mathbb{R}_{\geq 0}^{ng}$ are represent cost coefficients [$/kg] of sulfur dioxide and particulate matter, respectively; $SCC \in \mathbb{R}$ denotes the social cost of carbon [$/kg$\mathbf{CO_2}$], well-known as the carbon tax.

F. Decommissioning cost

Decommissioning [68] is the final process of power plants that are retired from electricity production. This process relates to the converting from the brownfield site (developed area) back to the greenfield site (pre-developed area). The cost of this restoration process includes dismantlement, waste disposal, environmental remediation, and so on. The decommissioning cost function can be expressed as follows;

$$DC(\boldsymbol{R}^{(t)}) = \sum_{t\in\mathcal{T}} \mathrm{NPV}^{(t)} \left(\sum_{r\in\mathcal{G}^R} \left(\gamma_g \mathrm{cap}_g R_g^{(t)} \right) \right) \quad (3.20)$$

Eq. (3.20) states that the retirement of retired units $\mathcal{G}^R$ equals to the product between decommissioning cost and retired capacity [MW] over the planning horizon $\boldsymbol{t}$. For unit $g \in \mathcal{G}^R$, let $\gamma_r \in \mathbb{R}_{\geq 0}^{nr}$ be a vector of the decommissioning factor [$/MW] depending on the individual project; The power plant retirement is assumed to occur in the ending of the planning year, and the all generating units set imply $\mathcal{G} = \mathcal{G} - \mathcal{G}^R$.

G. Salvage cost

The ending effect describes the phenomenon that the solving method is biased to choose the lowest investment cost of candidate options in the final year. The reasons are that: the remnant investment value has not been depreciated because it has remaining life to exercise electricity production, and the remnant operational cost has not been included after the final year. Based on literature reviews [69], the two methods that can mitigate the ending effect are described as follows;

- *Extended simulation* is straightforward to treat the remnant investment and operational costs; the extended simulation time should greater than the final year plus the longest life of power plants; the decision after the final year will be ignored, anyway the drawback is time computation.
- *Salvage value* is accounting the undepreciated capital cost into the objective function;

In this thesis, the salvage value approach is carried into the objective function using the straight-line depreciation assumption; the salvage cost function can be expressed as follows;

$$SC(\boldsymbol{X}^{(t)}) = \sum_{t=\mathrm{T}} NPV^{(t)} \left(\sum_{g \in \mathcal{G}} \left(C_g^{\mathrm{Inv}} \mathrm{cap}_g \theta(X_g^{(t)}) \right) \right) \tag{3.21}$$

In which,

$$\theta_g(\blacksquare) = 1 - \mathrm{UsageLife} \frac{\text{Capital Investment - Salvage Value}}{\text{Plant Lifetime}} \tag{3.22}$$

$\theta(\blacksquare)$ is defined as the salvage value function [%] relating to the usage life [year], capital investment [%], remaining salvage value [%] and plant lifetime [year] of power plants g; The NPV calculation is assumed to occur in the ending of study time T.

3.2.2 Constraints

For this thesis, the following constraints (generation adequacy, generation reliability, fuel diversification, new power plant limitation and carbon dioxide emission) are taking into considerations:

A. Generation adequacy

Generation adequacy [50,70] is the ability of the generation fleets to match the generation and electricity demand at all times. For this reason, the installed capacity should greater than future net peak demand plus planning reserve margins. There are two types of planning reserves: minimum reserve $\mathrm{RM}^{\min}$ is required to prevent generation shortage (practically, generation fleets face forced-outage and yearly scheduled maintenances), and the maximum reserve $\mathrm{RM}^{\max}$ is required to prevent the over-investment of electric utilities. The generation adequacy can be expressed mathematically as

$$\mathrm{NL}_t \times (1 + \mathrm{RM}^{\min}) \leq \sum_{g \in \mathcal{G}} \left(\mathrm{cap}_g X_g^{(t)} \leq \mathrm{NL}_t \times (1 + \mathrm{RM}^{\max}) \right), \forall t \in \mathcal{T} \quad (3.23)$$

Let $\mathrm{RM}^{\min}$ and $\mathrm{RM}^{\max}$ be the minimum and maximum reserve margins [%] at planning year t, respectively; NL_t represents the peak net load [MW] at planning horizon time t.

B. Generating system reliability

In practice, the generation, transmission, and distribution system have not 100% reliable operation to transmit the electrical energy to the end-use customers. The system planner evaluates the unsupplied-energy that system interruption should not greater than planning criteria (e.g., Loss-of-Load Probability index less than 0.00274 or 24 hours per year). In this study, the generating system reliability (Hierarchy-I) is evaluated by using the equivalent energy function method (EEF) [71]; The generating system reliability is stated as the following constraint:

$$LOLP\left(X_g^{(t)}\right) \leq \varepsilon \qquad , \forall t \in \mathcal{T} \quad (3.24)$$

We define a function $\mathrm{LOLP}(\blacksquare)$ to evaluate $LOLP \in \mathbb{R}_{\geq 0}^{ng}$ by using probabilistic production simulation (more details in section 3.2) at planning year t, and ε denotes generating system reliability criteria [%].

C. Investment limitation

The yearly new-build power plants were restricted for some reasons, e.g. limited financial budget, nuclear power plant limitation, and so on. The investment limitation is modeled in domain variables as following:

$$0 \leq U_g^{(t)} \leq \mathcal{D}_g \qquad , \forall c \in \mathcal{G}^c, \forall t \in \mathcal{T} \quad (3.25)$$

where $U_g^{(t)}$ denotes set of new candidate generating units over planning year t, associated with each candidate options $g \in \mathcal{G}^N$.

D. Fuel diversification

The energy mix describes the diversification of primary energy sources, e.g. natural gas, crude oil, bunker oil, LNG, and so on. For example, Thailand relies on almost 60% natural gas requirement. What if the gas field is disrupted for some reasons, the natural gas-fired power plants will shutdown. To minimize the insecurity of supply, natural gas dependence of Thailand is required to diversify to another resource [72]. Broadly speaking, the energy mix requirement is stated mathematically as follows:

$$M_f^{min} \leq \frac{\sum_{g\in\mathcal{G}}\left(\text{cap}_{g,f} X_{g,f}^{(t)}\right)}{\sum_{g\in\mathcal{G}}\left(\text{cap}_g X_g^{(t)}\right)} \leq M_f^{max} \qquad ,\forall t \in \mathcal{T}, \forall f \in \text{F} \quad (3.26)$$

Let M_f^{min} and M_f^{max} be the minimum and maximum energy mix for fuel type $f \in \text{F}$, respectively; Let F denotes the fuel set (1: foreign power purchase, 2: coal/lignite, 3:renewables, 4:imported LNG/natural gas, 5:nuclear and 6:remaining fuels); $X_{g,f}^{(t)}$ denotes the set of power plants group by fuel type f at time stage t; $\text{cap}_{t,f}$ denotes the plant type grouping by fuel type f at year t.

E. Carbon emission target

The carbon dioxide emission [tonne kg-CO_2] of the power sector is restricted by national policy. In general, the developing country requires the electricity demand for social development. In practice, an efficient pathway incorporating NAMA/INDC target calls for low carbon actions: (1) technological advancement (e.g., IGCC, ultra-supercritical technology and so on), and (2) renewable energy development to displace the produced energy by fossil-fired power plants [73]. The simple equation to limit the carbon dioxide emission is considered as follow;

$$\sum_{g\in\mathcal{G}} E_g^{\text{PPS}} \delta_g^{\text{CO}_2} \leq ET^{(t)} \qquad ,\forall t \in \mathcal{T} \quad (3.27)$$

Here, $ET^{(t)} \in \mathbb{R}_{\geq 0}^{\text{T}}$ indicates the yearly carbon dioxide emission target [tonne kg-CO_2] associated with NAMA/INDC policies in planning year t;

3.3 Probabilistic production simulation

Probabilistic methods for production cost simulation are that: (1) monte carlo simulation, and (2) convolution approach using equivalent load duration curve (ELDC). For this thesis, the convolution approach using the equivalent energy function (EEF) [71] is applied for probabilistic production simulation (PPS). The literature reviews [74] report that the EEF method has benefits in both accuracy and speed comparing to the well-renowned convolution approaches: recursive method [75], piecewise linear approximation method [76], segmentation method [77], mixture of normal approximation method [78], cumulant method [79], fast Fourier method [80] and equivalent interval frequency distribution [81]. This section is dedicated to basic principle to advance as follows:

3.3.1 Convolution approach using ELDC

A. Definitions

We first introduce the case of 100% generating reliability of thermal units $g \in \mathcal{G}^{th}$ over normalized load duration curve function $\overline{LDC}(\blacksquare)$ (see Section 2 sub section B). The total load energy [MWh] and unit $g \in \mathcal{G}^{\mathrm{th}}$'s produced energy with contracted capacity Cap_g can be calculated using the below equation:

$$E^{\mathrm{load}} = 8760 \int_{0}^{nh} \overline{LDC}\,(\mathrm{L})d\mathrm{L} \tag{3.28}$$

$$E_g = 8760 \int_{\mathrm{Cap}_g}^{\mathrm{C_{total}}+\mathrm{Cap}_g} \overline{LDC}\,(\mathrm{L})d\mathrm{L} \tag{3.29}$$

where $\mathrm{C_{total}}$ denotes the cumulative capacity of all generating units (decommiting status refer to $\mathrm{C_{total}} = 0$).

Since we are concerned with the planned and unplanned outages, ELDC plays an important tool for reliability evaluation and production cost calculation in generation expansion planning (it accounts for the unavailability of generating units in LDC through the convolution process). For sake of simplicity, the rigorous proof of the convolution equation (the two-state generation model with a load model) is given in [77]. The discrete version of the convolution equation is given below

$$\mathrm{ELDC(L)}^{(i)} = \mathrm{p}_g\mathrm{ELDC(L)}^{(i-1)} + \mathrm{q}_g\mathrm{ELDC}(\mathrm{L}-\mathrm{cap}_g)^{(i-1)} \tag{3.30}$$

Let unit g' ELDC function be $\mathbf{ELDC(L)}^{(i)}$ that mean probability $\mathbf{Prob} \in [0,1]$ of system net load greater or equal to netload $\mathbf{NL} \in \mathbb{R}$ [MW]; The ELDC function with superscript (i) refers to the i th convolution on LDC; $\mathrm{p}_g \in \mathbb{R}^{ng}_{\geq 0}$ denotes availability [fraction] of generating units g; so, unavailability $\mathrm{q}_g \in \mathbb{R}^{ng}_{\geq 0}$ [fraction] correspond to $\mathrm{q}_g = 1 - \mathrm{p}_g$;

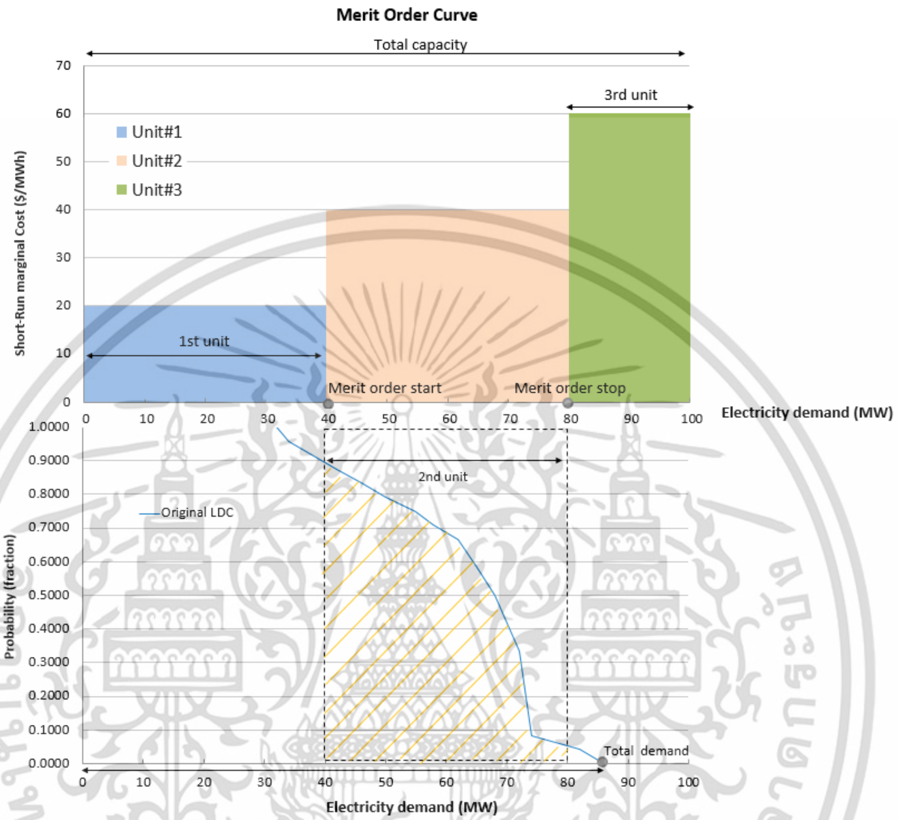

Figure 3.3 Produced energy of 2nd generating unit considering 100% generating reliability [66]

Recall equation (3.29) in probabilistic version as follows;

$$E_g = 8760 \int_{\mathrm{C_{total}}}^{\infty} \overline{ELDC}^{(i-1)}(\mathrm{L})dL \tag{3.31}$$

When all generating units are complete in the convolution process, the reliability indices, i.e. LOLP and EENS can be calculated as equations:

$$\mathrm{LOLP} = \overline{ELDC}(\mathrm{C_{total}}) \tag{3.32}$$

$$\mathrm{EENS} = 8760 \int_{\mathrm{C_{total}}}^{\infty} \overline{ELDC}^{(i)}(\mathrm{L})dL \tag{3.33}$$

Figure 3.4 visualizes the sequential convolution process of example (see Section 3.3.2 sub section C) using the ELDC approach.

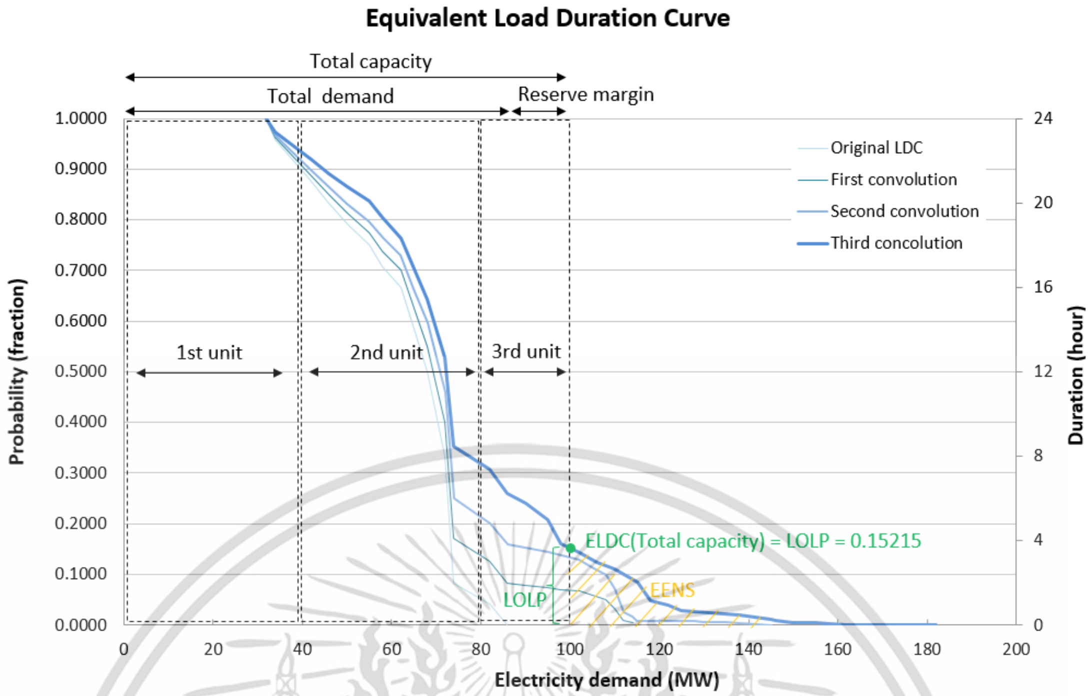

Figure 3.4 Equivalent load duration curve concept

3.3.2 Convolution approach using EEF

A. Definition

Let a function $\mathrm{ELDC(L)}^{(i)}$ is divided by $\Delta\mathrm{block}$ [MW] (the greatest common factor of total capacity $\mathrm{C_{total}}$ [MW]) to transform to discrete energy set $\mathcal{E} = \{1,2,..,e^{\max}\}$ corresponding to index e; The rigorous proof of equation is given in [82]. The total load energy can be calculated using the below equation:

$$E^{\mathrm{load}} = \sum_{e=1}^{e^{max}} EF(e) \tag{3.34}$$

where $EF(e)$ is an energy function which the maximum index e^{max} is calculated using the round-up of the quotient between peak load $\mathrm{NL}^{\max}$ divided by the energy block $\Delta block$. The unit g's expected produced energy [MWh] is calculated as below equation:

$$E_g^{PPS} = \mathrm{p}_g \sum_{e=e^{\mathrm{total}}}^{e^{\mathrm{total}}+K_g} EF(e) \tag{3.35}$$

Associated with,

$$K_g = \frac{\mathrm{Cap}_g}{\Delta\mathrm{block}} \tag{3.36}$$

$$e^{\mathrm{total}} = e^{\mathrm{total}} + K_g \tag{3.37}$$

where K^g [interger number] represents a movable index of generating unit g for discrete convolution process; The index of the cumulative energy function e^{total} is stated in equation (3.37); The convolution equation of energy function is given below:

$$\mathrm{EF}(e)^{(i)} = \mathrm{p}_g \mathrm{EF}(e)^{(i-1)} + \mathrm{q}_g \mathrm{EF}(\mathrm{e} - K_g)^{(i-1)} \tag{3.38}$$

When all generating units are complete in the convolution process, the reliability indices, i.e. LOLP and EENS can be calculated as equations:

$$EENS = \sum_{e>e^{\max}} \mathrm{EF}\,(\mathrm{e}) \tag{3.39}$$

$$LOLP \cong \frac{\mathrm{EF}(e^{max})^{(i)} + \mathrm{EF}(e^{max}+1)^{(i)}}{2\mathrm{T}\Delta\mathrm{block}} \quad ,i = g \tag{3.40}$$

B. Procedure

The convolution approach using EFF can be summarized as below pseudocode:

Table 3.1

The pseudocode of the convolution approach using EEF

Begin

- Prepare the power system data and power plant characteristics
- Prepare the netload duration curve (mentioned in section 2.2 sub section B).
- Prepare merit order dispatch (ascending order) by using Eq. (2.7).

For $g \le ng$,

- Perform the convolution process by using Eq. (3.38)
- Evaluate expected produced energy [MWh] by using Eq. (3.35)

End for loop

- Evaluate reliability indices by using Eq. (3.39) and Eq. (3.40)

End

C. Example calculation

If power plant A, B, C have 40-MW, 40-MW and 20-MW contracted capacity, respectively. The forced outage rates of power plants A, B, C are 0.1, 0.1 and 0.2 respectively. The chronological load (assumed step-wise data) is shown in Table 3.2;

Table 3.2

Example calculation of load duration curve

Chronological load				Load duration curve					
No. [hour]	Load [MW]	No. [hour]	Load [MW]	Load [MW]	Frequency [occurence]	Individual probability	Cumulative probability	Duration [hour]	Area [MWh]
1	32	13	68	32	1	0.0417	1	24	32
2	34	14	72	34	2	0.0833	0.9583	23	68
3	34	15	72	42	1	0.0417	0.8750	21	42
4	42	16	72	46	1	0.0417	0.8333	20	46
5	50	17	72	50	1	0.0417	0.7917	19	50
6	55	18	82	55	1	0.0417	0.7500	18	55
7	62	19	72	58	1	0.0417	0.7083	17	58
8	65	20	68	62	2	0.0833	0.6667	16	124
9	65	21	68	65	2	0.0833	0.5833	14	130
10	74	22	62	68	4	0.1667	0.5000	12	272
11	72	23	58	72	6	0.2500	0.3333	8	432
12	68	24	46	74	1	0.0417	0.0833	2	74
				82	1	0.0417	0.0417	1	82

Based on the procedure of Table 3.1, the example calculation of convolution using the EEF approach can be shown in Table 3.3.

Table 3.3

Example calculation of convolution using EEF approach

Gen No.	E_g^{PPS}	Energy not Served	Index of energy function of EEF						Symbols
			1	2	3	4	5	6	
0	0	1465	480	460	371	152	2		$\mathrm{EF}(e)^{(0)}$
1	0.9(480+460)	1465-846		480	480	460	371	152	$\mathrm{EF}(e-2)^{(0)}$
	= 846	= 619		462	381.9	182.8	38.9	15.2	$\mathrm{EF}(e)^{(1)}$
2	0.9(381.9+182)	619-508.2				462	381.9	182.8	$\mathrm{EF}(e-2)^{(1)}$
	= 508.23	= 110.77				210.7	73.2	31.9	$\mathrm{EF}(e)^{(2)}$
3	0.8(73.2)	110.8-58.6					210.7	73.2	$\mathrm{EF}(e-1)^{(2)}$
	= 58.56	= 52.21					100.7	40.2	$\mathrm{EF}(e)^{(3)}$

The LOLP can be read from Table 3.3 as 52.21 MWh; Therefore, the LOLP can be approximated using equation (3.40) as below:

$$LOLP \cong \frac{\mathrm{EF}(5)^{(3)} + \mathrm{EF}(5+1)^{(3)}}{2 \times 24 \times 20} = 0.145783 \tag{3.41}$$

3.3.3 PPS enhancement for load leveling application of ESS

The original PPS framework faces ‘order’ [83] and ‘logic’ [84] problems when deal with ESS. This section integrates the two techniques satisfying energy invariance property [85] to solve these issues for demand-side management (DSM) [86], hydroelectricity (with storage) [87], and the ESS operation. Firstly, probabilistic peak-shaving [88] and deconvolution techniques are applied for peak-shaving operation, and valley-filling operation of ESS’s generating units. Lastly, both techniques form the load leveling application (sometimes called *load shifting*) as shown in Figure 3.5. The optimal operation of ESS applies the *energy marginal analysis* using the concept of piece-wise constant benefit/cost curve (PCBC) [89].

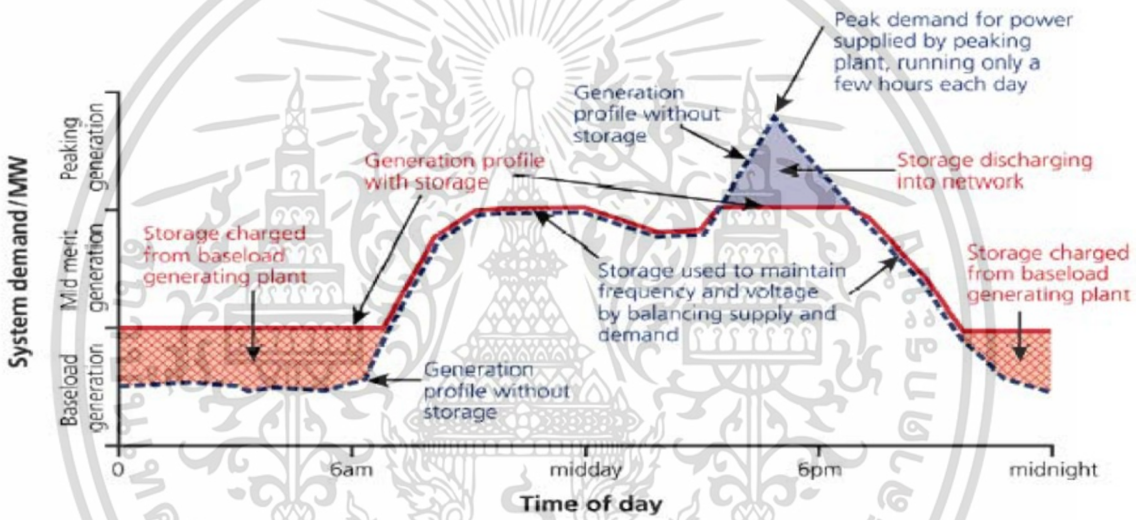

Figure 3.5 Load leveling application concept, adopt from [88]

A. Valley-filling and peak-shaving techniques

The intermediate energy function $\mathrm{EF}'(e)^{(i)}$ to perform the *valley-filling technique* and updating equation (additional pumping/charging load) are shown as below:

$$\mathrm{EF}'(e)^{(i)} = \mathrm{p}_g \mathrm{EF}(e - K_g)^{(i-1)} + \mathrm{q}_g \mathrm{EF}(\mathrm{e})^{(i-1)} \tag{3.42}$$

$$\mathrm{EF}(e)^{(i)} = \mathrm{EF}'(e)^{(i)} - \mathrm{EF}(e)^{(i)} \tag{3.43}$$

$$SOC_g^i = \eta_g^{\text{cycling}} \mathrm{p}_g \sum_{e=e^{\text{total}}}^{e^{\text{total}}+K_g} \mathrm{EF}(e)^{(i)} \tag{3.44}$$

Let SOC_g^i denotes the state of charging energy [MWh] of ESS generating units g ; the upper script means the i-th dispatch order in ascending arrangement; η_g^{cycling} denotes cycling/round-trip efficiency [fraction] of ESS generating units.

The intermediate energy function $\mathrm{EF}'(e)^{(i)}$ to perform the *peak- shaving technique* and updating equation (displace/discharge expensive load) are shown as below:

$$\mathrm{EF}'(e)^{(i)} = \mathrm{p}_g \mathrm{EF}(e + K_g)^{(i-1)} + \mathrm{q}_g \mathrm{EF}(e)^{(i-1)} \tag{3.45}$$

$$\mathrm{EF}(e)^{(i)} = \mathrm{EF}(e)^{(i)} - \mathrm{EF}'(e)^{(i)} \tag{3.46}$$

$$DoD_g^i = \mathrm{p}_g \sum_{e=e^{\mathrm{total}}}^{e^{\mathrm{total}}+K_g} \mathrm{EF}(e)^{(i)} \tag{3.47}$$

Let DoD_g^i denotes the depth of discharging energy [MWh] of ESS generating unit g; the upper script means the $i^{\text{-th}}$ dispatch order in ascending arrangement; The utilization level R [MWh] of ESS generating unit is described as below equation:

$$CP_g = \sum_{i \in \mathcal{G}^{\mathrm{th}}} SOC_g^i + R_0 \qquad , \forall g \in \mathcal{G}^{\mathrm{ESS}} \tag{3.48}$$

Let $\mathcal{G}^{\mathrm{ESS}}$ be the set of ESS generating units; CP_g denotes the ESS generating unit g's cumulative utilization level [MWh]; R_0 represents the initial utilization level [MWh].

B. Load leveling application using marginal analysis

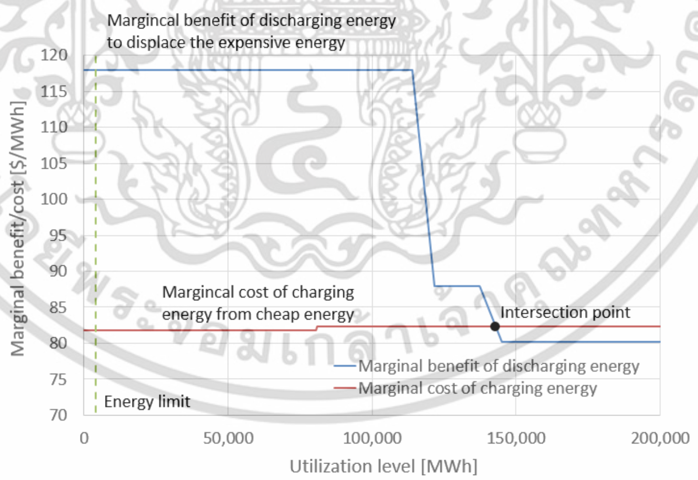

Figure 3.6 Optimal economic operation of the ESS unit using energy marginal analysis

The utilization level CP_g [MWh] of load leveling application of ESS generating unit can be evaluated using *energy marginal analysis* as depicted in Figure 3.6. The energy marginal analysis comprises piece-wise constant benefit/cost, so-called PCBC (represents the marginal benefit of discharging energy), and the marginal cost of charging energy. The area of marginal benefit above marginal cost (equation 2.6 multiply with fuel cost) represents the total benefit of ESS utilization. The intersection point indicates the unit g's optimal operation CP_g^* [MWh].

The short-run marginal cost of charging/pumping energy, and short-run marginal benefit of charging/pumping energy are calculated as follows:

$$MC_g^{\text{charing}} = \frac{\text{IHR}_g \text{FC}_f}{\eta_g^{\text{cycling}}} \quad ,\forall g \in \mathcal{G}^{\text{th}} \quad (3.49)$$

$$MC_g^{\text{discharing}} = \text{IHR}_g \text{FC}_f \quad ,\forall g \in \mathcal{G}^{\text{th}} \quad (3.50)$$

Equation (3.49) states the marginal cost of charging energy on ascending merit order of thermal units (convolution based-on thermal power plants $\mathcal{G}^{\text{th}}$); FC_f represent fuel cost indexed with fuel price set (1: pooled natural gas, 2: lignite, 3:imported coal, 4:nuclear, 5:diesel, and 6:bunker oil); IHR_g denotes the incremental heat rate curve as mentioned in Eq. (2.3); Equation (3.50) states the marginal benefit of discharging energy on descending merit order of thermal units. The data representing in Figure 3.6 are tabulated as below table:

Table 3.4

Energy marginal analysis of 2015 Thailand's generating system

Cumulative discharging energy [MWh]	$MC^{\text{discharging}}$ [\$/MWh]
0 -114,051	117.92
114,051 -145,023	87.94
152,875 -433926	80.26

Cumulative charging energy [MWh]	MC^{charging} [\$/MWh]
0 -114,051	81.74
80,998 - 245,143	82.26

For calculation example, 20-MW capacity, 99% reliability and 95% round-trip efficiency of BESS are adopted; The energy limit and expected produced energy are calculated as below equations:

$$\text{EL}_g = \eta_g^{\text{cycling}} \text{p}_g \text{Cap}_g \text{H}_g^{\text{operate}} \times 365 \quad (3.51)$$

$$= 0.95 \times 0.99 \times 20 \times 1 \times 365 = 5{,}420 \text{ MWh}$$

$$E_g^{\text{PPS}} = \min\{E_L, CP_g\} \quad (3.52)$$

$$= \min\{5{,}420{,}137{,}237\} = 5{,}420 \text{ MWh}$$

Equation (3.51) calculates the yearly produced energy approximation of BESS; The BESS have 20-MW capacity with 99% reliability; the round-trip efficiency is 95%; The expected operating hour per day is 1 hour per day. Equation (3.52) finalizes the expected produced energy of the ESS generating unit.

C. Proposed framework

Let $\mathcal{G}^{\mathbf{th}}$ denote the set of thermal power plants, the set of SPP units $\mathcal{G}^{\mathbf{SPP}}$, the set of hydroelectricity (with storage) $\mathcal{G}^{\mathrm{H}}$, and the set of ESS units $\mathcal{G}^{\mathbf{ESS}}$; It imply $\mathcal{G} = \mathcal{G}^{\mathrm{th}} \cup \mathcal{G}^{\mathrm{SPP}} \cup \mathcal{G}^{\mathrm{H}} \cup \mathcal{G}^{\mathrm{ESS}}$, indexed by g. The proposed framework can be described by the following steps:

Step 1. Read the system data, e.g. techno-economic data.

Step 2. Evaluate investment problem follow conventional GEP.

Step 3. Calculate the PPS framework as follows:

- Dispatch the unit-by-unit SPP generating, i.e., solar PV and wind farm (zero fuel cost) $g \in \mathcal{G}^{\mathrm{SPP}}$; Perform traditional PPS for thermal power plants G^{th} in increasing average heat rate. The economic loading dispatch of EES units is ranked by decreasing cycle efficiency
- Dispatch the unit-by-unit thermal units, indexed $g \in \mathcal{G}^{\mathrm{th}}$ in ascending SRMC until completely the most expensive units; and Dispatch the hydroelectricity and ESS by decreasing operating hours $\mathrm{H}_g^{\mathrm{operate}}$ as below equation:

$$\mathrm{H}_g^{\mathrm{operate}} = \frac{\mathrm{EL}_g/\eta_g^{\mathrm{cycling}}}{\mathrm{p}_g \mathrm{Cap}_g} \tag{3.53}$$

  where unit g's energy limit, e.g. reservoir capacity [MWh] or battery energy [MWh].

- Perform peak-shaving technique for hydroelectricity (with storage) follows Eq.(3.42), indexed $g \in \mathcal{G}^{\mathrm{H}}$ by decreasing discharging hours $\mathrm{H}_g^{\mathrm{discharge}}$ as below equation:

$$\mathrm{H}_g^{\mathrm{discharge}} = \frac{\mathrm{EL}_g}{\mathrm{p}_g \mathrm{Cap}_g} \tag{3.54}$$

  For simplicity, the availability is assumed the identical for loading and discharge power. In addition, the limited energy is adopted by using the statistics data.

- Perform load leveling application of ESS follows Eq. (3.45), indexed $g \in \mathcal{G}^{\mathrm{E}}$ according to decreasing cycling/round-trip efficiency $\eta_g^{\mathrm{cycling}}$. The expected discharge/shaving energy [MWh] is determined by the minimum value between limited energy $\mathbf{EL}_g$ and the intersection point of energy marginal analysis.

3.4 Study Case 1: Load Leveling Application of Lithium-ion battery for Thailand Generation Expansion Planning

3.4.1 Case study descriptions

Objective

To assess the load leveling application of Lithium-ion BESS on Thailand's generation system.

Problem formulation

The compact formulation of the multistage GEP without consideration of transmission constraint (**GEP-I**) is:

$$\min_{\Delta GEP\text{-}I}(3.15)-(3.19),(3.21)$$

$$\text{s.t.} \quad (3.23-3.26) \qquad \forall g \in \mathcal{G}$$

Assumptions

Appendix (test system 1) provides the techno-economic data of existing, candidate and ESS plants that follow an official PDP 2015. The chronological load and VRE generation are derived from practical data. The planning assumptions follow the criteria that are used in the PDP2015. The proposed method was programmed on MATLAB with 2.45 GHz CPU and 16 Gb RAM installation. The test cases are described as follows;

Test case 1: This case is designed by following an official PDP 2015; the pumped-hydroelectricity projects comprise of Lamtakong (PSH#1), Chulabhorn (PSH#2) and Srinagarind (PSH#3). The project sites are shown in Figure 3.7.

Test case 2: This case is alternative ESS technology that adopts the Lithium-ion BESS instead of hydroelectricity projects.

Figure 3.7 Future pumped-hydroelectricity projects based on PDP2015

3.4.2 Simulation results

The comparative result of the total cost is shown in Table 3.5. The breakdown cost of variable O&M are that Testcase 1 = 3,303.69 million $, Testcase 2 = 3,301.98 million$

Table 3.5

Comparative cost result of pumped-hydroelectricity and BESS

Name	Investment [million $]	O&M cost [million $]	Outage cost [million $]	Env cost [million $]	Salvage cost [million $]	Total cost [million $]
Test case 1	17,826	3,303.69	6.23-E05	38,196	6,880	201,949
Test case 2	17,826	3,301.98	6.22-E05	38,195	6,880	201,949

The carbon dioxide intensity [83] – reflects the atmospheric CO_2 emission from per-unit of produced energy in $kgCO_2/kWh$. The mathematical equation can be stated as below;

$$\text{Intensity}_t = \frac{\text{ET}_t}{E_t^{\text{load}}} \quad ,\forall t \in \mathcal{T} \quad (3.55)$$

where Intensity_t stand for the carbon dioxide intensity [$kgCO_2/kWh$] over year t; ET_t represents CO_2 emission [thousand tonne $kgCO_2$] over year t; E_t^{load} represents expected energy demand [MWh] over year t. The yearly carbon dioxide emission data [thousand tonne $kgCO_2$] of study case 1 can be shown in Table 3.6.

Table 3.6

Comparative carbon dioxide emission result of pumped-hydroelectricity and BESS

Planning year	Test case (1)	Test case (2)	(2) – (1)	Planning year	Test case (1)	Test case (2)	(2) – (1)
1	83,851	83,851	0	11	118,860	118,850	-10
2	92,738	92,738	0	12	121,040	121,050	10
3	95,486	95,486	0	13	122,610	122,630	20
4	98,062	98,046	-16	14	123,100	123,130	30
5	99,123	99,106	-17	15	123,710	123,730	20
6	101,590	101,560	-30	16	120,400	120,410	10
7	105,620	105,610	-10	17	116,840	116,850	10
8	107,270	107,270	0	18	111,140	111,150	10
9	116,840	116,840	0	19	107,840	107,840	0
10	118,170	118,170	0	20	108,660	108,640	-20
				Intensity	0.3791	0.3791	

3.5 Conclusions

The following conclusions can be drawn from this chapter:

- The techno-economic assessment for Lithium-ion BESS is demonstrated in Thailand's generation system. This result confirms the potential benefits of Lithium-ion BESS for load leveling application in Thailand generation systems. The results indicate the lower operation cost and lower carbon dioxide emission.
- The effective approaches are applied to PPS enhancement, successfully. Firstly, the probabilistic peak-shaving and deconvolution techniques are applied to solves the logic and order problems of ESS operations. Lastly, the *energy marginal analysis* can determine the economic operation of ESS.

Chapter 4
Metaheuristic Development for Simheuristic Approach

In practice, the GEP problem is observed as a large-scale nonsmooth nonlinear-constrained combinatorial optimization and is classified as the complexity as NP-hard (solution cannot be found in polynomial time) [92]. The majority formulations are a deterministic model that omits the stochastic parameters; in a contradictorily, the stochastic model accounts for the uncertainty of planning parameters. To solve the global optimal solution of deterministic GEP, dynamic programming is applied in full enumeration; unfortunately, the growth of the algorithm observes an exponential trend, so-called *curse of dimensionality*. From past to present, many researchers applied the algorithm-solving strategies that are: (1) direct method, (2) greedy algorithm, (3) dynamic programming, (4) mathematical programming, (5) nature-inspired metaheuristics, and (6) hybrid approaches.

The main objective of this chapter is to develop an efficient metaheuristic approach to solve deterministic GEP, and extend the proposed method to solve the stochastic GEP (more details in Chapter 5) by using Simheuristic approach. The proposed method is developed from cuckoo search (CS) and dynamic programming (DP), namely 'hybrid CS-DP' to solve the performance problems, i.e. poor solution quality and convergence characteristics. The effectiveness of the proposed method is evaluated to solve the scaled-down 1996 Korea generation system with 14-year and 20-year planning periods. The benchmark methods are derived from famous literature comprising classical and metaheuristic methods.

4.1 Solving methods for deterministic GEP

4.1.1 Current algorithm-solving strategies

A. Literature surveys

In the field of optimization, many researchers applied many algorithm-solving strategies to solve deterministic GEP, successfully. Table 4.1 summarizes the state-of-art methods from famous and reliable journals in the past two decades. Each solving method has different advantages and disadvantages in terms of solution quality, solution robustness, convergence characteristics and computational time. In addition, difficulties of fine-tuning parameters and algorithm flexibility are the important reasons for choosing an algorithm to solve the GEP problem in a specific context.

Table 4.1
Literature surveys for solving deterministic GEP

Algorithm-solving strategies	Methods
Direct method	Bruteforce
Greedy algorithm	Year-Year optimization [75]
Dynamic programming	Dynamic programming [93], Tunnel-constrained dynamic programming [94], Successive approximation dynamic progmmming [95], and so on.
Mathmatical programming	Linear programming [96], Nonlinear progeamming [97], Mixed-integer nonlinear programming [98-99], and so on.
Nature-inspired metaheuristics	Evolutionary programming [100], Genetics algorithm [101], Particle swarm optimization [102], Shuffled frog leaping algorithm [103], Differential evolution [104], Ant colony [105], Simulated annealing [106], Tabu search [107], and so on.
Hybrid approaches	GA Bender decomposition [108-109] and so on.

B. Nature-inspired metaheuristics

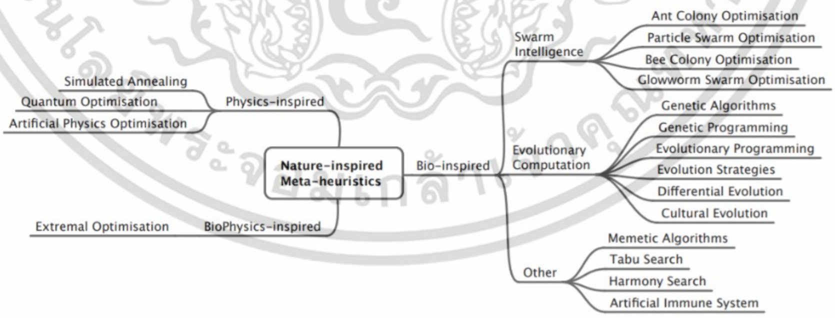

Figure 4.1 Classification of Nature-inspired metaheuristics, adopted from [110]

The metaheuristics [110] consist of two words that are (1) "*heuristics*" means a common-sense to solve a "compromising solution" in a reasonable time with the iterative procedure for solution quality, and (2) "*meta*" means a higher level. The two words are combined into the meaning of "higher-level framework of heuristic optimization aiming to solve the global optimal solution with local and exploration searches with not being trapped by local optimum". Figure 4.1 classifies the nature-inspired metaheuristics which metaphor from natures e.g., physics-, social-, bio-inspired and so on. This chapter focus on cuckoo search (CS), a subset of bio-inspired optimization.

4.1.2 Original CS

A. General descriptions

Cuckoos, developed by X.S. Yang [111] live widespread in Africa to Europe. They have more than 100 species around the world. Some species of cuckoo e.g. "ani" and "Guira", have aggressive hatching behavior. They act brooding parasitism in other host birds as follows: 1) A hidden female cuckoo await the host birds go hunting for food, 2) The female cuckoo lay 16 to 22 eggs in the other incubating bird, 3) The incubating bird mistaken for their eggs, and (4) The incubating bird may detect the cuckoo eggs; The incubating bird may remove cuckoo egg or may abandon the nest to the new habitat.

Figure 4.2 Cuckoo (scientific name: Cuculiformes)

Based on the strategy of egg laying of the cuckoo, it inspires the design of metaheuristic, explained the analogy as: (1) cuckoo sneak to lay its eggs on other nests (new solutions are generated by local search process), and (2) incubating bird may discover cuckoo eggs (exploration search process to diversify the solution by the discovering probability). The metaphor-descriptions [112] can be summarized in Table 4.2 to visualizes the concept of Cuckoo algorithm.

Table 4.2

Metaphor-based description of cuckoo search algorithm

Metaphor-based description	Optimization description	Parameters
Incubating bird's nest	Candidate solution of problem	$U_n^{(\text{iter})} \in \mathbb{Z}_+^{nt}$
Cuckoo sneaks to lay its eggs on other nests	Local search	$\alpha \in \mathbb{R}_+^{nt}$
Incubating bird may discover cuckoo eggs	Exploration seach	$\text{Prob}^{\text{discover}} \in [0,1]^{nt}$
The living thing continue the species	Iterative search	$\text{iter} = \{1,2..\text{iter}^{\max}\}$

As mentioned above, we consider the cuckoo algorithm with nt host nests and a set of tricked bird's host nests $\mathcal{C}$ which cuckoo bird sneak to lay its egg; For egg $n \in \mathcal{C}$, let $\boldsymbol{U}_n^{(\text{iter})} \in \mathbb{Z}_+^{nt}$ denotes decision vector with superscript (iter) refer to iter-th iteration of the searching process; we first introduce an equation (4.1) as below:

$$\boldsymbol{U}_n^{(\text{iter})} = \begin{bmatrix} \boldsymbol{U}_1 \\ \boldsymbol{U}_2 \\ \cdots \\ \boldsymbol{U}_{nt} \end{bmatrix}^{(\text{iter})} = \begin{bmatrix} \boldsymbol{U}_1 = \{U_1, U_2, .., U_{\text{T}}\} \\ \boldsymbol{U}_2 = \{U_1, U_2, .., U_{\text{T}}\} \\ \cdots \\ \boldsymbol{U}_{nt} = \{U_1, U_2, .., U_{\text{T}}\} \end{bmatrix}^{(\text{iter})} \tag{4.1}$$

B. Local search via lévy flight

Local search (sometimes called intensification) is a searching mechanism to guide the solver agents (some metaheuristic approaches). The local search mainly focuses on the neighboring solution through the search space via iterations. The local search of the CS algorithm relies on the *lévy flight* search pattern (originally, albatrosses's foraging route) [113].

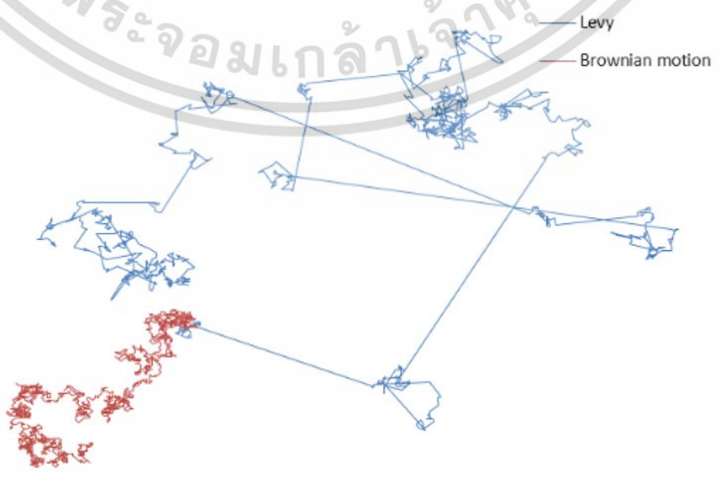

Figure 4.3 Example of Brownian motion walk and Le'vy walk

Scientists study the animal feeding behavior and discover the *lévy flight* (random walk according to Brownian motion with emigrating property to a new place). Later, the French mathematician, Paul Levy states the *lévy flight* as the Levy distribution which has infinite variance and infinity mean (random jumping with any large step is possible) [114]; Figure 4.3 illustrates the two-dimension random-walk comparison between Brownian motion and Levy motion.

The CS performs local search as below expression:

$$U_n^{(\text{iter}+1)} = U_n^{(\text{iter})} + \alpha \text{ Levy}(\blacksquare) \tag{4.2}$$

where $\alpha \in \mathbb{R}_+^{nt}$ denotes the scaling factor to match the search space (this doctoral thesis chooses 1.5); $\textbf{Levy}(\blacksquare)$ is a function of number generator to draw from Levy distribution; The recommended method to simulated a Levy distribution is Mantegna's algorithm [115]; The the step lengths according to the Mantegna's algorithm are calculated as below;

$$SL_n = \frac{\text{num}_n^1}{\sqrt[\bar{\beta}]{\text{num}_n^2}} \tag{4.3}$$

Let SL_n denotes the n nest's step lengths which derive from the ratio of randomized numbers $\textbf{num}_n^1, \textbf{num}_n^2$ which calculate as follows; $\bar{\beta} \in [1,2]$ is Mantegna's parameter.

$$\sigma_n^1 = \sqrt[\bar{\beta}]{\frac{\Gamma[1+\bar{\beta}] \times \sin(\frac{3.14\bar{\beta}}{2})}{\Gamma[\frac{1+\bar{\beta}}{2}] \times 2\beta \times 2^{(\frac{\bar{\beta}-1}{2})}}} \quad , \quad \sigma_n^2 = 1 \tag{4.4}$$

where σ_n^1, σ_n^2 denotes standard deviations of num_n^1 and num_n^2, respectively; $\Gamma(\blacksquare)$ is a gamma function.

C. Exploration search via randomization

Exploration search (sometimes called diversification) is a searching mechanism to explore the new solution throughout the whole search space. The original CS performs an exploration search using the randomization process (uniform distribution) as below conditions:

$$U_n^{(\text{iter}+1)} = \begin{bmatrix} U_1 \\ U_2 \\ \dots \\ U_{nn} \end{bmatrix}^{(\text{iter}+1)} = \begin{cases} \text{do nothing} & rand_n < 1 - \text{Prob}^{\text{discover}} \\ \text{randomization} & rand_n \geq 1 - \text{Prob}^{\text{discover}} \end{cases} \quad (4.5)$$

where $rand_n \in [0,1]^{nt}$ represents an n-th individual random number using a uniform distribution; $\text{Prob}^{\text{discover}} \in [0,1]^{nt}$ denotes the threshold of discovering probability to activate the exploration search (diversification process).

D. Procedure

The pseudocode of the CS algorithm can be described as the following:

Table 4.3

Pseudocode of original cuckoo search algorithm

Begin

Initialize CS parameters, i.e. the nest of a tricked bird nt, maximum iterations $\text{iter}^{\max}$ and discovering probability $\text{Prob}^{\text{discover}} \in [0,1]$.

While $[\text{iter} < \text{iter}^{\max}]$ or [stopping criterion]

Perform local search via by *lévy flight*;

Evaluate the fitness function;

If (the new objective function better than the former solution)

Replace a former solution (one-by-one comparison)

End

Perform exploration search via randomization process;

Evaluate the fitness function;

Rank the solutions (cuckoo nests)

End while

4.2 Proposed method

4.2.1 Analysis of CS

Even the CS is recognized as an efficient metaheuristic approach which comes up with unique local search using levy flight distribution, and exploration search using randomization can be overcome the local optimum. The original CS found performance problems based on the result of the test system. First, CS attempts the many iterations to reach a compromising solution for large-scale combinatorial optimization (the result of test system). Second, new generating solutions may move into the infeasible solution of generation adequacy (constraints 3.23) and investment limitation (constraints 3.25). Finally, the global search diversifies the new solution with explored solutions. These explainations are the reasons for poor solution quality and slow convergence characteristics of the original algorithm.

4.2.2 Description of the hybrid CS-DP

To overcome the mentioned performance problems, the tailor-made method, so-called, "hybrid CS-DP" is proposed. The three techniques are introduced to improve the solution quality and convergence characteristics that are: (1) hybrid concept, (2) feasible search concept, and (3) memory exploration search. The main differences between CS and hybrid CS-DP are summarized in Table 4.4.

Table 4.4

The main differences between CS and hybrid CS-DP

Descriptions	Original CS	Hybrid CS-DP
Problem-solving structure	Generates a decision variable simultaneously	Encode decision variable as dummy and generate sequentially follow dynamic programming structure
Constraints handling	Convert hard constraints to soft constraint using the penalty approach [116]	Eq. (3.23) and Eq. (3.25) are managed using a feasible search concept; The remaining handle with hard constraints
Local search	Levy distribution [117]	Levy distribution with a feasible search concept
Exploration search	Uniform distribution	Memory exploration

A. Hybrid concept

The DP algorithm can solve the optimal solution but the computation time is very large; On the other hand, the cuckoo search can trade-off between solution quality and computation time. The hybrid concept combines the advantage between DP and CS, so-called "CS-DP structure" to overcome the computational complexity of combinatorial optimization. Figure 4.4 illustrates the general concept of the hybrid concept of CS-DP structure. In each state, the iterative search is a process to improve the solution quality. The objective value of each state is derived, and select the n^{th}-

nests for the next stage. The iteration counter is a parameter to control the spent time of the algorithm

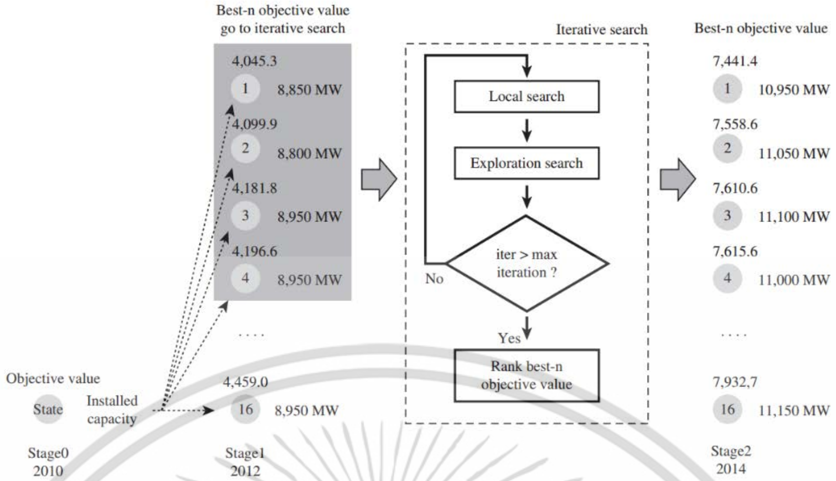

Figure 4.4 Hybrid concept based on cuckoo search and dynamic programming

B. Feasible search concept

In practice, the generation expansion planning is classified as NP-hard because it is observed a large-scale nonsmooth nonlinear function. For example, the decision spaces of the test system [101] in each state are 6 × 5 × 4 × 4 × 4 = 1920. Accordingly, the overall search spaces of 10 time stages are 1920^{10} = 6.81 × 10^{32} combinations. In this dissertation, the feasible search concept is introduced to cut-away the infeasible region of search space. Mathematically the equation can be stated as follows;

$$\mathrm{MinCap}_t = (1 + \mathrm{RM}^{\min})\mathrm{NL}_t - \mathrm{cap}_g X_g^{(t)} \qquad ,\forall t \in \mathcal{T} \quad (4.6)$$

$$\mathrm{MaxCap}_t = (1 + \mathrm{RM}^{\max})\mathrm{NL}_t - \mathrm{cap}_g X_g^{(t)} \qquad ,\forall t \in \mathcal{T} \quad (4.7)$$

where MinCap_t, MaxCap_t denotes the minimum and maximum requirement of new generating capacity [MW];

Figure 4.5 visualizes the feasible search concept mechanism which restricts the feasible region satisfying the adequacy Eq. (3.23) and construction limit Eq. (3.25).

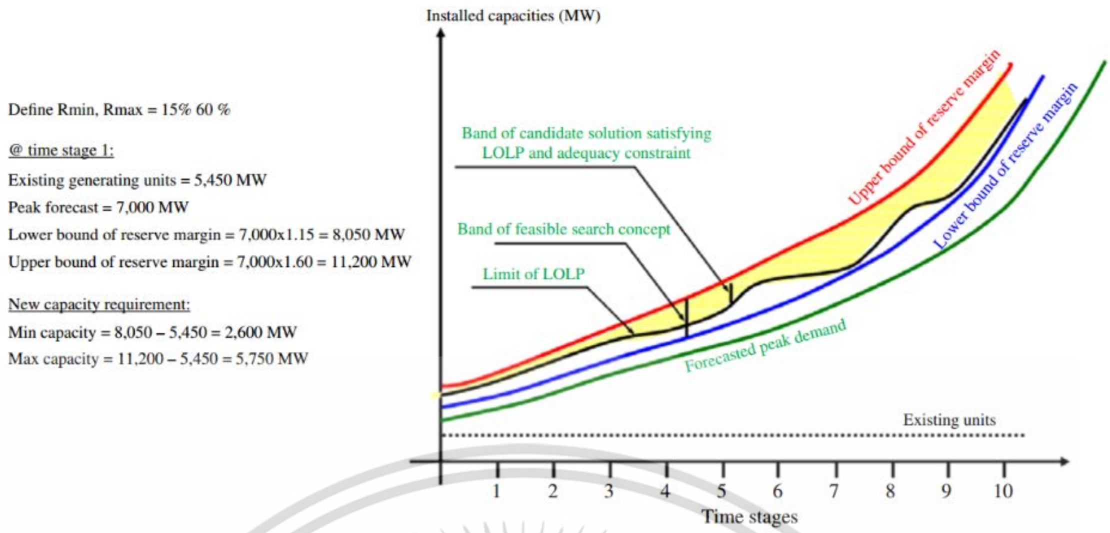

Figure 4.5 Concept of the feasible search concept

C. Memory exploration search

The exploration search using uniform distribution has a chance of repeated search in one-dimensional integer variables. Table 4.5 reports the example of the repeated candidate solutions (1 and 7 occur two times). To solve the repeated problem, the memory exploration search is proposed. The concept starts from (1) generate a set $[\mathcal{D}_1 \times \mathcal{D}_2 \times, \ldots, \mathcal{D}_{nn}]$, then check the remaining hard constraint (exclude adequacy and construction limit) for a feasible solution, (2) generate the memory table then shuffle the order randomly, (3) pick the number from memory table for the exploration search, and (4) delete the picked number, if the memory table is empty then stop the inner loop searching process.

Table 4.5

The example of exploration search using the uniform distribution for randomization

No.	1	2	3	4	5	6	7	8	9	10
Randomization	0.465	0.035	0.165	0.200	0.042	0.743	0.909	0.632	0.111	0.629
Discretize number	5	1	2	3	1	8	10	7	2	7

4.3 Example calculation for solving the deterministic GEP

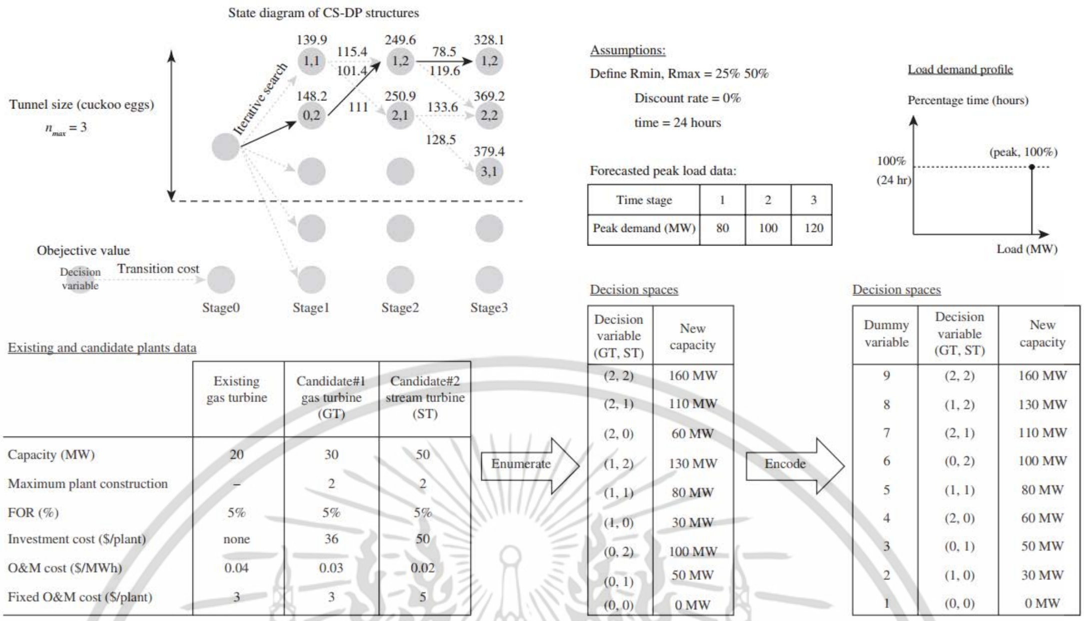

Figure 4.6 The simplest example for the hybrid CS-DP application

The simple example is adopted to describe the step-by-step hybrid CS-DP application for solving the deterministic GEP problem. The overall assumption is shown in Figure 4.6, the existing generation comprises the gas turbine; the candidate options are gas turbine (GT) and steam turbine (ST) to serve the flatten demand requirement. The state vector $X = [\text{Existing,GT,ST}]$ are containing the decision variables. The Bruteforce can analyze the algorithmic complexity as below equation;

$$\Theta = \prod_{c=1}^{G^C} (u_c^{max} + 1) \quad ,\forall c \quad (4.8)$$

where Θ denotes the growth of algorithm, e.g. decision spaces of each time stage are 3 × 3 = 9 combinations; So, the overall search spaces are $9^3 = 729$ combinations. The overall feasible solution of the problem is only six combinations after apply the feasible search concept (presented by dotted line graph in Figure 4.6). For simplicity, the salvage and outage costs are neglected. The fuel diversification and reliability constraints are omitted. Figure 4.7 presents the flowchart of the hybrid CS-DP algorithm. The step-by-step procedure can be described in the following steps:

Step 1. The assumption data are initialized such as the generation fleets, system load demand, and so on; The planning parameters are defined such as $\text{RM}^{\text{min}}, \text{RM}^{\text{max}}$ and so on; The parameters of hybrid CS-DP are set, i.e. maximum iteration $\mathbf{iter}^{\max}$, a maximum of host birds nt, and discovering probability $\mathbf{Prob}^{\text{discover}}$.

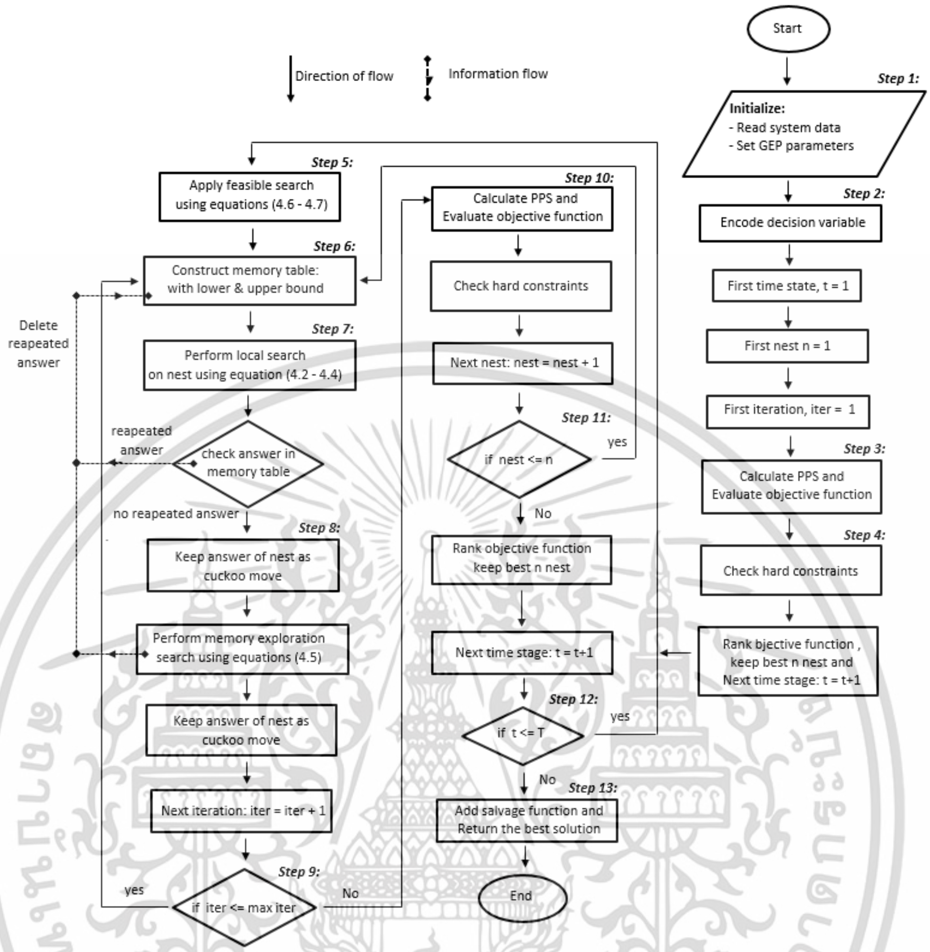

Figure 4.7 The simplest flowchart of hybrid CS-DP

Step 2. The decision variable is converted to the dummy space in the ascending order (the benefit of the dummy variable is provided in the literature [101]). First, enumerate all candidate options combinations and then calculate the total installed capacities. Lastly, rank the total capacities in the ascending order and then assign the numbers of dummy variables from the first to the last row. An example of dummy encoding is shown in Figure 4.7.

Table 4.6

An example of PPS calculation at time stage = 1

Decision variable	State variable	Expected energy served [MWh]				EENS [MWh]
		Existing	GT#1	ST#1	ST#2	
5	(1,1,1)	65	684	1,140	-	51.54
6	(1,0,2)	44.4	-	1,140	728	28.74

Step 3. For each time stages t, evaluate the probabilistic production simulation (PPS) based-on the equivalent energy function method. The LOLP and EENS are calculated according to Eq. (3.39-3.40). The example calculation of PPS using the EEF approach is demonstrated in Table 4.6.

Table 4.7

Example calculation of state diagram

Installed capacity	State variable	Decision spaces								minimum objective
		1	2	3	5	6	7	8	9	
$t = 1$										
120	(1,1,1)					148.3				148.3
100	(1,0,2)				139.9					139.9
$t = 2$										
150	(1,1,2)		249.6	255.3						249.6
130	(1,2,1)		250.9							250.9
$t = 3$										
180	(1,2,2)		369.2	384.5						369.2
160	(1,3,1)		379.4							379.4
150	(1,1,2)	328.1								328.1

Step 4. Check the hard constraints then rank the objective functions in the ascending order. The best $\boldsymbol{nt}$ nests are preserved for the next time stage. Increase the time stage, t = t + 1 and set the cuckoo nest, n = 1. Update the state diagram as detail in Table 4.7.

Step 5. Apply the *feasible search concept* using equation (4.6-4.7). For example, the minimum and maximum reserve requirements are the bound (80 × 1.25 = 100 MW, 80 × 1.5 = 120 MW). The minimum and maximum new capacity requirements are the bound (100–20 = 80 MW, 120–20 = 100 MW). The given dummy variable defines the feasible solution as the set {5,6}. These candidate solutions satisfied the adequacy and construction limit, simultaneously.

Step 6. Initialize the *memory table* for the first iteration (iter = 1). Otherwise, utilize the memory table to guide the new candidate solution for local and exploration search.

Step 7. Perform the local search using Eq. (4.2-4.4) with feasible search concept for the nest {5} at time stage = 2. The minimum and maximum reserve requirements are the bound [100× 1.25 = 125 MW, 100 × 1.5 = 150 MW]. The minimum and maximum new capacity requirements are the bound [125–100= 25 MW, 150–100 = 50 MW]. Therefore, the decision spaces of dummy variable {5} are the set {2,3}. The example calculation of local search is demonstrated as follows;

First, calculate σ^1 using Eq. (4.4) with $\bar{\beta}$ = 1.5 that gives results in Eq. (4.9). We have got $\mathrm{num}^1 \sim N(0, 69662^2)$ and $\mathrm{num}^2 \sim N(0, 1^2)$.

Second, random the two numbers with uniform distribution for the num^1 and num^2. For example, it is assumed that we got random numbers of 0.786 and 0.963. Therefore, the num^1 and num^2 generated numbers of 0.385 and 1.797, respectively.

$$\sigma^1 = \sqrt[\bar{\beta}]{\frac{\Gamma[1+1.5] \times \sin(\frac{3.14 \times 1.5}{2})}{\Gamma[\frac{1+1.5}{2}] \times 2 \times 1.5 \times 2^{(\frac{1.15-1}{2})}}} = 0.6966 \tag{4.9}$$

Third, the step length (SL) is calculated using Eq. (4.4) as in Eq. (4.10). If we assumed $U_1^{(1)} = 2$, we can calculate the new candidate solutions using Eq. (4.2) as in Eq. (4.10). Finally, we apply discretization using 2.26, we derived a decision variable = 2. Check repeated search, if any candidate solutions are repeated, then delete it from the memory table and try local search again. Otherwise, go to the next step.

$$U_1^{(2)} = U_1^{(1)} + \alpha \text{ Levy} = 2 + 1(0.26) = 2.26 \tag{4.10}$$

Step 8. Perform the memory exploration search using Eq. (4.5). For example, it is assumed that we got a number of 0.158, then exploration search is active. The memory exploration search guides the decision space {3}. Finally, check the repeated search the same as Step 7 and increase iteration, iter = iter + 1. Update the state diagram as detail in Table 4.7.

Step 9. Check maximum iteration. If $\mathrm{iter} \le \mathrm{iter}^{\max}$ go back to Step 6. Otherwise, go to Step 10.

Step 10. Calculate PPS and objective function the same concepts as Step 3. Check hard constraints the same concepts as Step 4. Change to the next nest, $\mathrm{n} = \mathrm{n} + 1$.

Step 11. Check the maximum nest. If $\mathrm{n} \le nt$, go back to Step 5 and reset iteration. Otherwise, evaluate the optimal path using bellman's equation Eq. (4.11), increase time stage t = t + 1 and go to Step 12.

$$Z(s)^{(t-1)} = \min_{d\in\mathcal{D}}\{ Z^{(t-1)}(s^{*}) + z(d)\} \qquad \forall t \in \mathcal{T}, \forall s \in \mathcal{S} (4.11)$$

where $Z_t(s)$ denotes the forward bellman's equation of objective function at state s, time stage t; $d \in \mathcal{D}$ represents the decision space from the possible previous time stage to time stage t correspond to $Z_{t-1}(s^{*})$ which means the optimal path at time stage t.

Step 12. Check the maximum time stages. If $t \leq \mathrm{T}$, go back to the Step 5, reset nest ($\mathrm{n} = 1$) and iteration (iter = 1). Otherwise, go to Step 13.

Step 13. Calculate salvage function using Eq. (3.21). Recalculate objective function and rank it in the ascending order. Finally, Figure 4.7 shows the state diagram for the overall example results and complete bellman's equation is tabulated in Table 4.7.

4.4 Study Case 2: An efficient hybrid CS-DP application for deterministic GEP

4.4.1 Case study descriptions

Objective

To develop an efficient metaheuristic approach for stochastic optimization

Problem formulation

The compact formulation of the multistage GEP considering generating reliability without external cost consideration (**GEP-II**) is:

$$\begin{aligned} &\min \quad (3.15) - (3.18), (3.20) - (3.21) \\ &\text{s.t.} \quad (3.23 - 3.26) \qquad\qquad \forall g \in \mathcal{G} \end{aligned}$$

Problem descriptions

In this chapter, the scaled-down Korea's generation system, provided in the Appendix (test system 2) is used to confirm the effectiveness of the proposed method. The initial existing capacity is 5,450 MW. There are 5 candidates (200-MW oil, 450-MW LNG combined cycle, 500-MW coal, 1,000-MW nuclear and 700-MW nuclear). The test cases are described as follows;

Test case 1: This case follows the assumptions in reference [101]; the planning period is set 14-year planning horizon; The number of trial experiments is set 100 trial run within 600 seconds.

Test case 2: This alternative case represents the long-term planning in a 20-year planning horizon; Unfortunately, the global optimal solution cannot be found within a reasonable time (more than 30 days); For this reason, the number of trial experiments is set 30 trial run within 800 seconds.

4.4.2 Empirical results

i) **Solution quality:** The best results obtained from the proposed method is compared with those from the famous journal (only 14-year planning horizon) and own programming (20-year planning horizon). It should be noted that the results obtained by DP, TCDP and Year-Year method represent global optimal, near-optimul and the fastest solutions, respectively. Table 4.8 clearly shows the 14-planning comparative details that the proposed method and GA-direct search are successful to find the global optimal solution. In the case of a 20-year planning horizon, the proposed method success to find the best-found solution (best results among the other methods) comparing to other methods (author program as it own).

Table 4.8

Best results comparasion among different appraoches

Methods	Cumulative discounted cost (million dollar)	
	Test case 1: 14-year planning horizon	Test case 2: 20-year planning horizon
Dynamic programming (DP)	14,896.9	N/A**
Tunnel-constrained DP (TCDP)	14,905.2	19,615.1***
Year-Year	15,001.2	19,735.5***
Genetics algorithm (GA)	*14,922.2	19,958.4***
Differential Evolution	*14,922.2	N/A**
Evolutionary programming	*14,958.4	N/A**
Expert system	*14,926.3	N/A**
Simulated annealing	*14,939.3	N/A**
Tabu search	*14,983.7	N/A**
GA-direct search [17]	*14,896.9	N/A**
Cuckoo search (CS)	15,022.5	19,860.3***
Hybrid CS-DP	**14,896.9**	**19,602.6**

* The best results are converted by using %Error, ** N/A means not applicable,

*** Author program as its own.

The cumulative capacity of optimal plans (CS and CS-DP) is provided in Figure 4.8. We can see the installed capacity satisfying the minimum and maximum reserve margins. Furthermore, the LNG-fired are retired in the end of the study period. Table 4.9 shows the optimal plan using a hybrid CS-DP approach for solving **GEP-II** with a deterministic model.

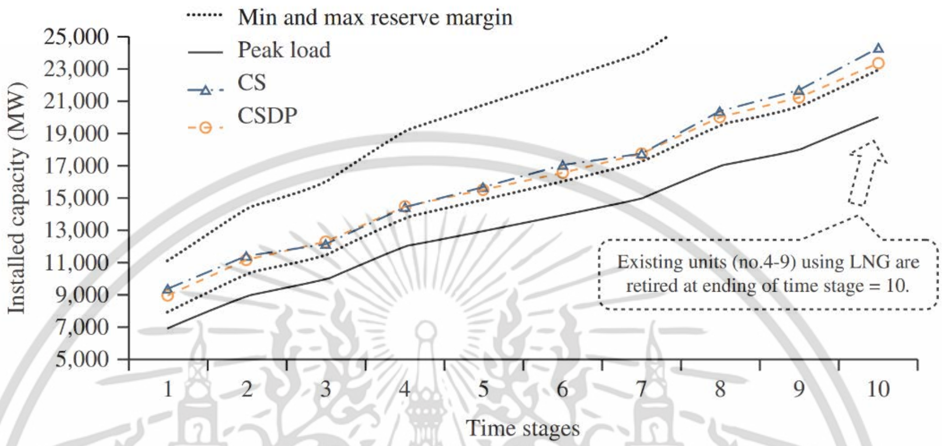

Figure 4.8 Cumulative capacity of optimal plans (CS and CS-DP)

Table 4.9

Optimal plan using hybrid CS-DP approach

Year	Candidate plants					New capacity (MW)	Installed capacity (MW)
	Oil (200 MW)	LNG (450 MW)	Coal (500 MW)	PWR (1,000 MW)	PHWR (700 MW)		
1998	3 (3)*	2 (2)	2 (2)	1 (1)	0 (0)	3,500	8,950
2000	1 (1)	0 (0)	2 (2)	1 (1)	0 (0)	2,200	11,150
2002	1 (1)	1 (1)	1 (1)	0 (0)	0 (0)	1,150	12,300
2004	1 (1)	1 (1)	1 (1)	1 (1)	0 (0)	2,150	14,450
2006	3 (3)	0 (0)	1 (1)	0 (0)	0 (0)	1,100	15,550
2008	3 (3)	1 (1)	0 (0)	0 (0)	0 (0)	1,050	16,660
2010	1 (1)	0 (0)	0 (0)	1 (1)	0 (0)	1,200	17,800
2012	1	1	3	0	0	2,150	19,950
2014	1	0	0	1	0	1,200	21,150
2016	1	1	3	0	0	2,150	23,300

* The figures within parenthesis denote the result of case1.

ii) **Solution robustness:** After performing the trial run experiments, the robustness of the proposed method is evaluated using statistical results (best, worst, average and standard deviation). Table 4.10 clearly shows that the proposed method has a better result than other methods with a 72% success rate (probability to find global optimum solution). Table 4.11 evidently shows that the proposed method achieves the best-found solution with a 0.06% improvement comparing to the second-best solution of TCDP.

Table 4.10

Comparison of solution robustness for case 1

Methods	Cumulative discounted cost (million dollar)					
	Best	Worst	Avg	Std Dev	%Error	%SR
DP	14,896.9	14,896.9	14,896.9	0	0.00%	100%
TCDP	14,905.2	14,905.2	14,905.2	0	0.06%	0%
Year-Year	15,001.2	15,001.2	15,001.2	0	0.70%	0%
GA	15,081.7	15,404.3	15,220.0	79.48	1.24%	0%
CS	15,022.5	15,378.7	15,194.3	74.85	0.84%	0%
CS-DP	**14,896.9**	**14,905.0**	**14,897.6**	**1.84**	**0.00%**	**72%**

Table 4.11

Comparison of solution robustness for case 2

Methods	Cumulative discounted cost (million dollar)				
	Best	Worst	Avg	Std Dev	%Error
DP	N/A*	N/A	N/A	N/A	N/A
TCDP	19,615.1	19,615.1	19,615.1	0	0.06%
Year-Year	19,735.5	19,735.5	19,735.5	0	0.68%
GA	19,958.4	20,230.4	20,052.4	74.33	1.81%
CS	19,860.3	20,284.9	20,052.0	101.35	1.31%
CS-DP	**19,602.6**	**19,604.9**	**19,603.3**	**0.80**	**0.00%**

* N/A means result not available due to long computational time.

iii) **Convergence characteristics:** After performing the trial experiments, the convergence characteristics of the proposed method is evaluated. Figure 4.9 indicates that the proposed method reaches the global optimal solution faster than other methods while other methods being trapped with local optimum. Figure 4.10 reports that the convergence characteristics of the proposed method reaches the best-found solution faster than other methods.

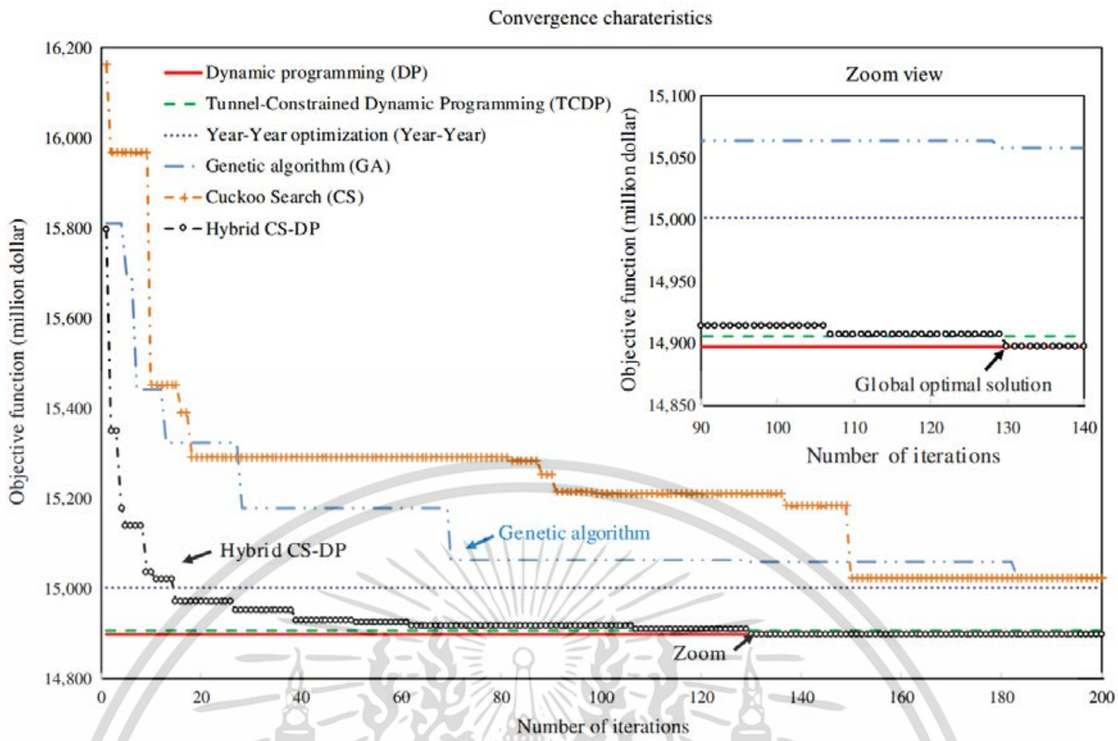

Figure 4.9 The convergence characteristic of case1

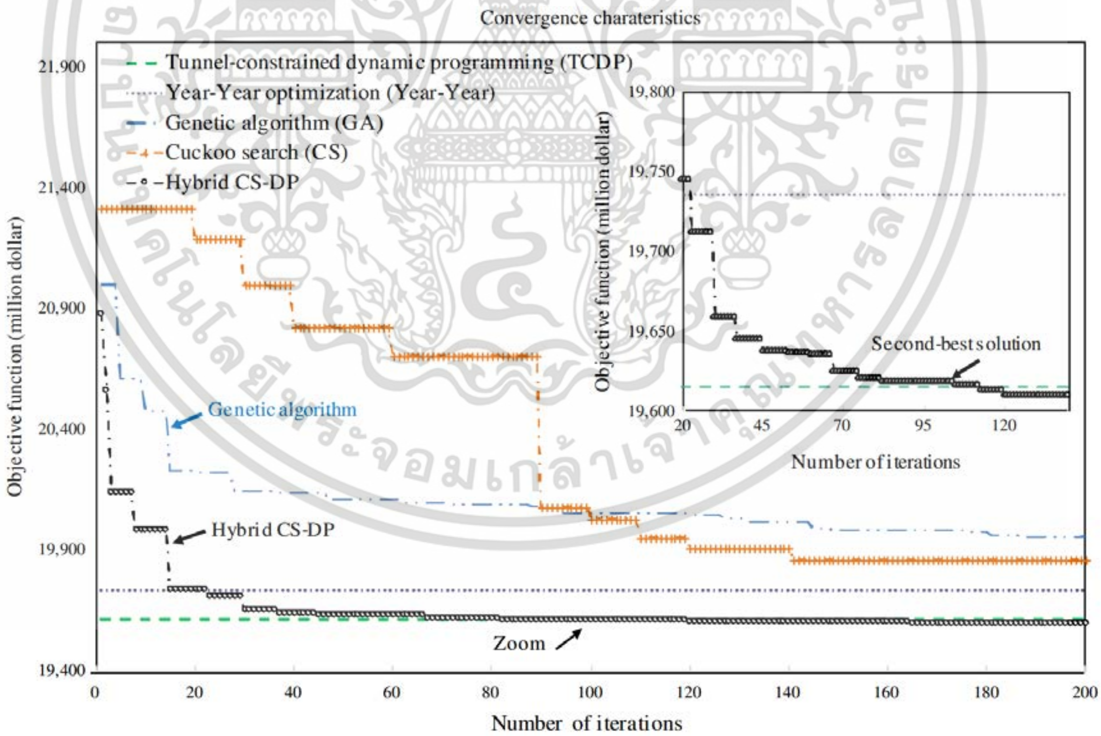

Figure 4.10 The convergence characteristic of case2

iv) **The complexity of algorithm:** The computational time comparison is depicted in Figure 4.11. The DP's result is referred to as the time resource to reach the optimal global solution. Since the **GEP-II** is recognized as NP-hard (solution cannot be found in polynomial time), the computational time will grow when the problem size increases. Figure 4.12 shows that the complexity of DP observes the exponential function, conversely the proposed method observes linear function.

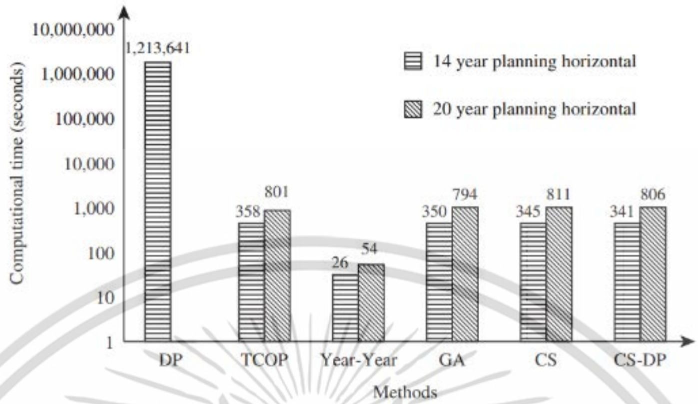

Figure 4.11 The computational time comparison

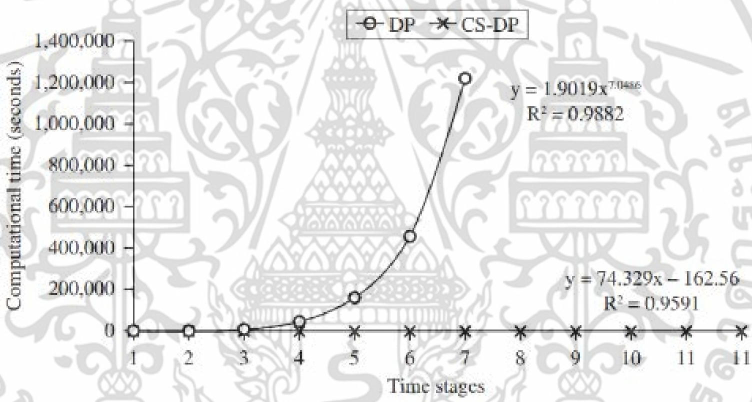

Figure 4.12 The complexity of proposed method

4.5 Conclusions

In this chapter, the development of metaheuristic method, namely "hybrid CS-DP" is described. The proposed method combines the advantages between dynamic programming (DP) and cuckoo search (CS) to solve the **GEP-II** while satisfying the constraints, i.e. energy mix requirement, generation adequacy, new power plant limitation and generation reliability.

The proposed method implements three efficient techniques to improve solution quality and convergence characteristics. First, the CS-DP structure solves the optimum solution under a reasonable time, regardless of the dimensional problem. Second, the feasible search concept succeeds to eliminate infeasible solutions from the searching process. Finally, the repeated search problem is solved after applying the memory exploration search. The test results confirm the effectiveness of practical metaheuristic approach.

Chapter 5

Stochastic Model for PDP

In real life, the policy-maker has to make the decision under risk and uncertainty [118]. The long-term electricity planning inherently observes the political-, economic-, social-, technological-, legal- and environmental-risks depending on the regime of the country [119]. For instance, the volatility of natural gas price induces the investment risk [120] of the natural gas-fired power plant which observes high capital expenditures (CAPEX) and medium operational expenditures (OPEX); The raising fuel price may lead the investment decision to phase-in the renewable energy [121], i.e. wind and solar PV, which LCOE can compete with the natural gas-fired power plant. In contradictory, the downward natural gas price may lead the investment decision to continue the natural gas-fired power plants [122]. Accounting the possible risks into the long-term electricity planning make the generation expansion plan more robust [123].

In the same way, fossil price uncertainty [124] and fuel availability [125] influences climate policy considerations, i.e. carbon tax scheme [126] and emission trading scheme [127]. In the case of the carbon tax scheme, the social cost of carbon is the main parameter for the switching effect [128] (changing the energy from carbon-intensive power plants to zero-emission power plants). The fuel price fluctuation distorts the “here-and-now” decision [129] which new power plants are constructed before uncertainty is realized. In the case of emission trading scheme, the risk of fluctuating fossil fuel costs may intervene the cap-and-trade target.

In this chapter, the Simheuristic approach is proposed to solve Thailand generation expansion planning considering fuel price uncertainty. This chapter is organized as (1) the introduction for stochastic optimization, (2) the development of proposed Simheuristics approach, (3) the insight-details of fuel price modeling with mean-reversion property, (4) the study case of Thailand electricity planning based-on official PDP2015, and (5) conclusion.

5.1 Stochastic Model for PDP

5.1.1 Stochastic optimization

A. General definition

Considering the six-times tossing of a die, each result of tossing is called *event* A, and the set containing the all possible outcomes, called *sample spaces* denoted by Ω. The combined outcomes that contain a die result in even number, denoted by $\mathcal{A}$, thus $A \in \mathcal{A}$ and $\mathcal{A} \subset \Omega$. The useful probability theories can be recalled, $\mathcal{P}(\emptyset) = 0$, $\mathcal{P}(\Omega) = 0$, $0 \leq \mathcal{P}(A) \leq 1$ and so on. We can define the *probability space* $(\Omega, \mathcal{A}, \mathcal{P})$ is a tripet of sample space Ω of all possible events $\mathcal{A}$ with a specified probability $\mathcal{P}$.

Refer to stochastic optimization, we consider the parameters of the optimization problem as *random variable* denoted by ξ to capture the uncertainty, e.g the possible outcomes of spot natural gas price, $\Omega \in \{\xi_1, \xi_2, ..\xi_5\}$. Let $\mathcal{F}$ be the domain of all feasible region. The compact model can be expressed as:

$$\min_{U \in \mathcal{F}} \quad \mathcal{Z} = \mathbb{E}\left[\mathcal{Z}(U, \xi)\right] \tag{5.1}$$

$$\text{subject to} \quad \varphi_i(U, \xi) \leq l_i, \qquad \forall i = 1,2, ..nd \tag{5.2}$$

$$\Psi_j(U, \xi) \leq r_j, \qquad \forall j = 1,2, ..np \tag{5.3}$$

where $\mathcal{Z}: \mathbb{R} \times \Omega \rightarrow \mathbb{R}$, the expected value $\mathbb{E}\left[\mathcal{Z}(U, \xi)\right]$ is derived from decision variables U and random variable ξ with specified probability $\mathcal{P}$ on the sample space $(\Omega, \mathcal{A})$; $\mathcal{F}$ denotes discrete space of feasible solutions; Equation (5.2) represents the probabilistic constraints relating to the specific problem; l_i denotes the probabilistic threshold, e.g. the outage probability should less than 0.00274; Equation (5.3) represents the typical deterministic constraints in combinatorial optimization; r_j denotes the planning parameters/constants; nd is a number of deterministic constraints and np is a number of probabilistic constraints.

B. Literature reviews

The birth of Stochastic optimization has to go back for more than 50 years. The researchers divide the algorithm-solving strategies are that: (1) the analytic methods solving the problem with a "pencil and a paper" based on mathematical theories; The result provides the generic solutions for any value of parameters, and (2) the simulation-based methods solving the problem as a deterministic equivalent model via different scenarios. Table 5.1 summarized the solving methods in the field of stochastic optimization. In practice, the simulation-based approach dominates the analytic methods because of flexibility and tractability.

Table 5.1

Literature reviews for solving stochastic GEP

Algorithm-solving strategies	Methods
Analytic methods	Two-stage recourse optimization [130], chance-programming [131], real option [132], mean-variance portfolio [133]
Simulation-based methods	Scenario tree [134], Sample-path optimization [135], Scenario-based optimization [136], Sensitivity [34],

5.1.2 Simheuristic approach

A. General description

Simheuristic approach [37] is stochastic optimization which combines the simulation-based optimization with the metaheurisric-driven search. The advantage of this method is to overcome the *curse of dimensionality* which problem size increases exponentially when the scenario increases. The current application is found only in transmission planning [137]. This is an opportunity to apply the Simheuristics in generation expansion planning.

B. Pseudocode

The pseudocode of the original simheuristic algorithm is summarized in Table 5.2. The detailed explanations of simulation-based and metaheuristic optimization are presented in section C and section D.

C. Simulation-based optimization

The role of simulation-based optimization [138] is a process to simulate the sample-path scenario and interact with the metaheuristic-driven search. The sampling techniques can be categorized into two approaches for simulation optimization. One approach uses sampling in an "interior" fashion [139]. The original stochastic problem is solved (sample while solving) with embedded different samples in each iteration. Another approach uses sampling in an "exterior" fashion (sample then solve). The complex stochastic optimization is transformed into an equivalent deterministic scenario and then solve it.

Table 5.2

Pseudocode of Simheuristic algorithm

Begin
Stochastic optimization be transformed into an equivalent deterministic scenario;
Simulation-based optimization generates sample-path scenarios $ns^{\max}$;
Perform simplification process using simple average scenario;
While $[ns < ns^{\max}]$ or [stopping criterion]
Scenario identification verifies the impact scenario;
Efficient metaheuristic approach solves the deterministic equivalent scenarios;
The promising solution is kept for risk analysis;
End while
Perform risk analysis;
Perform decision-making process;

The original Simheuristic aims to solve the stochastic problem in a deterministic fashion; the only impact scenarios are sent to the metaheuristic driven-search. It should be noted that the optimal solution of the deterministic equivalent does not need to be the optimal solution for the stochastic problem. However, it is observed that the simple average scenario tends to be a high-quality solution for the practical stochastic problem [37]. The interaction between simulation-based and metaheuristic-driven optimizations are depicted in Figure 5.1.

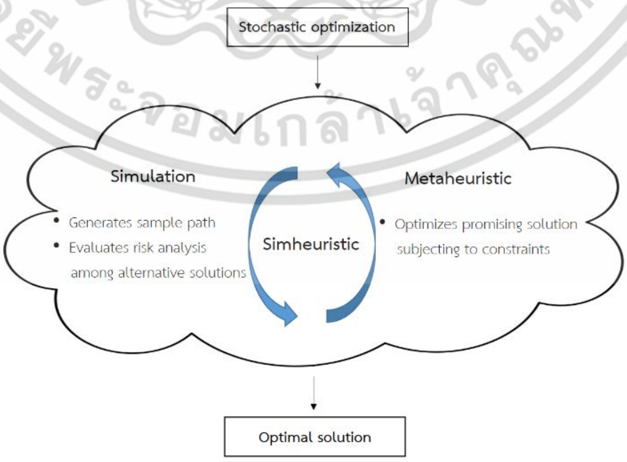

Figure 5.1 Interaction between simulation and metaheuristic-driven search.

D. Metaheuristic-driven optimization

The role of metaheuristic optimization is a process to search the compromising solutions for each sample-path scenario (it should be noted that the simulation is not a solving method as its own). This technique is similar to the *sample-path optimization* [135], for example, all random variables are replaced by the expected value to form the most likely scenario. Then the metaheuristic algorithm performs an iterative search to find a compromising solution of the original stochastic problem. This dissertation, the hybrid CSDP is adopted as an efficient metaheuristic approach due to the good tradeoff between the intensification and diversification process.

5.2 Proposed Simheuristic approach

Even if the Simheuristics is recognized as an efficient stochastic optimization that comes up with simulation-based optimization and metaheuristic driven-search. The original Simheuristics has practical limitations. First, monte carlo sampling requires so many samplings numbers to converge to the true expected and variance values. Second, a compromising solution derived from the average sample-path may not hedge to the critical scenario. Another representative scenario is required to provide moderate information for sample-path optimization. Finally, the decision-making based on the sample average approximation suits for risk neutrality; Generally, decision-maker is risk-aversion who cares the extreme scenario [140]. All of these explanations, the reasons for poor solution quality and computational expensive of the original algorithm.

5.2.1 Improved simulation process

A. The convergence of monte carlo sampling

Even if the simulation process using *monte carlo sampling* is practical to solve stochastic optimization. The drawback of monte carlo sampling is computationally expensive. The convergence performance can be stated as follows:

$$\Theta = \frac{1}{\sqrt{\mathrm{ns}}} \tag{5.4}$$

where Θ denotes the big-o notation of algorithm; $\mathrm{ns} \in \mathbb{R}_+$ represents the number of sampling scenarios; This equation implies that more 10 times faster convergence, more 100 times sampling numbers are required; The in-depth performance of monte-carlo sampling can be described by the *sample average approximation* principle [141].

Once we try to solve the equation (5.1) with exterior sampling. We generate a random sample $\xi_1, \xi_2, .. \xi_{\mathrm{ns}} \sim \mathcal{P}$ of ns realizations. The expectation $\mathbb{E}[z(U, \xi)]$ of equation (1) based on *sample average approximation* is provided as follows;

$$\hat{\mathcal{Z}}(U) := \frac{1}{\mathrm{ns}} \sum_{i=1}^{\mathrm{ns}} \mathcal{Z}(U, \xi_i) \tag{5.5}$$

$$Var(\mathrm{ns}) = \frac{{\sigma_{SAA}}^2}{\mathrm{ns}} \tag{5.6}$$

where $\hat{\mathcal{Z}}$ represents sample average approximation of stochastic cost function; $Var(\mathrm{ns})$ denotes the variance of the sampling distribution; $\mathrm{ns} \in \mathbb{R}_+$ represents the number of sampling or scenarios.

Let consider the rate of convergence of *sampling average approximation* [142]. $\mathcal{Z}^*$ and U^* be the optimal objective function and set of the optimal solution, respectively; In parallel, $\hat{\mathcal{Z}}^*$ and $\hat{U}^*$ be the estimation of optimal value and solution, respectively; The central limit theorem state that as $\mathrm{ns} \to \infty$, the sampling distribution tends to the unit normal distribution $N(0,1)$; Simultaneously, the theory of large number state that as $\mathrm{ns} \to \infty$, the sample mean converge to actual mean at a rate of $\Theta = {}^{1}/_{\sqrt{ns}}$; The sampling mean lie within the confidence intervals $(1 - \alpha^{\mathrm{CI}})$ as below;

$$\hat{\mathcal{Z}} \pm Z^{\mathrm{score}}_{\alpha^{\mathrm{CI}}/2} \frac{\sigma_{SAA}}{\sqrt{ns}} \tag{5.7}$$

where $\mathrm{Z}^{\mathrm{score}}$ denotes the standard score of the sample mean; σ_{SAA} denotes the standard deviation of sampling; $\boldsymbol{\alpha}^{\mathrm{CI}}$ denotes the significance value respecting to the confidence interval, for example, if $\alpha^{\mathrm{CI}} = 0.05$, thus $Z^{\mathrm{score}}_{0.025} = 1.96$.

B. Quasi monte-carlo simulation

Instead of monte carlo sampling, quasi-random sequences (sometimes called low-discrepancy sequences) [143] is used to replaced the uniform distribution in the sampling process. In reality, the name *quasi-random sequence* may be misleading because it is derived from a deterministic sequence. There are several low-discrepancy sequences, such as Halton [144], Faure [145], Neiderreiter [146], Van der Corput [147], and Sobol [148] are applied for quasi monte-carlo approach.

In this dissertation, the Sobol sequence (Sob) introduced by Ilya N. Sobol' [148], is utilized for a high multi-dimensional low discrepancy sequence. In the research area of the power system, Sobol sequence is applied in many fields such as transient stability [149], economic dispatch [150] and so on. The Sob generates successively a sequence between zero to one over d-dimensional space by a primitive polynomial of the following form:

$$\text{eqn} = A^{\text{degree}} + a_1 A^{\text{degree}-1} + a_2 A^{\text{degree}-2} + \cdots + a_{\text{degree}-1} A + A^0 \quad (5.8)$$

where eqn represents the primitive polynomial equation with coefficients $(a_1, a_2, \ldots a_{\text{degree}-1})$ are eigher 0 or 1; The coefficients of A^{degree} and A are unity.

Table 5.3 demonstrates the statistical estimation of renowned sequences for one-dimensional sequences.

Table 5.3

Statistical estimation comparison of one-dimension under 1,000 sampling point

	Uniform distribution	Pseudo-random	van der Corput	Sobol sequence
Minimum	0	0.000008	0.000098	0
Maximum	1	0.999004	0.998047	0.998047
Mean	0.5	0.492246	0.498866	0.498773
Median	0.5	0.484037	0.498047	0.499023
Standard deviation	0.288675	0.2851	0.288661	0.288806
Variance	0.083333	0.0813	0.083325	0.083409
Skewness	0	0.039117	0.000204	0.000030
Kurtosis	1.8	1.833361	1.794803	-1.20022

Figure 5.2 illustrates the advantage of the Sobol sequence. We can observe that the convergence rate can improve from $\Theta = {}^{1}/_{\sqrt{ns}}$ to $\Theta = {}^{1}/_{ns}$.

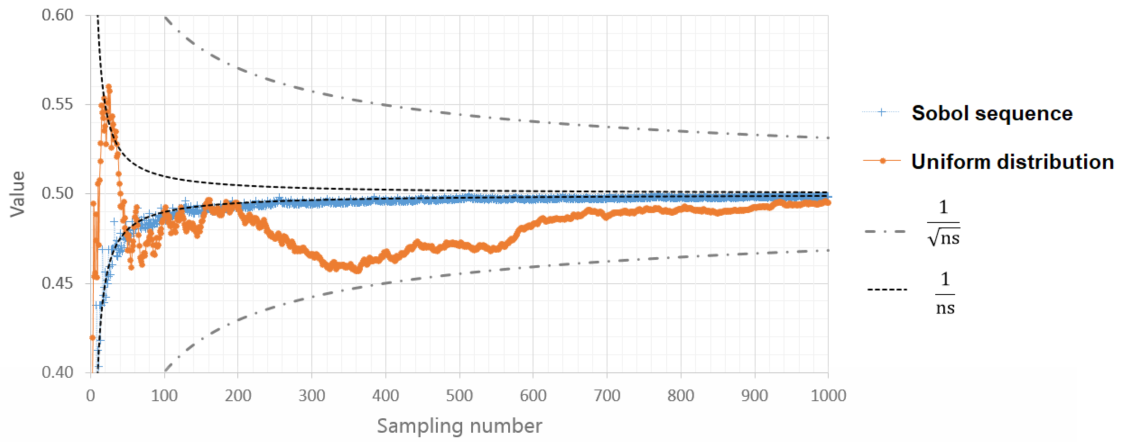

Figure 5.2 The convergence of 1,000 samples using pseudo-random number, and the Sobol sequence.

In the case of high dimensional sequences, the issue "filling the gaps" is a major drawback. The low-discrepancy sequences are needed to generate the new numbers over the whole region and avoid the clustering point. Figure 5.6 demonstrates the comparison between the uniform distribution and the Sobol. Moreover, the performances of the Sobol sequence are fast convergence and good accuracy.

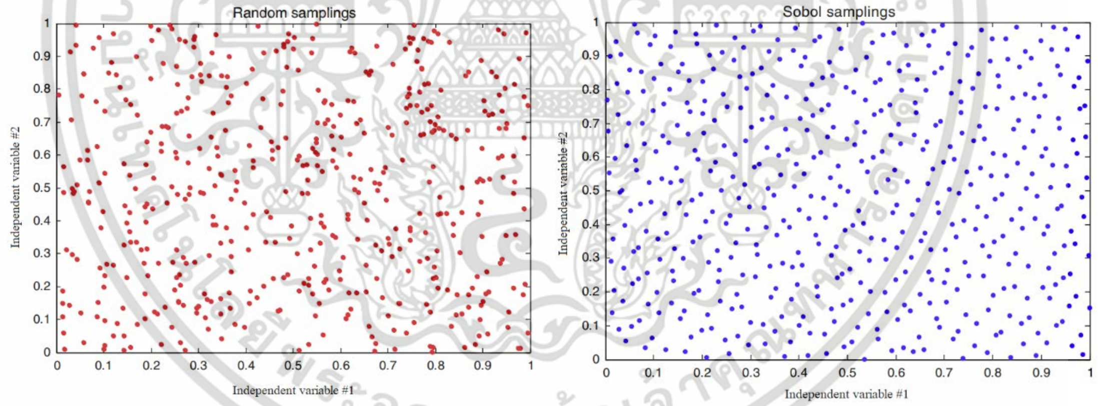

Figure 5.3 The 500 samples using pseudo-random number and Sobol sequence, adopt from [147]

5.2.2 Improved simplification process

A. The flaw of averages

The stochastic optimization using the average scenario may lead to "the flaw of averages" [151] which the single-point estimation obscures the uncertainty in the data. Figure 5.4 depicts the drunk man (represents random walk of the one-dimensionality) walking along the road; the central line (represents the mean value of randomization) separates the road to two one-way road. We can observe that the state of his average position is alive, but the average state of the drunk man is dead.

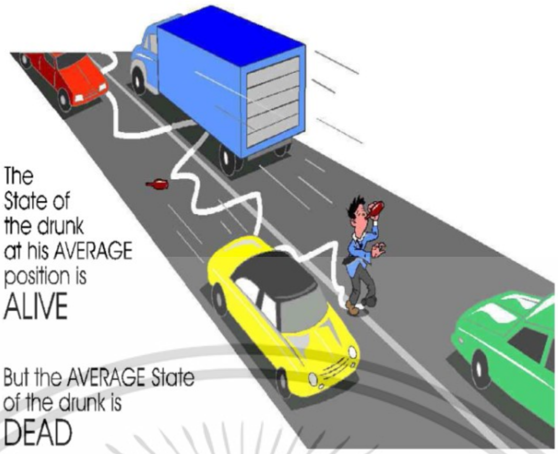

Figure 5.4 The flaw of average, adopted from [151]

B. Scenario aggregation using quantile for sample-path optimization

As a previous explanation, the simple average scenario may fall in the pitfall [151] and, the worst-case scenario may too conservative since it may never be realized in practice [152]. In this section, we propose the *scenario aggregation using quantile* to provide an effective scenario by using end-point quantile partitioning for sample-path optimization. This idea is similar to the scenario bucket in [153]. This approach comprises two steps: (1) quantile partitioning, and (2) scenario aggregation.

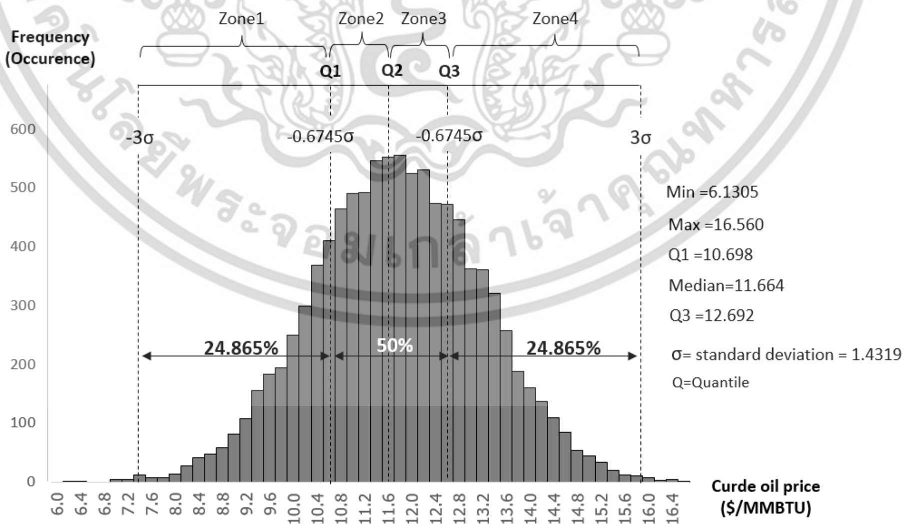

Figure 5.5 The aggregate crude oil price using a quantile classification

First, we describe how simulated scenarios can be partitioned using quantile. For example, Figure 5.5 shows histograms of the 25% quantile, median, 75% quantile as well as 0.27% quantile (both tails end). Second, the partitioning scenarios are aggregated based on Cartesian products of several sets. Table 5.4 demonstrates the aggregated scenarios of crude oil and natural gas prices by using Zone2 and Zone3 of the quantile. Finally, the alternative solutions are solved based on the aggregate scenarios to derive critical information covering risk and uncertainty. Identical alternative solutions are diminished. The remaining solutions are sent for representative solutions in the next process.

Table 5.4

Example of the aggregate scenario using quantile mapping

Aggregated Scenarios	Spot price [$/MMBTU]		Quantile mapping		Sample-path optimization
	Crude oil	Natural gas	Crude oil	Natural gas	
1	11.342	3.358	Zone2	Zone2	Sol#1
2	11.586	3.787	Zone2	Zone3	Sol#2
3	12.125	3.468	Zone3	Zone2	Sol#3
4	12.086	4.028	Zone3	Zone3	Sol#1

Remark: *Sol* denotes alternative solution

5.2.3 Efficient decision-making under risk and uncertainty

A. Risk preference

To understand the risk preference, it is assumed that we have two alternatives: (1) we do nothing and accept 500 baht, and (2) we need to play a "heads or tails" which if winning we will receive a prize of 1,000 baht, otherwise we receive nothing. It is noticed that the expected value of "heads or tails" game equal to surely 500-baht acceptance. It is different that the first alternative relates to the probability (risk) to gain/lose the reward, otherwise the second alternative is certainty way. The risk attitudes of decision-makers are divided into 3 types: (1) you are *risk-aversion* if you prefer the first alternative, (2) you are *risk-loving* if you prefer the second alternative, and (3) you are *risk-neutrality* if you are indifferent (either first- or second-alternative). We can measure how risk-averse you are by changing the surely offer money as Table 5.5.

Table 5.5

Decision-making choice based on risk attitude

Decision making attitude	Surely offer money [baht]									
	100	200	300	400	500	600	700	800	900	1,000
Risk-aversion	Alt2	Alt2	Alt2	Alt2	Alt1	Alt1	Alt1	Alt1	Alt1	Alt1
Risk-neutral	Alt2	Alt2	Alt2	Alt2	Alt1, Alt2	Alt1	Alt1	Alt1	Alt1	Alt1
Risk-lover	Alt2	Alt2	Alt2	Alt2	Alt2	Alt2	Alt2	Alt2	Alt2	Alt1

Remark: Alt1 denotes first alternative is chosen, Alt2 denotes second alternative is chosen

We can summarize the risk preference as three types:

Risk-neutrality: The instrumental decision-making which appropriates with the risk-neutrality is sample average approximation. This approach is described in Eq. (5.5-5.6) to minimize the expected cost across the individual scenarios.

Risk-aversion: Generally, the decision-makers are risk-averse behavior, i.e. they prefer a sure outcome over the uncertain outcome for the same expected benefits. They may prefer a less benefit with the lower risk. The instrumental decision-making corresponds to the risk-aversion are conditional value-at-risk [36], and minimizing the maximum regret [154].

Risk-lover: This risk attitude represents the gambler.

B. Minimizing the maximum regret for risk aversion

The decision approach that suits the risk-aversion is known as *maximum regret minimization* [155] (minimum regret maximization for a profit maximation problem). The "regret" is also called "worst-case avoidance" for the cost minimization problem or "opportunity loss" for profit maximation problem. We now describe the example calculation of minimum regret. It is assumed that we have two sample-paths with a certain probability (P1 with probability 0.1 and P2 with probability 0.9). Table 5.6 provides the costs if each alternative solution is decided. The regret score can be calculated based on the minimum cost of each sample-path, for example if P1 happens (the alternative solution is decided), then we have regret of 100-$40 = $60. We can do it in the same manner to fulfill Table 5.6. Finally, the maximum regret with respect to alternative solution 1 is decided is max {$60, $0} = $60; for alternative solution 2 is 35; for alternative solution 3 is $20. Based on instrumental decision-making, i.e. worst-case approach, sample-average approximation, and minimax regret. The risk analysis can be summarized: first, if the decision-maker is avoiding the worst-case event (low- probability high impact), the alternative solution number 2 is preferred; Second, if the decision-maker is risk-averse (avoid the less-likely high risk), the alternative solution number 3 is preferred; Third, if decision-maker is risk-neutral (equally accept the risk), the alternative solution number 1 is preferred.

Table 5.6

Example calculation of decision-making under uncertainty

Sample path	Probability	Cost				Regret score		
		Alt1	Alt2	Alt3	min	Alt1	Alt2	Alt3
P1	0.1	100	40	60	40	60	0	20
P2	0.9	20	55	30	20	0	35	10
Expected cost		28	54	33				
Maximum cost		100	55	60				
Maximum regret		60	35	20				

Remark: Alt denotes the alternative solution, P denotes the sample path

In this section, the mathematical formulation of min-max decision is reviewed. Equation 5.9 defines the regret score among the different discrete scenarios $\omega \in \Omega$ relateing to the uncertainty set $\xi = (\xi_1, \xi_2, \dots, \xi_\omega)$; Equation 5.10 states the optimal performance of each alternative $U \in \mathcal{F}$ corresponding to realization ω.

$$\text{Regret}(U, \omega) = |\mathcal{Z}(U, \xi_\omega) - U^*_\omega| \quad (5.9)$$

$$U^*_\omega = \min_{U \in \mathcal{F}} \mathcal{Z}(U, \xi_\omega) \quad (5.10)$$

Finally, we can calculate the mini max regret as following:

$$U^{\text{mini-max}} = \min_{U \in \mathcal{F}} \max_{\omega \in \Omega} \text{Regret}(U, \omega) \quad (5.11)$$

where $U^{\text{mini-max}}$ represents min- max decision of each alternative among different scenarios; $\text{Regret}(U, \omega)$ denotes the regret function of alternative U under discrete scenario ω.

5.2.4 Proposed framework

The simplest framework is shown in Figure 5.6 as below.

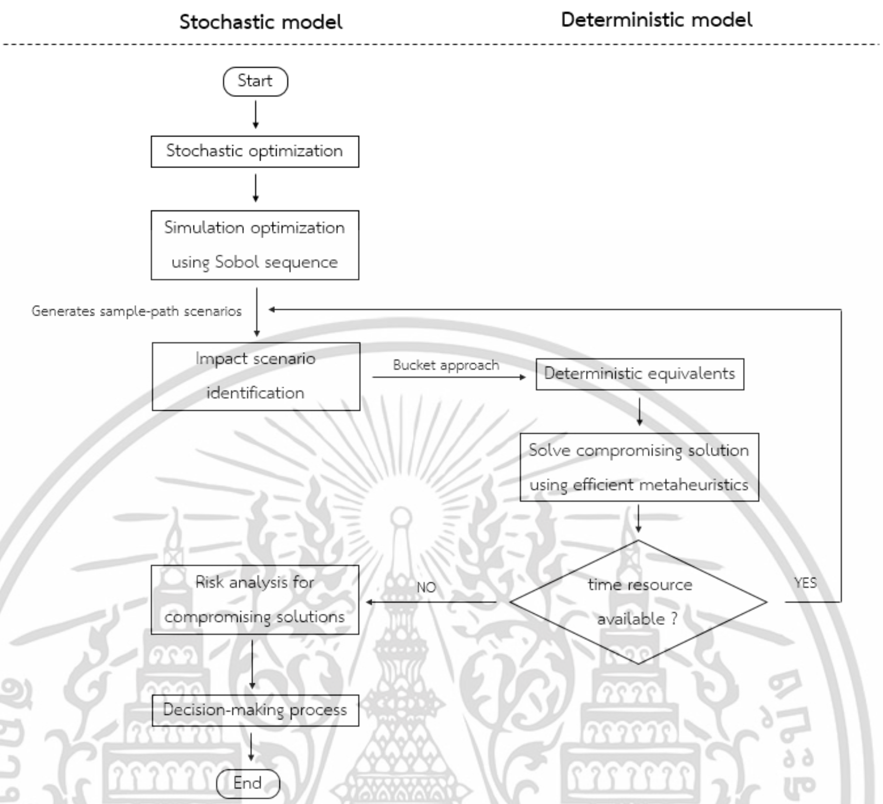

Figure 5.6 The simplest flowchart of proposed Simheuristic approach

Stage I (Simulation-based optimization): The original stochastic optimization is transformed into the deterministic equivalent. The scenarios presenting the uncertainty are generated using the Sobol sequence as described in section 5.2.1. The impact scenarios are indentified by using scenario aggregation using quantile mapping as described in section 5.2.2.

Stage II (Metaheuristic driven-search): The efficient CS-DP is used for the metaheuristic approaches. The detail about the algorithm is provided in The Chapter 3. The high-quality solution of each sample-path optimization is sent to the next process for the risk analysis.

Stage III (Risk analysis) Compromising solutions under particular sample-paths are considered risk analysis. Each alternative solution is tested with every generated scenario to get the information. The decision rule based-on the risk neutrality is provided in section 5.2.1 and risk aversion is provided in section 5.2.3.

Stage IV (Decision-making) This process is the selection of robust strategies. The alternative solutions are compared by using the risk preference to recommend a robust solution.

5.3 Fuel price modeling with mean-reversion property

A. Spot vs forward prices

Before starting with fuel price modeling, the definitions of spot and forward prices are described as following:

Spot price is the shot-term price which exhibits the three characteristics that are: (1) seasonal effect which variable to weather, climate and season, (2) mean-reversion tends to fluctuate around the long-run equilibrium price (affect by supply-demand law), and (3) price spike which changes abruptly cause by generation shortage or unexpected event.

Forward price is the future spot price providing by the forward market. The forward price tends to exhibit the three characteristics less than the spot price.

B. Fuel price modeling with drift and random components

In 1827, R. Brown discovered the pollen particle movement within water, so-called *Geometric Brownian motion*. The important property of Brownian motion is a random walk (originated by the classic problem of a drunk man aiming to go back home). Figure 5.7 illustrates the price modeling inspiring from Brownian motion (longer simulated time, the larger price uncertainty) which increases with $\sigma\sqrt{t}$. In 1973, Black-Sholes-Merton [156] developed the price modeling as below;

$$\pi_{t+1} - \pi_t = \Delta\pi = \pi_t + \pi_t[\mu\Delta t + \sigma\varepsilon\sqrt{\Delta t}\,] \quad (5.12)$$

where π_t represents the price over a period t; Δt refers time step in year; σ represents the annualized deviation (volatilities); ε represents the random component; μ represents the mean component. The square-root-of-time $\sqrt{\Delta t}$ allows us to annualize hourly, daily, weekly, monthly or any other volatilities. Sometimes, if the high volatilities situation occurs, the drift component ($\mu\Delta t$) dominates the random component ($\varepsilon\sqrt{\Delta t}$).

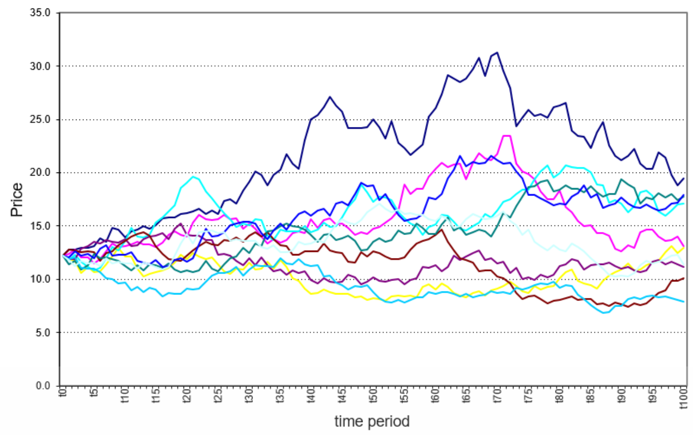

Figure 5.7 The sample-path simulation using Geometric Brownian motion

C. Fuel price modeling with mean reversion

Even though the standard Brownian motion can address the random walk characteristics, the long-term equilibrium electricity price can not be incorporated (usually spot price is governed by the "supply-demand" principle). For example, electricity price jumps from ฿3.8/MWh to ฿10/MWh momentarily due to supply-shortage; the Brownian motion would accept the ฿10/MWh price as a normal condition and proceed next electricity price from that starting point. Mean-reversion neglecting seems the unrealistic electricity price in long-term electricity planning.

To incorporate the mean-reversion property, the one-factor model developed by Schwartz [157] is provided as follows:

$$d\pi_t = \alpha^{\text{reversion}}(\mu^{\text{eq}} - \pi_t)dt + \sigma d\varepsilon_t \tag{5.13}$$

The first part represents the mean reversion component and the second part represents the random component; π_t denotes the spot price; μ^{eq} represents equilibrium price level; σ represent volatility; ε_t represents random shock from $t \rightarrow t + dt$; $\alpha^{\text{reversion}}$ denotes mean reversion rate (the speed which spot price reverts to the equilibrium price level); Equation 5.13 states that: (1) if spot price above equilibrium price level, the drift component is a negative value to pull spot price to the equilibrium price level, and (2) if spot price below equilibrium price level, the drift component is positive value to push spot price to the equilibrium price level.

The half life $t_{1/2}$ describing the characteristics of spot price to revert to half-way equilibrium price level is stated as below;

$$t_{1/2} = \frac{\ln 2}{\alpha^{\text{reversion}}} \tag{5.14}$$

Table 5.7 describes the relation between the mean-reversion rate and the half life.

Table 5.7

Mean reversion rate corresponding to the half life

$\alpha^{\text{reversion}}$	1	5	10	100	1000
$t_{1/2}$	8 months	1.66 months	25 days	2.53 days	6 hours

There are several techniques for estimating the mean-reversion rate. This dissertation, the linear regression approach is applied. Equation 5.15 can be stated in discrete form as follows;

$$\Delta\pi_t = \widehat{\beta_0} + \widehat{\beta_1}\,\pi_{t-1} + \sigma\varepsilon_t \tag{5.15}$$

where $\widehat{\beta_0}$, $\widehat{\beta_1}$ denotes intercept and slope parameters of linear regression equation; ε_t obeys normal distribution as $\varepsilon_t \sim \mathcal{N}(0,1)$; Δt is derived from $\frac{1}{\text{observation}}$.

D. Example calculation of fuel price used in PDP2015

Step 1: Monthly crude oil price (Jan-Dec 2019) is collected as in Table 5.8.

Table 5.8

Example calculation of monthly crude oil price

Month/Year	Price [$]	Price [$/MMBTU]	Volatilities [%]	Price changes [$/MMBTU]	Previous price [$/MMBTU]
Jan 2019	56.58	9.90		" Y-Axis "	" X-Axis "
Feb 2019	61.10	10.70	7.77%	0.80	9.90
Mar 2019	63.79	11.16	4.21%	0.46	10.70
Apr 2019	68.58	12.00	7.26%	0.84	11.16
May 2019	66.83	11.69	-2.62%	-0.31	12.00
Jun 2019	59.79	10.45	-11.21%	-1.24	11.69
July 2019	61.48	10.75	2.83%	0.30	10.45
Aug 2019	57.67	10.09	-6.34%	-0.66	10.75
Sept 2019	60.04	10.50	3.98%	0.41	10.09
Oct 2019	57.27	10.02	-4.68%	-0.48	10.05
Nov 2019	60.40	10.56	5.25%	0.54	10.02
Dec 2019	63.35	11.08	4.81%	0.52	10.56

Step 2: Calculates volatility using logarithmic price changes as below equation;

$$\text{price changes} = \ln[\frac{\pi_{t+1}}{\pi_t}] \tag{5.16}$$

Step 3: Calculates the standard deviation of volatilities. The standard deviation = 6.51%; Using square-root-of-time, assuming we have 250 days per year. Then, the annualized volatility is calculated as $6.51 \times \sqrt{250} = 21.59\%$.

Step 4: Analyse linear regression parameters. The obtained parameters are $\widehat{\beta_0} = 6.322 \pm 6.6678$, $\widehat{\beta_1} = -0.580 \pm 0.6214$ (anyway the $\widehat{\beta_1}$ should lie on $-1 < \widehat{\beta_1} < 0$), residual standard error = 0.581 and $\Delta t = 1$. The equilibrium price level and mean reversion rate can calculate as below equations.

$$\mu^{\text{eq}} = \frac{\widehat{\beta_0}}{\alpha^{\text{reversion}} \Delta t} \tag{5.17}$$

$$\alpha^{\text{reversion}} = \frac{-\widehat{\beta_1}}{\Delta t} \tag{5.18}$$

$$\hat{\sigma} = \frac{\text{standard error}}{\mu^{\text{eq}}} \tag{5.19}$$

Using equation (5.18), the mean reversion rate $\alpha^{\text{reversion}} = 0.580$, therefore half life $t_{1/2} = \frac{\ln 2}{0.580} = 1.19$ month; Using equation (5.19), equilibrium price level $\mu^{\text{eq}} = \frac{6.322}{0.580} = 10.8958$.

Step 5: Since $\alpha^{\text{reversion}}$ can not be a negative value, therefore we should confirm the coefficient $\widehat{\beta_1}$ that it is $1 < \widehat{\beta_1} < 0$ using t-test statistics as belows;

$$\text{t-test} = \frac{\widehat{\beta_1}}{\hat{\sigma}\sqrt{\sum_{t=1}^{T}(\pi_t - \bar{\pi})^2}} \tag{5.20}$$

$$= \frac{-0.580}{0.0534\sqrt{4.604}} = -5.068 \tag{5.21}$$

$$\Delta\pi_t = 6.322 - 0.580\,\pi_{t-1} + \sigma\varepsilon_t \tag{5.22}$$

Refer to 5% significance, the absolute value of t-test statistics should exceed 2. Given parameters, we can form the linear regression equation as in Eq. (5.22) for price modeling considering the mean-reversion property. Figure 5.8 depicts the three future crude oil prices with mean reversion.

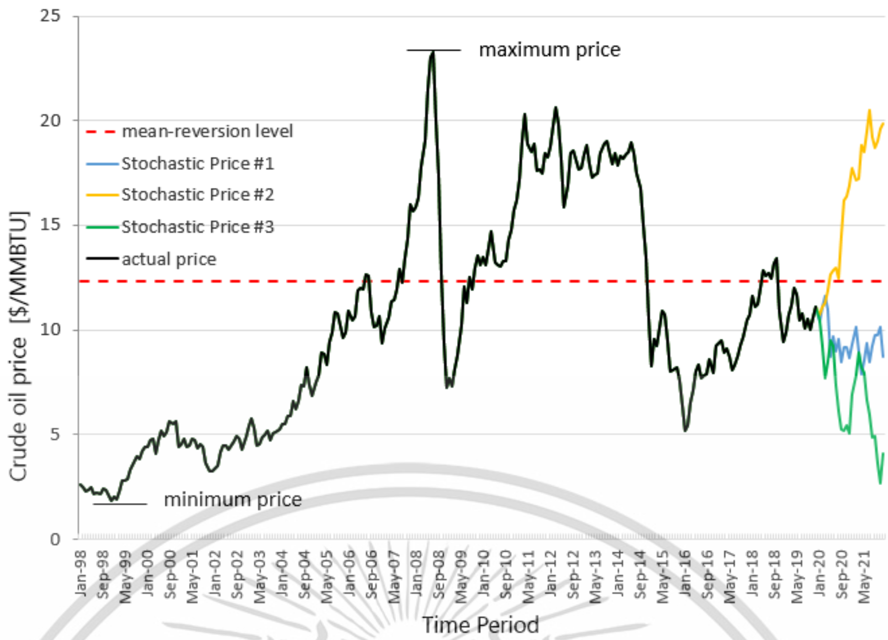

Figure 5.8 The simulation of three future crude oil prices with mean reversion.

5.4 Study Case 3: The proposed Simheuristic application for stochastic GEP

5.4.1 Case study descriptions

Objective

To develop the Simheuristic approach for generation expansion planning considering uncertainty.

Problem formulation

This study case illustrates the application of the proposed method to the electricity planning model considering fuel price uncertainty. The generation system adopts the official PDP2015 for input assumptions. The proposed method has confirmed the effectiveness via the back-testing during the period 2015 - 2020. The compact formulation of the multistage stochastic (**S-GEP-I**) is:

$$\begin{aligned} \min \quad & (3.15) - (3.21) \\ \text{s.t.} \quad & (3.23 - 3.26) \qquad \forall g \in \mathcal{G} \end{aligned}$$

Assumptions

1) The conventional PDP2015 relies on the deterministic model which input assumptions are typically represented as a simple average. The forward fuel price assumption based-on PDP2015 is shown in Table 5.9.

Table 5.9

Fuel price assumption based-on PDP2015

Fuel Type	2015	2021	2034
Domestic Natural gas	12.24	15.63	21.93
Imported Natural gas	13.46	17.19	24.12
Lignite	2.48	2.79	3.64
Imported coal	4.55	5.12	6.68
Fuel oil	15.33	18.37	24.59
Diesel	27.91	31.80	38.47
Nuclear	0.72	0.76	0.81

2) The historical fuel prices (January 1998 - April 2015) derive from the equally average spot price of Brent, Dubai and West Texas intermediate. In this study, the crude oil, natural gas, imported coal, and uranium prices are forecasted as the forward fuel prices. For the fuel prices of diesel, bunker oil and LNG, the fuel prices are obtained by multiplication factor 1.25, 1.23 and 0.93, respectively due to the oil-link price property as shown in Figure 5.9.

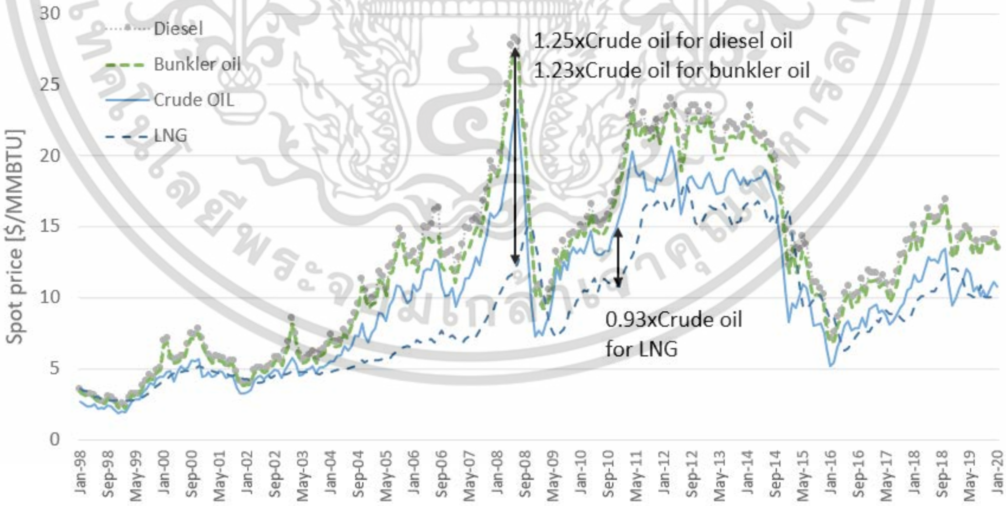

Figure 5.9 The diesel, bunker oil and LNG price assumptions

Table 5.10

Aggregate scenario assignment by using quantile mapping

No	Aggregated Scenario	No	Aggregated Scenario	No	Aggregated Scenario
1	Med/Med/Med/Med	28	Z3/Med/Med/Med	55	Z2/Med/Med/Med
2	Med/Med/Med/Z3	29	Z3/Med/Med/ Z3	56	Z2/Med/Med/ Z3
3	Med/Med/Med/Z2	30	Z3/Med/Med/ Z2	57	Z2/Med/Med/ Z2
4	Med/Med/ Z3/Med	31	Z3/Med/ Z3/Med	58	Z2/Med/ Z3/Med
5	Med/Med/ Z3/ Z3	32	Z3/Med/ Z3/ Z3	59	Z2/Med/ Z3/ Z3
6	Med/Med/ Z3/ Z2	33	Z3/Med/ Z3/ Z2	60	Z2/Med/ Z3/ Z2
7	Med/Med/ Z2/Med	34	Z3/Med/ Z2/Med	61	Z2/Med/ Z2/Med
8	Med/Med/ Z2/ Z3	35	Z3/Med/ Z2/ Z3	62	Z2/Med/ Z2/ Z3
9	Med/Med/ Z2/ Z2	36	Z3/Med/ Z2/ Z2	63	Z2/Med/ Z2/ Z2
10	Med/ Z3/Med/Med	37	Z3/ Z3/ Med / Med	64	Z2/ Z3/Med/Med
11	Med/ Z3/Med/ Z3	38	Z3/ Z3/ Med / Z3	65	Z2/ Z3/Med/ Z3
12	Med/ Z3/Med/ Z2	39	Z3/ Z3/ Med / Z2	66	Z2/ Z3/Med/ Z2
13	Med/ Z3/ Z3/Med	40	Z3/ Z3/ Z3/ Med	67	Z2/ Z3/ Z3/Med
14	Med/ Z3/ Z3/ Z3	41	Z3/ Z3/ Z3/ Z3	68	Z2/ Z3/ Z3/ Z3
15	Med/ Z3/ Z3/ Z2	42	Z3/ Z3/ Z3/ Z2	69	Z2/ Z3/ Z3/ Z2
16	Med/ Z3/ Z2/Med	43	Z3/ Z3/ Z2/ Med	70	Z2/ Z3/ Z2/Med
17	Med/ Z3/ Z2/ Z3	44	Z3/ Z3/ Z2/ Z3	71	Z2/ Z3/ Z2/ Z3
18	Med/ Z3/ Z2/ Z2	45	Z3/ Z3/ Z2/ Z2	72	Z2/ Z3/ Z2/ Z2
19	Med/ Z2/Med/Med	46	Z3/ Z2/ Med / Med	73	Z3/Z3/Med/Med
20	Med/ Z2/Med/ Z3	47	Z3/ Z2/ Med / Z3	74	Z3/Z3/Med/ Z3
21	Med/ Z2/Med/ Z2	48	Z3/ Z2/ Med / Z2	75	Z3/Z3/Med/ Z2
22	Med/ Z2/ Z3/Med	49	Z3/ Z2/ Z3/ Med	76	Z3/Z3/ Z3/Med
23	Med/ Z2/ Z3/ Z3	50	Z3/ Z2/ Z3/ Z3	77	Z3/Z3/ Z3/ Z3
24	Med/ Z2/ Z3/ Z2	51	Z3/ Z2/ Z3/ Z2	78	Z3/Z3/ Z3/ Z2
25	Med/ Z2/ Z2/Med	52	Z3/ Z2/ Z2/ Med	79	Z3/Z3/ Z2/Med
26	Med/ Z2/ Z2/ Z3	53	Z3/ Z2/ Z2/ Z3	80	Z3/Z3/ Z2/ Z3
27	Med/ Z2/ Z2/ Z2	54	Z3/ Z2/ Z2/ Z2	81	Z3/Z3/ Z2/ Z2

3) The aggregated scenario assignment follows the concept in section 5.2.2. Table 5. 10 shows the combination of quantile mapping of each fuel price. The aggregate scenarios are abbreviated, namely median (Med), second quantile (Z2), and third quantile (Z3). For example, Z3/Med/Z2/Med stands for the third quantile of crude oil, median for natural gas, second quantile for imported coal, and median for nuclear.

4) The parameters of fuel prices with the mean-reversion property are calculated based-on section 5.3. The calculated parameters are calculated based on the regression method. Table 5.11 reported the parameters.

Table 5.11

Calculated parameters of fuel prices with mean-reversion property

Fuel type	Crude oil	Natural gas	Imported Coal	Uranium
Linear regression parameters:				
$\widehat{\beta_0}$	+0.2516	+0.7492	+0.0715	+0.0047
$\widehat{\beta_1}$	-0.0189	-0.2007	-0.0238	-0.0184
Standard error	0.9529	0.4408	0.2711	0.0245
$\hat{\sigma}$	0.29	0.39	0.0901	0.01
Fuel price model:				
$\alpha^{\text{reversion}}$	0.0190	0.2007	0.0238	0.0184
μ^{eq}	13.2544	3.7331	3.009	0.2554
$t_{1/2}$	36.5	3.45	29.18	37.64

5.4.2 Simulation results

i) **Simulation generation:** The scenarios generated 10,000 sampling. Figure 5.10 depicts the convergence comparison between the conventional monte-carlo simulation using uniform distribution and quasi monte-carlo simulation using the Sobol sequence. As the sample scenario reaches 100 outcomes, it is observed that quasi monte-carlo converge to the truely expected mean. The simulation-based is improved from from $\Theta = {}^{1}/_{\sqrt{ns}}$ to $\Theta = {}^{1}/_{ns}$, obviously.

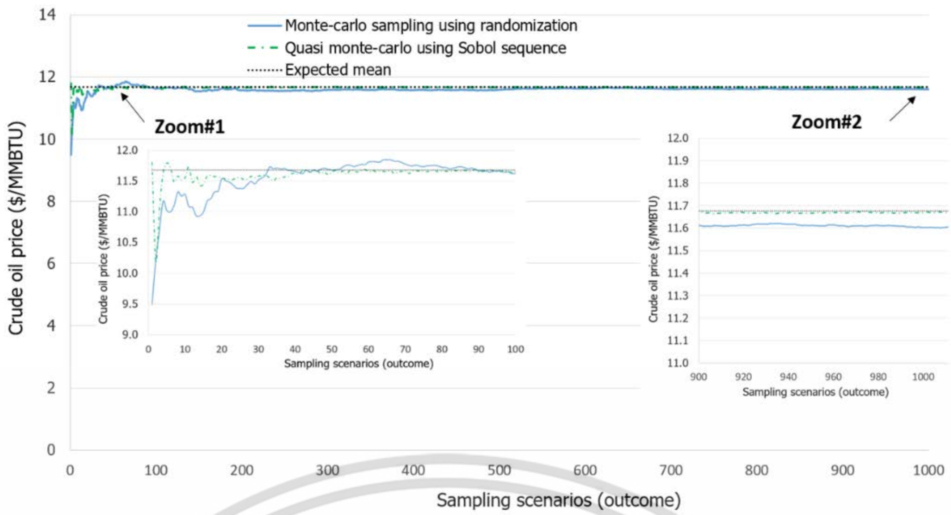

Figure 5.10 The convergence characteristic of quasi mote-carlo simulation

ii) **Sample-path optimization and risk analysis:** Table 5.12 reports the sample-path optimization of aggregated scenarios. Furthermore, similar representative solutions are grouped to verify the major alternative solutions. Based on the risk analysis by using 10,000 samplings, the Sol#5 is a consensus both risk neutrality and risk aversion.

Table 5.12

The risk analysis of representative solutions for risk neutrality and risk aversion

Alt.	SAA	MiniMax	Freq. (%)	Aggregated scenarios
Sol#1	46,889.99	74.6	13 (16%)	1, 6, 11, 27, 33, 34, 36, 54, 55, 63, 65, 67, 81
Sol#2	46,905.16	77.3	8 (9.9%)	4, 12, 15, 16, 40, 57, 73, 76
Sol#3	47,001.13	242.0	2 (2.5%)	50, 51
Sol#4	46,955.31	167.5	1 (1.2%)	48
Sol#5	**46,871.01**	**22.8**	**24 (29.6%)**	3, 5, 17, 18, 20, 21, 24, 28, 29, 30, 31, 32, 38, 39, 41, 43, 61, 62, 66, 69, 70, 71, 80
Sol#6	46,921.38	106.5	5 (6.2%)	23, 26, 64, 72, 74
Sol#7	47,017.32	275.7	1 (1.2%)	46
Sol#8	46,931.21	121.9	1 (1.2%)	13
Sol#9	47,027.58	300.2	3 (3.7%)	25, 52, 53
Sol#10	46,887.36	51.2	13 (16.0%)	10, 14, 19, 35, 37, 42, 45, 58, 60, 68, 75, 77, 79
Sol#11	46,981.16	219.4	1 (1.2%)	22
Sol#12	46,938.47	152.6	2 (2.5%)	47, 49
Sol#13	46,922.84	107.3	1 (1.2%)	78
Sol#14	46,903.87	54.59	6 (7.4%)	2, 7, 8, 9, 56, 59

Remark: SAA stand for sample average approximation, Alt. stand for representative solutions.

Table 5.13 reports the optimal plan of fifth solution (Sol#5)

Table 5.13

The optimal solution satisfying both risk neutrality and risk aversion

Year	Candidate plants			
	1,000-MW Coal	700-MW CC(gas)	240-MW gas turbine	20MW-Diesel
2015	0	2	0	0
2016	0	0	0	0
2017	0	0	0	0
2018	0	1	0	0
2019	0	0	0	0
2020	0	3	0	0

iii) **Back-test:** The future crude oil price is simulated with a 30% volatility $\hat{\sigma}$ based-on Table 5.11. Figure 5.11 depicts the cone of uncertainty in the shaded area representing 10%-90% quantiles (refer to 10,000 sampling). The back-test implies that the realization of crude oil price reverts to the long-term mean.

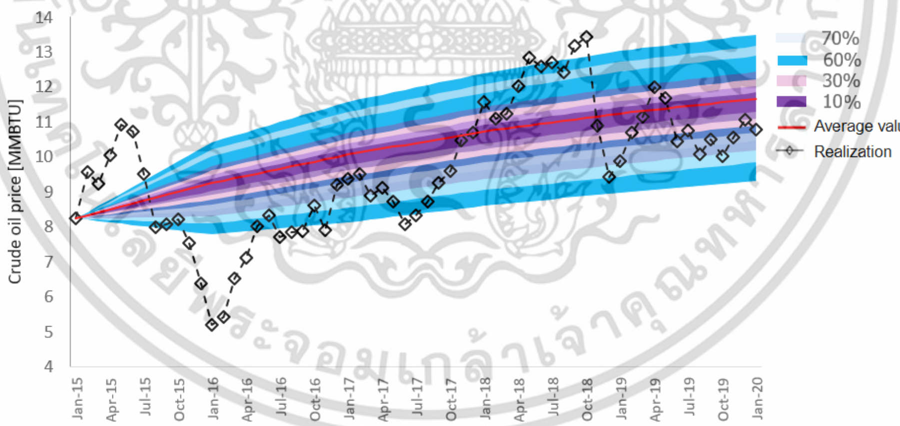

Figure 5.11 The future crude oil price projection with range of uncertainty

iii) **Hedge against fuel price uncertainty:** The importance of stochastic model can be measured by metric, namely EVPI (expected value of perfect information) as following;

$$\text{EVPI} = \text{stochastic model} - \text{realization} \qquad (5.23)$$

where realization denotes the stochastic problem which uncertainty is removed; The stochastic model denotes the representative solution solve by stochastic optimization;

There are many risk-hedging strategies [158] against fossil fuel price uncertainty for instance, renewables [159], nuclear [160] and so on. In this study case, the robust decision-making guides the Sol#5. Exactly, no alternative is the best under all possible circumstances. The useful metric to measure the hedging effect, namely $\mathbf{VSS}$ (value of the stochastic solution) measures the difference between stochastic and deterministic models. The mathematical equation provides as follows;

$$\mathbf{VSS} = \mathbf{deterministic\ model} - \mathbf{stochastic\ model} \tag{5.24}$$

The hedging effect implies that it has no single solution to suit all possible scenarios. Table 5.14 shows the deterministic model replacing the random variables by their simple average values is clearly optimistic. The difference between the perfect formation and simple average value is high. On the other hand, both $\mathbf{EVPI}$ and $\mathbf{VSS}$ of the stochastic model are lower than the deterministic model. This implies that the stochastic model tries to hedge against the range of uncertainty. So, the difference between perfect information and robust decision is minor.

Table 5.14

Hedging effect comparison between stochastic and deterministic models

Model	Appraoch	Obj.	EVPI	VSS
Realization	Perfect information	44,675.8	-	-
Deterministic	Simple average value	44,974.7	298.9	284.47
Stochastic	Sample average approximations	44,690.2	14.43	-
	Minimax regret	44,690.2	14.43	-

Remark: Obj. stand for objective function

iv) **Generation portfolio:** The energy mix of each generation has not changed significantly as shown in Figure 5.12.

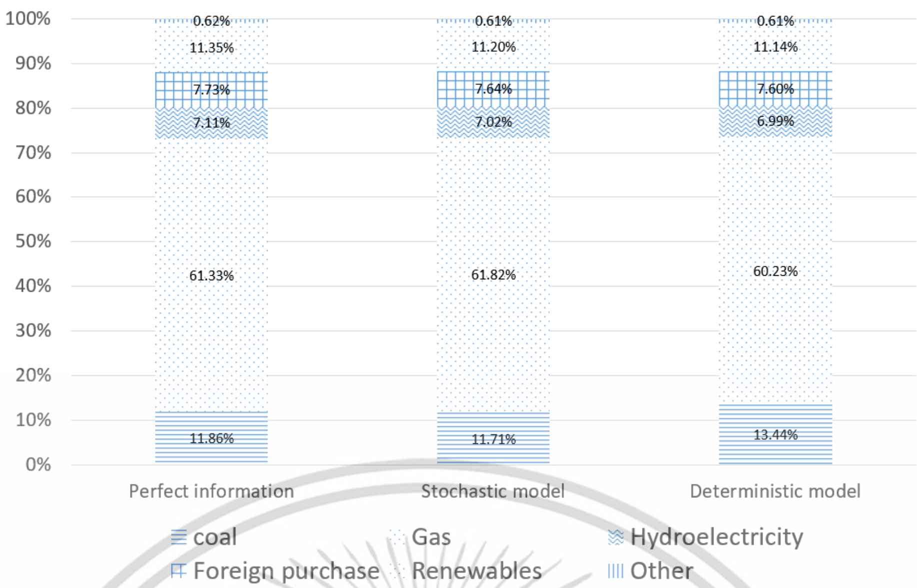

Figure 5.12 Energy mix in 2020 for each generation plan

5.5 Conclusions

Shifting from the deterministic model (least-cost planning) to the stochastic model (risk compromising) can reduce the investment and operational risks. In this chapter, the stochastic optimization, namely "Simheuristics" is developed to solve the generation expansion planning considering fuel price uncertainty. The main improvements are that: (1) the improved simulation optimization which applies the Sobol sequence can overcome the computationally intensive, (2) the efficient metaheuristic approach solves the deterministic equivalent (described in Chapter 4) to obtain the compromising solution, and (3) the robust decision making, namely "sample average approximation" and "minimax regret" are deployed to match the risk preferences. As a result of the study case, the Simheuristic approach is practical to solve generation expansion planning considering the fuel cost uncertainty.

Chapter 6

Flexibility and Frequency Security Enhancement to Generation Expansion Planning

The electricity planning can be categorized with frameworks is that: (1) long-term system planning (e.g., generation expansion planning, geospatial planning and so on) which focus on system adequacy assessment that defines what type, where, when, and how many of new-build power generation to serve the future electricity demand and (2) short-term operation planning (e.g., unit commitment, economic dispatch and so on) which focus on how generation and transmission system that can operate the supply-demand dispatching under security and reliability during the year-, month- and day operation [161]. For over 40 years, 'system adequacy' successfully optimize the new-build generation among various candidate options to maintain the electricity supply-demand balance for generation expansion planning. In a sense of increasing variable renewable energy [162], the original framework can not measure the flexibility shortages [163] and frequency security deterioration [164]. With these reasons, the proposed framework is demonstrated to encounter the new challenges on system flexibility and frequency security.

The first part of this chapter will discuss flexible generation planning [165]. The definitions relating to the flexibility shortages, i.e., *load shedding*, *generation shedding* and *VRE curtailment* [116] are described. The two-stage generation expansion planning comprising adequacy and flexible planning is proposed. As we have no standard metric as well as adequacy planning, the dispatch simulation (the dispatch simulation is divided into reduced unit commitment [167] and frequency-constrained economic dispatch [168]) is required to verify the unserved energy from flexibility shortages of power system operation.

The second part of this chapter provides the derivation of frequency-security constraint for generation dispatch simulation. The inertia definition [169] and the aggregated swing equation model [170] are reviewed to describe the *inertial frequency response* [171]. The proof of the swing equation is provided for the frequency-security constraint. The *Governor response* [172] as part of primary and secondary controls is realized. Finally, the modified IEEE-24 bus [173] is demonstrated for the proposed framework considering flexibility and frequency security.

6.1 System flexibility planning

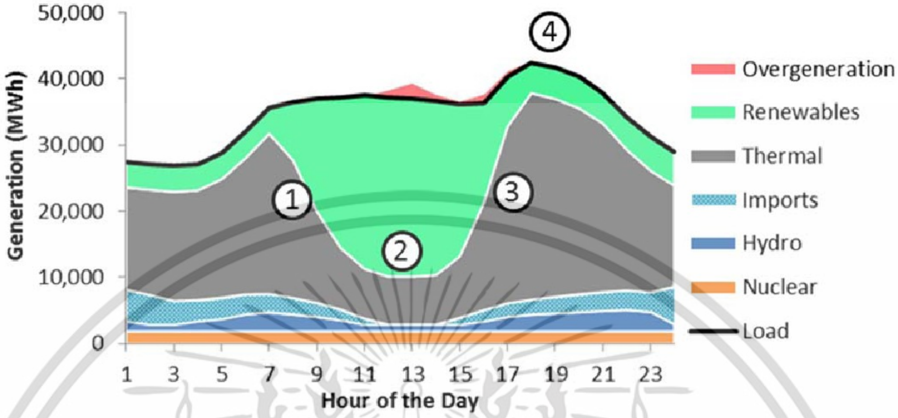

Figure 6.1 Typical daily load dispatch, derived from [14]

6.1.1 Flexibility shortage descriptions

All power systems require the operational ability to respond to the system's net load [174] at all operating periods (e.g. seconds, minutes, hours, and days). To understand how flexible resources are important (e.g. dispatchable powerplants, energy storage system, demand-side response, interconnection, and so on) [175], Figure 6.1 illustrates the operating dispatch under high penetration of solar PV. The four events are noticed as follows:

1) Decreasing netload or ramp down event: This event starts in the morning gradually by increasing solar PV generation. As higher solar PV installed, steeper net load occurs. The important characteristics of dispatchable generations are de-loading rate or downward ramping capability.

2) Low net load event: This event approximately occurs at noon because of the maximum power of solar PV received at the highest solar radiance from the sun. This event requires dispatchable generation to operate at minimum-stable output or shutdown for the surplus power plant.

3) Increasing netload or ramp up event: This event starts at noon gradually by decreasing solar PV generation. The important characteristics of dispatchable generations are loading rate or upward ramping capability.

4) Shorter peak net load event: Normally, tropical countries, e.g. Thailand, the peak netload occurs in the noon. As increasing solar PV, the peaknet load is shifted to the night period.

As the above descriptions, Figure 6.2 summarizes whether or not the flexible resources can operate the power system at various events. The unserved energies lacking the flexible resources are captured by the '*load shedding*', '*generation shedding*', and '*VRE curtailment*' [176]. These incidents can be used as flexibility metrics as well as the reserve margin or LOLP in the adequacy metrics.

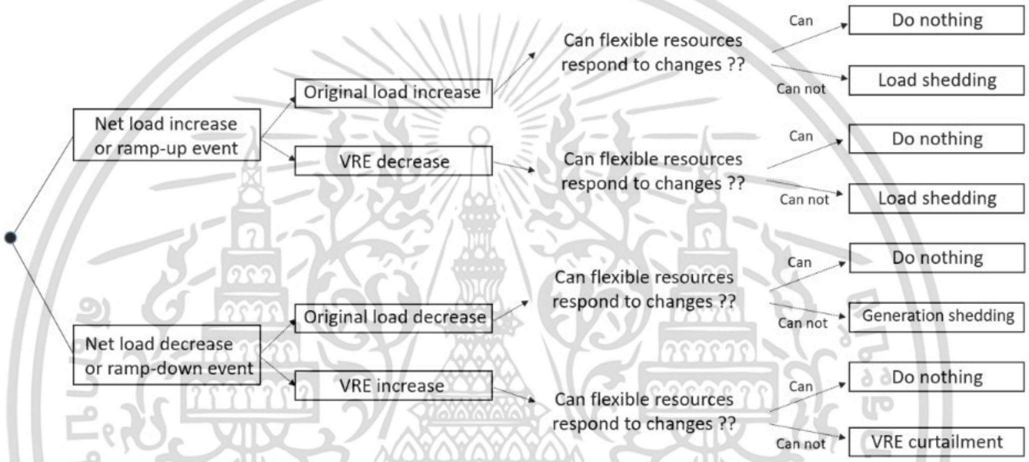

Figure 6.2 System flexibility shortage descriptions

6.1.2 Mathematical formulation

A. Objective and constraints function

The coupling objective function to solving the generation expansion planning considering adequacy and flexibility is expressed as follows;

$$\min\{\mathrm{NPV}^{(t)}(z^1 + z^2)\} \tag{6.1}$$

where the first-stage objective function (adequacy planning) z^1 is corresponding to the section 3; the second-stage objective function (flexibility planning) z^2 can be formulated as below general form:

$$\min z^2(\mathrm{X}) \tag{6.2}$$

subject to

$$g(\mathrm{X}) = 0 \tag{6.3}$$

$$h(\mathrm{X}) \leq 0 \tag{6.4}$$

$$\mathrm{X}_{\min} \leq \mathrm{X} \leq \mathrm{X}_{\max} \tag{6.5}$$

The objective function $z^2(\blacksquare)$ is minimizing the flexible generation investment subjecting to equality constraint, inequality constraint, and box constraints. In this thesis, $g(\mathrm{X}) = 0$ represents the real power balance; $h(\mathbf{X}) \leq 0$ represents the load shedding and VRE curtailments.

The aboved objective function can be described in the detailed equation as

$$z^2 = \min\left\{\sum_{t\in\mathcal{T}}\left(\mathrm{NPV}^{(t)}\left(\mathrm{inv}^{\intercal}\mathrm{U}^{flex,(t)}\right)\right)\right\} \tag{6.6}$$

It is clearly seen that the flexibility objective z^2 only concerns the flexibility shortages [14]. The constraints comply with the flexibility shortage concept described in Figure 6.2. The above constrained forms can be described in the detailed equation as Eq. (6.7-6.8)

(a) Load shedding criteria

$$\sum_{h=1}^{8760} P_{\mathrm{S}}^{(h)} \leq P_{\mathrm{S}}^{\max} \tag{6.7}$$

(b) Variable renewable curtailment criteria

$$\sum_{h=1}^{8760} P_{\mathrm{C}}^{(h)} \leq P_{\mathrm{C}}^{\max} \tag{6.8}$$

With the proposed formulation, equation (6.7) summarizes the total load shedding over an operating hour $h \in \mathcal{H}$; The variable renewable curtailment can be stated in equation (6.8). Moreover, the operation simulation is required for flexibility shortages simulation because we have no standard metrics to measure it like adequacy metrics

B. The operation simulation

To derive load shedding $P_{\mathrm{S}}^{(h)}$ and VRE curtailment $P_{\mathrm{C}}^{(h)}$ over operating time $h \in \mathcal{H}$, the operation simulation can be initially defined as follows:

$$P_{\mathrm{S}}^{(h)}, P_{\mathrm{C}}^{(h)} = OS(\blacksquare) = ED\left[UC\left(\mathbf{X}^{(t)}\right)\right] \tag{6.9}$$

$OS(\blacksquare)$ stand for the operation simulation function comprising the reduced unit commitment as the main problem [177] and economic dispatch [178] (consider a frequency-security constraint) as a sub-problem. The each planning horizon t

equivalent to 8,760 operating hours $h \in \mathcal{H}$. The state variable $\mathbf{X} = \{x_1, x_2, .., x_{ng}\}$ is set containing the individual number of generating units x_g.

Generally, the main problem considers the ON/OFF status (scheduling problem) of the power plant over operating hour $h \in \mathcal{H}$, and the sub-problem considers the dispatching power for power balancing. The state variable $\mathbf{X}^{(t)}$ is containing the existing generating units over the planning horizon year $t \in \mathcal{T}$.

$$\mathrm{W} = UC\left(\mathrm{X}^{(t)}\right) \tag{6.10}$$

Scheduling problem

$$\mathrm{W}^{(t+1)}\mathrm{P}^{\max} - \mathrm{W}^{(t)}\mathrm{P}^{\max} \leq \Delta\mathrm{P}^{\max} \tag{6.11}$$

$$\mathrm{W}^{(t)}\mathrm{P}^{\min} - \mathrm{W}^{(t+1)}\mathrm{P}^{\min} \leq \Delta\mathrm{P}^{\min} \tag{6.12}$$

$$\mathrm{ON}(\mathrm{X})^{(\mathrm{t})} \leq \mathrm{M}^{\mathrm{up}} \tag{6.13}$$

$$\mathrm{OFF}(\mathrm{X})^{(\mathrm{t})} \leq \mathrm{M}^{\mathrm{down}} \tag{6.14}$$

$$\mathrm{W} \in \mathbb{R}^{ng\times 1}, \mathrm{P} \in \mathbb{R}^{ng\times 1}, \mathrm{M}^{\mathrm{up}} \in \mathbb{R}^{ng\times 1}, \mathrm{M}^{\mathrm{down}} \in \mathbb{R}^{ng\times 1}, \Delta\mathrm{P}^{\min} \in \mathbb{R}^{ng\times 1}, \Delta\mathrm{P}^{\max} \in \mathbb{R}^{ng\times 1}$$

Constraints (6.11-6.12) represent the loading-, deloading- rate capabilities of generating units ($g = 1,2, \dots, ng$); Constraints (6.13-6.14) describe the minimum up/downtime of each generating unit ($g = 1,2, \dots, ng$) which imply the cycling capability.

From the above equations (6.13-6.14), there are some remarks are as follows;

- Once each thermal generating units are scheduled "ON", plants can not stop immediately and need to run for at least a minimum up-time $\boldsymbol{t}_i^{\mathrm{up,min}}$, and $\boldsymbol{t}_i^{\mathrm{up}}$ stand for the consecutive runtime hour of generating unit i.
- Once each thermal generating units are scheduled "OFF", the power plants can not start immediately and need to shutdown for at least a minimum down-time. $\boldsymbol{t}_i^{\mathrm{down,min}}$, and $\boldsymbol{t}_i^{\mathrm{down}}$ stand for the consecutive shutdown hour of generating unit i, respectively.

Dispatch problem considering primary frequency security

$$sum\{\mathbf{P}\} = \mathrm{P_L} - \mathrm{P_S} + \mathrm{P_C} \qquad g\epsilon\mathcal{G} \tag{6.15}$$

$$sum\{\mathbf{P}_\mathrm{R}\} \geq \Delta\mathrm{P} \qquad g\epsilon\mathcal{G}, g \neq g^{\cdot} \tag{6.16}$$

$$\boldsymbol{P}_R \leq \frac{\Delta\mathrm{P}}{GRC^{\min}}\boldsymbol{GRC}_g \qquad g\epsilon\mathcal{G}, g \neq g^{\cdot} \tag{6.17}$$

$$\mathbf{P} + \mathbf{P}_{\mathrm{R}} \leq \mathbf{P}^{\max} \qquad g\epsilon\mathcal{G} \qquad (6.18)$$

$$\mathbf{P}^{\min} \leq \mathbf{P} \qquad g\epsilon\mathcal{G} \qquad (6.19)$$

$$\mathbf{P} \in \mathbb{R}^{ng\times 1}, \mathbf{P}_{\mathrm{R}} \in \mathbb{R}^{ng\times 1}, \boldsymbol{GRC_g} \in \mathbb{R}^{1\times ng}, \mathbf{P}^{\min} \in \mathbb{R}^{ng\times 1}, \mathbf{P}^{\max} \in \mathbb{R}^{ng\times 1}$$

From the above formulations, there are some additional descriptions are as follows;

- Constraint (6.15) defines the total power balance [MW] of all generating units which net load comprise of original load P_L [MW] minus load-shedding power P_S [MW] and renewable curtailment P_C [MW].
- Constraint (6.16) defines a necessary operating reserve [179] of all generating units except the largest-generating unit $g^{\cdot}$ for N-1 contingency by tripping the largest-generating unit $g^{\cdot}$.
- Constraint (6.17) describes the minimum governor-ramping capability $GRC^{\min}$ [MW/s] of total generating units that adequate for governor action both primary- and secondary- controls during disturbance. The derivation of governor-ramping capability is presented in section 6.2.1 sub-section C; The equation be re-written as follows;

$$\mathrm{GRC}^{\min} = \frac{\frac{1}{2}\Delta \mathrm{P}^2}{\mathrm{M_H}(\mathrm{freq_0} - \mathrm{freq_{min}} - \mathrm{freq_{db}})} \quad [\mathrm{MW/s}] \qquad (6.20)$$

where ΔP stand for the loss of generating unit [MW]; $\mathrm{M_H}$ represent a total system inertial constant [MW-s/Hz] after N-1 contingency condition; $\mathrm{freq_0}$ represent a set-point frequency [Hz]; $\mathrm{freq_{min}}$ represent a minimum frequency nadir performance [Hz]; $\mathrm{freq_{db}}$ represent a dead-band frequency [Hz].

The vector of governor ramping capability $\boldsymbol{GRC_g}$ is containing the individual governor's ramping capability. In reality, the governor response has dead time before an active period [180]. In reality, the governor response's characteristics performs the overshoots in frequency excursion.

- Constraint (6.18) represents the maximum power output [MW] of generating units that quantify the individual spinning reserve for the governor used.
- Constraint (6.19) represents minimum stable power output [MW] of individual generating units.

6.2 Frequency security requirement

6.2.1 Frequency security descriptions

A. Frequency response and control

The typical frequency response [181] after the instantaneous tripping of the largest generation is depicted in Figure 6.3. During the first period (0-5 seconds), the frequency excursion is resisted by only the aggregated system inertia, referred to as *inertial frequency response*. After system frequency falls below the dead-band frequency, the governor control of each power plant will stabilize the frequency deviation by using the primary reserve. At this moment, the frequency response reaches the new equilibrium state after governor control, called "*primary control*". After that, if system frequency can not back to the nominal value, the load-frequency control takes action by re-scheduling the set-point power and participation factor of each power plant, refer to as "*secondary control*". The other control, so call "*tertiary control*" re-establishes the economic set-point and commitment of each power plant. The secondary and tertiary controls perform in a range of timescale 30 seconds to 15 minutes.

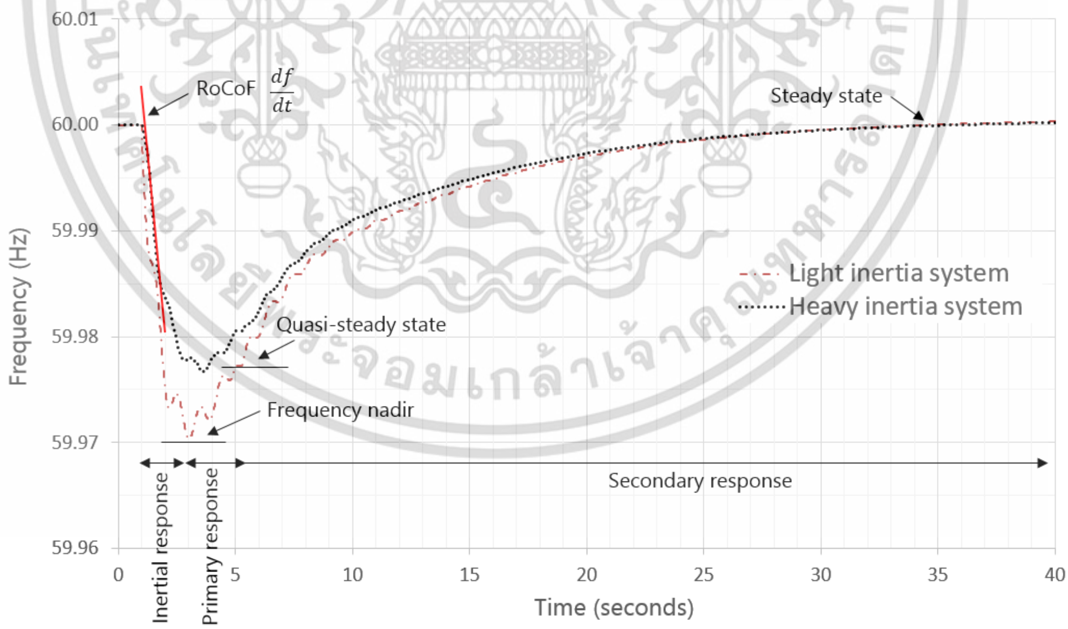

Figure 6.3 System frequency security with light and heavy inertia

The power system is designed to dispatch an electrical load at the nominal frequency. *Frequency security* [182] defines the ability to maintain the nominal frequency after large disturbances, i.e. tripping of large generation and load rejection.

For example, the power system is called "secured" if a single contingency (N-1 criteria) is satisfied. In contrast, the power system is called "insecure" if frequency collapse (frequency drops to zero) or the rate of change of frequency (RoCoF) [183] can not manageable.

B. Aggregated frequency response

The frequency dynamics of each synchronous generator g can be described by using the classical swing equation [184] as below;

$$\frac{d}{dt}\Delta\mathrm{freq}_g(t) = \frac{\Delta P_g}{2\mathrm{H}_g} - \frac{\mathrm{D}^{\mathrm{load}}\Delta\mathrm{freq}_g(t)}{2\mathrm{H}_g} \qquad g\epsilon\mathcal{G} \quad (6.21)$$

$$\mathrm{H}_g = \frac{\mathrm{S}_g \times \mathrm{h}_g}{\mathrm{freq}_0} \qquad g\epsilon\mathcal{G} \quad (6.22)$$

$$\mathrm{D}^{\mathrm{self}} = \mathrm{D}^{\mathrm{GOV}} + \mathrm{D}^{\mathrm{load}} \quad (6.23)$$

where $\Delta\mathrm{freq}_g(t)$ denotes frequency deviation [Hz] which derive from individual electrical frequency freq_g [Hz] minus nominal frequency freq_0 [Hz] at timeframe t; ΔP_g is individual power difference [MW] between mechanical power $\mathrm{P}_g^{\mathrm{mech}}$ [MW] and electrical power $\mathrm{P}_g^{\mathrm{elec}}$ [MW]; $\mathrm{D}^{\mathrm{self}}$ stands for the self-regulation property [185] of power system [per unit]; $\mathrm{D}^{\mathrm{load}}$ represents the damping factor of frequency-dependent load [per unit]; $\mathrm{D}^{\mathrm{GOV}}$ represents the governor response [per unit]; H_g represents inertia constant [MW-s/Hz] which derive from inertia parameter h_g [MJ/MW] multiply with rating machine [MVA].

To analyze the system frequency dynamics, the center of the inertia method (COI) [186] is applied. The individual synchronous machines are aggregated into the lumped machine. The equation 6.21 is rewritten to aggregated swing equation as below;

$$\frac{d}{dt}\Delta\mathrm{freq}(t) = \frac{\Delta P}{2\mathrm{H}^{\mathrm{sys}}} - \frac{\mathrm{D}^{\mathrm{load}}\Delta\mathrm{freq}(t)}{2\mathrm{H}^{\mathrm{sys}}} \quad (6.24)$$

In which,

$$\mathrm{H}^{\mathrm{sys}} = \frac{\sum_{g\epsilon\mathcal{G}} \mathrm{S}_g \times \mathrm{h}_g}{\sum_{g\epsilon\mathcal{G}} \mathrm{S}_g} \quad (6.25)$$

$$\Delta P = \Delta P^{\mathrm{mech}} - \Delta P^{\mathrm{elec}} = \sum_{g\epsilon\mathcal{G}} \mathrm{P}_g^{\mathrm{mech}} - \sum_{g\epsilon\mathcal{G}} \mathrm{P}_g^{\mathrm{elec}} \quad (6.26)$$

Here $\Delta\mathrm{freq}(t)$ denotes the weighted average frequency [Hz] which oscillate around the center of inertia; ΔP represents the total balance between mechanical and electrical power [per unit]; $\frac{d}{dt}\Delta\mathrm{freq}(t)$ represents the RoCof [Hz/second].

C. Frequency deviation equation and characterisics

For sake of simplicity, equation 6.24 can be solved as the frequency deviation equation. Insight details are found in [187]. The frequency deviation can be expressed as below;

$$\Delta\text{freq}(t) = \frac{\Delta P}{\text{D}^{\text{load}}}\left(1 - e^{-\frac{\text{D}^{\text{load}}}{M_H}t}\right) \tag{6.27}$$

where M_H represents inertia coefficient which derives from $M_H = 2 \times \sum_{g\epsilon\mathcal{G}} \text{S}_g \times \text{h}_g \div 60$.

Early in the inertial frequency response, the aggregated system inertia compensates the stored energy to stabilize the unbalance power, $\Delta P < 0\,[MW]$. The frequency drops to nadir frequency depends on many factors: the size of power unbalance, aggregated system inertia, the droop of generation, load-characteristics, and etc. Lately, the frequency recovers to a quasi-steady state $\Delta\text{freq}_{\text{quasi}}$ due to the governor response, called the power-frequency characteristics [188]. The mathematical equation expresses as follows:

$$\text{PFC} = \frac{\Delta P}{\Delta\text{freq}_{\text{quasi}}} \tag{6.28}$$

where PFC stand for power-frequency characteristics [MW/second]; $\Delta\text{freq}_{\text{quasi}}$ represents the frequency deviation after reachs quasi-steady state [Hz].

6.2.2 Adequacy of primary reserve

The system frequency dynamics requires the primary reserve for governor response (Droop-P control). After a large disturbance, each synchronous machine (deployed the primary control) will compensate the frequency deviation depend on Droop-P control. Figure 6.4 illustrates the approximation of governor response after tripping of the largest power plant. The adequacy analytics of primary reserve provided in [172]. However, this thesis summarizes the main idea as follows:

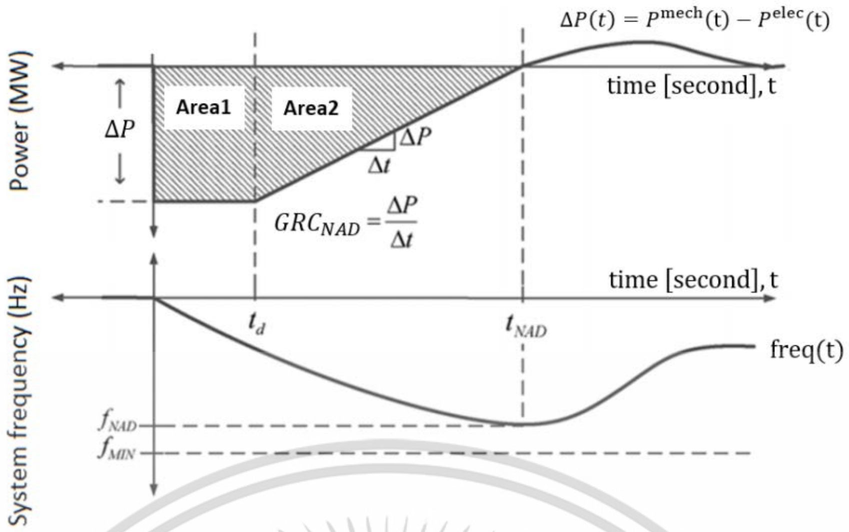

Figure 6.4 Droop-P control for governor reponse, adapted from [172].

Reconsider the classical swing equation by neglecting the self-regulation property ($D^{self} = 0$) as equation 6.28 and integrates from $t = 0$ to $t = t_{NAD}$ to derive equation 6.30.

$$\frac{d}{dt}\text{freq}(t) = \frac{1}{M_H}\{P(t)^{\text{mech}} - P(t)^{\text{elec}}\}\text{dt} \tag{6.29}$$

$$\int_0^{t_{NAD}} \frac{d}{dt}\text{freq}(t)\,dt = \frac{1}{M_H}\int_0^{t_{NAD}} \{P(t)^{\text{mech}} - P(t)^{\text{elec}}\}\text{dt} \tag{6.30}$$

Mathematically speaking, $\int_0^{t_{NAD}} \frac{d}{dt}\text{freq}(t)\,dt$ is equivalent to $\text{freq}(t_{\text{NAD}}) - \text{freq}(0)$ for the left-hand side. Furthermore, it should be noted that the right-hand side of equation comprises of rectangular and triangular areas; we can split equation 6.30 as second part from $t = 0 \rightarrow t_{NAD}$ and $t = t_d \rightarrow t_{NAD}$ as below;

$$\text{freq}_{\text{NAD}} - \text{freq}_0 = \frac{1}{M_H}\int_0^{t_d} \{-\Delta P\}\text{dt} + \frac{1}{M_H}\int_0^{t_{\text{NAD}}-t_d} \{C^{NAD}t - \Delta P\}\text{dt} \tag{6.31}$$

where C^{NAD} denotes the ramping capability of governor response approximation [MW/second]; ΔP represents the size of credible contingency; freq_{NAD} represent the nadir frequency [Hz] corresponding to nadir time t_{NAD} [second]; The pre-contingency frequency is defined as freq_0 [Hz]; The dead time t_d [second] relates to the frequency dead band freq_{db} as $\text{freq}_{\text{db}} = t_d \times \Delta P \div M_H$.

As a result of integration, the simple form of the equation can be shown in equation 6.32. Rearranging the equation to derive the governor ramping capability GRC_{NAD} as equation 6.33.

$$\mathrm{freq}_{NAD} - \mathrm{freq}_0 = \frac{-1}{M_H}(\Delta \mathrm{P}t_d + \frac{\Delta \mathrm{P}^2}{2\mathrm{GRC}_{\mathrm{NAD}}}) \tag{6.32}$$

$$\mathrm{GRC}_{\mathrm{NAD}} = \frac{\frac{1}{2}\Delta \mathrm{P}^2}{\mathrm{M_H}(\mathrm{freq}_0 - \mathrm{freq}_{\mathrm{NAD}} - \mathrm{freq}_{\mathrm{db}})} \tag{6.33}$$

In sense of system planning, we can replace the minimum time $t_{\min}$ with nadir time t_{NAD} corresponding to the under-frequency criteria $\mathbf{freq_{min}}$ as follows;

$$\mathrm{GRC}_{\min} = \frac{\frac{1}{2}\Delta \mathrm{P}^2}{\mathrm{M_H}(\mathrm{freq}_0 - \mathrm{freq}_{\min} - \mathrm{freq}_{\mathrm{db}})} \tag{6.34}$$

6.3 Proposed framework

6.3.1 Two-stage generation expansion planning

The adequacy planning is defined as the first stage planning. The candidate plans satisfying the adequacy criteria are sent to the second stage, so-called 'flexibility planning'. Figure 6.5 demonstrates the simplest concept of two-stage planning framework. The second stage determines the candidate plans whether flexible to operate or not; If the judgment is a flexible plan, the candidate plan is considered to be the possible generation portfolio; If the judgment is not a flexible plan, the flexible generations are added to increase the system flexibility of candidate plan. Finally, the total cost comprises of the adequacy and flexibility costs.

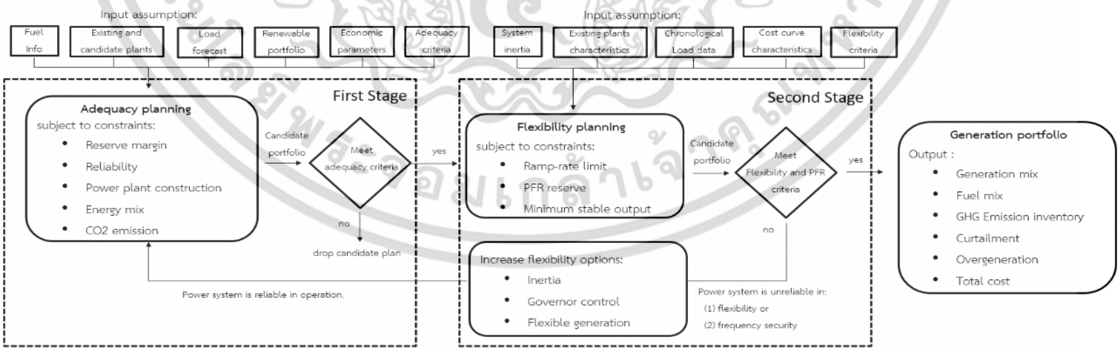

Figure 6.5 Proposed two-stage generation expansion planning framework

6.3.2 Simplest procedure

The simplest procedure of proposed framework is described as Table 6.1.

Table 6.1

The pseudocode of proposed two-stage generation expansion planning framework

```
Begin
    Read the system data for adequacy and flexibility planning, e.g. existing and
candidate plant, original and netload forecasting;
While t ∈ T
    Perform the adequacy planning in the same manner of section 3;
    Evaluate the objective function of 1st stage planning for each candidate plan;
    Perform the operation simulation;
    If renewable curtailment and load shedding can not satisfy constraints (6.7-6.8)
        Add flexible generation to increase the system flexibility;
        If frequency is not "secure"
            Drop the candidate plan
        End
    End
    - Evaluate the objective function of 2nd stage planning for candidate plan;
    - keep candidate plans;
End while
    - Rank the total cost in ascending order, then summarize the optimal plan;
End
```

6.4 Study Case 4: Flexibility and Frequency Security Enhancement to Generation Planning Framework

6.4.1 Case study descriptions

Objective

The objective is to demonstrate the two-stage generation expansion planning facing the flexibility shortage and insecurity of frequency response problems.

Assumptions

The modified IEEE-24 bus system is adopted for the two-stage generation expansion planning (**GEP-III**). The original load data is modified to expedite the flexibility shortage and insecurity of frequency. Table 6.2 shows the modified data. The adequacy and flexibility planning are programmed in the MATLAB software. To confirm the load-frequency control, DIgSILENT software is used for power system simulation. Refer to the IEEE-24 bus data, the information is summarized as Table 6.2.

Table 6.2

Modified original load data of IEEE-24 bus for study case 4

Descriptions	2018	2019	2020	2021	2022	2023	2024	2025	2026	2027	2028
Original load (MW)	2,850	3,135	3,448	3,793	4,173	4,590	5,049	5,554	6,109	6,720	7,392
Net load (MW)	2,850	3,070	3,377	3,715	4,086	4,495	4,944	5,438	5,982	6,581	7,239
Utility-scale solar PV (MW)	0	188	396	556	712	952	1,187	1,447	1,780	2,175	2,670
PV penetration (%) (based-on installed capacity)	0%	6.0%	11.5%	14.7%	17.1%	20.7%	23.5%	26.1%	29.1%	32.4%	36.1%

Figure 6.6 shows the chronological load profile of the IEEE-24 bus and actual utility-scale solar PV generation which are derived from Thailand's 2014 generation system. Finally, the solar PV generation is normalized and then scaling-up the installed capacity.

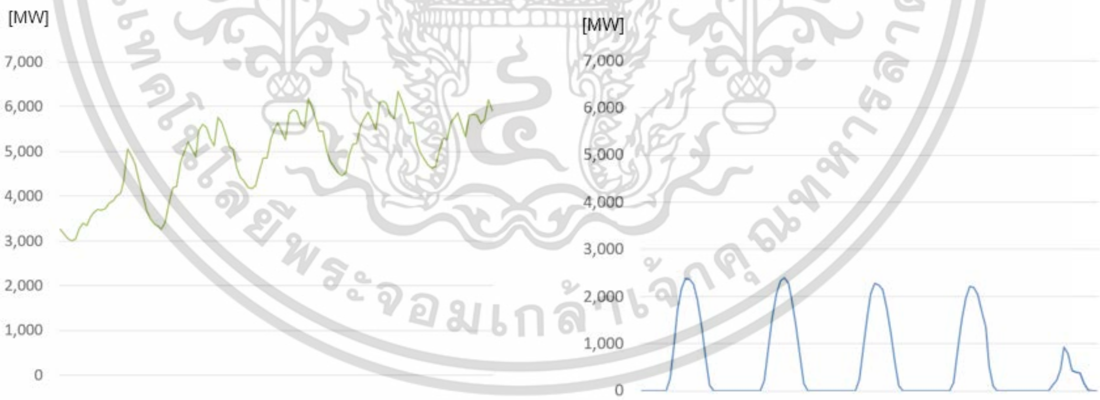

Figure 6.6 Original Chronological load profile and utility-scale solar PV generation

The main assumptions are summarized as follows:

- The flexibility information and the governor response data use the same data as the original information of the IEEE RTS. The recommended control block refers to [142].
- The typical netload profile is illustrated as shown in Figure 6.7.

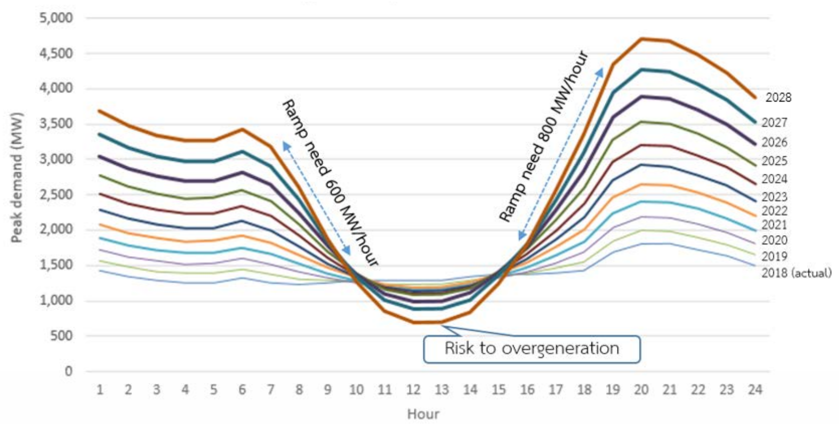

Figure 6.7 Typical daily net load profile forecasting on 2019-2028 periods

- The quadratic cost functions of generating units are estimated using method in this [189].
- The frequency security information follows the reference [190]. The governor models [191] of each dispatchable generation are set as: (1) the oil-fired power plants are set a "GGOV1", (2) the coal-fired power plants are set an "IEEEG1", (3) the hydropower plants are set an "HYGOV2", and the nuclear power plants are assumed as a non- governor control.
- The power plants are clustered using the fuel type and ramp capability as result in Table 6.3.

Table 6.3

Assumption informations based on modified IEEE RTS

General informations				Quadratic cost function			Frequency security informations*			Flexibility informations				Clustering power plants
type	Unit size (MW)	Num. of units	Fuel/Tech	aX^2	bX	c	Governor control	Governor response (MW/s)	Inertia (MJ/MW)	Min down time (hour)	Min up time (hour)	Min stable output (MW)	Ramp capability (MW/s)	
U12	12	5	Oil/Stream	2.87	157	305	GGOV1	1.13	2.8	2	4	2.4	1	High flexible plant (oil)
U20	20	4	Oil/Stream	2.1	166	301	GGOV1	1.9	2.8	1	1	16	3	Gas turbine
U50	50	6	Hydro	0.001	11	200	HYGOV2	1	3.5	N/A	N/A	N/A	N/A	Hydroelectricity
U76	76	4	Coal/stream	0.07	19	323	IEEEG1	7.6	3.0	4	8	15	2	Medium flexible plant (coal)
U100	100	3	Oil/stream	0.22	136	2352	GGOV1	9.3	2.8	8	8	25	7	Medium flexible plant (oil)
U155	155	4	Coal/stream	0.01	18.2	444	IEEEG1	15.6	3.0	8	8	53	3	Low flexible plant (coal)
U197	197	3	Oil/stream	0.09	139	698	GGOV1	18	2.8	10	12	67	3	Low flexible plant (oil)
U350	350	1	Coal/stream	0.001	17.9	780	IEEEG1	34.4	3.0	48	24	140	4	Inflexible plant (coal)
U400	400	2	Nuclear/stream	0	6.2	410	-	-	5.0	1	1	100	20	Nuclear plant

PI controller for load-frequency control

The proportional-integral controller (PI controller) is adopted for the load-frequency control (regulation mode) to stabilize the set-point frequency within 40 seconds. The trial and error method is applied for the gain tuning (gains are selected 1 and 0.1 for the proportional-integral controller, respectively). The time delay is assumed

0.5 seconds, and the forward bias gain chooses the value as 0.16. It is noticed that the following mode is out of the scope of this chapter. Finally, frequency security is considered the N-1 condition (the largest power plant) under the regulation mode.

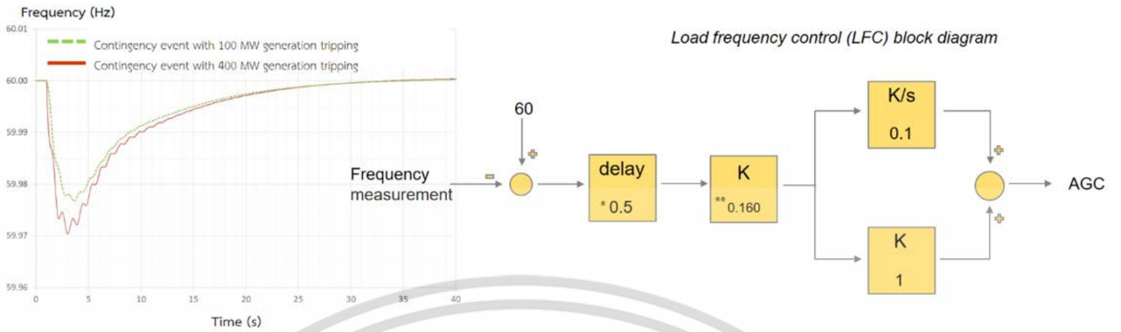

Figure 6.8 Load frequency control's block diagram with PI controller.

Frequency control policy

In this study, the frequency control policy for regulation mode is summarized in Table 6.4.

Table 6.4

Frequency control policy for regulation mode

Frequency Threshold [Hz]	Descriptions
$63 < \text{freq}$	Perform the generation-shedding scheme to disconnect the power plant for the system frequency restoration
60 ± 0.36	Normal operation within deadband of 360 mHz
$\text{freq} \leq 59.64$ or $60.36 \leq \text{freq}$	Perform load-frequency control
$\text{freq} < 57$	Perform the load-shedding scheme to disconnect the load for the system frequency restoration

Test case descriptions

The comparative test cases are designed to demonstrate the proposed framework as follow;

Test case 1: It is referred to as the 'base case' considering adequacy planning.

Test case 2: It is referred to as the 'proposed framework' considering adequacy and flexibility. It should be pointed out that the result is a preliminary study for demonstration purposes. The planning assumptions are summarized as follows:

- The adequacy metric: The planning reserve is required between the boundaries $[\mathrm{RM}^{\min}, \mathrm{RM}^{\max}]$.
- The flexibility metric: In practice, we have no standard flexibility metric, so the data from the operation simulation is utilized for the flexibility shortage. To consider the worst case, the load shedding $P_S^{\max}$ and renewable curtailment $P_C^{\max}$ are considered as the zero energy. Thus, the candidate plan that violates the constraints (6.7-6.8) will be judged as a flexibility shortage. The dummy gas turbine [20 MW] will be added to mitigate the deficit of flexible generation. As the test system has no neighboring system, the overgeneration is assumed as the zero energy, also.
- The frequency security criteria: The frequency security considers the N-1 condition which the largest generating unit is tripped. The minimum frequency $\mathbf{freq}_{\min}$ is assumed 57 Hz with a dead time 0.5 seconds (the dead band frequency $\mathrm{freq}_{\mathrm{db}}$ is greater than or equal to 360 mHz).

6.4.2 Simulation results

A. Two-stage planning result

The adequacy investment is conducted based on the details in Chapter 3. The flexibility investment is based on the flexibility shortages, i.e. renewable curtailments and load-shedding. In the case of unsatisfied flexibility requirements, the dummy gas turbines are added to increase the flexible generation. Table 6.5 shows the investment comparison between test case 1 and test case 2.

Table 6.5

Comparison of adequacy and flexibility investment

Name	Adequacy investment [million $]	Flexibility investment [million $]	Total cost [million $]
Test case 1	1,108	0	1,108.0
Test case 2	1,108	140.6	1,248.7

The two-stage generation expansion planning suggests an optimal solution as Table 6.6. The installed capacity is 9,000 MW satisfying the reserve margin.

Table 6.6

Optimal plan of proposed framework

Descriptions		Year									
		2019	2020	2021	2022	2023	2024	2025	2026	2027	2028
Adequacy planning:											
U75	Medium flexible plant (Coal)	0	0	0	0	1	1	1	1	1	1
U100	Medium flexible plant (Oil)	1	1	1	1	2	1	2	1	2	2
U150	Low flexible plant (Coal)	0	0	0	0	1	0	0	1	1	1
U190	Low flexible plant (Oill)	0	1	0	1	1	1	0	1	1	1
U350	Inflexible plant (Coal)	1	0	0	0	0	0	1	0	0	0
U400	Nuclear plant	0	0	1	0	0	1	0	0	0	0
Flexibility planning considering frequency security:											
U20	dummy gas turbine	0	0	0	0	2	2	2	2	4	4
	Reserve margin [%]	12.3	12.0	12.2	11.8	12.2	12.7	12.7	12.5	12.4	12.2

B. System flexibility analysis

The typical daily dispatch is demonstrated by using the long-holiday (14 April 2028) which is the most risk of the overgeneration. Table 6.7 reports the minimum and maximum netload as 686 MW and 4,701 MW, respectively. Furthermore, the downward- and upward- ramping which are required to follow the morning and evening loads, are 988 MW/hour and 746 MW/hour, respectively.

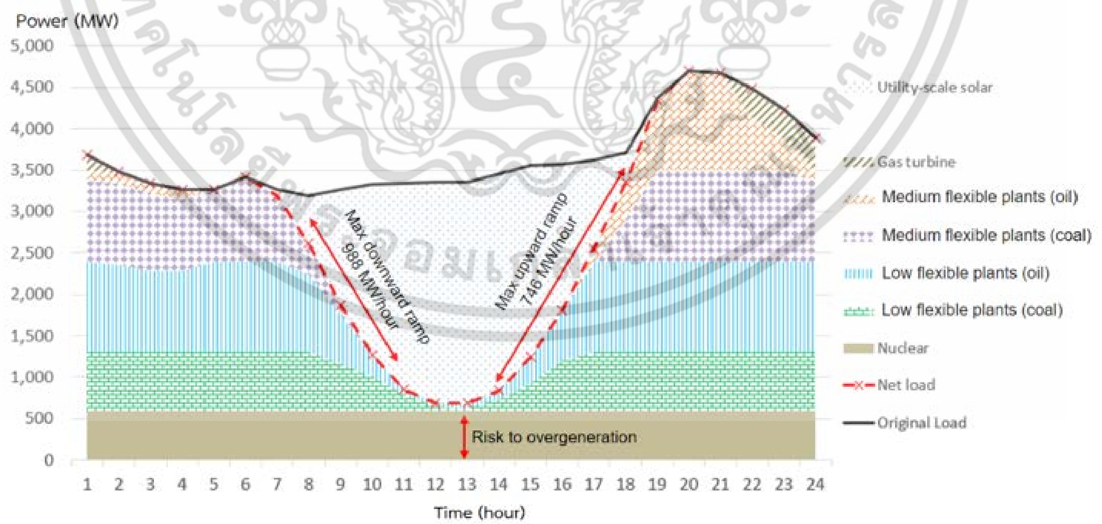

Figure 6.9 Typical daily dispatch at 14 April 2028 (risk to violate the operating dispatch)

Refer to the demonstrated load profile as shown in Figure 6.9, the flexible generations are adequate with medium flexible plants (U75 and U100) and dummy gas turbines (U20). The baseload power plants which are nuclear and inflexible plants (U350) are reduced the plant utilization. An analysis between flexible generation and system net load shows that the generation system is sufficiently flexible to respond to the ramping requirements.

Table 6.7

Dispatching data on 14 April 2028

Hour	Original load	Variable generation	Net load	Ramp net load	Dispatching net load	Maximum reserve
1	3,683	0	3,682	-267	3,682	2,528
2	3,476	0	3,476	-206	3,476	1,794
3	3,341	0	3,341	-135	3,341	1,929
4	3,262	0	3,262	-79	3,262	2,008
5	3,267	0	3,267	5	3,267	483
6	3,419	0	3,418	151	3,418	332
7	3,265	78	3,187	-231	3,187	563
8	3,184	569	2,615	-572	2,615	1,135
9	3,260	1391	1,869	-746	1,869	681
10	3,323	2055	1,267	-602	1,267	1,283
11	3,347	2492	854	-413	854	1,696
12	3,356	2670	685	-169	689	1,865
13	3,356	2661	695	10	695	2,255
14	3,460	2616	843	148	843	2,107
15	3,555	2311	1,244	401	1,244	1,306
16	3,576	1771	1,804	560	1,804	746
17	3,626	1072	2,554	750	2,554	1,516
18	3,716	356	3,360	806	3,360	1,910
19	4,365	17	4,347	987	4,347	923
20	4,701	0	4,700	353	4,700	570
21	4,671	0	4,670	-30	4,670	600
22	4,480	0	4,480	-190	4,480	1,190
23	4,230	0	4,229	-251	4,229	1,441
24	3,886	0	3,885	-344	3,885	2,325

C. Load dispatch considering the primary reserve

The 12th hour on 14 April 2028 is demonstrated for the primary reserve. This operation scenario represents the "worst-case frequency security". This scenario observes the lowest system inertia and the lowest governor capability resulting from de-commitment thermal generation. Using equation (6.34), the governor ramping capability is calculated as below;

$$GRC^{min} = \frac{\frac{1}{2}\Delta P^2}{M_H(freq_0 - freq_{min} - freq_{db})} = \frac{\frac{1}{2}300^2}{116.21(60-57-0.516)} \tag{6.35}$$
$$= 277.16\ MW/second$$

Using equation (6.26), the system inertia is calculated as below;

$$M_H = 2 \times \frac{\sum_{g\epsilon\mathcal{G}} S_g \times h_g}{60} = 2 \times \frac{(3\times 89\times 3 + 1\times 119\times 2.8 + 1\times 471\times 5)}{60} \tag{6.36}$$
$$= 116.21 \quad MW - s/Hz$$

In this operation scenario, the running power plants are dispatching 689 MW. The primary reserve prepares 439 MW for the governor use with 32.1 MW/second. The dispatching data of generating units is shown in Table 6.8.

Table 6.8
Generating units dispatching at hour 12

Name	Installed Capacity [Num x MVA]	Dispatch Power [MW]	Inertia Constant [MJ/MW]	Reserve for Primary control [MW]	Reserve for Secondary control [MW]
U76	3x89	3x20	3	3x11	3x56
U100	1x119	1x35	2.8	1x10	1x65
U400	2x471	2x300	5	0	2x100

D. Frequency security analysis

The N-1 frequency security is considered by tripping the largest-power plant (U400). The disturbance started at 1.01167 seconds using the time step 0.01 second in the simulation program. This study compares the three responses, i.e. inertial frequency-, primary- and secondary responses. The basic parameters are calculated as below;

- Generation loss ΔP:

$$\Delta P = \frac{\text{power loss}}{\text{base power}} = \frac{-300}{700} = -0.428571 \text{ per unit} \tag{6.37}$$

The frequency excursion is shown in Figure 6.10. The system is considered as ‘frequency security’ since the quasi-steady state stays upper the minimum frequency requirement (57 Hz).

- System inertia coefficient M_H:

  Based-on the simplified single machine model [7.27], the system inertia coefficient can be calculated as below;

$$M_H = \frac{\Delta P}{\frac{d}{dt}\Delta \text{freq}} = \frac{-0.428571}{\frac{(59.851-60)/(60)}{0.05}} = 8.63 \text{ seconds} \tag{6.38}$$

where $\frac{d}{dt}\Delta\text{freq}$ (refer to RoCoF) derives from tangent at $t = 0$; From Figure 6.10, we choose the coordinate (1.011667,60) and (1.061667, 59.85098).

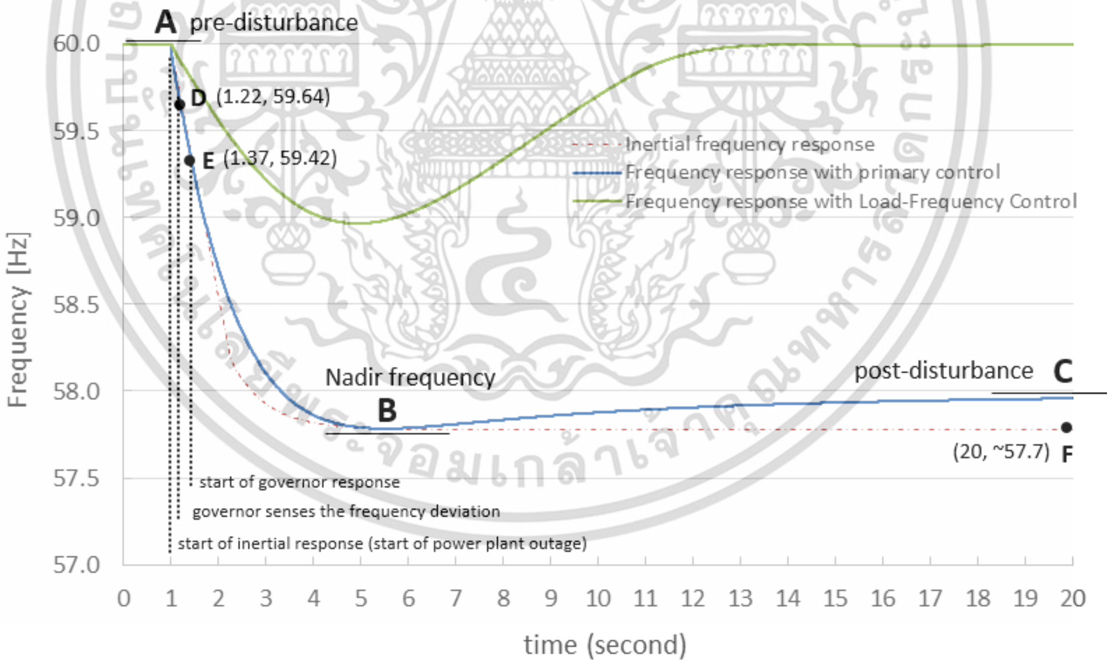

Figure 6.10 Frequency excursion after tipping largest power plant (400 MW)

The analysis of the different control schemes is described as following:

<u>Inertial frequency response</u>: This frequency excursion only relies on the system self-regulation (system inertia and dynamic characteristics of electrical load). The lowest

frequency is observed at 57.784 Hz within 4.47 second, equation 6.34 is applied as below;

$$\Delta\text{freq(t)} = \frac{\Delta\text{P}}{\text{D}^{\text{load}}}\left(1 - e^{\frac{-\text{D}^{\text{load}}}{M}t}\right) = \frac{-0.428571}{\text{D}^{\text{load}}}(1 - e^{\frac{-\text{D}^{\text{load}}}{8.63}t}) \qquad (6.39)$$

To duplicate the inertial response, we apply the coordinate (4.47, 57.784). So, the per-unit frequency deviation $\Delta\mathbf{freq(t)}$ **is** $(\mathbf{60} - \mathbf{57.784})/\mathbf{60} = \mathbf{0.0369}$. Solve it by using goal-seek (Mircosoft's excel), gives $\text{D}^{\text{load}} = 11.575$ (a positive value means the self-regulation property).

$$0.0369 = \frac{-0.428571}{11.575}(1 - e^{\frac{-11.575}{8.63}4.47}) \qquad (6.40)$$

<u>Primary response</u>: In this case, the secondary control is deactivated. From Figure 6.10, the frequency deviation reaches a new equilibrium point at coordinate (20, 57.7). Using equation (6.28), the power frequency characteristic (PFC) [MW/Hz] is calculated as below;

$$\text{PFC} = \frac{\Delta\text{P}}{\Delta\text{freq}_{\text{quasi}}} = \frac{-300}{60 - 57.7} = -130.4 \qquad (6.41)$$

From Figure 6.10, the frequency deviation reaches the nadir frequency at the coordinate (5.4817, 57.784). The rate of change of frequency (RoCoF) [MW/Hz] can be calculated as below equation;

$$\text{RoCof} = \frac{\Delta\text{P}}{\Delta\text{freq}_{\text{NAD}}} = \frac{-300}{60 - 57.784} = -135.379 \qquad (6.42)$$

We can calculate the self-regulation property and governor response as follows:

$$D^{\text{self}} = \frac{\Delta\text{P}}{\text{freq}_{\infty}} = \frac{0.4286}{0.0336} = 12.75 \text{ per unit} \qquad (6.43)$$

$$\text{D}^{\text{GOV}} = D^{\text{self}} - \text{D}^{\text{load}} = 12.75 - 11.575 = 1.175 \text{ per unit} \qquad (6.44)$$

where $\mathbf{freq}_{\infty}$ represents the steady-state frequency [per unit] without the primary and secondary control.

<u>Secondary response</u>: In this case, the regulation mode applies both primary- and secondary- controls. It is observed that the primary reserve of on-line power plants is

sufficient to cover the tripped power plant. So, the system frequency rebounds to the set-point frequency within 12 seconds.

6.5 Conclusions

This chapter demonstrates the two-stage generation expansion planning that incorporating the adequacy, flexibility, and frequency security. First planning stage, the adequacy planning aims to finds a least-cost plan which satisfying system constraints, e.g., reserve margin and LOLP criteria. The candidate plans of the early stage are selected for the next planning horizon. The second planning stage, so-called 'flexibility and frequency security planning' examines the candidate plans which are not capable to balance between supply and demand, are required the flexible power plant. The operation simulation is carried out for flexibility and frequency security assessment at hourly resolution and is slid over the planning horizon.

Within this chapter, the modified IEEE RTS has magnified the flexibility shortages and frequency collapse problems by adding 30% utility-scale solar PV into the load profile. As a result of the proposed framework, the generation portfolio can operate reliably under (1) steeper upward- and downward ramping, (2) higher cycling requirement, and (3) decreasing the system inertia.

Chapter 7
Strategic Choices of Climate Change Policies for Clean Energy Investment

In the 21st century, the developed and developing nations have been focusing on the global climate change caused by atmospheric carbon dioxide (CO_2) and other greenhouse gases (GHGs) [192]. The ultimate goal provided by the United Nations Framework Convention on Climate Change (UNFCCC) is to stabilize the atmospheric GHGs concentration on avoiding the level of dangerous anthropogenic interference [193]. Naturally, the global carbon cycle exchanges the carbon among the atmosphere, hydrosphere, biosphere, and geosphere through photosynthesis, deposition, respiration and, so on [194]. The CO_2 gaseous is accumulated in the atmosphere because of the net unbalance of carbon source and carbon sink [195]. The human-driven activities disturb the net balance of the carbon cycle in two main ways: through the combustion of fossil fuels for the industrialization and the removal of the forest for urbanization [196].

The latest observations measured by the Earth System Research Laboratory in Mauna Loa reveal [3] that the atmospheric CO_2 reached a new high in April 2020 with 416.03 parts per million (ppm) which significantly has increased 47.89% from 280 ppm since the pre-industrial revolution [197]. The increasing CO_2 concentration is likely to raise the Earth's average temperature exceeds 2°C temperature rise. According to the fourth assessment of the Intergovernmental Panel on Climate Change (IPCC) [198], the average surface temperature had increased 0.74±0.18°C compared to the pre-industrial era which harms the climate system. Through the Paris Agreement, limiting temperature rise to well below 1.5°C by 2100 minimizes the risky trigger to the climate tipping point [199]. It requires the negative anthropogenic CO_2 emission by 2070 [200] to stabilizing GHGs concentration within 450 ppm for avoided long-term irreversible changes.

This chapter studies electricity planning in Thailand electric supply industry with consideration of the prospect on the carbon emission trading scheme and carbon tax scheme to increase competitiveness to go beyond 2°C global climate change policy.

7.1 Background to Thailand's electricity sector

7.1.1 Current status based-on PDP2018

Based-on PDP2018, the utility's electricity demands in Thailand was estimated peak and energy at 53,997 MW and 367,458 GWh, respectively. In 2037, the generation fleet comprises: (1) existing capacity 11,792 MW, (2) new coal-fired generation 4,420 MW, (3) new gas-fired generation 18,720 MW, (4) new energy efficiency 3,980 MW, (5) new hydroelectricity 4,698 MW and renewables 10,623 MW.

Based-on energy balance analysis, the generated energy comprises (1) large hydroelectricity 38,308 GWh, (2) gas-fired generation 196,062 GWh, (3) bunker generation 32 GWh, (4) diesel generation 69 GWh, (5) lignite-fired generation 21,619 GWh, (6) imported coal 24,468 GWh, (7) renewables 66,270 GWh, and (8) energy efficiency 20,499 GWh. As a result of generation fleets, CO_2 emission and intensity data are summarized in Table 7.1.

Table 7.1

Electricity demand and carbon dioxide emission based-on PDP2018

Year	Utility's Electricity		System's electricity		Carbon dioxide	
	Peak [MW]	Energy [GWh]	Peak [MW]	Energy [GWh]	Intensity [kgCO_2/kWh]	Emission [MtCO_2]
2020	32,732	219,946	37,437	258,549	0.386	84,825
2025	38,780	261,100	44,396	306,774	0.337	88,021
2030	44,781	303,138	51,341	355,789	0.326	98,743
2035	51,265	348,302	58,803	408,281	0.295	102,717
2037	53,997	367,458	61,965	430,693	0.283	103,845

7.1.2 Low-carbon economy development

In the context of sustainable development goal 13 of The United Nations, the government of Thailand decided to include the Nationally Appropriate Mitigation Actions (NAMAs) target into the energy policy to reduce the CO_2 emission by 7-20 % of the energy sector in 2020. Furthermore, Conference of Parties 21 (COP21) held in Paris, Thailand intends to reduce the CO_2 emission by 20-25 percent from the 2010 business-as-usual (BAU) level by 2030 as Nationally Determined Contribution (NDC) target. As these commitments, Thailand's NDC roadmap [211] set a 20% reduction target as 115.6 million metric tons of CO_2 emission (MtCO_2) in economy-wide, hereafter referred to as

"444 MtCO_2 pathway". The electricity sector (sub-group in energy sector) committed a reduction target of 24 MtCO_2 contribution to achieve the national NDC target. According to the 2019 emission inventory, the Thailand energy sector emits 316 MtCO_2 which below the 2010 baseline emission (330 MtCO_2). Even if the NAMA's 20% reduction target is achieved, the government of Thailand is considering the appropriate policy instruments, i.e. carbon tax scheme (CTS) and emission trading scheme (ETS) to go farther 444 MtCO_2 pathway. The country-level inventory of CO_2 emission is reported in Table 7.2.

Table 7.2

Country-level CO_2 emission projection based-on PDP2018 (unit: GtCO_2)

Descriptions	2010	2015	2020	2025	2030	2035	2037
Agriculture, forestry, and Fishery	14.60	18.30	22.90	26.90	30.90	37.90	39.90
Commercial & Residential	6.40	7.70	9.10	10.60	12.10	8.60	9.20
MFG industrial process	42.60	52.60	65.30	79.80	92.30	65.80	71.60
Petroleum refining	8.50	10.70	13.30	15.80	18.30	20.80	21.80
Transport	63.80	74.40	77.90	87.30	96.70	65.10	68.86
Agriculture	55.05	57.55	63.05	69.80	76.55	83.30	86.00
Industrial process	32.00	39.10	57.10	74.10	91.10	107.50	114.30
Landuse	15.10	17.70	18.80	18.80	18.80	18.80	18.80
Waste	13.80	15.00	16.60	18.10	19.60	19.10	19.70
Electricity generation	90.88	97.54	84.83	88.02	98.74	102.72	103.85
Energy sector	258.78	300.34	306.43	327.02	346.54	408.42	429.51
Total	342.74	390.59	404.88	428.73	444.50	529.62	555.00

7.1.3 A strategic choice for candidate options

The Levelized cost of energy (LCOE) which is a metric to compare the economy of generating electricity, is calculated in Baht/kWh (the exchange rate is 32 baht/USD). Based-on 2019, Thailand energy mix relies on 59.64% of the natural gas-fired combined cycle plant. Figure 7.1 shows the LCOE comparison among generating technologies which the natural gas-fired combined-cycle dominates the others. However, the solar PV is competing with the natural gas-fired technology because the electricity cost is falling from the learning effect (more detail in section 7.3). The cost of the integrated gasification combined cycle (IGCC), the new clean energy option, is going down for the commercial phase.

The abatement cost is calculated in Baht/kWh, which is a metric to compare the cost of the negative externalities reducing from the environment. Based-on PDP2018, the abatement cost of candidate options is shown in Figure 7.1 which the pulverized coal with sub-critical boiler technology is used for reference. The natural gas-fired combined cycle is the economy in point of abatement cost while the IGCC, the new clean energy option, has too expensive compared to the others.

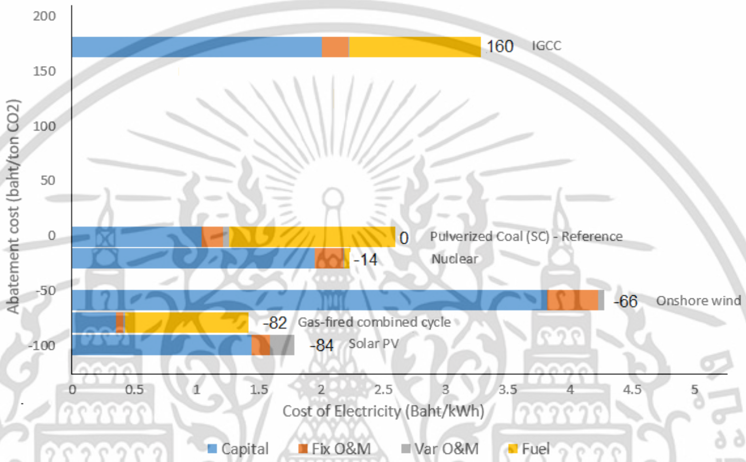

Figure 7.1 The abatement cost vs cost of electricity, refers to PDP2018 [202].

7.2 New clean energy investment

7.2.1 Valley of death of new energy technologies

Generally, the candidate options of GEP comprise the cost-competitive technologies which product phase is either maturity or commercialization. Unfortunately, current technology can not go beyond 0.283 $kgCO_2/kWh$ without the high-efficiency low emission technology. Table 7.3 summarized the new clean energy technology choices for mitigation potential by 2020-2037 [203].

Generally, technological innovation can be described as four stages of development: research & development (R&D), demonstration, scale-up, and fully commercial phases. In the early stage, basic and applied researches discover the new technology [204]. The conceptual plant is built to prove the concept which cost of the lab-scale is very low. As any innovation is technically viable, the pilot plant is required for the showcase. At this step, the unit-cost increases sharply and need participation from the governmental and private funds. For example, the beginning of renewable development in Thailand is technically feasible, but most project sites it is uncompetitive without subsidies.

Table 7.3
Clean energy technology choices for mitigation potential

Types	Technologies	Stage	Descriptions
Clean coal	Advance ultra- and ultra- Supercritical steam boiler	R&D to Commercial	High-temperature materials requirement.
	IGCC	Demonstration	Cost barrier and full-scale demonstration.
	Carbon capture and storage	Demonstration	Cost barrier and full-scale demonstration.
Renewables	Hybrid SPP/VSPP firm, Hydro-floating solar PV, Solar rooftop.	Scale-up	Flexibility and frequency security concern; Distribution system concern
Nuclear	II and III generation. IV generation	Commercial to R&D	Postponed since the Fukushima Daiichi disaster in 2011.
Energy efficiency	End-use efficiency, vehicle, heating, cooling	Scale-up to commercial	Requres technical work to bring the product to fully commcercial

The cost barrier to transition from the demonstration phase to the scale-up phase is called the "valley of death". It is a gap between discovery and commercial viability as shown in Figure 7.2.

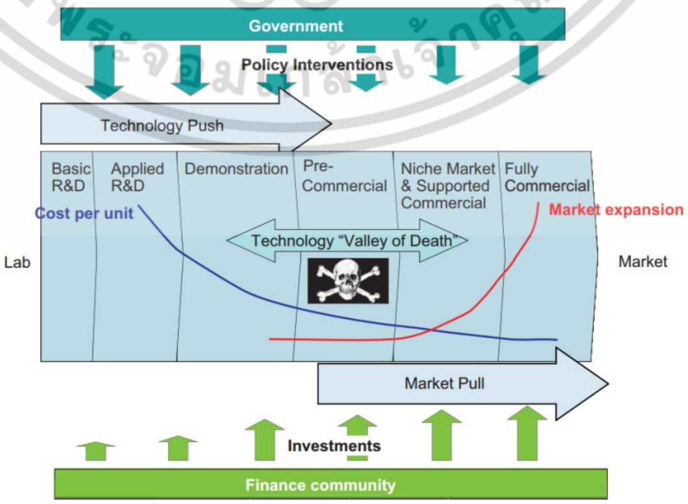

Figure 7.2 The valley of death of new energy technologies, adopt from [204].

7.2.2 Integration of the learning by doing effect

From historical observation, the price/cost trend comprises of 4 phases: (1) development, (2) price umbrella, (3) shakeout, and (4) stability phases [205]. For the new technology innovation, the price/cost evolution of falling per-unit cost (see Figure 7.3) is referred to as the "learning by doing" which reducing cost is influenced by an experienced worker, economies of scale, and technological development.

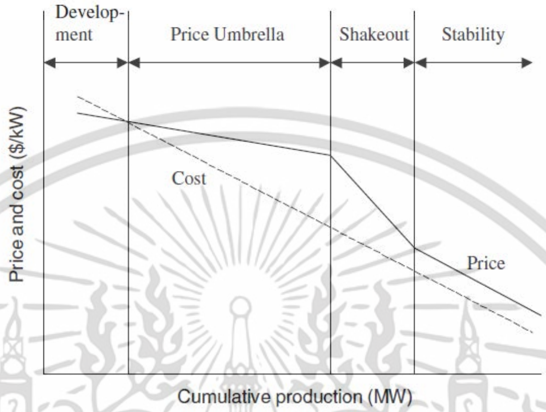

Figure 7.3 Price and cost evolution affect by learning effect, adopt from [205].

The concept of learning by doing (LBD) [205] is the phenomenon that double cumulative capacity, constantly decreases unit cost (or market price). For example, a progress ratio PR of 95% describes that for every double cumulative capacity, the investment cost decrease by 5% (learning rate factor: LR). The basic LBD can be expressed mathematically as follows:

$$C_{g,t}^{\mathrm{Inv}} = \alpha_g^{\mathrm{LBD}} \times \mathrm{I}_{g,t}{}^{\mathrm{const}_g} \qquad g \in \mathcal{G}^N, t \in \mathcal{T} \quad (7.1)$$

Which,

$$\mathrm{I}_{g,t} = \mathrm{I}_g^0 + \sum_{t=1}^{\mathrm{T}} \mathrm{I}_{g,t} \qquad t \in \mathcal{T} \quad (7.2)$$

$$\mathrm{const}_g = \frac{\log(\mathrm{PR})}{\log(2)} \quad (7.3)$$

$$\mathrm{LR} = 1 - \mathrm{PR} \quad (7.4)$$

where $C_{g,t}^{\mathrm{Inv}}$ represents the unit investment cost [$/kW] of candidate option g at time t; α_g^{LBD} represents the constant of LBD model; I_t represents the cumulative installed capacity [MW] of technology g at time t; I_g^0 represents the initial cumulative installed capacity [MW]; LBD is constant which derive from log of progress ratio PR divide by log 2; The LBD is useful to forecast the unit investment cost (external and variable O&M costs do not reduce on LBD). Equation 3.15 is modified as following equation.

$$CC\left(U^{(t)}\right) = \sum_{t\in\mathcal{T}} \mathrm{NPV}^{(t)} \left(\sum_{g\in\mathcal{G}^N} \alpha_g^{\mathrm{LBD}} \mathrm{I}_{g,t}^{\frac{\log(\mathrm{PR})}{\log(2)}} \mathrm{Cap}_g U_g^{(t)} \right) \qquad g \in \mathcal{G}^N, t \in \mathcal{T} \quad (7.5)$$

7.2.3 Integration of thermal efficiency and emission factor improvement

Generally, the relationship between CO_2 emission rate [$\mathrm{kgCO_2/MWh}$] and thermal efficiency [%] is approximated as the linear trend as Figure 7.4.

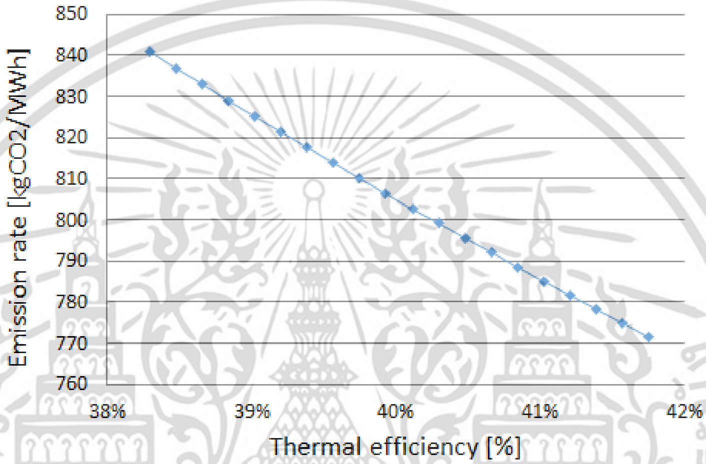

Figure 7.4 Relationship between CO_2 emission rate and thermal efficiency

As the average heat rate [MMBtu/MWh] defines $\mathrm{AHR} = \frac{3.41}{\eta_g^{\mathrm{th}}}$; Equation 3.15 is modified as the following equation.

$$EP\left(X^{(t)}\right) = \sum_{t\in\mathcal{T}} \mathrm{NPV}^{(t)} \left(\sum_{g\in\mathcal{G}} E_g^{\mathrm{PPS}} \left(\frac{3.41}{\eta_g^{\mathrm{th}}} FC_g + C_g^{\mathrm{VOM}}\right) \right) \qquad g \in \mathcal{G} \ (7.6)$$

To improve the CO_2 emission factor [$\mathrm{kgCO_2/MWh}$], the carbon capture and storage (CCS) technology is introduced. The CCS can equip with thermal power plants, i.e. coal-fired power plant, IGCC plant, natural gas-fired combined-cycle plant, and so on. For example, the pulverized coal supercritical boiler with 30% and 90% CCSs have 796 $\mathrm{kgCO_2/MWh}$ and 115 $\mathrm{kgCO_2/MWh}$, respectively. Figure 7.5 depicts the CO_2 emission factor improvement. Unfortunately, the thermal efficiency is degraded, so-called "thermal efficiency penalty" [206] that range around 10%-15%.

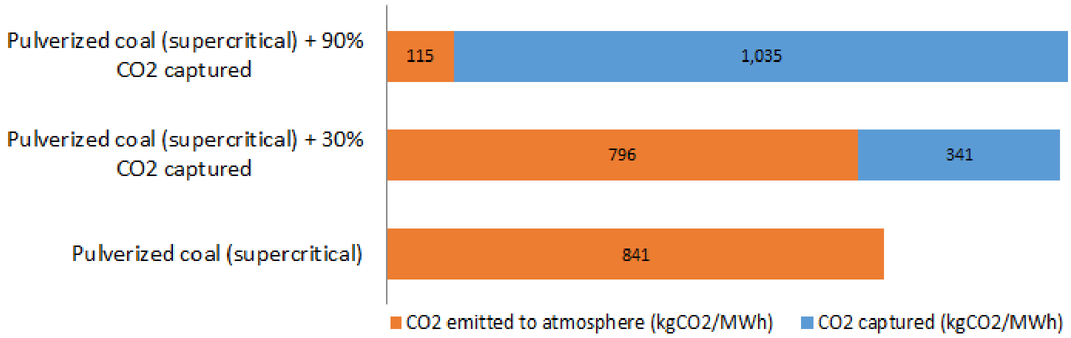

Figure 7.5 Boosting near-zero emissions by carbon capture and storage (CCS)

7.3 Policy instruments to accelerate the clean energy options

Bridging the valley of death, the policy instruments to accelerate the clean energy options are described as following:

7.3.1. Emission trading scheme (ETS)

The emission trading scheme (ETS) [207] is a quantity-based incentive by putting a price on carbon. The concept of ETS is a market mechanism on a nation-wide sector to drive the high-emission technologies to low-emission ones via the "cap and trade" principle. A "cap" in this context means the baseline CO_2 emission (2010 emission inventory). A "trade" in this context means the selling and buying capabilities of carbon credit to become carbon neutral. The simplest concept to describe the ETS can be described as follows;

Step 1 Target setting: To set the emission reduction target, equation 3.27 is rewritten as below;

$$VT_t = ET_t - \sum_{g \in \mathcal{G}} E_g^{PPS} \delta_g^{CO_2} \quad , \forall t \in \mathcal{T} \quad (7.7)$$

where ET_t indidates the CO_2 emission target [ton-kgCO_2] associated with NAMA/INDC targets in planning horizon t; VT_t represents the carbon neutral [ton-kgCO_2] that a positive value implies the unused allowance which can be sell in the carbon market (the total cost will be reduced); Conversely, a negative value implies the carbon credit that can be purchased form the carbon market (the total cost will be increased).

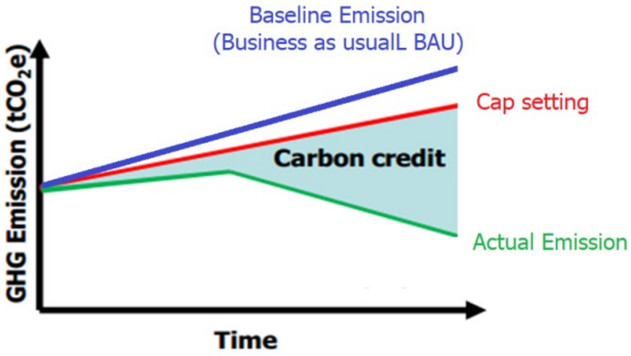

Figure 7.6 CO_2 emission reduction target of Thailand electricity sector, adapted from [137]

Step 2 Allowance allocation: The main approach to allocate the permit allowance are (1) grandfather basis which the initial allowance is neglected and, (2) 0% allowance which no allowance is distributed. The main concept is shown in Figure 7.7.

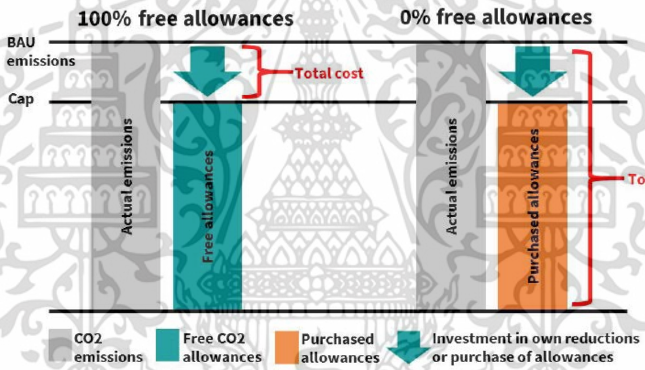

Figure 7.7 Allocations approach with 100% and 0% allowance, adopted from [137]

Step 3 Emission trading: With the market environment, the CO_2 emitter can exchange the carbon credit to buy or sell them from the foreign system under market value (SCC) [\$/tone-kgCO_2]. The equation 3.19 is rewritten to include the carbon cost as below;

$$EC(X^{(t)}) = \sum_{t\in\mathcal{T}} \mathrm{NPV}^{(t)} \left(\sum_{g\in\mathcal{G}} E_g^{\mathrm{PPS}} \left(C_g^{\mathrm{SO_2}} \delta_g^{\mathrm{SO_2}} + C_g^{\mathrm{PM}} \delta_g^{\mathrm{PM}} \right) - SCC \cdot VT_t \right) \quad ,\forall t \in \mathcal{T} \quad (7.8)$$

7.3.2 Carbon tax scheme (CTS)

Carbon tax scheme (CTS) is a price-based incentive which aims to discourage the CO_2 emission and other GHGs that cause climate problem by taxing it (well-known as Pigouvian tax [208]). Generally, the CTS affects the power system both supply and demand-side responses. The supply-side response refers to as the "substitute effect" which carbon tax penalizes the carbon-intensive power plant. The generation technology may change from the coal-fired generation to gas-fired generation, called "fuel switching". Furthermore, the demand-side response refers to the "demand effect" which electricity demand decreases when electricity price increases.

In theoretical, grandfathering a CTS is equivalent to the ETS under the free allocation of permits. The simplest concept to describe the ETS can be described as follows;

<u>Step 1</u> **Design a carbon tax rate:** Ideally, the optimal tax rate should be equal to the marginal abatement cost. However, the screening curve can be used for carbon tax rate design. Figure 7.8 demonstrates the tax rate which activates the technological substitute between IGCC plant and coal-fired generation in the year 2033.

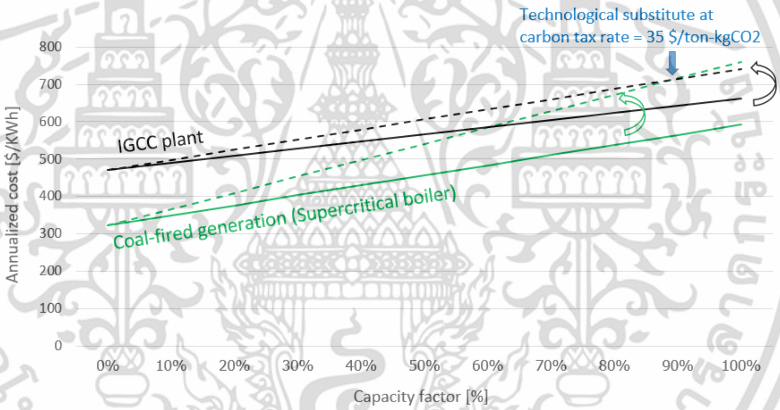

Figure 7.8 Screening curve including the carbon cost

<u>Step 2</u> **Evaluate the increasing price:** To calculate the electricity price effect, the average incremental cost of electricity (AIC) is applied for the incremental cost from proxy electricity price (e.g., cost from IPP purchase cost is 2.62 baht/kWh). The AIC can be expressed mathematically as follows;

$$\mathrm{AIC} = \frac{\mathrm{TotalCost}}{\mathrm{Incremental\ Demand}} \tag{7.9}$$

where **TotalCost** represents the total cost during the planning horizon $t \in \mathcal{T}$ follows equation 3.14; **Incremental Demand** denotes the incremental demand refer to the beginning of the planning horizon. For simplicity, the new electricity price equals to the AIC plus with the IPP purchase cost (2.62 baht/kWh or 0.0819 $/kWh).

<u>Step 3</u> Evaluate the reducing demand: In this dissertation, the price elasticity of electricity demand is adopted –0.001. It should be noticed that the price elasticity of electricity demand is not a constant (it varies depending on the magnitude of electricity demand). The price elasticity of electricity demand can be expressed mathematically as follows;

$$\tau = \frac{\Delta \text{demand}}{\Delta \text{price}} \tag{7.10}$$

where τ represents the price elasticity of electricity demand [dimensionless]; Δdemand represents the change in electricity demand [%]; Δprice represents the change in electricity price.

<u>Step 4</u> Evaluate the new equilibrium: The equilibrium point between the new electricity price and new electricity demand after applied CTS is illustrated in Figure 7.9.

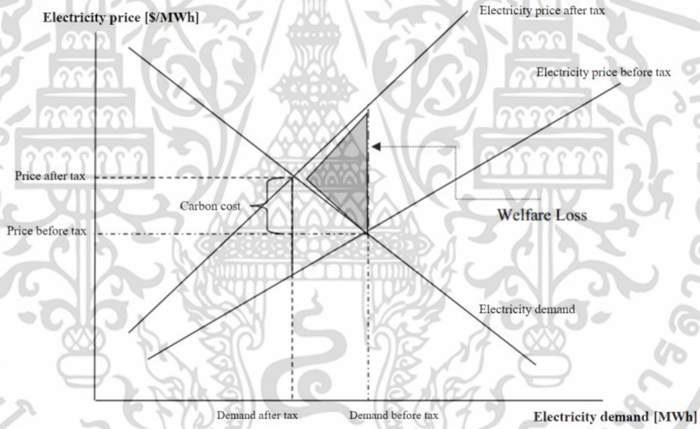

Figure 7.9 The new equilibrium after applies CTS, adapted from [208]

7.4 Study Case 5: Strategic choices for climate change investment

7.4.1 Case study descriptions

Objective

To demonstrate the climate change policies to go beyond the 444 MtCO_2 pathway in the context of PDP2018.

Problem formulation

The compact formulation of **S-GEP-II** considering the extended conditions is:

$$\begin{aligned} \min \quad & (3.15) - (3.21) \\ \text{s.t.} \quad & (3.23 - 3.26) \qquad \forall g \in \mathcal{G} \end{aligned}$$

Scenario descriptions

The scenario analysis designs to different three storylines (refer to as BAU, CTS, and ETS). The three scenarios are described as follows;

- BAU is a scenario that follows the continuation of official PDP2018 in existing policies for the reference case.
- CTS is a scenario in which the carbon tax is applied in the electricity sector. The tax rate is fixed throughout the planning horizon. In order to make IGCC plant competitive with fossil-based plants, a carbon tax is included in fuel costs.
- ETS is a scenario in which the carbon emission trading market is assumed to happen in Thailand. The market environment can exchange the carbon credit to the foreign system. The carbon price is fixed for selling/buying in the market environment throughout the planning horizon.

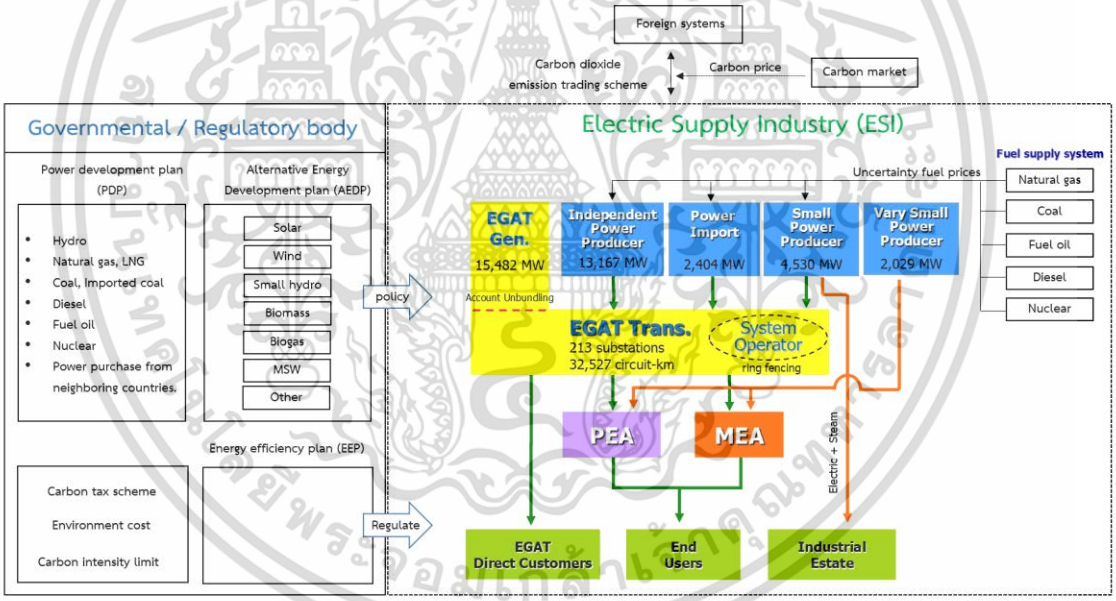

Figure 7.10 Proposed ESI for both ETS and CTS enhancements

Assumptions

1) For this study, Eq. (2.8) and Eq. (2.12) are applied.
2) The fuel assumption follows similar assumptions in PDP2018.
3) The ETS applies the grandfather right to make it apart from CTS. The carbon price is fixed at 5$/ ton-kg$CO_2$.
4) The CTS applies the fixed tax rate at 35$/ ton-kg$CO_2$ (the first year is 2026).

5) Due to strong public resistance against new coal-fired generation, the new coal capacity is restricted to the same energy mix as the PDP2018.
6) Generally, the CCS technology has negative effects: thermal penalty 8%-16%, capacity penalty 50-100MW, and double FOM and triple VOM. This study applies 10% for thermal penalty and applies 100 MW capacity reduction. The CCS equips with 700-MW pulverized coal (ultra-supercritical boiler). The incremental per unit cost is 1,000 $/kW.
7) The learning rate applies 5% for all candidate options.
8) The thermal efficiency advancement is assumed yearly 0.25% addition for ultra-supercritical boiler, advance ultra-supercritical boiler, and IGCC plants.

7.4.2 Scenario results

i) **BAU:** The generation fleet of the BAU scenario is depicted in Figure 7.11. The generation fleets follow the assumption of the official PDP2018. The major different change between PDP2015 and PDP2018 are (1) the nuclear plan is dropped because of the Fukushima Daiichi disaster, (2) energy efficiency replaces the nuclear with superior CO_2 emission, (3) the new coal-fired generation requires the new clean coal technologies, i.e. advance ultra-supercritical boiler, (4) the new natural gas-fired generation uses the imported fuel from foreign spot market (100% imported LNG in 2028).

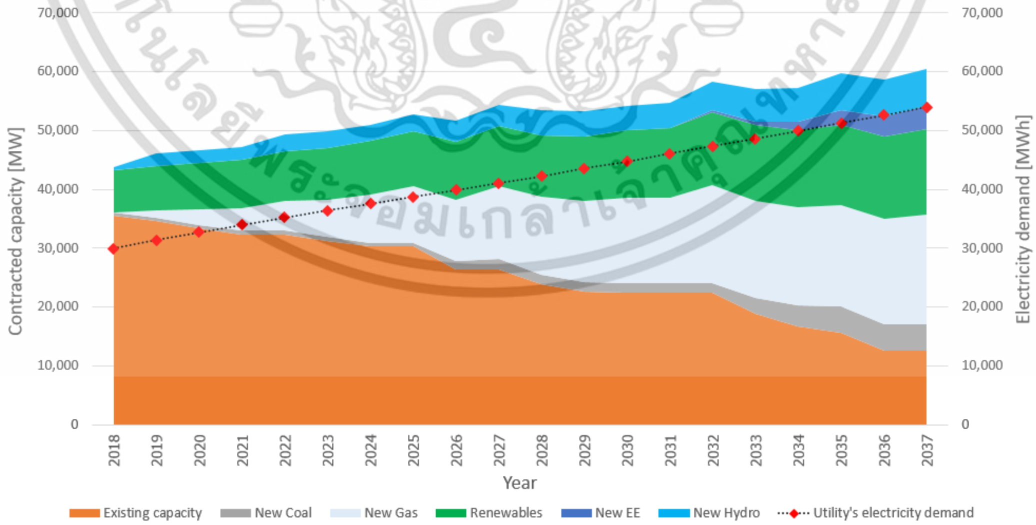

Figure 7.11 Generation fleets of BAU scenario

The energy mix of the BAU scenario is depicted in Figure 7.12. The new coal initially introduces in Thailand's generation system when the indigenous gas is depleted.

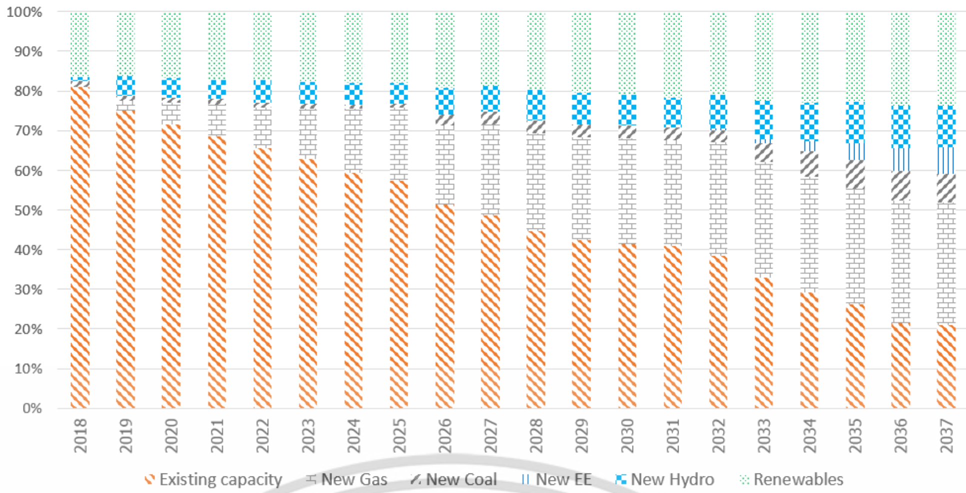

Figure 7.12 Energy mix of BAU scenario

ii) **CTS:** In order to make the IGGC can compete with the coal-fired generation (ultra-supercritical boiler), the carbon tax rate applies 35$/ ton-kg$CO_2$ in 2026. As a result of the carbon tax, the first IGCC plant phase-in at the beginning of 2026. The cumulative capacity of the IGCC plant is 3,300 MW. The generation fleet of the CTS scenario is depicted in Figure 7.13.

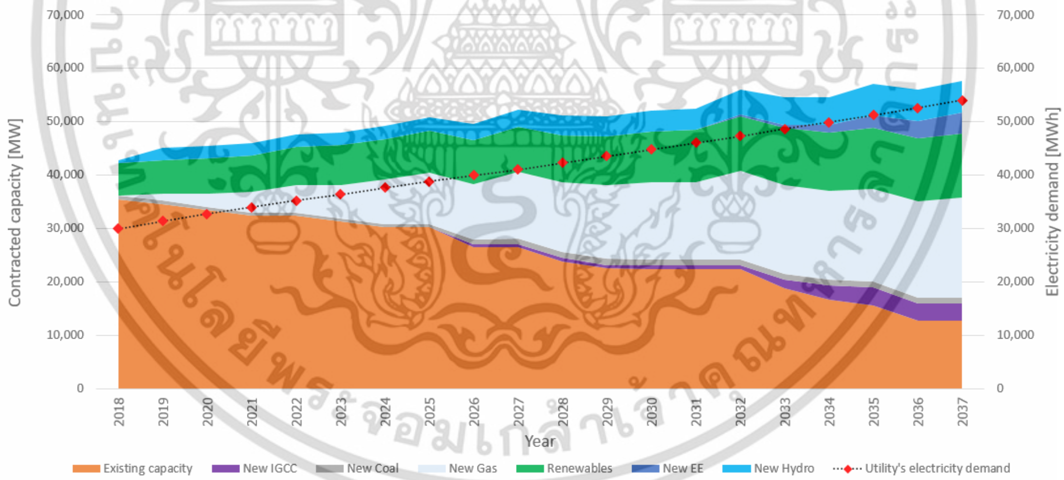

Figure 7.13 Generation fleets of CTS scenario

The energy mix of the CTS scenario is depicted in Figure 7.14. The new coal-fired generation is dominated by the IGCC because of the technological substitute effect.

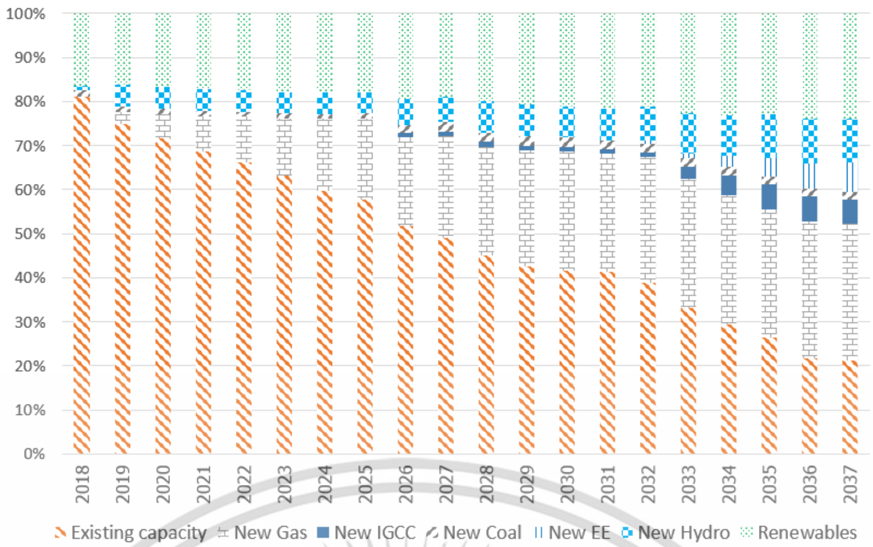

Figure 7.14 Energy mix of CTS scenario

iii) **ETS:** In this scenario, the emission of the BAU scenario is used for cap-setting. The carbon price utilizes 5$/ ton-kg$CO_2$ (160 baht$/ ton-kg$CO_2$ @ exchange rate at 32 baht/$). The generation fleet of the ETS scenario is depicted in Figure 7.15. At the beginning of 2034, the first CCS plant is introduced in the generation portfolio. The cumulative capacity of the CCS plant is 1,500 MW. The remaining capacities of new coal power plant are 1,600-MW IGCC plant and 1120-MW ultra-supercritical boiler.

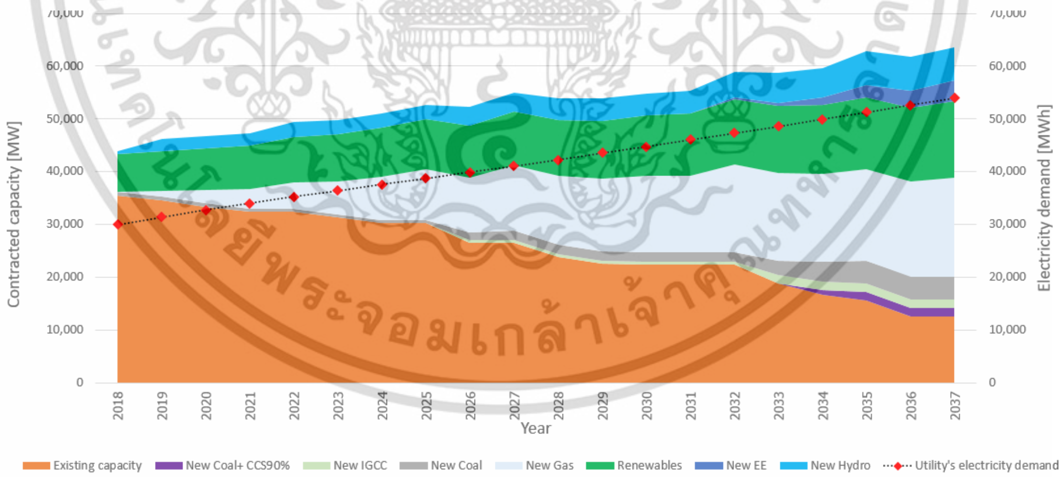

Figure 7.15 Generation fleets of ETS scenario

The energy mix of the ETS scenario is depicted in Figure 7.16. The three types of new coal technology share the energy mix.

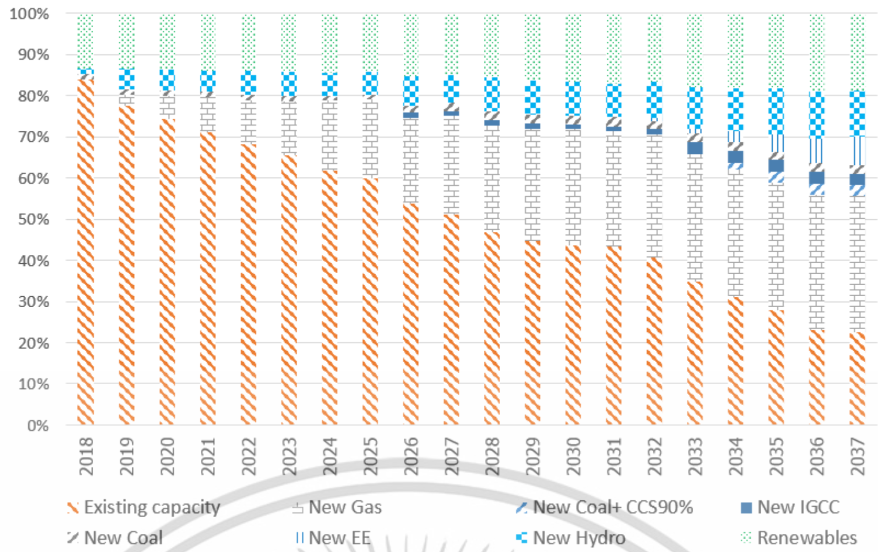

Figure 7.16 Energy mix of ETS scenario

7.4.3 Scenario analysis

i) **The economics of the three scenarios:** Table 7.4 reports the cost comparison among the BAU, CTS, and ETS. Refer to the electricity price, the burden from the carbon tax is transferred to the electricity price. The AIC between ETS and CTS is comparable. Refer to the abatement cost, the ETS scenario is cheaper than the CTS scenario.

Table 7.4

Cost comparison among BAU, CTS and ETS

Scenario	Total Cost [million $]	Energy [GWh]	AIC [$/kWh]	LRMC [$/kWh]	CO_2 emission [ktone-CO_2]	Abatement cost [k$/ton-kg$CO_2$]
BAU	97,809	362,720	0.081	0.163	102,834	-
CTS	109,798	362,358	0.097	0.179	101,572	12.10
ETS	98,858	363,710	0.098	0.171	101,842	0.32

The breakdown cost can be shown in Figure 7.17. We can see the amount of carbon tax cost from the CTS scenario and observe the negative carbon cost (sell the carbon credit to the foreign system) from the ETS scenario.

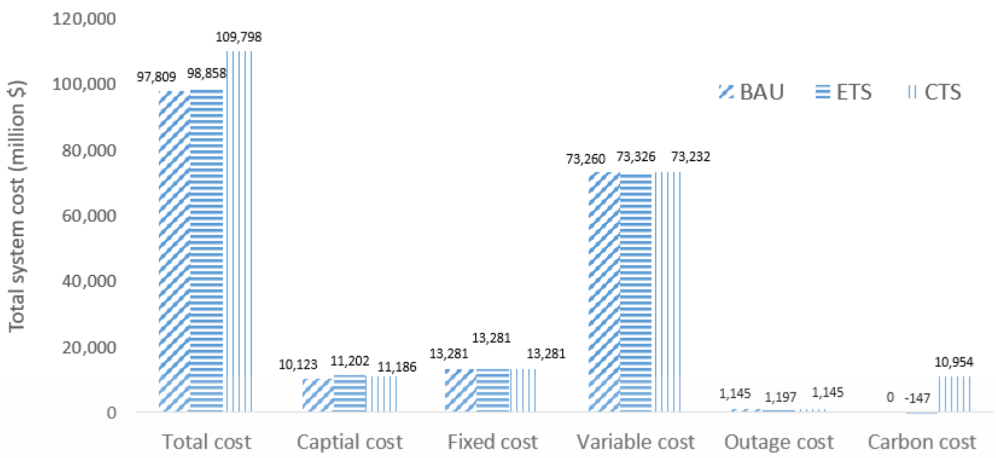

Figure 7.17 The breakdown cost comparison among BAU, CTS and ETS

ii) CO_2 **emission and intensity:** The CO_2 profile is depicted in Figure 7.18. The ETS outperform the others because of the CCS power plant (with 90% carbon captured). The CTS scenario slightly improves from the phase-in IGCC power plant.

Figure 7.18 CO_2 emission profile

The intensity profile is depicted in Figure 7.19. The ETS profile can go beyond the 0.283 $kgCO_2/kWh$. The new clean energy option has confirmed the effectiveness.

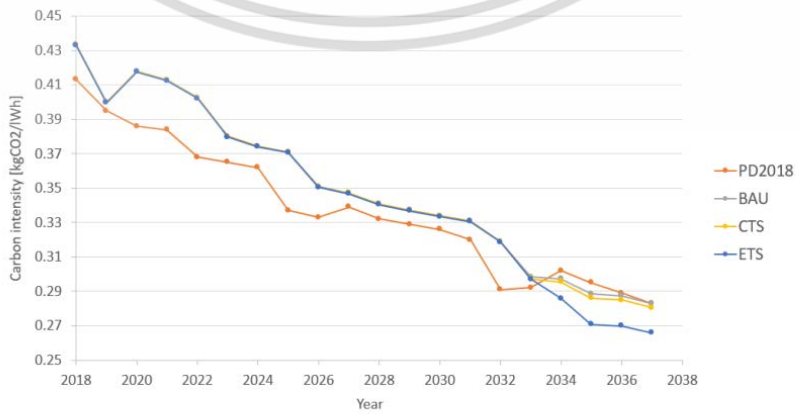

Figure 7.19 CO_2 intensity profile

7.4.4 Flexible generation evaluation

Due to Thailand generation system is a large-scale problem. The cluster approach [209] is adopted for a reduction of time computation. The flexible generation investment (dummy gas turbine) is assumed a 304$/kW. The flexibility criteria (i.e., renewable curtailment and load shedding) are considered as zero for the tightest criteria. The result of flexibility evaluation is approximated as Table 7.5. The result shows that Thailand's generation system has no problem with the flexibility and frequency security issues.

Table 7.5

Flexibility evaluation based-on PDP2018

Operation scenario	Peak netload [MW]	Min. netload [MW]	Up/Dn Ramp [MW per hour]	Load shedding [MW]	Renewable curtailment [MW]	Reliable operation
New year's day (1-2 January 2037)	23,793	12,734	3,340/1,702	0	0	Reliable
Songkran day (13-15 April 2037)	27,265	17,003	3,916/2,228	0	0	Reliable
2037 system peak (30 May 2037)	43,236	32,740	4,190/3,299	0	0	Reliable

7.5 Conclusion

The proposed method has been tested with Thailand's generation system following the official power development plan (PDP2018) over a 20-year planning horizon (2018-2037). To evaluate the climate change mitigation, the three scenarios have been conducted. Firstly, business-as-usual (BAU) is used for reference which the natural gas-fired generation dominates the other fuel types because of the lowest abatement and electricity costs. Secondly, the carbon tax scheme (CTS) sets up the tax to activate the technological substitute effect from the ultra-supercritical coal power plant to the integrated gasification combined cycle (IGCC) technology. Finally, the emission trade scheme (ETS) sets the baseline emission and put the price on it for the tradable market system. As a result of the three scenarios, the ETS pathway performs the efficient mitigation option to achieve the 1.5°C global climate change.

Chapter 8

Conclusions

In this chapter, the research results about the generation expansion planning under extended conditions are summarized. It is noted that the research results in this thesis and the author's published papers have never been addressed in any thesis or previous researches. Besides, the research gaps about this doctoral thesis that can be further developed are also introduced.

8.1 Summary

Table 8.1 summarizes the planning model, extended conditions and cost model for each chapter as follows;

Table 8.1

The summary of the extended condition, and the planning and cost models

	Case study 1 (Chapter 3)	Case study 2 (Chapter 4)	Case study 3 (Chapter 5)	Case study 4 (Chapter 6)	Case study 5 (Chapter 7)
Planning model:	**GEP-I**	**GEP-II**	**S-GEP-I**	**GEP-III**	**S-GEP-II**
Test system	Thailand (PDP2015)	1996 Korea (Scale-down)	Thailand (PDP2015)	Modified IEEE RTS	Thailand (PDP2018)
Extended conditions:					
Energy storage utilization	✓	-	-	-	✓
Flexibility planning	-	-	-	✓	✓
Fuel price uncertainty	-	-	✓	-	✓
1.5°C climate change	-	-	-	-	✓
Cost model:					
Investment cost	✓	✓	✓	✓	✓
Availability payment	✓	✓	✓	✓	✓
Energy payment	✓	✓	✓	✓	✓
Outage cost	✓	✓	✓	✓	✓
External cost	-	-	✓	-	✓
Decommissioning cost	-	✓	-	-	✓
Salvage cost	✓	✓	✓	✓	✓

The detailed summary of study cases can be provided as follows;

For Chapter 3, the GEP incorporates the enhanced valley-filling and peak-shaving techniques to form the load leveling application synergized with the energy marginal analysis. The proposed method is demonstrated for the viable study of Lithium-based battery energy storage system (Lithium BESS) in the Thailand generation system (official PDP2015). The result reveals the potential benefits of Lithium BESS for load leveling application in Thailand generation systems because of lower carbon dioxide emission and operation cost.

For Chapter 4, the development of a metaheuristic approach to solve deterministic GEP is evaluated in the 1996 scale-down Korea’s generation system. The proposed method is a hybrid approach between the cuckoo search and the dynamic programming, so-called “hybrid CSDP”. The efficient techniques, i.e. feasible search concept, hybrid structure, and memory exploration search are applied because of the solution quality and convergence characteristics. The simulation results conclude that the hybrid CSDP outperforms the other methods with high solution quality (higher probability to find the global optimal solution), good robustness (lower standard deviation), and fast convergence characteristics (lower iteration to reach the optimal solution). Moreover, the hybrid CSDP is adopted for the efficient metaheuristic approach in Chapter 5.

For Chapter 5, the stochastic approach, the so-called “Simheuristics” is developed to solve the GEP considering the uncertainty of fuel price. The efficient techniques, i.e. aggregated scenario, and quasi-mote carlo using Sobol sequence are applied because of the solution quality and convergence characteristics. The proposed method has demonstrated the effectiveness by using the Thailand generation system (PDP2018). Base on the backtest of the period 2015-2020, the Simheuristics provides a robust GEP than the deterministic approach.

For Chapter 6, the flexibility and frequency security planning are enhanced into conventional generation planning. The proposed framework is tested with the modified IEEE RTS considering 30% solar PV generation. Based on the simulation result, the flexible generation is invested to prevent the flexibility shortages, and the adequacy of frequency security is taken into account.

For Chapter 7, The GEP using the Simheuristics approach is demonstrated base on the extended conditions of Thailand generation system (official PDP2018). The three scenarios are defined to evaluate the climate change mitigation options. Firstly, business-as-usual (BAU) is used for reference which the natural gas-fired generation dominates the other fuel types because of the lowest abatement and electricity costs. Secondly, carbon tax scheme (CTS) sets up the CO_2 tax to activate the technological substitute effect from the ultra-supercritical coal power plant to the integrated gasification combined cycle (IGCC) technology. Finally, the emission trade scheme (ETS) sets the CO_2 reduction target and put the price on it for the tradable market system. As a result of the three scenarios, the ETS pathway performs the efficient mitigation option to go beyond the 444 MtCO_2 pathway.

8.2 Further works

The research questions are achieved with interesting results. Anyway, the following points and research gaps are suggested to continue the further researches:

1. The transmission system is recommended for the generation expansion planning model. The paper [210] is recommended to deal with regional planning getting the attention for Thailand system planners and policymakers.
2. The time resolution of system flexibility is limited to 60 minutes (hourly load profile). This may underestimate the flexibility challenge.
3. The clustering technique [209] used for the unit commitment to overcome the curse of dimensionality has not been assessed the accuracy and effectiveness. Further study is required to improve the dispatch problem considering the flexibility issue.
4. The social cost of carbon and the carbon tax rate are not the optimal value. The insight study is needed to obtain the positive/negative effects.

References

[1] Power Development Plan:2018 (PDP), **Electricity Generating Authority of Thailand**, 2015.

[2] System planning division, **Electricity Generating Authority of Thailand.**

[3] Retrieved from https://www co2.earth/daily-co2

[4] International Energy Agency (IEA), **Thailand Renewable Grid Integration Assessment**, 2018.

[5] WMO Greenhouse Gas Bulletin, **"The State of Greenhouse Gases in the Atmosphere Based on Global Observations through 2016,"** No.13, 2017.

[6] Alternative Energy Development Plan: AEDP 2015, **Ministry of Energy**, 2015.

[7] IPCC, **"Summary for Policymakers. In: Global warming of 1.5°C**

[8] Office of Natural Resources and Environmental Policy and Planning (ONEP), **"Thailand's Nationally Determined Contribution Roadmap on Mitigation 2021 - 2030,"**

[9] A. Wattanakuljarus, **"Carbon Taxes to Cool Earth: Costs and Benefits to Thai Economy,"**, vol.4, No. 2, NIDA case research journal, 2012.

[10] S. Kim, J. Koo, C.J. Lee and E.S. Yoon, **"Optimization of Korean energy planning for sustainability considering uncertainties in learning rates and external factors,"** Energy, vol. 44, pp.126-134, 2012.

[11] Alternative Energy Development Plan 2015 (AEDP2015), **Ministry of Energy**, 2015.

[12] International Renewable Energy Agency (IREA), **Planning for the renewable future: Long-term modeling and tools to expand variable renewable power in emerging economies**, 2017.

[13] W. Wonglimamornlert, T. Lubpanagawgiat and C. Thammarak. **"Thailand's Duck Curve: Proposed Alleviated Schemes and Affected Costs**," CIGRE AORC 2018.

[14] J. Hargreaves, E. Hart, R. Jones and A. Olson, **"REFLEX: an adapted production simulation methodology for flexible capacity planning,"** IEEE trans. on power systems, vol. 30, no. 2, pp. 1306-1315, 2014.

[15] Energy Analysis and Environmental Impacts Division Lawrence Berkeley National Laboratory, **Frequency Control Requirements for Reliable Interconnection Frequency Response**, 2018.

[16] M.S. Debry, T. Prevost, F. Xavier and A. Menze, **"Maximizing the penetration of inverter-based generation on large transmission systems: the MIGRATE project,"** 6th Solar Integration Workshop and published in the workshop's proceedings.

[17] E. Lannoye, D. Flynn and M.O. Malley, "**Evaluation of Power System Flexibility",** IEEE trans. on power systems, vol. 27, no. 2, pp. 922-209, 2012.

[18] O. Leitermann, **"Energy storage of frequency regulation on the electric grid,"** doctor of philosophy, 2012.

[19] F.D.Gonzalezm A.Sumper and O.G.Bellmunt, **"Energy Storage in Power Systems,"** WILEY: New Delhi India, 2016.

[20] K.Staschus, A. Bell and E. Cashman, **"Usable hydro capacity and electric utility production simulation and reliability calculations,"** IEEE trans. power sys., Vol.5, No.2, 1990.

[21] P.J.R. Torrealba, **The role of flexibility in generation expansion planning of power system with a high degree of renewables & vehicle electrification.** D.Eng. Thesis, Imperial College London, 2012.

[22] M.G. Molina, **Energy storage and power electronics technologies: a strong combination to empower the transformation to the smart grid,** IEEE trans. sys, pp.1-28, 2017.

[23] International energy agency (IEA), **Prospects for large-scale energy storage in decarbonized power grids,** working paper, 2009.

[24] International energy agency (IEA), **Technological roadmap of energy storage**, 2014.

[25] Y.E.Lee and Y.B. Jung, **"Challenges of nuclear power for sustainable role in Korean energy policy,"** Vol.49, energy Conversion & management, pp.1951-1959, 2008.

[26] Electricity Generating Authority of Thailand, **Contracted natural gas management (in Thai),** 2017.

[27]A. Geiger, **Strategic power plant investment planning under fuel and carbon uncertainty,** working paper, 2009.

[28] Neuhoff, K., Von Hirschhausen, **"Long-term vs. Short-term Contracts: A European Perspective on Natural Gas,"** Cambridge Working Papers in Economics, 2006.

[29] Retrieved from source: https://www.indexmundi.com

[30] A. Alim, **"Asian spot prices for LNG and other energy commodities,"** The University of Western Australia, 2015.

[31] F. Kesicki, **"Marginal abatement cost curves for policy making – expert-based vs. model-derived curves commodities,"** UCL energy institute The University of Western Australia, 2011.

[32] F. Bayatloo and A.B. Amiri, **"A novel optimization model for dynamic power grid design and expansion planning considering renewable resources,"** journal of cleaner production, Vol.229, pp. 1319-1334, 2019.

[33] P. Jirutitijaroen and C. Singh, **"Power system reliability consideration in energy planning,"** Electric power systems, Springer, 2006.

[34] F. Kesicki, **"Sensitivity-based chance-constrained Generation Expansion Planning,"** Electric power system research, Vol.127, pp.309-317, 2015.

[35] H.T. Mogulkoc, D.W Coit and F.A. Felder **"Mean-risk stochastic electricity generation expansion planning problems with demand uncertainties considering conditional-value-at risk and maximum regret as risk measures,"** Electrical Power and Energy Systems, Vol.13, pp.309-317, 2016.

[36] Z. Lu, J. Qi, B. Wen and X. Li, **"dynamic model for generation expansion planning based on Conditional Value-at-Risk theory under Low-Carbon Economy,"** Electric power system research, Vol.141, pp.363-371, 2016.

[37] A. Juan, J. Faulin, S.E. Grasman, M. Rabe and G. Figueira, **"A review of simheuristics: Extending metaheuristics to deal with stochastic combinatorial optimization problems,"** Operation research perspectives, Vol. 2, pp.62-72, 2015.

[38] Energy efficiency plan 2015: EEP2015, **Ministry of Energy**, 2015.

[39] Gas plan 2015, **Ministry of Energy**, 2015.

[40] Oil plan 2015, **Ministry of Energy**, 2015.

[41] **Kyoto Protocol to the United nation framework convention on climate change**, United nations, 1998.

[42] **Communication on Thailand's Nationally Appropriate Mitigation Actions (NAMAs)**, Office of Natural Resources and Environment 2014.

[43] **Thailand's Intended Nationally Determined Contribution (INDC)**, Office of Natural Resources and Environmental Policy and Planning, 2015.

[44] **Thailand's Nationally Determined Contribution Roadmap on Mitigation 2021 – 2030**, Ministry of Natural Resources and Environment, 2017.

[45] **The NDC and JCM status in Thailand**, Thailand greenhouse gas management organization, 2017.

[46] F. Ueckerdt, RJ. Brecha, G. Luderer and et.al., "**Variable renewable energy in modeling climate change mitigation scenarios,**" International energy workshop, pp.1-22, 2011.

[47] J. Zhong, **Power System Economics and Market Operations**. New York; CRC Press; 2018.

[48] K. Komasatid, **Long-term Thailand energy consumption forecasting with an artificial neural network approach.** M.Eng. Thesis, Chulalongkorn university, 2012.

[49] International Energy Agency (IEA), **The Fukushima Daiichi accident**, technical volume, 2015.

[50] North American Electric Reliability (NERC), **methods to model and calculate capacity contributions of variable generation for resource adequacy planning**, 2011.

[51] J. Lim, J. Jang and J. Choi, "**Probabilistic production cost simulation and reliability evaluation of power system including renewable generators**," pp. 1-7, 2012.

[52] International Energy Agency (IEA), **Modelling the capacity credit of renewable energy sources**, 2011.

[53] C. Naksrisuk and K. Audomvongseree, "**Dependable capacity evaluation of wind power and solar power generation systems**," ECTI trans. on electrical and communications, vol. 11, No.2 august pp. 58-66, 2013.

[54] K. Chaiamarit and S. Nuchprayoon, "**Modeling of renewable energy resources for generation reliability evaluation**," renewable and sustainable energy reviews, vol.57, pp.34-41, 2013.

[55] K.Rajesh, K.Karthikeyan, S. Kannan, C. Thangaraj, "**Generation expansion planning based on solar plants with storage**," renewable and sustainable energy reviews, vol.57, pp.953-964, 2016.

[56] California energy commission, **The use of heat rates in production cost modeling and market modeling**, 1998.

[57] Annual report 2018, **Department of mineral fuel**, 2018.

[58] S.Shibata, N.Zarlin, H.Shimada, et al., "**Preliminary study on design of longwall mining from final highwall at Mae Moh lignite mine in Thailand**," Mine Planning and Equipment Selection, 2014.

[59] Statistical review of world energy 2018, **British petroleum**, 2018.

[60] O. Godal and J. Fuglestvedt, "**Testing 100-year global warming potentials: impacts on compliance costs and abatement profile**," Microchimica Acta, vol.52, pp.93-127, 2002.

[61] The Intergovernmental Panel on Climate Change, **Fifth Assessment Report**, 2019.

[62] S. Rao, "**Engineering optimization: theory and practice,**" WILEY: New Canada, 2009.

[63] A.L. Arancibia, G. F Marques and C.A. Mendes, "**Systems capacity expansion planning: Novel approach for environmental and energy policy change analysis**," Environmental modeling & software., Vol. 85, pp. 70-79, 2016.

[64] H. Tekiner, D.W. Coit and F.A. Felder, "**Multi-period multi-objective electricity generation expansion planning problem with Monte-Carlo simulation**," EPSR., Vol. 80, pp. 1394-1405, 2010.

[65] S. Awerbuch, "**Portfolio-based electricity generation planning: policy implications for renewables and energy security**," Mitigation and adaptation strategies for global change., Vol. 80, pp. 1394-1405, 2010.

[66] J R.Billington and R. Allan, **Reliability evaluation of power system,** 2nd edition: Plenum Press; New York, 1996.

[67] J. Srikum and A. Techanitisawad, "**Power generation expansion planning with emission control: a nonlinear model and a GA-based heuristic approach,**" International Journal of Energy Research, Vol. 30, pp. 81-89, 2006.

[68] D. Raimi, "**Decommissioning US power plants: decisions, costs, and key issues,**" Technical report, 2017.

[69] V. Krishnan and J.D. McCalley, "**Building Foresight in Long-Term Infrastructure Planning Using End-Effect Mitigation Models,**" IEEE systems journal, vol. 11, pp.2040-2051, 2017.

[70] S. Oren, "**Ensuring generation adequacy in market electricity markets,**" pp.1-21, 2003.

[71] X. Wang and J.R. McDonald, **Modern power system planning.** New York: McGraw-Hill; 1990.

[72] T. Nakawiro, S.C. Bhattacharyya and B. Limmeechokchai, "**Electricity capacity expansion in Thailand: An analysis of gas dependence and fuel import reliance,**" Energy, vol. 33, pp.712-723, 2008.

[73] D. Weusbach and G.E Metcalf, "**The design of a carbon tax,**" SSRN, pp.1-67, 2009.

[74] M. Lin, A. Breipohl and F. Lee, "**Comparison of probabilistic production cost simulation methods**," IEEE transaction on power system, vol. 4, pp. 1326-1334, 1989.

[75] International Atomic Energy Agency (IAEA), **Expansion Planning for Electrical Generating Systems-A Guidebook,** No.241, 1984.

[76] H. Baleriaux, E. Jamoulle and Fr. L. Geurtechin, "**Simulation de L'explotation d'unparc de machines thermiques de production d'electricite couples a des stations de pompag**," Revu E., vol. 5, pp. 3-24, 1967.

[77] K.F. Schenk, R.B. Misra, S. Vassos and W. Wen, "**A new method for the evaluating of expected energy generation and loss of load probability**," IEEE transaction on power system, vol. 2, pp. 294-303, 1984.

[78] G.Gross, N.V. Garapic and B. McNutt, "**The mixture of normals approximation technique for equivalent load duration curves**," PES summer meeting Paper, 1986.

[79] J.P.Stremel, R.T.Jenkins, R.A.Babb and W.D. Bayless, "**Production costing using cumulant method of representing the equivalent load duration curve**," IEEE transaction on power system, vol. 5, pp. 1947-1956, 1980.

[80] J.W. Cooly and J.W. Turkey, "**An Algorithm for the machine calculation of complex fourier series,**" Mathematics of computation 19, pp. 336-342, 1965.

[81] L. Jin, L. Xie, W. Shi and C. Shao, "**Power System Probabilistic Production Simulation Based on Equivalent Interval Frequency Distribution Including Wind Farms**," International Conference on Power System Technology (POWERCON 2014), pp. 336-342, 2014.

[82] X. Wang, "**Equivalent energy function approach to power system probabilistic modeling**," PES winter meeting paper, 1987.

[83] A.J. Conejo, M.C. Caramanis and J.A. Bloom, "**An efficient algorithm for optimal reservoir utilization in probabilistic production costing**," IEEE transaction on power systems, vol. 5, pp. 439-447, 1990.

[84] B. Manhire, and R.T. Jenkins, "**A new technique for simulating the operation multiple assigned-energy generating units suitable for use in generation system**

expansion planning models," IEEE transaction on power apparatus and systems, vol. PAS-101, pp. 3861-3869, 1982.

[85] A.S. Malik, and B.J. Cory, "**Efficient algorithm to optimise the energy generation by pumped storage units in probabilistic production costing**," IET gen trans dist, vol.143, pp. 546-552, 1996.

[86] A.S Malik, "**Simulation of DSM Resources as Generating Units in Probabilistic Production Costing Framework**," IEEE transaction on power system, vol. 13, No.4, pp. 531-538, 1998.

[87] K. Staschau, A. Bell and E. Cashman, "**Usable hydro capacity and electrical utility production simulation and reliability calculations**," IEEE transaction on power system, vol. 5, pp. 531-538, 1990.

[88] A.S. Malik, B.. Cory and P.D.C. Wijayatunga, "**Application of probabilistic peak-shaving technique in generation planning**," IEEE transaction on power system, vol. 14, pp. 1543-1548, 1999.

[89] A. Ramos, and J. Arrojo, "**Storage plants energy optimization in probabilistic production cost models**," IET Proceedings - Generation Transmission and Distribution, vol. 143, pp. 546-552, 1996.

[90] A. Joseph and M. Shahidehpour, "**Battery storage systems in electric power systems**," 2006 IEEE Power Engineering Society General Meeting, Montreal Canada, pp. 1-8, 2006.

[91] G.P. Hammond and J. Spargo, "**The prospects for coal-fired power plants with carbon capture and storage: A UK perspecti**ve," Energy conversion & management, vol.89, pp. 476-489, 2014.

[92] E. Chong and S.H. Zak, "**An introduction to optimization,**" WILEY: USA, 2013.

[93] P.S. Neelakanta, M.H. Arsali, and N.P. Padhy, "**Integrated resource planning using segmentation method based dynamic programming,**" IEEE Trans on Power Systems, vol. 14, no. 1, pp.375-385, 1999.

[94] S.H. Karaki, F.B. Chaaban, N. Al-Nakhl and K.A. Tarhini, "**Power generation expansion planning with environment consideration for Labanon,**" IJEPE, vol. 24, pp.611-619, 2002.

[95] R. Tanabe, K. Yasuda and R. Yokoyama, "**Practical method for generation expansion planning based on dynamic programming,**" IJEPE, vol. 112, No.8, pp.114-127, 1992.

[96] P. Masse and R. Gilbrat, "**Application of linear programming to investments in the electric power industry,**" Management Science, vol. 3, No.2, pp.1326-1334, 1957.

[97] A. Ramos and J. Bogas, "**A nonlinear programming approach to optimal generation expansion planning,**" IEEE trans. on power sys, vol. 4, No.3, pp.1140-1146, 1989.

[98] C.H. Antunes, A. Martins and S.B. Isabel, "**A multiple objective mixed integer linear programming model for power generation expansion planning,**" Energy, vol. 29, pp.613-627, 2004.

[99] J. Srikum, A. Techanitisawad and V. Kachitvichayanakul, "**A new efficient GA-Benders' decomposition method: for power generation expansion planning with emission controls,**" IEEE trans. on power sys, vol. 22, No.3, pp.1092-1100, 2007.

[100] Y.M. Park, J.R. Won, J.B. Park and D.G Kim "**Generation expansion planning based on an advanced evolutionary programming,**" IEEE trans. on power sys, vol. 14, No.1, pp.299-305, 1999.

[101] J.B. Park, Y.M. Park, J.R. Won and K.Y. Lee "**An improved genetic algorithm for generation expansion planning,**" IEEE trans. on power sys, vol. 15, No.3, pp.916-922, 2000.

[102] S. Kannan, S. Slochanal, P. Subbaraj and N.P. Padhy "**Application of particle swarm optimization technique and its variant to generation expansion planning problem,**" EPSR, vol. 70, No.3, pp.203-210, 2010.

[103] M. Jadidoleslam and A. Ebrahimi "**Reliability constrained generation expansion planning by a modified shuffled frog leaping algorithm,**" IJPES, vol. 64, No.3, pp.743-751, 2015.

[104] R. Storn and K. Price "**Differential evolution – a simple and efficient heuristic for global optimization over continuous spaces,**" Journal of global optimization, vol. 11, pp.341-359, 1997.

[105] S. Kannan, S. Slochanal and N.P. Padhy "**Application and comparison of metaheuristic techniques to generation expansion planning problem,**" IEEE trans. on power sys, vol. 20, No.1, pp.466-475, 2005.

[106] K.P. Wong and Y.W. Wong "**Combined genetic algorithm/simulated annealing/fuzzy set approach to short-term generation schedule with take-or-pay fuel contract,**" IEEE trans. on power sys, vol. 11, No.1, pp.128-136, 1996.

[107] D. Nualhong, S. Chusanapiputt, S. Jantarang and V. Pungprasert "**Generation expansion planning including biomass energy sources with global environmental consideration using improved Tabu search,**" TENCON Region 10 conference, pp.1-5, 2005.

[108] Y.M. Park, J.B Park and J.R. Won"**A hybrid genetic algorithm/dynamic programming approach to optimal long-term generation expansion planning,**" IJPES, vol. 20, No.4, pp.295-303, 1998.

[109] S. Kannan, S Basjar, M.D. McCalley and P. Murugan "**Application of NSGA-II algorithm to generation expansion planning,**" IEEE trans. on power sys, vol. 24, No.1, pp.1790-1797, 2009.

[110] P.S. Meneses, **Extremal optimisation applied to constrained combinatorial multi-objective optimisation problems.** D.Eng. Thesis, Bond university, 2012.

[111] X.S. Yang , **Engineering Optimization - An introduction with Metaheuristic Applications**, WILEY, 2010.

[112] K. Sorensen "**Metaheuristics—the metaphor exposed,**" International Transactions in Operational Research, vol. 22, No.1, pp.1-20, 2015.

[113] G.M. Viswanathan, V. Afanasyev, S.V. Buldyrev and et. al. "**Levy flight search pattern of wandering albatrosses,**" Nature, vol. 381, pp.413-415, 1996.

[114] X.S. Yang, "**Nature-Inspired Metaheuristic Algorithms,**" Luniver Press, 2010.

[115] R.N. Mantegna" **Fast, accurate algorithm for numerical simulation of Levy stable stochastic**

processes," Physical Review E, vol. 49, pp.4677-4683, 1994.

[116] S. Salcedo-Sanz "**A survey of repair methods used as constraint handling techniques in evolutionary algorithms,**" Computer science review, vol. 3, No.3, pp.175-192, 2009.

[117] X.S. Yang "**Cuckoo search via Levy flight,**" World Congress on Nature & Biologically Inspired Computing (NaBIC), Coimbatore India, pp.1-7, 2009.

[118] **Risk Hedging Strategies under Energy System and Climate Policy Uncertainties**, International Institute for Applied Systems Analysis, 2009.

[119] A. Ioannou, A. Angus and F. Brennan, “**Risk-based methods for sustainable energy system planning: A review,**” Renewable and Sustainable Energy Reviews, vol. 74, pp. 602-615, 2017.

[120] O. Tietjen, M. Pahle and S. Fuss, “**Investment risks in power generation: A comparison of fossil fuel and renewable energy dominated markets,**” Energy economics, vol. 58, pp. 174-185, 2016.

[121] **The Use of Solar and Wind as a Physical Hedge against Price Variability within a Generation Portfolio**, National renewable energy laboratory, 2013.

[122] M. Bolinger, R. Wiser and W. Golove, “**Accounting for fuel price risk when comparing renewable to gas-fired generation: the role of forward natural gas prices,**” Energy policy, vol. 34, pp. 706-720, 2006.

[123] M.J. Santos, P. Ferreira and M. Araujo, “**A methodology to incorporate risk and uncertainty in electricity power planning,**” Energy, vol. 115, pp. 1400-1411, 2016.

[124] N. Bauer, I. Mouratiadou, G. Luderer and et al., “**Global fossil energy markets and climate change mitigation – an analysis with REMIND,**” Climate change, vol. 1, pp. 1-14, 2012.

[125] I.C Perez, I. Arto, J.M. Polanco-martinez and Et al., “**Likelihood of climate change pathways under uncertainty on fossil fuel resource availability,**” Energy & environtmental science, vol. 9, pp. 2482-2496, 2016.

[126] R.M. Shrestha, R. Shrestha and S.C Bhattacharya “**Environmental and electricity planning implications of carbon tax and technological constraints in a developing country,**” Energy policy, vol. 26, pp. 527-533, 1998.

[127] S. Kim, J. Koom C.J. Lee and E.Y. Yoon, **Emissions trading and electricity sector regulation**, Energy, vol. 44, pp. 126-134, 2018.

[128] P.M. Pardalos, **Energy Systems.** Springer; 2012.

[129] International carbon action partnership, “**Critical mid-term uncertainties in long-term decarbonisation pathways**, 2018.

[130] J.R Birge and F. Louveaux, **Introduction to stochastic programming.** Springer; 2010.

[131] M. Mazadi, W.D Rosehart, O.P. Malik and J.A. Aguado, “**Modified Chance-Constrained Optimization Applied to the Generation Expansion Problem,**” IEEE trans. on power sys, vol. (3)24, pp. 1635-1636, 2009.

[132] S. Fuss and J. Szolgayova, **"Fuel price and technological uncertainty in a real options model for electricity planning,"** Applied energy, vol. 87, pp. 2938-2944, 2010.

[133] M. Bierlaire, **"A mean-variance portfolio optimization of Califonia generation mix to 2020,"** California Energy Commission, 2007.

[134] B. Defourny, D. Ernst and L. Wehenkel, **"Multistage Stochastic Programming: A Scenario Tree Based Approach to Planning under Uncertainty,"** Systems and Modeling Research Unit, pp. 1-51, 2011.

[135] G. Guerkan, A.Y. Oezge and S.M. Robinson, **"Sample-Path Optimization in Simulation,"** International institute for applied systems analysis, 1994.

[136] R.T. Rockafellar and J.B. Roger, **"Scenarios and Policy Aggregation in Optimization Under Uncertainty,"** Mathematics of operations research, pp. 1-32, 1991.

[137] R.M. Sanchez, L.R. Villacres, S.P. Torres and Castro, **"Transmission Expansion Planning Considering Uncertainty,"** 2019 IEEE PES Innovative Smart Grid Technologies Europe (ISGT-Europe), pp. 1-5, 2019.

[138] M. Bierlaire, **"Simulation and optimization: A short review,"** Transportation research part C, vol. 1, pp. 1-10, 2015.

[139] J.L. Higle and S. Sen, **Stochastic decomposition.** Springer; 1996.

[140] S. Pineda and A.J. Conejo, **"Scenario reduction for risk-averse electricity trading,"** IET Generation Transmission & Distribution, Vol. 4(6), pp. 694-705, 2010

[141] A. Shapiro, **"Monte Carlo simulation approach to stochastic programming,"** Proceedings of the 2001 Winter Simulation Conference, Arlington USA., pp. 428-431, 2001.

[142] D. Bertsimas, V. Gupta, N. Kallus, **"Robust Sample Average Approximation,"** *Math. Program.*, Vol. 171, pp. 217-282, 2018.

[143] **An introduction to Quasi Monte Carlo methods**, Norwegian university of science and technology, 2005.

[144] J.Halton, **"Algorithm 247: Radical-inverse quasi-random point sequence,"** Communications of the ACM, vol. 7, pp. 701-707, 1964.

[145] H. Faure. **"Discrepancy of sequences associated with a number system (in dimension s),"** Acta. Arith, vol. 41, pp. 337-351, 1982.

[146] H. Niederreiter. **"Points sets and sequences with small discrepancy,"** Monatsh. Math, vol. 104, pp. 273-337, 1987.

[147] V.D. Corput. **"Verteilungsfunktionen (Erste Mitteilung),"** Proceedings of the Koninklijke Akademie van Wetenschappen te Amsterdam, vol. 38, pp. 813-821, 1935.

[148] I.M. SOBOL. **"Uniformly distributed sequence with an additional uniformity property,"** USSR Comput. Maths. Math. Phys, vol. 36, pp. 236-242, 1976.

[149] S. Phootrakornchai and S. Jiriwibhakorn, **"Transient Staiblity Analysis by Adaptive Neuro Fuzzy Inference System and Sobol Sequence,"** 2018 15th International Conference on Electrical Engineering/Electronics, Computer, Telecommunications and Information Technology, pp. 49-53, 2018.

[150] W. Khamsawang and S. Jiriwibhakorn, **"DSPSO–TSA for economic dispatch problem with nonsmooth and noncontinuous cost functions,"** Energy conversion and management, vol. 51, pp. 365-375, 2010.

[151] **The flaw of averages**, European Working Group, pp. 1-3, 2003.

[152] P.V. Gomes, J.T. Saraiva, L. Carvalho and et al. **"Impact of decision-making models in Transmission Expansion Planning considering large shares of renewable energy sources,"** *EPSR*, vol. 174, pp. 1-13, 2019.

[153] C. Uckun, A. Botterud and J.R Birge **"An Improved Stochastic Unit Commitment Formulation to Accommodate Wind Uncertainty,"** IEEE trans. on power sys, vol. (4)3, pp. 2507-2517, 2016.

[154] S. Li, D.W. Coit and F. Felder, **"Stochastic optimization for electric power generation expansion planning with discrete climate change scenarios,"** EPSR, Vol. 140, pp. 401-412, 2016.

[155] M. Pantos, **"Stochastic generation-expansion planning and diversification of energy transmission paths,"** Electric power system research, vol. 98, pp. 1-10, 2013.

[156] C. Blanco, S. Choi and D. Soronow, **"Energy Price Processes Used for Derivatives Pricing & Risk Management,"** Commodity now, pp. 74-80, 2001.

[157] S. Pineda and A.J. Conejo, **"Estimation of mean reversion in Oil and Gas markets,"** Technical report, MITSUI/2008-10-14, 2008.

[158] J. Morris, V. Srikrishnan, M. Webster and Reilly, **"Hedging Strategies: Electricity Investment Decisions under Policy Uncertainty,"** Energy journal, vol. 39(1), pp. 101-122, 2018.

[159] **The Value of Renewable Energy as a Hedge Against Fuel Price Risk: Analytic Contributions from Economic and Finance Theory**, Lawrence Berkeley National Laboratory; 2009.

[160] C. Mari, "**Hedging electricity price volatility using nuclear power,**" Applied energy, vol. 141, pp. 615-621, 2014.

[161] A. Ulbig and G. Andersson "**Analyzing operational flexibility of electric power systems**", Electrical power & energy systems, vol. 72, pp. 155-164, 2015

[162] B. Kroposki, B. Johnson, Y. Zhan and et al., "**Achieving a 100% Renewable Grid: Operating Electric Power Systems with Extremely High Levels of Variable Renewable Energy**", IEEE power and energy magazine, vol. 15(2), pp. 61-73, 2016.

[163] K. Kongrith, W. Sanpat, S. Kornphat and L. Juthamard, "**Operational Flexibility Assessment for Thailand Generation Planning Enhancement**", CIGRE AORC, Bali Indonesia, pp.1-8, 2019.

[164] N.W. Miller, K. Clark and M. Shao, "**Impact of frequency responsive wind plant controls on grid performance,**" IEEE Power and Energy Society General Meeting, USA, pp. 1-7, 2011.

[165] National Renewable Energy Laboratory (NREL), **Power System Planning: Emerging Practices Suitable for Evaluating the Impact of High-Penetration Photovoltaics**, technical report NREL/SR-581-42297, 2008.

[166] A. Olsen, R. Jones, E. Hart and J. Hargreaves, "**Renewable curtailment as a power system flexibility resource**", The electricity journal, vol. 27(9), pp. 49-61, 2014.

[167] J. Ma, V. Silva, R. Bellhomme, and et al., "**Evaluating and planning flexibility in sustainable power systems,**" IEEE trans. on sustainable energy, vol. 4(1), pp. 200-209, 2013.

[168] H. Chavez and R. Baldick, "**Inertia and governor ramp rate constrained economic dispatch to assess primary frequency response adequacy**," International conference on renewable energies and power quality, Spain, pp.1-8, 2012.

[169] R. Eriksson, N. Modig and K. Elkington, "**Synthetic inertia versus fast frequency response: a definition,**" IET renewable power generation, vol. 12(5), pp. 1-8, 2018.

[170] A. Ulbig, T. Borsche and G. Andersson "**Impact of low rotational inertia on power system stability and operation**," IFAC proceeding volumes, vol. 47(3), pp. 7290-7297, 2014.

[171] S. Sharma, S. Huang and N. Sama, "**System inertial frequency response estimation and impact of renewable resources in ERCOT interconnection**," IEEE power and energy society general meeting, USA, pp.1-8, 2011.

[172] H. Chavez, R. Baldick and S. Sharma **"Governor rate-constrained OPF for primary frequency control adequacy,"** IEEE trans. on power sys, vol. 29(3), pp. 1473-1480, 2014.

[173] C. Barrows, A. Bloom, A. Ehlen and et al., **"The IEEE reliability test system: a proposed 2019 Update,"** IEEE trans. on power sys, vol. 35(1), pp. 119-127, 2020.

[174] F. Ueckerdt, R. Brecha, G. Luderer and et al. "**Representing power sector variability and the integration of variable renewables in long-term climate change mitigation scenario: A novel modeling approach",** Energy, Vol. 90, pp. 1799-1814, 2015.

[175] J. Kopiske, S. Spieker and G. Tsatsaronis, "**Value of power plant flexibility in power systems with high1 shares of variable renewables: A scenario outlook for Germany 2035**," Energy, vol. 137, pp. 823-833, 2017.

[176] International electrotechnical commission (IEC), **"Grid Integration of large-capacity renewable energy source and use of large-capacity electrical energy storage",** white paper, 2012.

[177] E. Balkirtzis, P. Biskas, D. Labridis and et al., "**Multiple Time Resolution Unit Commitment for Short-term Operations Scheduling under High Renewable Penetration"**, IEEE transactions on power sys, vol. 29(1), pp. 149-159, 2014.

[178] T. Adhinarayanan and M. Sydulu, **"Efficient lambda logic based optimisation procedure to solve the large scale generator constrained economic dispatch problem"**, Journal of Electrical Engineering & Technology, vol. 4(3), pp. 301-309, 2009.

[179] National renewable energy laboratory (NREL), **Operating reserves and variable generation**, technical report, 2011.

[180] G. Kou, P. Markham, S. Hadley and et al., **"Impact of governor deadband on frequency response of the eastern interconnection"**, IEEE transactions on smart grid, vol. 7(3), pp. 1368-1377, 2015.

[181] H. Ahmadi and H. Ghasemi, **"Security-constrained unit commitment with linearized system frequency limit constraints"**, IEEE transactions on power sys, vol. 29(4), pp. 1536-1545, 2014.

[182] R. Doherty, A. Mullane, G. Nolan and et al., **"An assessment of the impact of wind generation on system frequency control"**, IEEE transactions on power sys, vol. 25(1), pp. 452-460, 2010.

[183] G. Chown, J. Wright, R.V. Heerden and M. Coker, **"System inertia and rate of change of frequency (RoCoF) with increasing nonsynchronous renewable energy penetration,"** CIGRE 2017, pp. 1-19, South Africa, 2017.

[184] A Ahmadyar and S. Riaz, **"A framework for frequency stability assessment of future power systems: An Australian case study"**, Mathematics, Computer Science, pp. 1-8, 2017.

[185] B. Porretta and S. Porretta, **"Self regulation of electrical power systems"**, IEEE Texas Power and Energy Conference (TPEC), USA, pp. 1-6, 2019.

[186] European network of tansmission system operators for electricity (ENTSO), **Nordic future system inertia**, technical report, 2018.

[187] B. Porretta and S. Porretta, **"Calculation of power systems inertia and frequency response,"** Texas Power and Energy Conference (TPEC), pp. 1-6, USA, 2018.

[188] D. Delille, B. Francois and G. Malarange, **"Dynamic frequency control support by energy storage to reduce the impact of wind and solar generation on isolated power system's linertian"**, IEEE transactions on sustainable energy, vol. 3(4), pp. 931-939, 2012.

[189] Y. Wen, W. Li, G. Huang and X. Liu, **"Frequency dynamics constrained unit commitment with battery energy storage"**, IEEE transactions on power sys, vol. 31(6), pp. 5115-5125, 2016.

[190] Electricity generating authority of Thailand (EGAT), **"Minimum requirement for frequency regulation and control of interchange in the inter-connectors",** technical report, 2020.

[191] The institute of electrical and electronics engineers (IEEE), **Dynamic models for turbine-governors in power system studies,** technical report PES-TR1, 2013.

[192] Y. Gao, X. Gao and X. Zhang, **"The 2 °C Global Temperature Target and the Evolution of the Long-Term Goal of Addressing Climate Change—From the United Nations Framework Convention on Climate Change to the Paris Agreement," engineering"**, Engineering, vol. 3, pp. 272-278, 2017.

[193] M.E. Mann, **"Defining dangerous anthropogenic interference,"** Proceedings of the National Academy of Sciences (PNAS), vol. 11, pp. 4065-4066, 2009.

[194] L. Hannar, **Climate change biology**, Academic press, pp. 13-53, 2014.

[195] A. Gambhir, J. Rogelj, G. Luderer and T. Napp, **"Energy system changes in 1.5 °C, well below 2 °C and 2 °C scenarios"**, Energy strategy, vol. 23, pp. 69-80, 2019.

[196] F.M. Pulselli, **Global warming potential and the net carbon balance**, Encyclopedia of ecology, 2008.

[197] world meteorological organization (WMO), **The state of greenhouse gases in the atmosphere based on global observations through**, 2019.

[198] Intergovernmental Panel on Climate Change (IPCC), **Fourth assessment of IPCC**, 2007.

[199] T.M. Lenton, J.Rockstrom, O.Gaffney and et al., **"Climate tipping points — too risky to bet against"**, Nature, vol. 575, pp. 592-595, 2019.

[200] H.A. Daggash and N.M. Dowell, **"Higher Carbon Prices on Emissions Alone Will Not Deliver the Paris Agreement",** Joule, vol. 3, pp. 2120-2133, 2019.

[201] Office of natural resource and environment policy and planning, **"Thailand's Nationally Determined Contribution Roadmap on Mitigation 2021 -2030",** in report, 2017.

[202] Power Development Plan:2015 (PDP), **Electricity Generating Authority of Thailand**, 2015.

[203] World bank, **Accelerating Clean Energy** , working paper No.138, 2008.

[204] R. Wustenhagen and E. Menichetti, **"Strategic choices for renewable energy investment: Conceptual framework and opportunities for further research"**, Energy policy, vol. 40, pp. 1-10, 2012.

[205] P. H. Kpbps, J. D. Erickson and T. E. Drennen, **"Technological learning and renewable energy costs: implications for US renewable energy policy,"** Energy Policy, vol. 34, pp. 1645-1658, 2006.

[206] D. Surang and J. Skerlos, **"Reassessing the efficiency penalty from carbon capture in coal-fired power plants,"** Environmental science & technology, pp. 2576-2584, 2015.

[207] Thailand greenhouse gas management organization, **development of carbon market in Thailand**, 2014

[208] M. Dobranschi and D. Nerudova, "**Pigouvian carbon tax rate: can it help the European union achieve sustainability?,**" Energy Policy, vol. 34, pp. 1645-1658, 2006.

[209] J. Choi, T. Tran, J. Kwon, R. Thomas, T. Mount and R. Billington, "**Nodal probabilistic production cost simulation considering transmission system unavailability,**" IET Proc.-Gener. Transm. Distrub., vol. 2, No.1, pp. 33-42, 2008.

[210] J. Choi, T. Tran, J. Kwon, R. Thomas, T. Mount and R. Billington, "**Nodal probabilistic production cost simulation considering transmission system unavailability,**" IET Proc.-Gener. Transm. Distrub., vol. 2, No.1, pp. 33-42, 2008.

Appendix

Appendix A

Test System 1:
Thailand's Generation System (PDP2015)

The Thailand generation system is based on the official PDP2015. The Techno-economic data of existing and candidate plants are shown in Table A1.1-A1.2. The details of the energy storage system are provided in Table A1.3. Finally, the commited power plants are assumed as a report in Table A1.4.

Table A1.1

Techno-economic data of Existing Plants

Plant type	Owner	Cum cap (MW)	FOR (%)	Envi cost. $/MWh	FOM $/kW/y	VOM $/MWh
TH-Lignite	EGAT[a]	2,180	5~10	47.4	25	2.0
CC-Gas	EGAT	9,182	4~7	11.9	20	0.7
TH-Gas	EGAT	1,152	5	11.9	20	0.5
TH-Oil	EGAT	315	0.5	59.3	20	0.5
GE-Diesel	EGAT	4	1	59.3	20	0.5
Hydro	EGAT	3,444	0.5	11.9	40	5.0
TH-Coal	IPP[b]	2,007	5	35.6	20	0.5
CC-Gas	IPP	9,650	4~7	11.9	20	0.2
TH-Gas	IPP	1,510	5	11.9	20	0.3
Hydro	Foreign	2,404	0.5	11.9	40	5
HVDC	Foreign	300	0.5	-	70	-
Cogen-Coal	SPP-F[c]	370	46.8	35.6	40	0.5
Cogen-Gas	SPP-F	2,927	25.7	11.9	40	0.5
Cogen-Oil	SPP-F	5	41	59.3	40	0.5
Biomass	SPP-F SPP-NF[d]	314	28.3	11.9	40	0.5
Waste gas	SPP-NF	498	63.3	11.9	40	0.5
Small hydro	SPP-NF	12.2	74.1	11.9	40	0.5
Solar	SPP-NF	175	76.6	7.1	40	0.5
Wind	SPP-NF	180	80	0.6	40	0.5

a. EGAT = Electricity Generating Authority of Thailand
b. IPP = Independent Power Producer
c. SPP-F = Small Power Producer (firm)
d. SPP-NF = Small Power Producer (non-firm)

TABLE A1.2

TECHNO-ECONOMIC DATA OF CANDIDATE PLANTS

Plant type	Cum. cap (MW)	FOR (%)	Envi cost. $/MWh	FOM $/kW/y	VOM $/MWh
TH-Nuclear	1000	5	0	60	0.37
TH-Coal	1000	6	1.8	30	2.39
IGCC-Coal[a]	420	6	0.9	35	3.63
CC-Gas	700	4	0.25	15	1.13
TH-Fuel oil	600	6	0.05	25	0.91
GT-Diesel	240	5	0.05	1.8	1.83
GE-Diesel	20	6	0.05	0.9	0.90

[a] IGCC = Integrated Gasification Combined Cycle

TABLE A1.3

TECHNO-ECONOMIC DATA OF ESSS

Description	PSH #1	PSH #2	PSH #3	BESS
Unit investment cost (million $/MW)	0.9 – 1.2			0.645
Investment cost (million $/block)	465	744	483.6	16.13
Product status	Majority			Commercial
Installed capacity (MW)	500	800	520	25
Effective capacity (MW)	450	720	468	20
Number of Block	1	1	1	100
Depth of Discharge $\mathbf{DOD}_{\max}$	0.9	0.9	0.9	0.8
Round-trip efficiency η_g^{cycling}	0.75	0.75	0.75	0.9
Assigned Limited Energy $\mathbf{EL}_g$ (MWh)	300,000	400,000	300,000	413,920, 745,040, 496,700
SCOD (Year)	2018	2026	2028	2018, 2026, 2028

TABLE A1.4

COMMITTED POWER PLANTS BASED ON PDP2015

Project name	Plant type	Contracted Cap. [MW]	SCOD (MW)
Hongsa	Lignite-fired power plant	1,480	2016
NPS #1-2	Gas-fired power plant	280	2016
Kanom	Gas-fired power plant	640	2016
NPS3-4	Gas-fired power plant	280	2017
Gulf #1	Gas-fired power plant	800	2017
Gulf #2	Gas-fired power plant	800	2017
Lamtakong #3-4	Pumped- hydroelctricity	500	2018
Chulabhorn	Pumped- hydroelctricity	800	2026
Dummy foreign purchase 1	Hydroelctricity	700	2026
Dummy foreign purchase 2	Hydroelctricity	700	2027
Srinagarind	Pumped- hydroelctricity	520	2028
Dummy foreign purchase 3	Hydroelctricity	700	2028
Dummy foreign purchase 4	Hydroelctricity	700	2029
Dummy foreign purchase 5	Hydroelctricity	700	2030
Dummy foreign purchase 6	Hydroelctricity	700	2031
Dummy foreign purchase 7	Hydroelctricity	700	2032
Dummy foreign purchase 8	Hydroelctricity	700	2033
Dummy foreign purchase 9	Hydroelctricity	700	2034

Test System 2:

Scaled-down 1996 Korea's generation system

The 1996 Korea's generation system [101] is scaled-down to be a test system which consists of 15 generating units and 5 candidate options. The forecasted peak demand and load shape characteristics are assumed as shown in Figure A2.1. The planning assumptions are provided in Table A2.2.

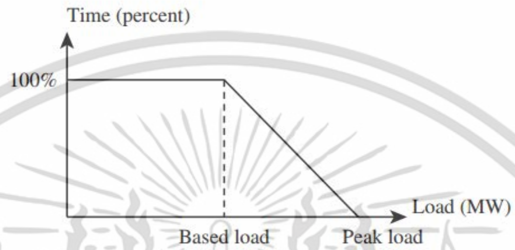

Time stage (year)	0 (1996)	1 (1998)	2 (2000)	3 (2002)	4 (2004)	5 (2006)	6 (2008)	7 (2010)	8 (2012)	9 (2014)	10 (2016)
Peak demand (MW)	5,000	7,000	9,000	10,000	12,000	13,000	14,000	15,000	17,000	18,000	20,000

Figure A2.1 Assumption of future load

Table A2.1

Planning assumption of test system 2

Parameters	Value	Unit
Discount rate	8.5	%
Reliability criterion	0.00274	-
EENS cost	0.05	Million$/GWh
Lower & upper bound of reserve margin	[0 30]	%
Salvage factor	15	%
Oil-fired power plants	[0 30]	%
Liquefied natural gas (LNG)-fired power plants	[0 40]	%
Coal-fired power plants	[20 60]	%
Nuclear power plants	[30 60]	%
Oil-fired power plants	50	thousand$/MW
Liquefied natural gas (LNG)-fired power plants	50	thousand$/MW
Coal-fired power plants	450	thousand$/MW
Nuclear power plants	1500	thousand$/MW

Test System 3:
The Modified 1996 IEEE RTS 1996

The modified IEEE RTS 1996 adopts from [142]. The net load assumption is shown in Figure. A3.1. The details of the modified IEEE RTS are depicted in Figure. A3.2.

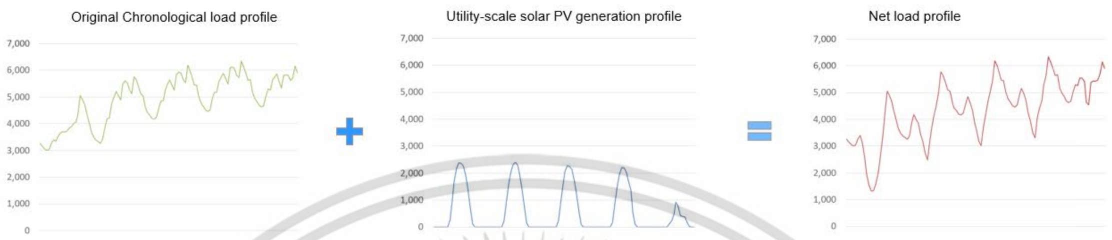

Figure A3.1 Net load assumption

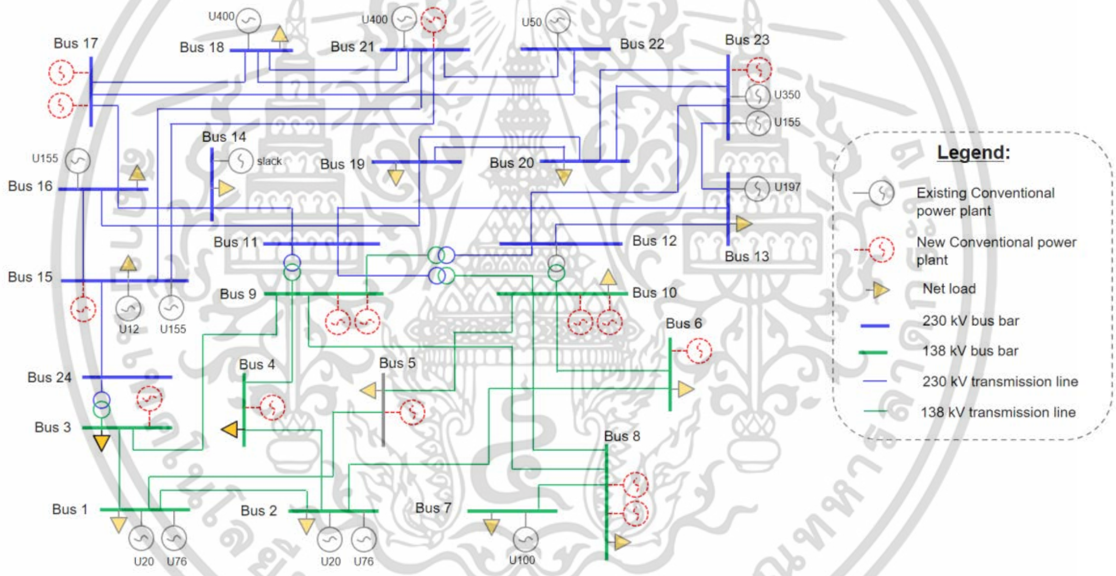

Figure A3.2 Network configuration of the modified IEEE RTS 1996

Appendix B

List of Publications

International Journals

[1] K. Komasatid and S. Jiriwibhakorn. "**An Efficient Hybrid CS-DP Application for Generation Expansion Planning Problem,**" IEEJ transactions on Electrical and Electronic Engineering: (Power and Energy), Vol 14: Issue 7, pp. 1023-1032, 2019. DOI: 10.1002/tee.22897

[2] K. Komasatid and S. Jiriwibhakorn. "**Thailand Electricity Planning under Extended Conditions using Simheuristics Approach,**" (Submitted to Electric Power System Research).

International Conferences

[1] K.Komasatid and S.Jiriwibhakorn. "**Load Leveling Application of Energy Storage System for Generation Expansion Planning,**" Proceedings of 2018 IEEE Region 10 Conference (TENCON 2018), Jeju Korea, pp. 122-127, 28-31 October 2018. DOI: 10.1109/TENCON.2018.8650357

[2] K. Komasatid and S. Jiriwibhakorn. "**Flexibility and Frequency Security Enhancement to Generation Expansion Planning Framework,**" Proceedings of IEEE-PES GTD Grand International Conference & Exposition Asia 2019 (IEEE-PES GTD Asia 2019), Bangkok Thailand, 19-23 March 2019. DOI: 10.1109/GTDAsia.2019.8715928

Biography

Kongrith Komasatid was born in Loei province, Thailand, on August 26, 1985. He received B.Eng. degree in electrical engineering from King Mongkut's Institute of Technology Ladkrabang (KMITL), in 2008 and M.Eng. degree in industrial engineering from Chulalongkorn Univerity, Thailand in 2012. Currently, he is acting as an electrical engineer at the transmission project section, transmission investment planning department, generation and transmission planning division, Electricity Generating Authority of Thailand (EGAT). He is working toward the Doctor of Engineering's degree in electrical engineering at KMITL and researching interests are long-term electricity load forecasting and optimization technique for power system operation and planning.